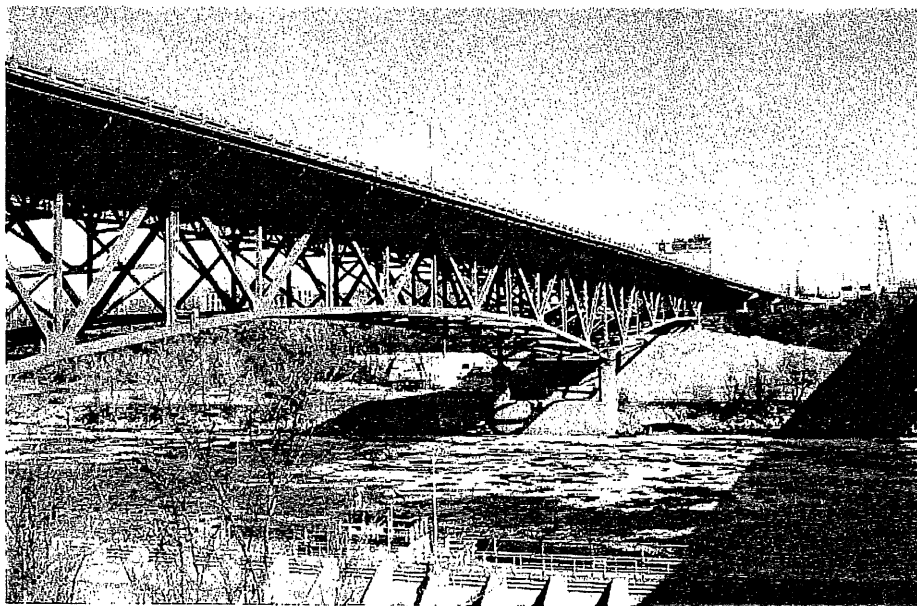


DRAFT REPORT

FATIGUE EVALUATION AND REDUNDANCY ANALYSIS

**BRIDGE NO. 9340
I-35W OVER MISSISSIPPI RIVER**



Prepared for
Mn/DOT

July, 2006

URS Corporation
700 South Third Street, Suit 600
Minneapolis, MN 55416
Project No. 31809166.01201

Consultant's Report

Recommendations on Truss Members Retrofit

The following table lists the identified 13 fracture critical truss members on one half of each truss. Due to the double symmetry of the deck truss, there are a total of 52 fracture critical main truss members on the bridge structure. Figure 1 shows all the fracture critical members on one truss, or 26 members. These include the corresponding chord members on the opposing side of the zero-force vertical from the fracture critical members identified by the redundancy analysis.

Table. Infinite Fatigue Life Check of Fracture Critical Members on One Half of Each Truss

Truss Member	Dead Load Axial Stress	Fatigue Guide Specs Fatigue Truck Method				LRFR Manual Fatigue Truck Method			
		LL+I Stress Range S_r	Factored Stress Range $R_s S_r$	Limiting Stress Range S_{FL} Cat. D	Limiting Stress Range S_{FL} Cat. E	LL+I Stress Range Δf I = 15%	Max Stress Range Factored $2.0R_s \Delta f$	Fatigue Threshold $(\Delta f)_{th}$ Cat. D	Fatigue Threshold $(\Delta f)_{th}$ Cat. E
		(ksi)	(ksi)	(ksi)	(ksi)	(ksi)	(ksi)	(ksi)	(ksi)
L1-L2	1.50	1.53	2.58	2.60	1.60	1.63	3.10	7.00	4.50
L2-L3	1.50	1.42	2.38	2.60	1.60	1.51	2.86	7.00	4.50
U0-U1	9.76	1.19	2.00	2.60	1.60	1.30	2.48	7.00	4.50
U1-U2	8.54	0.68	1.15	2.60	1.60	0.74	1.41	7.00	4.50
U4-U5	11.61	1.17	1.97	2.60	1.60	1.25	2.37	7.00	4.50
U5-U6	10.95	1.16	1.95	2.60	1.60	1.24	2.35	7.00	4.50
L11-L12	15.73	0.71	1.20	2.60	1.60	0.75	1.42	7.00	4.50
L12-L13	15.73	0.71	1.19	2.60	1.60	0.75	1.42	7.00	4.50
L13-L14	17.54	0.58	0.97	2.60	1.60	0.61	1.16	7.00	4.50
U6-U7	18.06	0.38	0.65	2.60	1.60	0.41	0.78	7.00	4.50
U7-U8	18.58	0.43	0.73	2.60	1.60	0.46	0.88	7.00	4.50
U8-U9	17.45	0.36	0.61	2.60	1.60	0.39	0.74	7.00	4.50
U9-U10	17.33	0.34	0.58	2.60	1.60	0.36	0.69	7.00	4.50

The table also summarizes AASHTO criteria for infinite fatigue life check in accordance with the Fatigue Guide Specifications and the LRFR Manual using the fatigue truck method. The Fatigue Guide Specifications is more conservative than the LRFR Manual in that it applies a 1.75 reliability factor (vs. 1.0 in LRFR) to the calculated stress range due to the fatigue truck for fracture critical members and uses an infinite fatigue life limiting stress range of 0.367 times (vs. 0.5 times in LRFR) the constant amplitude fatigue threshold developed from fatigue tests. As shown in the table, all members satisfy the LRFR requirements for infinite fatigue life although the first six members fail to satisfy the Fatigue Guide Specifications for the Category E fatigue detail (U1-U2 is included in this group because of its counterpart U0-U1).

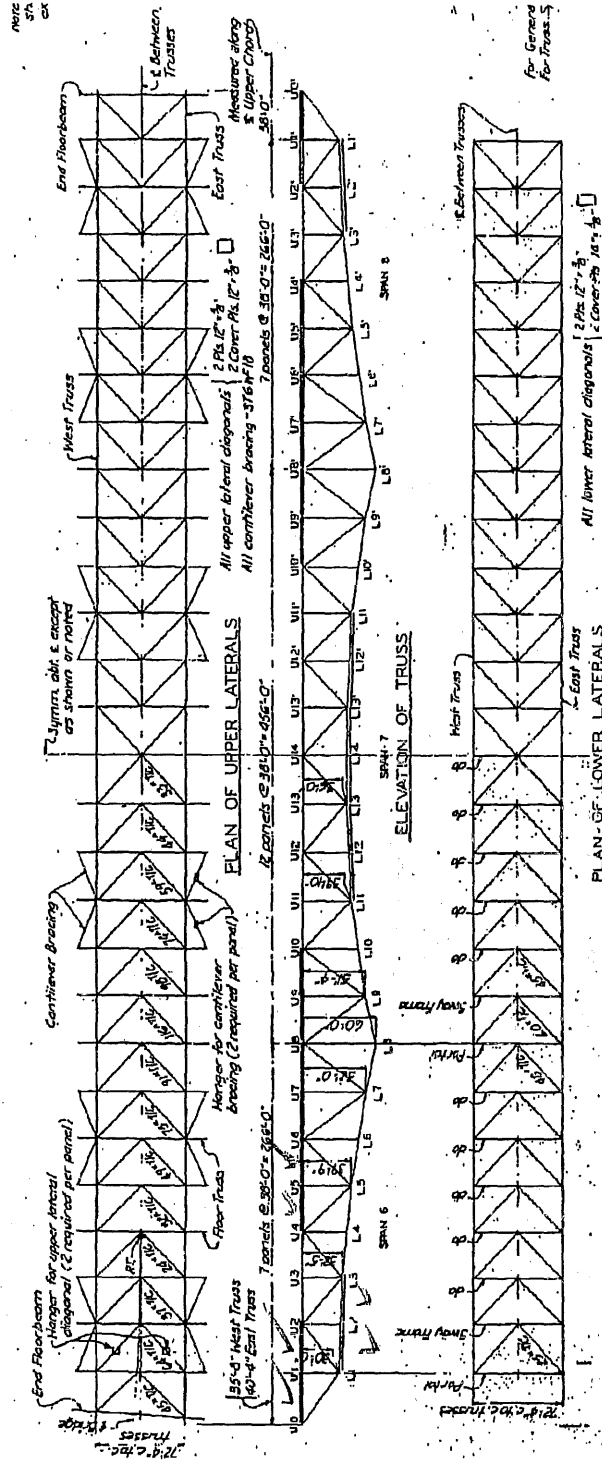


Figure 1: Deck Truss Framing Plan and Elevation from Original Contract Plans
 (Highlighted Members are Identified Fracture Critical Members)

The fracture critical members can be divided into two general groups: (1) relatively more fatigue sensitive members (L1-L2, L2-L3, U0-U1, U1-U2, U4-U5, and U5-U6), these members are subject to higher fatigue load stress ranges, not satisfying the Fatigue Guide Specifications' infinite fatigue life check for Category E, but are subjected to lower total stresses and have thinner web plates that are more forgiving for brittle fracture; and (2) relatively more fracture sensitive members (L11-L12, L12-L13, L13-L14, U6-U7, U7-U8, U8-U9, and U9-U10), these members have larger cross sections and are subject to very low fatigue load stress ranges, satisfying all AASHTO infinite fatigue life checks for Category E, but are subjected to higher total stresses and have thicker web plates that do not tolerate the existence of through-thickness cracks before the occurrence of brittle fracture.

It is very important to emphasize that neither a fatigue crack would propagate under repeated fluctuating load nor a brittle fracture would occur under some heavy load without a preexisting flaw or crack. As the results of a fracture mechanics analysis indicated in Section 9, the dimensions of preexisting cracks need to be quite large in order to propagate under the traffic load and grow to a critical size to induce a brittle fracture of the truss chord web plate. Since the locations of fatigue susceptible details are clearly known on Bridge 9340, one alternative retrofit approach to steel plating is to perform an in-depth non-destructive examination (NDE) of all the suspected details for existing cracks and flaws. For any weld-induced flaws or cracks discovered by the NDE efforts, a suitable procedure (e.g. grinding) should be carried out to remove the sources of localized stress concentration. After all the fracture critical members are assured of no existence of measurable cracks or flaws, confidence should be obtained for these members for infinite fatigue life under the traffic load.

Based on the analysis results described in this report, three equally viable retrofit approaches are recommended as follows:

- (1) Steel plating of all 52 fracture critical truss members. This approach will provide member redundancy to each of the identified fracture critical members via additional plates bolted to the existing webs. The critical issue of this approach is to ensure that no new defects

are introduced to the existing web plates through the drilled holes. This approach is generally most conservative but its relatively high cost may not be justified by the actual levels of stresses the structure experiences.

- (2) Non-destructive examination (NDE) and removal of all measurable defects at suspected weld details of all 52 fracture critical truss members. The critical issue of this approach is to ensure that no measurable defects are missed by the NDE efforts. The fracture mechanics analysis has indicated that the dimensions of preexisting surface cracks need to be at least one quarter of the web plate thickness in order to grow and subsequently cause member fracture under the traffic load. This approach is most cost efficient.

- (3) A combination of the above two approaches: steel plating of the 24 more fatigue sensitive members (L1-L2, L2-L3, U0-U1, U1-U2, U4-U5, and U5-U6 in each half of each truss), and NDE of the 28 more fracture sensitive members (L11-L12, L12-L13, L13-L14, U6-U7, U7-U8, U8-U9, and U9-U10 in each half of each truss).

TABLE OF CONTENTS

<u>Section</u>	<u>Page</u>
Executive Summary.....	1
Section 1 – Introduction.....	1-1
1.1 Bridge Structure Overview.....	1-1
1.2 Project Objectives and Work Scope.....	1-7
1.3 General Approach and Work Procedure.....	1-8
Section 2 – Bridge Inspection and Data Collection.....	2-1
2.1 Overview.....	2-1
2.2 Bridge Field Inspection.....	2-1
2.2.1 Inspection Overview.....	2-1
2.2.2 Condition of Truss Members.....	2-2
2.2.3 Condition of Bearings.....	2-2
2.2.4 Condition of Deck Expansion Joints.....	2-4
2.2.5 Bearing and Joint Marking.....	2-4
2.2.6 Inspection of Fatigue Susceptible Details Inside Truss Chords.....	2-5
2.2.7 Summary.....	2-6
2.3 Review of Previous Inspection Report.....	2-7
2.3.1 Cracks in the Steel or Welds.....	2-7
2.3.2 Deck Slab Expansion Joints.....	2-7
2.3.3 Stringer Expansion Seats.....	2-8
2.3.4 Structural Changes.....	2-8
2.3.5 Corrosion and Section Loss.....	2-9
2.3.6 Condition of Bearings.....	2-9
2.4 Review of Shop Drawings.....	2-10
2.5 Measurement of Bearing Movement.....	2-12
2.6 Collection of Traffic Data.....	2-14
2.6.1 Total Traffic Volume from Loop Detector Data.....	2-14
2.6.2 Heavy Vehicle Volume from Manual Count.....	2-16
2.7 Review of Relevant Weigh-In-Motion Data.....	2-22
Section 3 – Computer Modeling of Truss Spans.....	3-1
3.1 Development of 3-D Finite Element Model.....	3-1
3.1.1 Overview.....	3-1
3.1.2 General Assumptions.....	3-4
3.1.3 Main Trusses.....	3-5
3.1.4 Floor Trusses.....	3-5
3.1.5 End Floor Beams.....	3-8
3.1.6 Portal and Sway Frames.....	3-9

3.1.7 Upper Lateral, Lower Lateral, and Cantilever Bracing Members.....	3-10
3.1.8 Stringers and Diaphragms.....	3-11
3.1.9 Floor Truss Bracing Members.....	3-14
3.1.10 Deck and Barriers.....	3-15
3.1.11 Connection between Deck and Stringers.....	3-19
3.1.12 Connection of Stringers to Floor Trusses and End Floor Beams.....	3-20
3.1.13 Connection between Floor Trusses and Main Trusses.....	3-22
3.1.14 Stringer Supports on Floor Trusses.....	3-23
3.1.15 Main Truss Bearings.....	3-24
3.1.16 Piers.....	3-25
3.1.17 Approach Spans.....	3-29
3.2 Model Calibration per Field Testing Results.....	3-29
3.3 Summary.....	3-32
Section 4 –Strength Evaluation of Truss Members.....	4-1
4.1 Member Capacities.....	4-1
4.1.1 Main Truss Members.....	4-1
4.1.2 Floor Truss Members.....	4-8
4.1.3 Secondary Members.....	4-9
4.2 Truss Member Forces Under Camber and Dead Loads from 3-D Analysis.....	4-10
4.2.1 Camber Loads from 3-D Analysis.....	4-11
4.2.2 Non-Composite Dead Loads from 3-D Analysis.....	4-14
4.2.3 Composite Dead Loads from 3-D Analysis.....	4-16
4.2.4 Total Dead Loads from 3-D Analysis.....	4-17
4.2.5 Dead Load Member Forces from Original Contract B Plans.....	4-23
4.3 Truss Member Forces Under Live Loads.....	4-26
4.3.1 From Original Contract B Plans.....	4-26
4.3.2 Lateral Live Load Distribution.....	4-27
4.3.3 3-D Analysis – Unfactored Live Load and Ultimate Capacity.....	4-28
4.3.4 3-D Analysis – LFD Factored Live Load and Ultimate Capacity.....	4-29
4.3.5 3-D Analysis – LRFD Factored Load and Capacity.....	4-31
4.3.6 Summary and Comparison.....	4-31
4.4 Truss Member Forces Under Combined Dead and Live Loads.....	4-35
4.4.1 From Original Contract B Plans.....	4-35
4.4.2 3-D Analysis Unfactored Dead and Live Load and Ultimate Capacity.....	4-36
4.4.3 3-D Analysis LFD Factored Dead and Live Load and Ultimate Capacity.....	4-37
4.4.4 3-D Analysis LRFD Factored Dead and Live Load and Capacity.....	4-38
4.4.5 Summary and Comparison.....	4-39
Section 5 –Fatigue Evaluation of Truss Members.....	5-1
5.1 AASHTO Fatigue Specifications.....	5-1
5.2 Truss Member Fatigue Evaluation.....	5-3
5.3 Truss Member Fatigue Evaluation per AASHTO Fatigue Guide Specifications.....	5-6
5.4 Truss Member Fatigue Evaluation per Field Strain Measurements.....	5-11
5.5 Fatigue Evaluation Summary.....	5-11

Section 6 – Structural Redundancy Analysis.....	6-1
6.1 Identification of Eight Critical Truss Members.....	6-1
6.2 Objective and Key Issues of Bridge Redundancy Analysis.....	6-2
6.3 Literature Review on Bridge Redundancy Analysis.....	6-3
6.3.1 AASHTO LRFD Bridge Design Specifications.....	6-3
6.3.2 AASHTO LRFR Manual.....	6-5
6.3.3 NCHRP Report 406.....	6-6
6.3.4 NCHRP Report 319.....	6-8
6.3.5 NCHRP Synthesis 354.....	6-8
6.4 Proposed Procedure for Redundancy Analysis.....	6-9
6.5 Live Load for Redundancy Analysis.....	6-13
6.6 Criteria for Capacity Check of Remaining Bridge System.....	6-14
6.6.1 Member Capacity Check.....	6-15
6.6.2 Connection Capacity Check.....	6-16
6.7 Results Summary of Redundancy Analysis.....	6-19
6.7.1 Member Failures of Intact Structure under Dead Load.....	6-19
6.7.2 Member Failures of Intact Structure under Combined Dead and Live Load.....	6-20
6.7.3 Deformed Shapes of Failed Structure.....	6-21
6.7.4 General Summary of Redundancy Analysis Results.....	6-25
6.7.5 Load Case 1: Dead Load Only (Bridge Closed to Traffic).....	6-28
6.7.6 Load Case 2: Eight HS-20 Trucks at Slow Speed (MPF=1.0; IM=1.0).....	6-39
6.7.7 Load Case 3: Eight Lanes of Standstill HS-20 Truck & Lane Load (Rush Hour “Parking Lot”) (MPF=1.0; IM=1.0).....	6-55
6.7.8 Load Case 4: LRFD Design Load - Seven HS-20 Truck & Lane Load Lopsided (MPF=0.65; IM=1.33).....	6-75
6.7.9 Stringers.....	6-95
6.7.10 Deck.....	6-96
6.7.11 Summary of Fracture Critical Members.....	6-104
6.8 Effects of Truss Bearing Properties.....	6-105
6.8.1 Possibility of Movement of Locked Expansion Roller Bearings.....	6-106
6.8.2 Consequence of Expansion Bearing Movement from Member Failure.....	6-108
Section 7 – Retrofit Schemes for Improving Structural Safety and Performance.....	7-1
7.1 Contingency Repairs to Eight Critical Truss Members.....	7-1
7.1.1 Carbon Fiber Reinforced Polymer (CFRP) Plating.....	7-1
7.1.2 Pre-Tensioned Bars.....	7-2
7.1.3 High Performance Steel Plating.....	7-3
7.2 Deck Replacement for Reducing Stresses and Improving Redundancy.....	7-5
7.2.1 Alterations to Computer Model.....	7-6
7.2.2 Effect of Deck Replacement on Truss Member Axial Forces under Dead Load.....	7-7

7.2.3 Effect of Deck Replacement on Truss Member Force Interaction Ratio under Dead Load.....	7-9
7.2.4 Effect of Deck Replacement on Truss Member Forces under Live Load.....	7-11
7.2.5 Effect of Deck Replacement on Bridge Redundancy.....	7-12
7.2.6 Results Summary on Deck Replacement with a Continuous Slab...	7-17
Section 8 – Conceptual Plan for Deck Replacement.....	8-1
8.1 General Considerations.....	8-1
8.2 Deck Replacement Analysis.....	8-3
8.2.1 Structural Impact of Unsymmetrical Loading on Main Trusses.....	8-3
8.2.1.1 Case 1: Analysis of Existing Structure with Half the Deck and Stringers Removed – Using Unfactored Load and Ultimate Capacity.....	8-4
8.2.1.2 Case 2: Analysis of Existing Structure with Half the Deck and Stringers Removed – Using LRFD Factored Load and LRFD Factored Capacity.....	8-6
8.2.1.3 Case 3: Analysis of Existing Structure – Using LRFD Factored Load and LRFD Factored Capacity.....	8-9
8.2.1.4 Case 4: Analysis of Redecked Structure – Using LRFD Factored Load and LRFD Factored Capacity.....	8-12
8.2.1.5 Comparison of Four Cases Evaluated.....	8-15
8.2.2 Reinforced Concrete Pouring Sequence for Deck Replacement.....	8-17
8.3 Summary and Conclusions.....	8-19
 Appendices	
Appendix I – Model Test Member Comparison Graphs.....	AI-1
Appendix II – Member Forces.....	AII-1
Appendix III – Fatigue Evaluation of Truss Members.....	AIII-1
Appendix IV – Redundancy Analysis Results.....	AIV-1
Appendix V – Axial Force Comparison for Existing and Redecked Structures and Conceptual Retrofit Plans.....	AV-1
Appendix VI – Truss Member Force Interaction Ratios for Various Deck Replacement Structural Configurations.....	AVI-1

EXECUTIVE SUMMARY**Introduction**

Bridge 9340, I-35W over the Mississippi River, is a three-span continuous deck truss for the main crossing. Built in 1967, the steel superstructure contains a number of fatigue susceptible details in the main truss members and floor truss members. Most pronounced are the welded attachments at the diaphragms inside the box section of the main truss tension chords, which are Category D fatigue details according to current AASHTO fatigue provisions. The bridge was designed in accordance with the 1961 AASHTO *Standard Specifications for Highway Bridges*, which was based on a completely different fatigue design method that was revamped in the 1974 interim edition. The poor fatigue details on the truss spans, particularly those inside the main truss tension chords that are difficult to inspect, have raised concerns on the consequence of a possible main truss member failure triggered by a fatigue crack.

URS Corporation was retained by Minnesota Department of Transportation (Mn/DOT) to evaluate the integrity of the truss-arch superstructure in light of fatigue and fracture characteristics. The results from this study will be utilized by Mn/DOT as a reference for the development of future renovation work to be performed on the bridge. The primary objectives of the project include: (1) identify critical superstructure members that are most susceptible to cracking, (2) evaluate structural consequences if one of the critical members should sever, in terms of load redistribution and load carrying capacities of remaining members, (3) develop contingency repairs to selected fracture critical members, and (4) establish measures for improving structural redundancy and minimizing tensile stresses in the trusses, and develop a preferred deck replacement staging plan.

Computer Modeling

A 3-D finite element model was developed that includes all the structural components of the truss spans: deck, stringers, floor beams, floor trusses, main trusses, as well as all bracing members. All the piers and the adjacent approach span at each end were also included in the model. All steel components were modeled with space frame members through their center of gravity lines. Link members of proper stiffness properties were used at the joints to address the eccentricities due to the actual dimensions of members and connections. The reinforced concrete deck, with the existing transverse and longitudinal expansion joints, was modeled with shell elements at its mid-thickness and connected to supporting stringers with rigid shear link members for the composite action. Based on field inspection and measurements, the main truss expansion bearings have been found not to behave as intended and the actual force-displacement relationship of the bearings is rather erratic. In the computer modeling, two extreme bearing conditions were investigated for their impact: (1) the "as-designed" condition based on the original contract plans; and (2) the fully "locked" condition. Additionally, the stringers also have expansion shoes at certain locations on the supporting floor trusses. Both the "as-designed" and "locked" conditions were considered for these expansion shoes in the computer modeling.

The model was compared with previous strain gage test results of the bridge by University of Minnesota for truss member stresses under known loading conditions. Adjustments were made to the model for various support and connection stiffness properties to achieve a reasonable agreement with the test results. Based on the model-test comparison and a calibration process, the following conditions of the computer model were determined to yield the best prediction of truss member axial forces: (1) all main truss expansion bearings were completely fixed at the piers for the live load, different from the "as-designed" condition; (2) the substructure was included for the stiffness of all piers and their foundations; (3) all stringer expansion bearings were completely fixed at the floor truss and end floor beam locations, also different from the "as-designed" condition; (4) the link members at the stringer-to-floor truss and floor truss-to-main truss connections had a longitudinal stiffness that reflects the low out-of-plane web stiffness of the floor truss top chord and the actual connection properties; and (5) the link members at the

deck-to-stringer and stringer-to-floor truss connections had a transverse stiffness that reflects the low out-of-plane web stiffness of the stringer and the actual connection properties.

Strength Evaluation of Truss Members

The strength of the truss members were evaluated using the 3-D computer model in terms of the force interaction ratio, defined as the sum of the ratios of force to section capacity for axial force and bending moments in two principal directions, considering the axial force and bending moments. This is different from the traditional design of truss bridges when only the axial force is considered.

Truss members of Bridge 9340 were originally designed using the axial force only with member capacities determined from the 1961 AASHO *Standard Specifications for Highway Bridges*. A “design ratio”, defined for comparison purposes as the ratio of the calculated axial force under design load to the allowable axial capacity of the member, was used to measure the axial force design margin, similar to the force interaction ratio concept for combined force effects. Based on the information in the original contract plans, the design ratio was found to range between 0.730 and 1.004 for all the main truss members. This indicates that some of the members were sized very tightly in terms of the axial capacity and any bending moments would likely cause a localized overstress in relation to the design criteria.

Since truss members of Bridge 9340 were connected as frame members in reality, they are subject to axial force as well as in-plane and out-of-plane bending moments. To measure the combined force effects, the force interaction ratio was calculated for all truss members based on member force results of 3-D analysis as well as section capacities determined per the 1985 AASHTO *Guide Specifications for Strength Design of Truss Bridges (Load Factor Design)* and the 2004 AASHTO *LRFD Bridge Design Specifications*, respectively. The calculation of the force interaction ratios included the loads due to camber, non-composite dead load, composite dead load, and live load.

The cambering of the main trusses and floor trusses was included in the computer model as a uniform axial member distortion load to account for the built-in forces this process would induce. The calculated vertical deflections of the trusses due to camber were compared with the camber diagram in the original contract drawings and excellent agreement was observed. Ideally, the truss member bending moments due to the total dead loads would cancel out those due to the camber and the truss members would be subject to axial forces only under the dead load. The 3-D analysis indicated that after applying the camber and all the dead loads, including those at the truss ends that support the approach spans, significant bending moments may still remain in some truss members although the bending moments due to camber do counteract with those from dead loads in most members.

The force interaction ratio under the total load (camber, dead load and maximum live load) was calculated for three cases: 1) unfactored load and ultimate capacity; 2) LFD factored load and ultimate capacity; and 3) LRFD factored load and capacity. For all truss members, the LRFD loading was found to produce highest magnitudes of the force interaction ratio. For the "as-designed" truss bearing condition, the maximum values of the interaction ratio are: upper chords 1.452 (U1'-U0'), lower chords 1.120 (L8-L9), diagonals 1.773 (U0-L1), and verticals 1.321 (U1'-L1'). The maximum values of the force interaction ratio for the "locked" bearing condition (for live load) are: upper chords 1.504 (U1'-U0'), lower chords 1.264 (L8-L9), diagonals 1.827 (U0-L1), and verticals 1.310 (U1-L1). One distinct feature of the LRFD loading is the inclusion of both truck and lane loads as compared with the LFD loading that uses the higher of truck or lane load. The analysis indicated that using the unfactored loads and the ultimate capacities, no truss member has a force interaction ratio exceeding 1.0.

Further investigation was made for truss members with force interaction ratios greater than 1.0 using the LFD and LRFD criteria. It was found that for all the cases considered, the axial component of the force interaction ratio is either less than 1.0 or slightly above 1.0 (1.039 maximum). This indicates that if the truss were evaluated based on the design assumption that the members take axial load only, the members would be acceptable. A comparison between the force interaction ratios of the same members under the LRFD and the LFD criteria indicates that the LRFD produces higher interaction ratios for all but two of the sections, or 98% of the

members. This indicates the impact of the heavier LRFD loading. In diagonal member L1-U0' the force interaction ratio per the LRFD was found to be almost 30% greater than that per the LFD. For the two sections where the LFD produces a higher interaction ratio, the value was only about 5% greater than the LRFD interaction ratio (U1-L1) and the magnitude was low. The highest force interaction ratio occurred in member U0-L1, the diagonal supporting the truss cantilever at the end of the truss spans. Using the LRFD criteria the total force interaction ratio was calculated to be 1.858 with 1.038 from axial, 0.819 from in-plane bending, and essentially zero from out-of-plane bending. A large portion of this axial load and in-plane bending can be directly attributed to the approach span loads that are applied at the upper joint U0. For the same member (U0-L1) using the LFD criteria the total interaction ratio was 1.464 with 0.871 from axial, 0.590 from in-plane bending, and essentially zero from out-of-plane bending.

A force interaction ratio greater than or equal to 1.0 for the existing structure does not necessarily indicate a member "failure", but rather a localized overstress beyond the elastic limit under the factored design load and section capacities. Besides, the occurrence of a local yielding in a structural system there typically is a load redistribution, and thus a reduction of loading forces at the overstressed section, based on the change of member/connection stiffness properties. It is important to note that no interaction ratios greater than 1.0 were observed in the analysis using the unfactored load and the ultimate capacity. This indicates that the actual design load should not cause overstress in any truss members. No signs of overstress have been reported in the service history of the bridge for more than 40 years. Although some members exhibited large interaction ratios using the LRFD criteria, this is mainly because the LRFD loading can be significantly greater than the original design load for some members. Another difference between the current analysis and the original design is the assumption that the truss member end connections are rigid rather than "pinned". This assumption of rigid connections, although tending to maximize bending moments in the truss members, should better represent the actual truss joint condition.

In summary, a close examination of the force interaction ratios indicates that bending effects are not negligible in truss members when the members are assembled with moment connections. Such bending effects become significant when there are special sources for concentrated forces,

such as the truss span ends that serve as supports to the approach spans. Additionally, the LRFD loading was also found to produce more severe load effects than the traditional ASD and LFD design load, due to the use of combined truck and lane load as well as a greater vehicle impact. The 3-D analysis showed force interaction ratios greater than 1.0 in some member sections using the LRFD and LFD criteria. However, a force interaction ratio exceeding 1.0 does not necessarily indicate a section failure but rather a localized overstress under the factored load which should result in a consequent load reduction at the overstressed section due to a load redistribution.

Fatigue Evaluation of Truss Members

Using the 3-D computer model and the fatigue truck for live load stress analysis, the truss members were determined to have infinite fatigue life in accordance with the AASHTO *Guide Manual for Condition Evaluation and Load and Resistance Factor Rating (LRFR) of Highway Bridges* (LRFR Manual) and the *Guide Specifications for Fatigue Evaluation of Existing Steel Bridges* (Fatigue Guide Specifications). The University of Minnesota also concluded that fatigue cracking is not expected in the deck truss of this bridge based on field strain measurements and load tests in 2001. Therefore, it can be concluded that the probability for fatigue crack development at the concerned Category D details is very remote.

However, the fatigue concern should not be completely discounted for the following reasons: (1) the access to the fatigue susceptible details inside the truss sections is very limited for crack inspection at the weld toes and therefore a timely discovery is unlikely to happen should a crack occur for some unusual causes; (2) the length of the welded tabs at the box section diaphragms was specified 3.5" in length in the original contract plans, which is very close to the lower limit of 4" for the Category E detail. Should a fabrication error or the workmanship modify the detail to the extent that it has the fatigue resistance of a Category E detail, the infinite fatigue life requirement would not be satisfied per the AASHTO Fatigue Guide Specifications; (3) the traffic on the bridge is heavy compared with the average highway bridge and therefore the use of a single fatigue truck may be underestimating the repetitive load effects on the structure.

Structural Redundancy Analysis

For the investigation of structural redundancy and retrofit need, eight critical main truss members were selected from one half of each truss. The eight members actually represent thirty-two main truss members due to the nearly double symmetry of the trusses. Using the 3-D computer model calibrated with field testing results, the selection of the eight truss members was based on the following criteria: (1) subject to tension under combined dead load and live load; (2) containing the fatigue susceptible welded details at the interior diaphragm; and (3) among members subject to the highest magnitude of fatigue load stress range. The eight truss members selected based on these criteria are: L3-U4, L1-L2, U0-U1, U4-U5, U3-U4, L4-L5, L12-L13, and L13-L14. They cover all truss member types except the vertical, because the verticals are either compression members or do not have the fatigue susceptible detail.

The redundancy analysis was to evaluate the structural consequence for the sudden failure of each of the eight critical truss members, using the calibrated computer model. Based on the conventional planar analysis method used in truss bridge design, most tension truss members would be classified as fracture critical due to the statically determinant nature of trusses. The primary objective of the redundancy analysis was to assess the three-dimensional bridge structural system's ability to redistribute the load upon failure of a main truss member, considering the participation of all structural components. The force effects of load redistribution after a sudden member failure were to be calculated and compared with load carrying capacities of the remaining members.

After a literature review on structural redundancy evaluation, an analysis procedure was established to evaluate the force effects for the sudden failure of a main truss member and compare them with the load carrying capacities of the remaining members. Four live load cases were used for the redundancy analysis, which intend to represent realistically possible loading conditions on the bridge: (1) dead load only without live load; (2) eight lanes of slow moving HS-20 truck load (without multiple presence factor or vehicle impact); (3) eight lanes of standstill HS-20 truck and lane load (without multiple presence factor or vehicle impact); and (4)

the LRFD design load (seven lanes of HS-20 truck and lane load pushed to one side with a multiple presence factor of 0.65 and a dynamic load allowance of 33%).

For each live load case, the remaining bridge system (members and connections) were checked for their structural capacities against the consequent forces resulting from the sudden member failure. The member and connection capacities were checked using the force interaction ratio, including the effects of axial force and in-plane and out-of-plane bending moments for section capacities at the ultimate state. According to AASHTO specifications for connection design, the connections were designed with capacities between 75% and 100% of those of the main members, depending on the magnitude of design forces. The force interaction ratios were calculated both without and with a dynamic impact factor of 1.854 applied to magnify the static results to account for the dynamic effects caused by a sudden member failure. The calculated force interaction ratio presents a measurement of the load effects in terms of the ultimate capacities, or the probability of a section failure, at either the member or the connection.

Results of the redundancy analysis include the following items: (1) number of consequent main truss member failures; (2) number of consequent floor truss member failures; (3) impact on the floor truss members that “failed” in the intact structural condition; (4) consequent impact on reactions at the expansion bearings; and (5) consequent maximum bridge deflections. Table 1 and Table 2 present results of the redundancy analysis for all eight members under each of the four live load cases, based on member capacities and connection capacities, respectively.

**Table 1. Consequent Main Truss Member Failures due to a Critical Member Failure
(Based on Member Capacities)**

Number of Consequent Member Failures - Member Capacities					
Critical Member	Dynamic Impact	Load Case	Load Case	Load Case	Load Case
		1	2	3	4
L3-U4 (Diagonal)	w/o Dynamic Impact	0	0	0	0
	w/ Dynamic Impact	0	0	0	0
L1-L2 (Lower Chord)	w/o Dynamic Impact	0	0	0	0
	w/ Dynamic Impact	0	0	1	0
U0-U1 (Upper Chord)	w/o Dynamic Impact	2	2	2	2
	w/ Dynamic Impact	3	4	6	4
U4-U5 (Upper Chord)	w/o Dynamic Impact	0	0	0	0
	w/ Dynamic Impact	0	0	0	0
U4'-U3' (Upper Chord)	w/o Dynamic Impact	0	0	0	0
	w/ Dynamic Impact	0	0	0	0
L4-L5 (Lower Chord)	w/o Dynamic Impact	0	0	0	0
	w/ Dynamic Impact	0	0	0	0
L12-L13 (Lower Chord)	w/o Dynamic Impact	0	2	4	3
	w/ Dynamic Impact	2	3	7	5
L13-L14 (Lower Chord)	w/o Dynamic Impact	0	4	7	6
	w/ Dynamic Impact	6	7	10	7

**Table 2. Consequent Main Truss Member Failures due to a Critical Member Failure
(Based on Connection Capacities)**

Number of Consequent Member Failures - Connection Capacities					
Critical Member	Dynamic Impact	Load Case	Load Case	Load Case	Load Case
		1	2	3	4
L3-U4 (Diagonal)	w/o Dynamic Impact	0	0	0	0
	w/ Dynamic Impact	0	0	0	0
L1-L2 (Lower Chord)	w/o Dynamic Impact	0	0	0	0
	w/ Dynamic Impact	0	0	2	1
U0-U1 (Upper Chord)	w/o Dynamic Impact	2	2	3	2
	w/ Dynamic Impact	4	5	6	5
U4-U5 (Upper Chord)	w/o Dynamic Impact	0	0	0	0
	w/ Dynamic Impact	0	0	1	0
U4'-U3' (Upper Chord)	w/o Dynamic Impact	0	0	0	0
	w/ Dynamic Impact	0	0	0	0
L4-L5 (Lower Chord)	w/o Dynamic Impact	0	0	0	0
	w/ Dynamic Impact	0	0	0	0
L12-L13 (Lower Chord)	w/o Dynamic Impact	1	2	5	3
	w/ Dynamic Impact	3	5	9	6
L13-L14 (Lower Chord)	w/o Dynamic Impact	0	4	9	6
	w/ Dynamic Impact	6	7	11	7

BRIDGE 9340 STUDY

The tables summarize the number of additional main truss members that would fail as a result of the failure of the critical member both without and with the application of the dynamic impact factor. As shown in the tables, five of the eight critical members are fracture critical, i.e., their failure would result in the failure of at least one other main truss member and thus cause instability of the structural system. The five fracture critical main truss members are: Lower Chord L1-L2, Upper Chord U0-U1, Upper Chord U4-U5, Lower Chord L12-L13, and Lower Chord L13-L14. These five members actually represent twenty main truss members due to the nearly double symmetry of the trusses. Accounting for the connection capacities yields more total consequent main truss member failures, but Upper Chord U4-U5 is the only additional fracture critical member that would not be considered as such if the connection capacities were neglected.

Retrofit Concepts for Improving Structural Safety and Performance

For strengthening the eight critical truss members on one half of each truss, several retrofit alternatives have been investigated, including the use of Carbon Fiber Reinforced Polymer (CFRP) strips or sheets, pre-tensioned steel strands or CFRP bars, and high performance steel plating. The general objective of the retrofit is to replace the strength of a member in an event that the member should completely fail due to a fracture initiated from the concerned fatigue susceptible detail. The added benefit is that the retrofit would also reduce the live load stresses and thus retard or minimize the development of fatigue cracks in the repaired members.

The steel plating concept was considered most suitable for this application and is recommended. The retrofit involves installing steel plates on the exterior surfaces of both webs of the truss member, with high strength anchor bolts properly located beyond the fatigue susceptible details. The retrofit steel plates, and the bolted connections at both ends, were designed to take over all the member forces and replace the lost capacity in the case of a member fracture. To minimize the plate weight for field erection and installation, high performance steel of 100 ksi yield strength was used with two steel plates on each side of the truss member with each plate width equal to approximately one half of the member web depth. Preliminary plans have been developed for the thirty-two truss members on the bridge.

2
0
des. it
After if
it is
moved
- not?
looks
they
need
to off
plating.

Discussed 9/6/06 - Prefer to be 10 with deck on.

Another retrofit strategy is to alter the structural system by replacing the existing deck with a new deck that is continuous throughout the main truss spans and composite with the truss system. This structural alteration aims to reduce live load stresses in most members and improve structural redundancy. Combined with the steel plating member retrofit for selected critical members, the structural performance and redundancy of the redecked bridge is further improved.

Analyses results from the computer model indicate that replacing the existing deck with a continuous deck of the same thickness throughout the truss spans significantly reduces stresses in most truss members under both dead and live loads. The largest stress reductions typically occur in the members near the existing deck joint locations. Some truss members near the span contra-flexural areas experience minor stress increases due to a continuous deck under both the dead and live loads, but the consequence is not detrimental since those member forces are of low magnitudes. Under live load, further stress reduction can be achieved by using a thicker structural deck and by stiffening the connections between the floor truss and the main truss. The further stress reduction due to each of these two measures, however, is insignificant to the upper chords and nearly negligible to the lower chords and diagonals. Therefore, further enhancement of the deck-truss composite action by stiffening the connections between the main truss and floor truss top chord does not seem to be worthwhile.

The casting procedure of the new deck is critical to achieving the maximum benefit of stress reduction in truss members. Since the weight of wet concrete is carried by the steel system alone and any dead load applied after the deck concrete cures is carried more efficiently by the composite deck-truss system, the design and construction of the new deck should aim to minimize the thickness of the initial pour. For example, casting a continuous new deck with a 7" structural thickness plus a subsequently applied 2" overlay is more advantageous than a monolithically poured deck of 9" thickness. In addition, the use of light-weight concrete for the new deck should also be evaluated in the final design of deck replacement.

The impact of a continuous deck on the improvement of structural redundancy was also investigated using the 3-D computer model. The analyses indicated that replacing the existing

deck with a continuous deck of the same thickness improves the structural redundancy by reducing the number of consequent member failures after the failure of truss lower chord L13-L14, and the failure of truss upper chord U7-U8, respectively. However, the continuous deck would likely not eliminate the consequent failures of main truss members and thus would likely not change the fracture-critical nature of either member. The amount of longitudinal deck reinforcement above Piers 6 and 7 shall be carefully determined in the final design of deck replacement.

While the condition of the expansion bearings was assumed locked under live load, both “as-designed” and “locked” conditions were considered in the redecking dead load analysis for their uncertain and erratic nature. The analysis results indicated that the effect of bearing condition is complicated and can be significant on truss member forces. In the final design of deck replacement, both bearing conditions should be taken into consideration and the governing situation to be used in the design.

Conceptual Plan for Deck Replacement

A conceptual plan for deck replacement was studied to maintain a minimum of four lanes open to traffic during construction and to minimize traffic interruptions during necessary transportation and placement of construction materials and equipment. Based on the layout of existing bridge ramps, it is easier to replace the half deck width on the east side and then the other half on the west side, or vice versa, resulting in unbalanced loading about the bridge centerline during the deck replacement construction. It is also possible, although more difficult, to maintain traffic for the outer lanes and then the inner lanes, or vice versa, during the deck replacement to keep balanced dead loading to the trusses.

Since truss bridges have generally been designed with symmetrical dead load between the two trusses, the suitability of the structure, particularly the floor trusses, to the transversely unbalanced half-deck loading condition was investigated. Using the LRFD design load on the 3-D computer model, the analysis indicated that member forces in the main trusses and the floor trusses are no higher in the half-deck condition than the full-deck condition. Therefore, the

removal of half of the deck does not create a worse loading condition than what the existing structure is currently experiencing. However, it is likely that the original design of the floor trusses (members and connections) and other lateral bracing members did not consider the 3-D behavior of the truss system under transversely unbalanced half-deck loading. If the unbalanced half-deck procedure is to be considered, a more complete detailed analysis should be performed in the final design to evaluate the impact on all transverse members and their connections between the two main trusses.

Based on the total available space between the existing side curbs of the bridge, it was determined possible to allow the maintenance of four traffic lanes in each of the two half-deck construction stages while having the median area serving as a path for transporting concrete. Using the 3-D computer model, a map of deck longitudinal axial stress contours was provided over the entire truss bridge, which can be used as a basis to determine the sequence of deck concrete pouring for placing concrete in the compression areas first and tension areas last. The exact sequence will depend on the volume capacity for each pour as well as traffic maintenance details.

Recommendations

Based on results of our study, the following recommendations are made:

- (1) Five main truss members in one half of each truss, representing twenty members in the bridge, have been identified as fracture critical and should be retrofitted with the steel plating scheme developed, using high performance steel and high strength bolts. The retrofit, although not changing the fracture critical nature of the truss member, adds internal redundancy to the member and eliminates the possibility of a member fracture due to the fatigue of susceptible welded details at the internal diaphragms.
- (2) Before the retrofit takes place, the fatigue susceptible details at the internal diaphragms inside the identified fracture critical truss tension chords should be inspected with the access hole cover plates removed during the normal inspections. The toe of the

longitudinal fillet weld between the tab and the truss chord web is a primary location for the development of a fatigue crack.

- (3) A deck replacement with a new deck that is continuous throughout the main truss spans, and composite with the truss system, can significantly reduce live load stresses in most truss members and improve the redundancy of the truss system. To minimize dead load stresses, the replacement deck should be placed in two stages, with a structural deck of minimum required thickness, plus an overlay. Alternatively, the use of light-weight concrete for the new deck can also reduce dead load effects and should be evaluated in the final design of the deck replacement.
- (4) A preliminary analysis using the LRFD design load indicated that member forces in the main trusses and the floor trusses are no higher in a transversely unbalanced half-deck condition than the full-deck condition. However, since truss bridges have generally been designed with symmetrical dead load between the two trusses, it is more desirable to keep this symmetrical loading condition during deck replacement as much as possible. If the unbalanced half-deck procedure is to be considered, a more complete detailed analysis should be performed in the final design to evaluate the impact on all transverse members and their connections between the two main trusses.
- (5) Based on a map of the deck longitudinal axial stress contours provided, the sequence of deck concrete pouring can be determined for placing concrete in the compression areas first and tension areas last.

SECTION 1

1. INTRODUCTION

1.1 Bridge Structure Overview

Bridge 9340 carries Interstate 35W across the Mississippi River just east of downtown Minneapolis. Built in 1967, the structure is a three-span continuous deck truss with steel multi-girder and continuous concrete approach spans. The bridge carries eight lanes of traffic, four lanes in each direction, and has a total length of nearly 2,000-ft including the approach spans. The span configuration of the deck truss is approximately 266-ft, 456-ft, and 266-ft. Each side span also has an approximately 38-ft cantilever that supports the cross-girder of the adjacent approach span. The reinforced concrete deck has a total of seven transverse expansion joints in the truss spans: one at each end of the cantilevers, one at the center of each of the three spans, and one at each pier of the center span. Additionally, there is a longitudinal deck joint along the bridge centerline, under the median barriers.

Figure 1-1 shows the general plan and elevation of the bridge; and **Figure 1-2** depicts the framing plan of the deck truss, both extracted from the 1965 original plans of contract B. **Figure 1-3** shows an overview of the bridge looking north-west, and **Figure 1-4** is a view above the bridge deck looking north.

The steel superstructure contains a number of fatigue susceptible details in the main truss members and floor truss members. Most pronounced are the welded attachments at the diaphragms inside the box section of the main truss tension chords, as shown in **Figure 1-5** and **Figure 1-6**. In the main truss tension chords the original contract plan specified eight $3\frac{1}{2}$ " \times $\frac{3}{8}$ " \times $3\frac{1}{2}$ " steel bars welded to both the truss chord and the diaphragm and located along the perimeter of the diaphragm. According to current AASHTO fatigue provisions, the weld toe of fillet welded longitudinal attachments of lengths equal to or greater than 2" and less than 4" are Category D fatigue details. If poor workmanship or fabrication errors resulted in welds at some locations being 4" in length the details would be classified as a Category B fatigue detail.

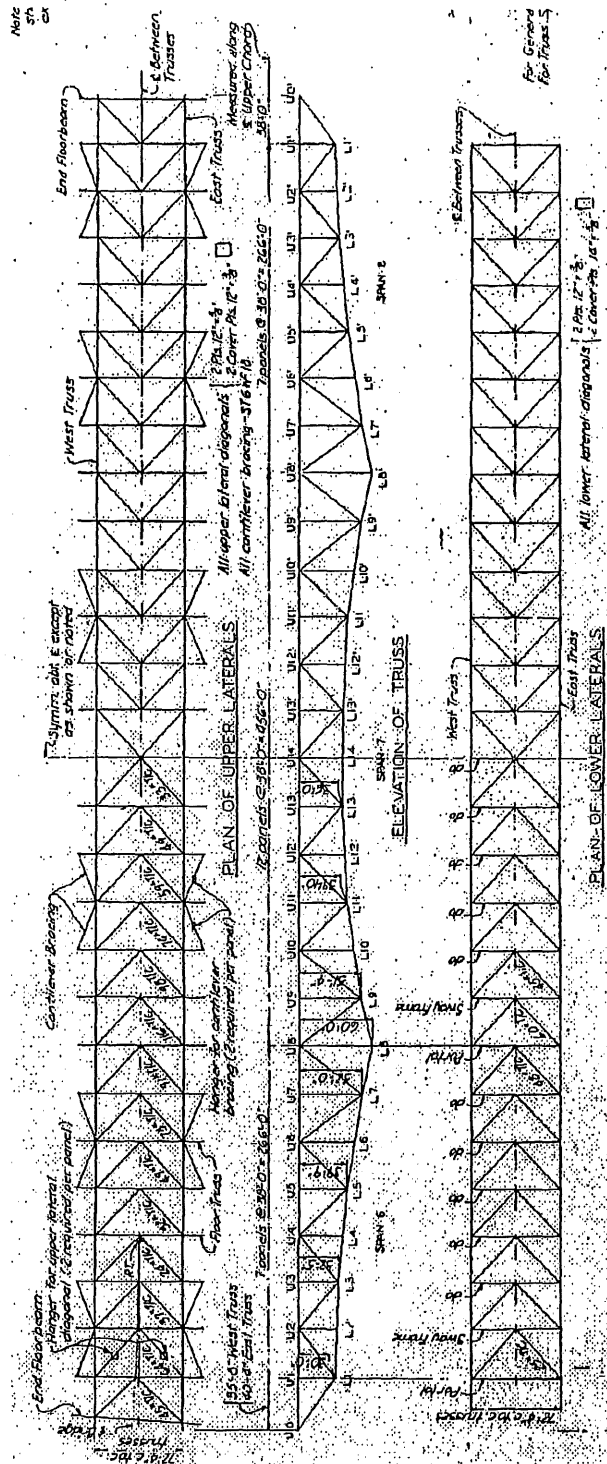


Figure 1-2. Deck Truss Framing Plan from Original Contract Plan



Figure 1-3. Bridge 9340 Overview Looking North-West



Figure 1-4. Bridge 9340 Deck View Looking North

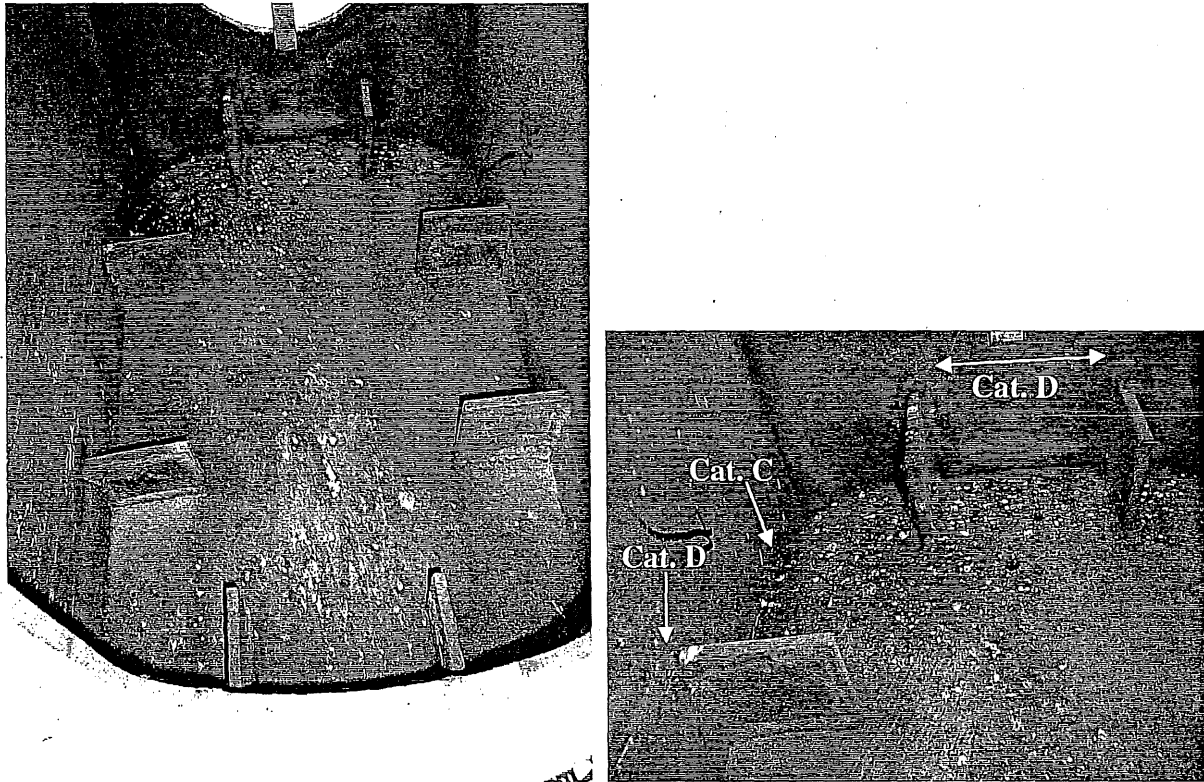


Figure 1-5. Fatigue Susceptible Details inside Main Truss Tension Chords

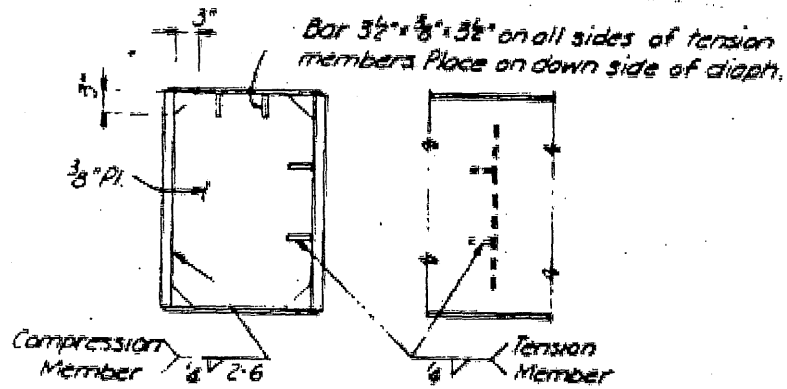


Figure 1-6. Welded Diaphragm Details in Main Truss Members from Original Contract Plan

Additionally, the floor truss members also have welded attachments of approximately 13" in length at the joint gusset plate, as shown in **Figure 1-7**. Such fillet welded longitudinal attachments of lengths equal to or greater than 4" are classified as Category E fatigue details at the weld toes according to current AASHTO fatigue provisions. It should be noted that the bridge was designed in accordance with the 1961 AASHTO *Standard Specifications for Highway Bridges*, which was based on a completely different fatigue design method that was revamped in the 1974 interim edition.

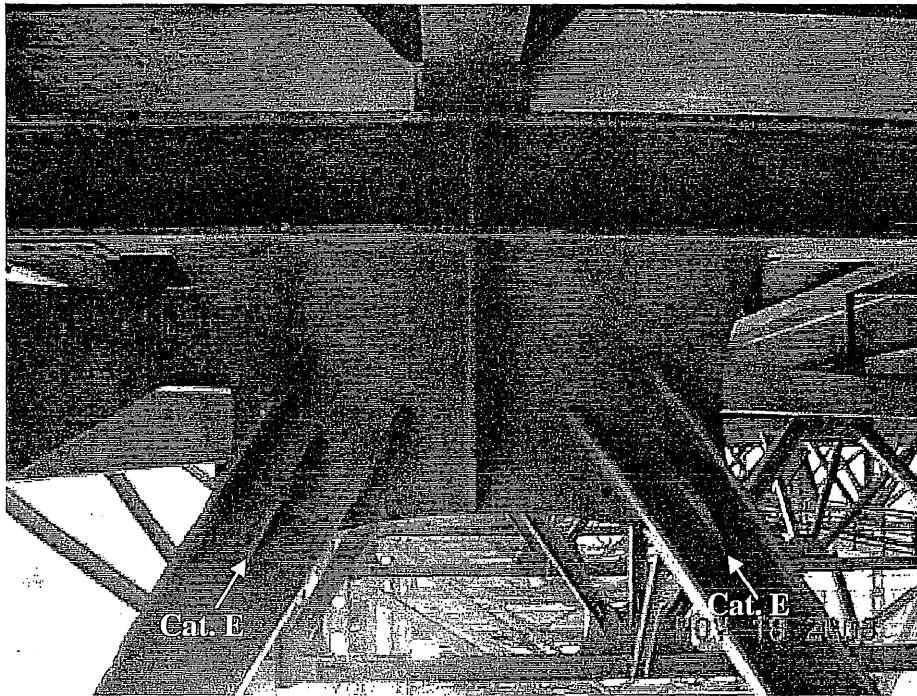


Figure 1-7. Fatigue Susceptible Details at Floor Truss Joints

The poor fatigue details on the truss spans, particularly those inside the main truss tension chords that are difficult to inspect, have raised concern on the consequence of a possible main truss member failure triggered by a fatigue crack.

The Office of Bridges and Structures of Minnesota Department of Transportation (Mn/DOT) issued a Request for Interest (RFI) in March 2003 for a comprehensive fatigue evaluation of Bridge 9340. URS Corporation was selected to undertake this study to evaluate the integrity of the truss-arch superstructure in light of fatigue and fracture characteristics. The results from this

study will be utilized by Mn/DOT as a reference for the development of future renovation work to be performed on the bridge.

1.2 Project Objectives and Work Scope

The primary objectives of the project include the following:

- A. Identify critical superstructure members that are most susceptible to cracking.
- B. Evaluate structural consequences if one of the critical members should sever, in terms of load redistribution and load carrying capacities of remaining members.
- C. Develop contingency repairs to selected fracture critical members
- D. Develop measures for improving structural redundancy and minimizing tensile stresses in the trusses.
- E. Establish a preferred deck replacement staging plan.

The scope of key work tasks is summarized as follows:

- (1) Evaluate performance of expansion bearings and joints through visually monitoring and recording of movements of specifically made marks at different temperatures.
- (2) Develop a 3-dimensional computer model that can reasonably predict truss member forces for dead, live and temperature loads.
- (3) Fatigue evaluation of critical fatigue details on truss members.
- (4) Identification of fracture critical members through evaluation of structural consequences for the loss of a tension member.
- (5) Prepare plans for contingency repairs of eight most critical members.
- (6) Develop schemes of altering bridge floor system for improving structural redundancy and minimizing tensile stresses in truss members.
- (7) Develop a sequence of deck removal, structural changes and deck replacement for structural improvement.

1.3 General Approach and Work Procedure

The URS approach and procedure for completing the work tasks to achieve the project objectives are described in the following:

- (1) Data Collection and Tabulation. Bridge plans, shop drawings, University of Minnesota fatigue evaluation report that includes field strain measurement results, as well as actual bridge traffic data, have been collected.
- (2) Bridge Condition Inspection and Bearing Movement Measurement. Two condition inspections of the bridge and its fatigue details were performed in July and November of 2003, and bearing movements were monitored at a few different temperatures from June 2003 to July 2004.
- (3) Development of a Computer Model for Truss Spans. A 3-D finite element model was developed that includes all the structural components of the truss spans: deck, stringers, floor beams, floor trusses, main trusses, as well as all bracing members. The piers and the stiffness of the approach spans were also included to study the effects of frozen bearings.
- (4) Calibration of Computer Model with Bridge Load Test Results. The model was used to predict member stresses under the test trucks used by University of Minnesota and compared with their measurement results. Certain adjustments were made to the support conditions and connection properties of the model to obtain better agreement with the test results.
- (5) Maximum Member Forces and Strength Ratings. The calibrated computer model was used to calculate member forces under the dead load and maximum member forces under the design live load. Load ratings were also calculated using the AASHTO Allowable Stress and Load Factor rating methods.
- (6) Fatigue Evaluation of Truss Members. Stress ranges due to the AASHTO fatigue load were calculated using the computer model. Fatigue life of truss members was evaluated per AASHTO fatigue provisions using the calculated stress ranges and in reference to University of Minnesota's field strain measurement.
- (7) Redundancy Analysis of Eight Fracture Critical Members. Based on stress results from the calibrated computer model, eight tension members were identified that are most susceptible to fatigue-induced fracture. A structural redundancy analysis, which

evaluated structural consequences for the sudden failure of a member, was performed for each of the eight truss members. The effects of load redistribution were calculated and load carrying capacities of the remaining members were evaluated. These eight members actually represent thirty-two main truss members due to the nearly double symmetry of the trusses, and they cover all types of truss members.

- (8) Contingency Repair Plans for Fracture Critical Members. Based on a study of different alternatives, contingency member repairs were designed and conceptual plans prepared for selected fracture critical members based on the redundancy analysis.
- (9) Retrofit Concepts for Improving Structural Redundancy and Performance. The computer model was used to study different retrofit schemes to improve the overall structural redundancy of the trusses and to reduce tension member stresses.
- (10) Conceptual Plans for Preferred Deck Replacement Sequence. Conceptual plans have been developed for a preferred sequence of deck removal, structural changes and new deck concrete placement.

The following sections of the report explain details of each work task, discuss results of the analyses, and present conceptual plans for contingency member repairs and deck placement sequence for structural improvement.

SECTION 2

2. BRIDGE INSPECTION AND DATA COLLECTION

2.1 Overview

Data on Bridge 9340 was collected from several different sources. These sources included the Minnesota Department of Transportation (Mn/DOT), University of Minnesota and five field inspections by URS at the bridge site.

Mn/DOT provided data such as contract drawings, boring data, shop drawings of the superstructure, fabrication records, material property records, previous inspection reports, traffic volume and weight data, as well as reports prepared by the University of Minnesota regarding fatigue evaluation of the bridge. Also provided was a copy of "Fracture Critical Bridge Inspection In-Depth Report" dated May 2002, prepared by the Mn/DOT Metro District, Maintenance Operations, Bridge Inspection Department, based on an inspection of the bridge for the Office of Bridges and Structures.

Data was also collected by URS during five field investigations including bearing and joint displacements/movements at different temperatures, and general condition of the truss and fatigue prone details. Additionally URS used the traffic monitoring system of Mn/DOT Regional Transportation Management Center (RTMC) and the City of Minneapolis to collect traffic data. One hundred sixty-eight hours of video were reviewed by URS staff to determine the number of heavy vehicles in each direction at the bridge site.

2.2 Bridge Field Inspection

2.2.1 Inspection Overview

URS made a total of five field investigations at the bridge site. The initial visit was made in June 2003 with subsequent visits in November 2003, January 2004, March 2004 and July 2004.

During the first two visits, members of URS staff participated with Mn/DOT inspection personnel in Mn/DOT's annual inspection in a snoopier to assess the condition of key superstructure components.

The purpose of URS participation with Mn/DOT in their field inspection was to observe the condition of identified fatigue susceptible details on the truss and the overall condition of the truss members, floor beams, truss bearings, truss connections, miscellaneous connections and bracing members. URS marked the bearing position for all truss bearings and recorded the temperature so that bearing movements could be ascertained later. URS also documented the condition of key members and created a photo log of the inspection photographs to document the general condition of the truss. Finally URS commented on the inspection effort of the fatigue susceptible details within the truss tension chords, advising that a more comprehensive inspection of the welded details along the diaphragms inside the box sections should be made in future inspections.

2.2.2 Condition of Truss Members

The overall condition of the truss members was found to be relatively good from a corrosion standpoint. Minimal surface rusting was found on the exterior of the truss members. Corrosion on the truss members and connections was generally concentrated near the deck joints, leading to the conclusion that leakage from the bridge deck is the primary contributing factor. There was also corrosion found at the welded tab attachments of the internal diaphragms inside the welded box section of some truss members.

2.2.3 Condition of Bearings

The truss spans have a fixed bearing at Pier 7 and three roller bearings at Piers 5, 6 and 8, respectively. While the conditions of the bearings at Piers 6 and 7 were relatively poor since they both are under deck expansion joints (**Figure 2-1**), the bearings at Piers 5 and 8 appear to be in good physical condition (**Figure 2-2**). At Pier 6, there was significant surface corrosion, debris

and dirt packed into various areas of the bearing. All the roller bearings seem to have thick coatings of paint and did not appear to be functioning as intended under the live load.

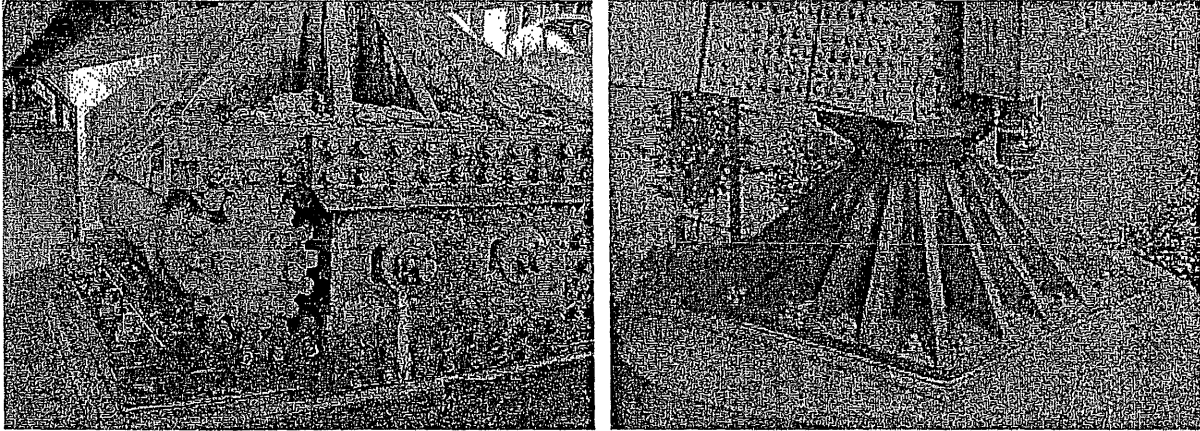


Figure 2-1. Roller Bearing at Pier 6 (Left) and Fixed Bearing at Pier 7 (Right)

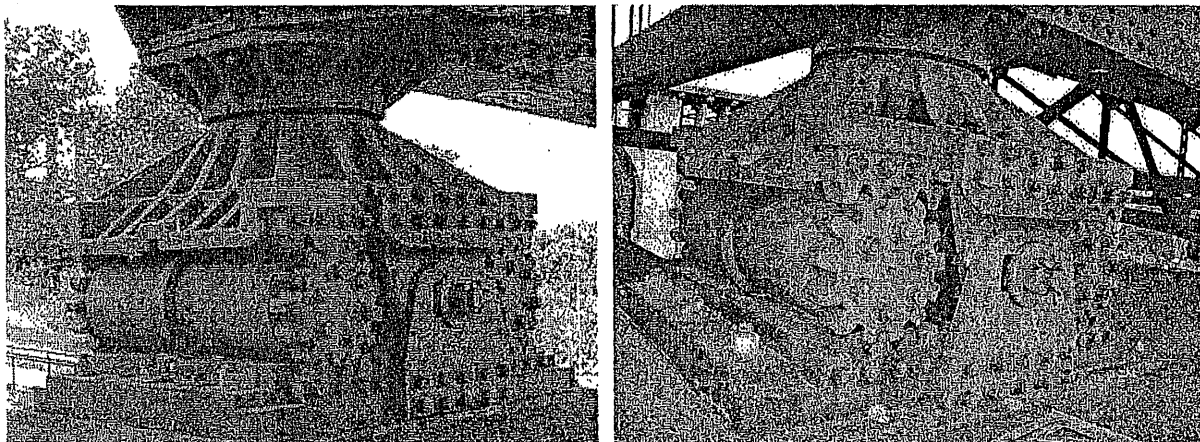


Figure 2-2. Roller Bearings at Pier 5 (Left) and Pier 8 (Right)

For the rocker bearings of the approach span at each approach span cross girder supported by the trusses at panel point U0 and U0', the access to observe the bearing condition was difficult due to the construction details. The bearings were built in the "pockets" in the cross girders with little clearance to either side. Some debris was noted in some bearing pockets and it was very difficult to visually determine if the bearings were functioning. **Figure 2-3** shows the rocker bearings at both the north and south ends of the west truss, each of which was viewed from the approach span side.

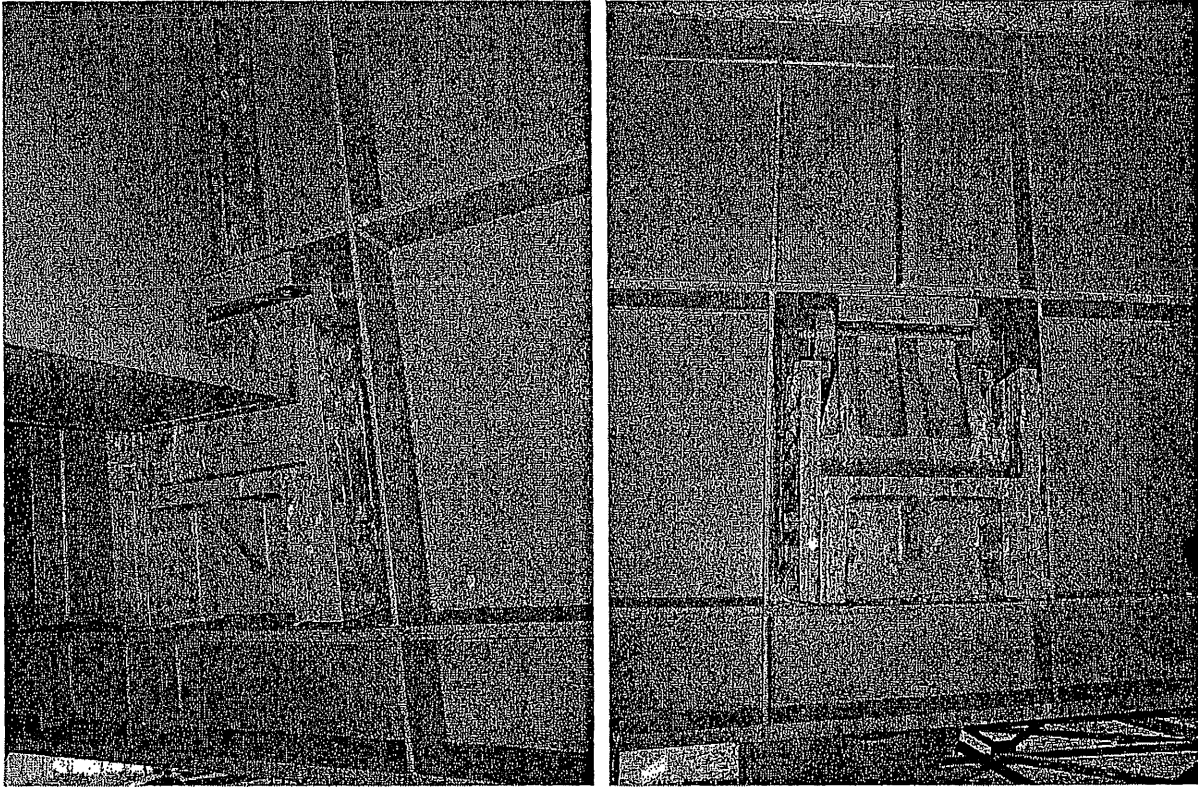


Figure 2-3. Rocker Bearings at North End (Left) and South End (Right) of West Truss

2.2.4 Condition of Deck Expansion Joints

The condition of the deck joints was found to be good except for a few bent fingers in the finger joints. However, the condition of the waterproofing was hard to determine. There was evidence that the deck joints had leaked or were currently leaking as indicated by the concentrated rusting of superstructure steel members at or near the deck joints.

2.2.5 Bearing and Joint Marking

URS marked truss span bearings and joints by scribing and use of permanent marker to determine if the bearings and joints were moving with temperature changes. All of the truss roller bearings, rocker bearings and truss end deck expansion joints were marked to document their positions and the temperature was recorded at each inspection. Figure 2-4 shows the

markings on a truss roller bearing. Scribed marks on the rocker bearing are visible in the left photo in **Figure 2-3**.

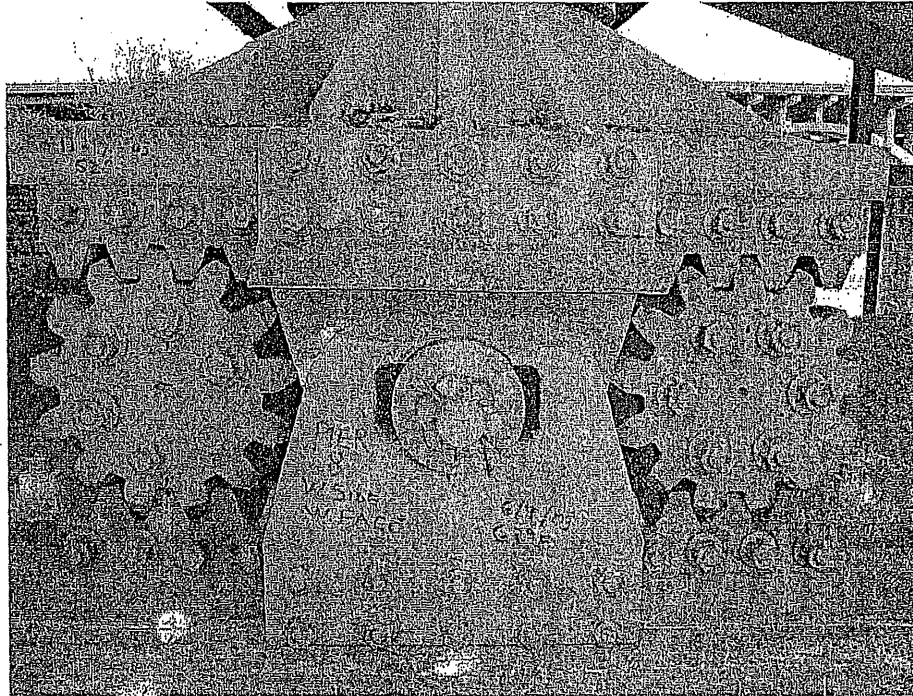


Figure 2-4. Markings on West Roller Bearing at Pier 8 for Movement Measurement

2.2.6 Inspection of Fatigue Susceptible Details inside Truss Chords

The most critical fatigue susceptible details on Bridge 9340 are the welded tabs along the diaphragms inside the box section of tension truss chords, as depicted in **Figures 1-4** and **1-5**. The inspection of these details, therefore, is one of the most important field efforts.

The access holes in the truss members are currently covered to keep birds out of the truss members and the fatigue details are not readily accessible without removal of the covers. During the first two URS inspections, the cover plate was removed at selected locations for observing the fatigue prone details inside the truss chord. It was noticed that some access holes are not located directly adjacent to the diaphragm locations and visual inspection of the fatigue details have to be made from a distance. Minor amounts of corrosion were found to be present within some truss members with corrosion being concentrated at the welded tab connections and at the

diaphragms themselves. There was also an accumulation of debris/dirt around the perimeter of some diaphragms.

Since the fatigue susceptible details exist on truss tension chords which by definition are fracture critical members, we recommend that these details be inspected at a minimum interval of one-year until retrofitted. Removing the cover plate adjacent to each of the diaphragm locations is necessary to facilitate the inspection of these details. The toe of the longitudinal fillet weld between the tab and the plate of truss chord is one of the primary locations that one would expect a critical fatigue crack to develop in the truss member.

2.2.7 Summary

The overall condition of the truss members and connections was, from a corrosion standpoint, found to be good. Corrosion was found in localized areas, generally concentrated near the deck joints. Minor corrosion, or rusting, inside the truss members was observed at some diaphragm locations away from the deck joints, likely due to water from the manholes trapped by the diaphragms.

All of the truss bearings were marked for their positions at the first inspection and temperature and movement readings were recorded in subsequent inspections to determine the movement-temperature relationships. The bearings did not appear to be moving under the live load due to surface friction, thick paint, rust, and debris build-up. The bearing movement-temperature relationships are discussed in more detail later in this section.

The fatigue susceptible details at the welded tabs along the interior diaphragms of the tension truss chords are difficult to inspect. The access openings are covered and observations can only be made after the cover is removed. It is our understanding that the cover plates are not removed as part of Mn/DOT's regular inspection. Due to the cracking potential of these details on the fracture critical truss members, we recommend that Mn/DOT inspect all of these details during the normal inspections. It is also recommended that scope equipment be procured to enable close

visual inspection of these details. This critical inspection should be done on an annual basis until such time as the structure can be retrofitted.

2.3 Review of Previous Inspection Reports

Previous inspection reports for bridge 9340 were obtained from Mn/DOT. The inspection reports were reviewed for specific information that would affect the fatigue and fracture evaluation of the truss spans.

2.3.1 Cracks in the Steel or Welds

The reports were reviewed for locations of cracks in the steel or welds in the deck truss spans, including the truss chords, floor trusses and the connections. Locations of the cracks, date of initial discovery and any subsequent monitoring were noted. Cracks were noted during the June 2003 inspection. There was a crack noted in the tack weld inside of the box on member U21-U22 (U7'-U6') approximately 2 feet north of joint U21 (U7'). There was another crack noted at joint U14 at the upper lateral stringer connection starting at a tack weld. The photos showing these cracks were noted in the inspection report for the June 2003 inspection.

2.3.2 Deck Slab Expansion Joints

The inspection reports were also reviewed for problems at the deck slab expansion joints. Finger joints were used at both the north end (near Pier 5) and the south end (near Pier 8) of the truss spans, respectively. In addition, transverse strip seal deck expansion joints exist at Panel Point 4 (near middle of the south span), Panel Point 8 (at Pier 6), Panel Point 14 (at middle of the center span), Panel Point 8' (at Pier 7) and Panel Point 4' (near middle of the north span). These joints were initially open joints sealed with elastic joint sealer but were replaced with strip seals during the 1977 joint repair. Finally, there is also a longitudinal deck joint along the centerline of the bridge under the median barrier. The longitudinal deck joint is an open gap running the entire length of the truss spans. It is not easily accessible due to the presence of the precast median cap on the top of the deck and the use of stay-in-place forms on the underside of the deck. No significant problems were noted at these locations in the inspection reports.

2.3.3 Stringer Expansion Seats

The reports were reviewed for performance of the stringer expansion seats. Sheet 22 of the original Contract B plans shows the layout of the expansion seats across the structure. The expansion seat consists of a bronze plate with or without hold down bars, as shown on sheet 23 of the contract plans. The performance of these expansion seats directly affects the composite behavior of the truss-floor-deck system. These joints do not appear to be functioning as designed and some cracking is noted at tack weld attachments and there are also notations of loose or missing bolts.

2.3.4 Structural Changes

The inspection reports and remodel plans were reviewed for changes made to the structural system from the original plans. Changes such as the addition or removal of members or plates, changes to the structural connections, changes to the stringer expansion bearings, modifications to the deck expansion joints or replacement of rivets with bolts were noted.

In 1986 braces were installed between the end floor beam and beams #2 & #3 on the approach spans to reinforce the area damaged as the result of the frozen southeast rocker bearing. The southeast rocker bearing hinge was also replaced in 1986. In 1992 braces were installed between the end floor beam and the approach span beams near the northeast rocker bearing to reinforce the area damaged by a frozen rocker bearing.

On the approach spans, there are numerous locations where cracks have been drilled out and/or repaired with bolted plates. Cracking in the vertical web stiffeners on the cross beam at the southeast rocker bearing (resulting from the 1986 southeast rocker bearing failure) were welded and the crack ends drilled out. There were missing or loose bolts noted at the stringer to floor beam connections.

BRIDGE 9340 STUDY

In 1998 the split median Jersey barrier was installed and bridge railings were reconstructed. The bridge railings were retrofitted by the addition of a 32" high concrete face and removal of the horizontal steel railings.

2.3.5 Corrosion and Section Loss

The inspection reports and the Fracture Critical Bridge Inspection In-Depth Report were reviewed for notations of significant corrosion and section loss for the members and connections throughout the deck truss spans. **Table 2-1** includes pertinent sections extracted from the Mn/DOT's June 2004 inspection report.

In general, the approach spans had many notations regarding fatigue cracks and repairs in the inspection reports. There was also section loss and moderate surface pitting noted at the ends of the beams. The interiors of the truss members were noted as having section loss, flaking and surface rust, and pigeon debris. The floor beams and sway frame brace connections were noted for having pack rust, some section loss and surface pitting. There was a Pontis Inspection general smart flag noting section loss, pitting, flaking and surface rust on the steel.

2.3.6 Condition of Bearings

The inspection reports and the Fracture Critical Bridge Inspection In-Depth Report were reviewed for notations of corrosion or deterioration of the bearing devices. The bearings on the bridge consist of rocker and roller bearings. **Table 2-1** includes pertinent sections extracted from the Mn/DOT's June 2004 inspection report.

In general the bridge bearings were noted to be in poor condition. The bearings did not appear to be functioning uniformly as designed. Some of the abutment bearings were corroded as a result of leaking joints. The south abutment bearings were in full contraction. The hinge bearings at span 2 were all locked in full expansion with the ends of the beams in contact. There were notations of previous bearing failures at the rocker bearings at each end of the main spans. There was also section loss with flaking and surface rust at the rocker bearings at the open finger joints.

BRIDGE 9340 STUDY



The main truss roller bearings were noted as having section loss, flaking and surface rust with moderate corrosion.

Table 2-1: Portions of June 2004 Mn/DOT Bridge Inspection Report

Mn/DOT BRIDGE INSPECTION REPORT 06-16-2004		
Elem. No.	Element Name	Notes
131	PAINT STL DECK TRUSS	Main truss members have numerous poor weld details (some cracked tack welds). [1995] Interiors of truss members have section loss, flaking & surface rust, severe pigeon debris, at the floorbeam & sway frame brace connections (with pack rust & surface pitting). [1999] Pigeons screens placed on truss member openings.
152	PAINT STL FLOOR BEAM	[1986] Crossbeam web stiffeners cracked at SE rocker hinge (rocker bearing had frozen). Cracks were welded/drilled out, and bracing was added (attached to approach span beams). [1992/98] Several cracks found in crossbeam & end floorbeam at the NE rocker hinge. Some cracks were drilled out, and bracing was added (attached to approach span beams). [1998/99] End floorbeams & "crossbeams re-painted. The face exposed to the open finger joints have extensive section loss (surface pitting & holes in stiffeners). Floorbeam trusses have numerous poor weld details, section loss, flaking & surface rust, some have holes, (plug welds & tack welds in tension zones). [1994] Floorbeam trusses have chalking throughout. [1999] Median portions of floorbeam trusses (and sway braces) re-painted. [2004] Crack found in cope north approach crossbeam at beam G1C bottom flange 2 1/2" east side, 2" west side.
373	STEEL HINGE	[1986] SE crossbeam rocker hinge pin replaced. Section loss at hinges, (open finger joint) steel has flaking & surface rust. [1999] Crossbeam rocker hinge bearings re-painted (all show evidence of recent movement). [1995] Span 2: all hinge bearings are locked in full expansion (beam ends contacting). [1999] Span 2 hinge bearings re-painted.
311	MOVEABLE BEARING	[94/2000] Some abutment bearings are rusty (joints leaking). [1996] South abutment bearings are in full contraction. [1994] Main truss roller bearings have section loss, flaking & surface rust, moderate corrosion.
356	STEEL FATIGUE SMFLAG	[98/2000] Numerous fatigue cracks found in approach spans. Cracks were located at negative moment diaphragm connections where the stiffener was not welded to the top flange. In span 9, the 3rd beam from the east had a 4 FT long crack in the web (it was reinforced with bolted plates). Most existing cracks were drilled out, and the diaphragm connections were lowered to reduce stress levels. [2004] Crack found in cope north approach crossbeam at beam G1C bottom flange 2 1/2" east side, 2" west side.
357	PACK RUST SMART FLAG	[1995] Truss members have flaking & surface rust corrosion at the floorbeam & sway brace connections (with pack rust & some section loss, surface pitting).
363	SECTION LOSS SMFLAG	Section loss: pitting, flaking & surface rust on steel.

2.4 Review of Shop Drawings

Mn/DOT provided the original shop drawings. The originals were returned to Mn/DOT after copies were made by URS. Upon review of the shop drawings, it was determined that several

rolls of the existing shop drawings were missing. Mn/DOT was unable to find the missing shop drawings as noted below and described in the Mn/DOT shop drawing key:

- ?-36 (Assumed to be roll R-36, the key is not legible): This roll was listed between Q-60 and R-37. Based on the sheet index on sheet GN1 of M-36, the sheets included in this missing roll would be 1110-1113, 1201-1208, and 1301-1304.
- P-37: This roll was listed on page 2 of the key and was labeled as missing. The sheets included in this missing roll should be 1611-1614, 1701-1705 and 1901-1905.
- X-36: This is listed on the third page of the key and is labeled missing. The missing roll contains sheets 22-46 covering the South Approach Spans, and was not necessary for this investigation.
- J-60: This is listed on the fourth page of the key. The missing roll contains sheets 1-18 covering the drainage systems, and was not necessary for this investigation.

There were no shop drawings available for two of the most critical members: L13-L14 and U4'-U3'. Dimensions for design considerations were estimated from similar members and from the contract plan drawings. Additionally, no shop drawings were available for the following main truss and floor truss members:

- Main Truss Upper Chords: U12-U13, U13-U14, U14-U13', U13'-U12', U6'-U5', U5'-U4', and U3'-U2'
- Main Truss Lower Chords: L13-L13', L7'-L6', and L6'-L5'
- Main Truss Diagonals: L3'-U2'
- Floor trusses: FT12, FT13, FT14, FT15 (PP 13'), FT16 (PP 12'), FT18 (PP10'), FT19 (9'), FT23 (PP 5'), and FT24 (PP 4')

Shop drawings were used to verify contract plan dimensions, details and plate sizes and to verify the camber/blocking as shown on the original plans. Discrepancies in the truss camber were discovered between the contract plans and the shop drawings, but were found to be due to adjustments from the leveled geometry to the final profile geometry. The contract plan camber/blocking data was utilized for the main truss member analysis since it was determined that this camber data was essentially the same as that on the shop drawings once the geometry

adjustments were accounted for. The floor truss camber details were consistent between the contract plans and the available shop drawings. For the main truss members and the floor truss members without available shop drawings, the camber values were assumed to correlate with the contract plan values based on the available shop drawings for other members.

Discrepancies were also noted between the truss member plate sizes as listed on the "Table of Truss Members and Stresses" on sheet 20 of the Contract B plans, the Truss Details on sheets 28 through 31 of the contract plans, and the shop drawings. The sizes as listed on the shop drawings were used in the analysis of the truss members. The differences were as noted below:

- Lower Chords L7-L8, L8-L9, L9'-L8', and L8'-L7': The center web thickness is listed as 0.9375" (sheet 20 of the plans), 0.875" (sheet 30 of the plans) and 0.875" (L7-L8 Roll N-36, L8-L9 and L9'-L8' Roll O-36, and L8'-L7' Roll Q-60 of the shop drawings)
- Diagonal U2-U3: The center web thickness is listed as 0.375" (sheet 20 of the plans), 0.625" (sheet 28 of the plans), and 0.625" (Roll Q-36 of the shop drawings). Note that the effective gross area listed on sheet 20 and 28 is the same and calculated based on a 0.375" center web thickness, the shop drawings match the 0.625" value.

2.5 Measurement of Bearing Movement

URS made marks for the initial positions of the truss bearings in the first field visit in June 2003 and recorded the movements of the marks in the four subsequent field visits in November 2003, January 2004, March 2004, and July 2004, respectively. However, movements of the truss bearings on Piers 6 and 8 were not measured in the last three visits since no snooper was used. Only the locations that were accessible were measured for bearing displacements. This data was recorded and compared with the previous data and the theoretical displacements based on ideal expansion bearings, as summarized in **Table 2-2**.

A review of the bearing measurement data indicates a large and erratic discrepancy between the measured and theoretical bearing movements for temperature changes. It appears that each bearing behaves in its own way in terms of overcoming the friction for longitudinal movement:

BRIDGE 9340 STUDY

No clear patterns are visible for the bearings on each pier or along each truss. Based on the available measurements, the following observations can be made:

- No truss roller bearings appear to move under the live load.
- Most bearings move with the temperature change, although to varying degrees. However, the amounts of thermal movements are significantly different than the theoretical movements of ideal expansion bearings.
- Under temperature changes the roller bearings at Pier 5, which appear to be clean and in good physical condition, move significantly more than those at Pier 6, which are under a deck expansion joint and have significant surface corrosion and debris build-up.

Table 2-2: Bridge 9340 Bearing Movement Measurements

Bridge 9340 Bearing Movement Measurements

Notes: (1) Bearing movement ΔL and temperature change ΔT are recorded as the increment from the previous measurement.
 (2) Bearing movement ΔL is positive when moving away from the fixed bearing at Pier 7 and negative when moving towards it.
 (3) $(\Delta L)_{theor} = (\Delta T)(L)(0.0000085)$, where L is the distance to fixed bearing at Pier 7.
 (4) Longitudinal locations of the rocker bearings and the expansion dam to the approach span are assumed to be the same at each end of the bridge.
 (5) "-" = "not measured"

East Truss

Bearings		Distance To Pier 7		Initial mark June 03	1st measurement - November 03				2nd measurement - January 04				3rd measurement - March 04				4th measurement - July 04				
Location	Type	L (ft)	L (in)	Temp. (F)	T (F)	ΔT (F)	$(\Delta L)_{meas}$	$(\Delta L)_{theor}$	T (F)	ΔT (F)	$(\Delta L)_{meas}$	$(\Delta L)_{theor}$	T (F)	ΔT (F)	$(\Delta L)_{meas}$	$(\Delta L)_{theor}$	T (F)	ΔT (F)	$(\Delta L)_{meas}$	$(\Delta L)_{theor}$	
S Appr.	Exp. dam	762.00	9144.00	62	46	-16	-0.6875	-0.9510	-	-	-	-	-	-	-	-	-	-	-	-	-
S Appr.	Rocker	762.00	9144.00	67	45	-22	-0.7500	-1.3076	1	-44	-2.9200	-2.6152	28	27	1.9625	1.6048	70	42	2.1875	2.4963	
Pier 5	Roller	721.67	8660.00	66	45	-21	-0.5625	-1.1821	1	-44	-0.8750	-2.4768	28	27	1.0625	1.5198	71	43	0.5000	2.4205	
Pier 6	Roller	456.00	5472.00	67	45	-22	-0.0938	-0.7826	-	-	-	-	-	-	-	-	-	-	-	-	-
Pier 7	Fixed	0.00	0.00	67	45	-22	-0.0938	-0.7826	-	-	-	-	-	-	-	-	-	-	-	-	-
Pier 8	Roller	265.90	3190.75	68	50	-18	-0.0938	-0.3733	-	-	-	-	-	-	-	-	-	-	-	-	-
N Appr.	Rocker	303.90	3646.75	68	50	-18	-0.7500	-0.4267	-	-	-	-	34	-16	-1.3600	-0.3793	69	35	1.7500	0.8296	
N Appr.	Exp. dam	303.90	3646.75	66	50	-16	-0.3750	-0.3793	-	-	-	-	-	-	-	-	-	-	-	-	-

West Truss

Bearings		Distance To Pier 7		Initial mark June 03	1st measurement - November 03				2nd measurement - January 04				3rd measurement - March 04				4th measurement - July 04				
Location	Type	L (ft)	L (in)	Temp. (F)	T (F)	ΔT (F)	$(\Delta L)_{meas}$	$(\Delta L)_{theor}$	T (F)	ΔT (F)	$(\Delta L)_{meas}$	$(\Delta L)_{theor}$	T (F)	ΔT (F)	$(\Delta L)_{meas}$	$(\Delta L)_{theor}$	T (F)	ΔT (F)	$(\Delta L)_{meas}$	$(\Delta L)_{theor}$	
S Appr.	Exp. dam	757.33	9088.00	66	54	-12	-0.5000	-0.7089	4	-50	-2.5625	-2.9536	-	-	-	-	-	-	-	-	-
S Appr.	Rocker	757.33	9088.00	-	63	-	-	-	1	-52	-2.2500	-3.0717	28	27	1.8750	1.5949	70	42	2.1250	2.4810	
Pier 5	Roller	721.67	8660.00	68	54	-14	-0.5000	-0.7881	1	-53	-0.8750	-2.9834	28	27	1.0000	1.5198	71	43	0.8750	2.4205	
Pier 6	Roller	456.00	5472.00	68	54	-14	0.0000	-0.4980	-	-	-	-	-	-	-	-	-	-	-	-	-
Pier 7	Fixed	0.00	0.00	68	54	-14	0.0000	-0.4980	-	-	-	-	-	-	-	-	-	-	-	-	-
Pier 8	Roller	265.90	3190.75	63	52	-11	0.0000	-0.2281	-	-	-	-	-	-	-	-	-	-	-	-	-
N Appr.	Rocker	303.90	3646.75	-	54	-	-	-	-	-	-	-	34	-20	-0.3750	-0.4741	69	35	1.3750	0.8296	
N Appr.	Exp. dam	303.90	3646.75	70	52	-18	-1.2500	-0.4267	4	-48	-3.3750	-1.1378	-	-	-	-	-	-	-	-	-

As a summary, the bearing measurement data indicates that the bridge expansion bearings are not functioning as designed. There have been notations in previous bridge inspection reports referring to "frozen" rocker bearings and corrosion and section loss at the truss roller bearings. The erratic nature of the bearing measurements can be explained by the bearings components "sticking" in place. There is enough frictional resistance due to corrosion and debris to keep the

bearing from moving until there is enough thermal force built up in the system to cause a drastic and quick movement of the bearing to relieve the force. The bearings are not allowing the structure to move linearly with changes in the ambient temperature.

2.6 Collection of Traffic Data

An estimate of the total traffic and heavy trucks at the bridge site was made by using the loop detector records, manually counting vehicles from the actual traffic video recordings, and projections for future growth, all based on data from Mn/DOT.

2.6.1 Total Traffic Volume from Loop Detector Data

Mn/DOT maintains permanent loop detector stations on the Trunk Highway system in the Twin Cities metropolitan area. The detectors record hourly traffic volumes and speeds, and are saved by Mn/DOT. The loop detector station data was used to determine the total traffic volume on Bridge 9340 for the same time period for which the heavy vehicle volumes had been collected. The detector stations used were located on I-35W at University Avenue (between the entrance and exit ramps of the diamond interchange). To obtain the total traffic volume crossing the Mississippi River, the volume from detectors on the northbound University Avenue exit ramp and the southbound University Avenue entrance ramp were added to the northbound and southbound mainline volumes, respectively. Table 2-3 summarizes the total daily traffic on Bridge 9340 over the Mississippi River for both the northbound and southbound directions. The average weekday traffic was 78,500 vehicles northbound and 80,310 vehicles southbound, or 158,810 total vehicles. The overall peak hour was found to be 4:00-5:00 PM, with an average northbound volume of 6,330 vehicles and an average southbound volume of 4,980 vehicles, or 11,310 total vehicles in the peak hour. The heavy vehicle peak hour was found to be 10:00-11:00 AM weekdays with average volumes of 350 heavy vehicles per hour in each direction.

The traffic volumes obtained from the loop detector stations were validated using manual counts of all vehicles from the video recordings for two time periods. Manual counts of the total traffic volume were completed for the 8:00-9:00 AM time period of the September 27 and September

BRIDGE 9340 STUDY



28, 2004 video files. Table 2-4 shows the traffic volumes obtained from the Mn/DOT detector stations and the URS manual counts. The percentage of the manually counted heavy vehicles in relation to the counted traffic volume and the loop detector determined traffic volume is shown in the table. The percentage of heavy vehicles for the loop detector traffic are based on the assumption that the heavy vehicle percentage is the same as that determined by actual counts.

Table 2-3: I-35W Bridge 9340 Total Traffic Volume from Loop Detectors

Time Period	Directional Volume		Total Traffic Volume
	NB	SB	
9/23/04 (Thursday)*	NB	43,030	79,430
	SB	36,400	
9/24/04 (Friday)	NB	84,120	168,080
	SB	83,960	
9/25/04 (Saturday)	NB	66,410	135,090
	SB	68,680	
9/26/04 (Sunday)	NB	55,990	115,640
	SB	59,650	
9/27/04 (Monday)	NB	74,150	151,130
	SB	76,980	
9/28/04 (Tuesday)	NB	77,120	156,920
	SB	79,800	
9/28/04 (Wednesday)	NB	77,960	157,180
	SB	79,220	
9/30/04 (Thursday)*	NB	36,120	81,270
	SB	45,150	

* Data was collected for a partial day only.

Data Source: Regional Traffic Management Center Loop Detector Stations

Table 2-4: Validation of Loop Detector Volume Data by URS Manual Count

	Total Traffic Volume			Number of Heavy Vehicles			Heavy Vehicle Percentage		
	NB	SB	Total	NB	SB	Total	NB	SB	Total
9/27/2004									
Manual Count ¹	4,076	6,269	10,345	256	489	745	6.28%	7.80%	7.20%
Loop Detector Station ²	4,182	6,342	10,524				6.12%	7.71%	7.08%
9/28/2004									
Manual Count ¹	4,078	6,044	10,122	195	204	399	4.78%	3.38%	3.94%
Loop Detector Station ²	4,223	6,162	10,385				4.62%	3.31%	3.84%

¹ Data Source: Manual counts, URS Corporation

² Data Source: MnDOT Loop Detector Station

The traffic volumes obtained from the loop detector stations were validated using manual counts of vehicles from video recordings for two time periods. Manual counts of the total traffic volume

BRIDGE 9340 STUDY



from video files were completed for the 8:00 to 9:00 AM time period on September 27th and 28th. As shown in Table 2-4, the volumes obtained from the loop detector stations were slightly (around 2%) greater than the volumes obtained from the manual counts for every case. This difference is likely due to the tendency of loop detectors to over-count heavy vehicles because of their multiple axles and the length of vehicles with a tractor-trailer combination. This difference was not considered to be significant, and the hourly loop detector station volumes were used to calculate the percentages of heavy vehicles on the bridge.

2.6.2 Heavy Vehicle Volume from Manual Count

URS utilized the Minnesota Department of Transportation (Mn/DOT) and the City of Minneapolis' traffic monitoring system to perform vehicle classification counts on the I-35W Bridge. Mn/DOT's Regional Traffic Management Center (RTMC) and the City of Minneapolis maintain closed circuit television cameras on select freeway and roadway networks in the Minneapolis-St. Paul metropolitan area to monitor traffic operations. The cameras are viewed in real time at the RTMC. The City of Minneapolis camera used to monitor and record traffic is mounted on the University Avenue Bridge over I-35W, immediately north of the Mississippi River. This camera was used to digitally record the video feed of traffic on I-35W that would travel on Bridge 9340 over the Mississippi River. Both northbound and southbound traffic can be viewed simultaneously from this location.

The digital recordings were saved onto a computer hard drive, which was located at the RTMC for the project. The recording was started at 2:00 PM on September 23, 2004 and ended at 2:00 PM on September 30, 2004, providing a total of 168 hours of video over the full 7-day period. The digital files were then viewed by URS staff to conduct manual counts of heavy vehicles traveling in each direction by the hour. Based on Mn/DOT's vehicle classification system, heavy vehicles were determined and counted as any vehicle having 2 or more axles with 6 or more tires.

Subsequent to the initial count of heavy vehicles over the full 168-hour period, two weekdays were recounted for 12 hours (6:00 a.m. – 6:00 p.m.) each to define the percentages of the

different classes of heavy vehicles in the overall traffic composition. The 6:00 a.m. – 6:00 p.m. period encompassed 70-75 percent of the daily traffic, so it was assumed to be a representative sample of the entire week of traffic. The Mn/DOT form for vehicle classification as shown in Figure 2-5, which includes category for 13 types of vehicles, was used for the detailed classification counts. Using this classification, the digital video files were viewed a second time by URS staff to conduct manual counts of each type of heavy vehicle traveling in each direction per hour.

Mn/DOT VEHICLE CLASSIFICATION SCHEME

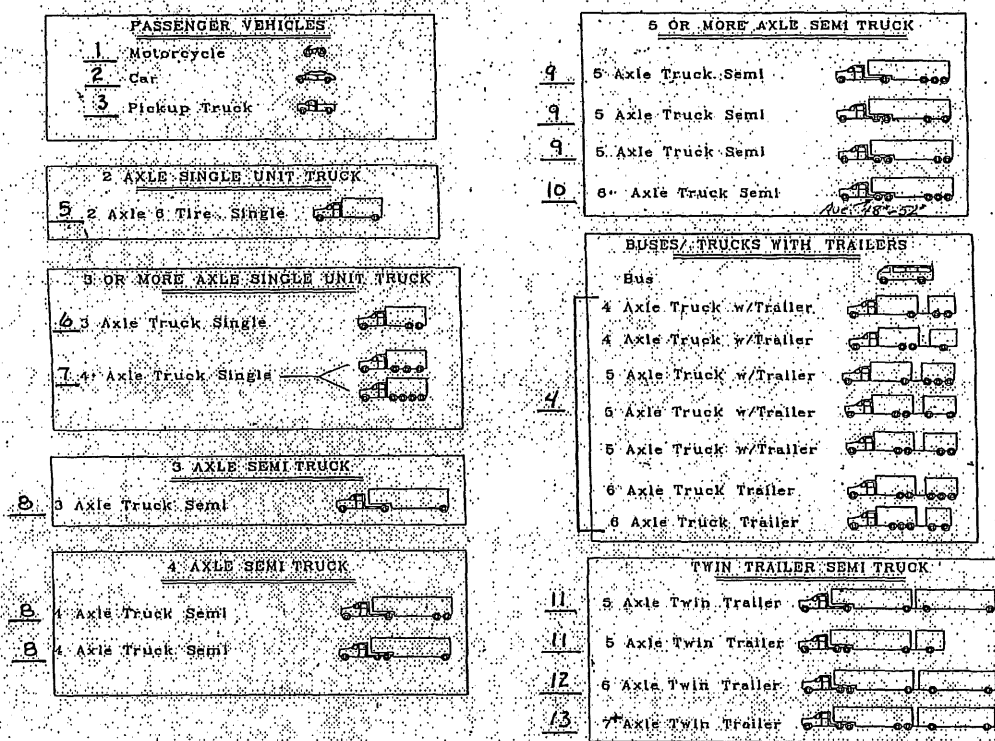


Figure 2-5: Mn/DOT Vehicle Classification Scheme

Table 2-5 shows the hourly and daily heavy vehicle (two-axle, six-tire and larger) percentages of the total traffic volume for the 7-day data collection period for both the northbound and southbound I-35W directions.

The results indicated that the average weekday heavy vehicle percentages were generally between 5.0 and 6.0 percent of the total traffic for both northbound and southbound directions. The heavy vehicle percentage averaged over all weekday hours was calculated as 5.58 percent. The average heavy vehicle percentage was approximately 2.0 percent on Saturday and approximately 1.5 percent on Sunday.

Of particular concern with respect to loading on the bridge is the percentage of total traffic that is heavy vehicles with five or more axles, as these vehicles have the greatest average weights. The data from the detailed classification counts (i.e., the two twelve-hour periods using the thirteen-category vehicle classification) were used to calculate the percentage for these categories of heavy vehicles for each direction on I-35W. The percentage of heavy vehicles having five or more axles relative to total traffic volume for two 12 hour periods that were recounted can be seen in **Table 2-6**.

The average percentages of heavy vehicles with five or more axles, shown in **Table 2-6**, were similar for September 28th and 29th when these specific heavy vehicles were counted and it was assumed that the same vehicle type distribution would be applicable to the other hours and days that were not included in the second, more-detailed classification count. Based on this assumption, the percentage of vehicles with five or more axles was calculated with respect to the total traffic volume for the entire 7-day period, and the results of this analysis can be seen in **Table 2-7**. The percentage of heavy vehicles with 5 or more axles, averaged over all weekday hours, was calculated as 1.61 percent. The percentages for Saturday and Sunday were 0.57 percent and 0.43 percent, respectively.

Table 2-5: I-35W Bridge 9340 Heavy Vehicle Percentages (Two-Axle, Six-Tire Vehicles or Larger) – URS Manual Count

Time Period	5/23/2004		5/24/2004		5/25/2004		5/26/2004		5/27/2004		5/28/2004		5/29/2004		5/30/2004	
	NE	SB														
0:00 AM - 1:00 AM			5.73%	5.46%	2.49%	1.83%	1.59%	1.79%	4.21%	6.05%	5.23%	10.00%	6.78%	5.45%	5.22%	6.14%
1:00 AM - 2:00 AM			8.39%	7.94%	2.39%	3.41%	1.95%	2.01%	5.73%	8.38%	8.65%	12.80%	6.01%	4.66%	7.02%	10.56%
2:00 AM - 3:00 AM			9.52%	10.76%	2.22%	2.90%	2.40%	1.98%	7.19%	5.65%	10.69%	16.70%	12.27%	8.21%	11.76%	11.22%
3:00 AM - 4:00 AM			12.50%	13.92%	7.01%	6.64%	4.91%	2.76%	17.74%	18.73%	18.31%	27.65%	15.65%	18.41%	15.27%	14.46%
4:00 AM - 5:00 AM			12.75%	13.53%	5.73%	8.95%	6.16%	5.91%	13.20%	12.86%	15.57%	24.92%	14.25%	14.37%	13.36%	15.09%
5:00 AM - 6:00 AM			9.06%	8.25%	5.49%	8.96%	4.29%	4.99%	8.76%	7.65%	8.37%	10.10%	8.40%	7.36%	8.15%	7.65%
6:00 AM - 7:00 AM			6.44%	5.65%	6.70%	5.52%	3.73%	3.97%	6.41%	5.58%	6.27%	4.85%	6.30%	5.36%	6.39%	4.44%
7:00 AM - 8:00 AM			5.11%	5.32%	3.60%	4.75%	2.07%	3.54%	4.61%	5.61%	3.55%	4.53%	3.81%	4.74%	3.72%	4.65%
8:00 AM - 9:00 AM			6.50%	7.78%	3.53%	4.70%	1.67%	1.48%	6.19%	7.79%	4.65%	6.44%	5.01%	7.37%	5.61%	7.01%
9:00 AM - 10:00 AM			8.68%	8.59%	2.91%	2.96%	1.89%	1.87%	9.06%	9.03%	7.00%	7.81%	8.34%	7.85%	7.39%	7.70%
10:00 AM - 11:00 AM			9.14%	9.56%	2.55%	2.73%	1.16%	1.15%	9.33%	9.72%	9.65%	8.68%	9.90%	10.31%	9.20%	9.13%
11:00 AM - 12:00 PM			6.73%	6.61%	3.05%	1.64%	1.04%	1.37%	8.97%	9.12%	6.62%	7.80%	8.42%	9.24%	7.76%	8.03%
12:00 PM - 13:00 PM			7.44%	6.97%	1.79%	1.80%	0.77%	1.16%	7.90%	8.73%	6.04%	7.10%	7.53%	7.82%	7.39%	7.98%
13:00 PM - 14:00 PM			6.74%	7.49%	1.67%	1.72%	1.53%	1.27%	8.59%	8.48%	7.65%	8.75%	8.55%	9.00%	8.04%	7.89%
14:00 PM - 15:00 PM	6.63%	5.92%	5.70%	5.41%	1.47%	1.54%	1.52%	1.41%	7.19%	7.16%	6.65%	7.06%	6.70%	6.93%		
15:00 PM - 16:00 PM	4.14%	4.71%	4.31%	4.14%	1.47%	1.42%	0.93%	1.37%	5.21%	5.39%	4.62%	5.12%	4.47%	5.18%		
16:00 PM - 17:00 PM	3.55%	1.95%	3.52%	2.92%	1.59%	1.42%	0.73%	0.82%	4.00%	3.40%	4.40%	3.53%	4.50%	2.89%		
17:00 PM - 18:00 PM	3.01%	2.12%	3.29%	2.24%	1.30%	1.21%	0.97%	1.11%	3.52%	2.81%	3.33%	2.65%	3.52%	2.51%		
18:00 PM - 19:00 PM	2.61%	2.22%	2.97%	2.30%	1.04%	0.91%	1.25%	1.15%	3.27%	2.49%	2.94%	2.53%	3.71%	2.48%		
19:00 PM - 20:00 PM	2.22%	2.20%	2.47%	2.84%	1.37%	1.29%	1.01%	1.40%	3.67%	3.62%	2.87%	2.74%	3.21%	2.97%		
20:00 PM - 21:00 PM	2.45%	3.23%	2.48%	2.55%	1.21%	0.90%	1.23%	1.67%	3.20%	4.55%	1.76%	4.34%	2.43%	2.94%		
21:00 PM - 22:00 PM	1.95%	2.29%	1.93%	2.11%	1.18%	0.99%	1.71%	1.19%	2.42%	3.91%	2.33%	4.45%	2.27%	3.08%		
22:00 PM - 23:00 PM	3.10%	2.44%	1.34%	2.24%	0.39%	0.69%	1.46%	1.40%	3.13%	3.68%	2.83%	5.43%	3.21%	3.14%		
23:00 PM - 24:00 PM	2.80%	3.24%	2.06%	2.35%	0.64%	0.83%	2.99%	2.35%	4.69%	3.63%	4.46%	6.67%	4.46%	4.25%		
Daily Average	3.44%	3.17%	5.17%	5.51%	1.98%	2.02%	1.40%	1.50%	5.85%	6.28%	5.18%	6.07%	5.59%	5.83%	7.15%	7.18%

Data Source: URS Corporation

Table 2-6: Bridge 9340 Five-Plus-Axle Heavy Vehicle Percentages – URS Manual Count

Time Period	9/28/2004		9/29/2004	
	5+ Axles		5+ Axles	
	NB	SB	NB	SB
6:00 AM - 7:00 AM	2.43%	1.45%	2.21%	1.35%
7:00 AM - 8:00 AM	1.00%	1.42%	1.35%	1.22%
8:00 AM - 9:00 AM	1.73%	2.42%	1.23%	1.85%
9:00 AM - 10:00 AM	2.69%	2.89%	2.52%	2.53%
10:00 AM - 11:00 AM	3.80%	3.42%	2.80%	2.96%
11:00 AM - 12:00 PM	2.38%	3.19%	2.28%	2.73%
12:00 PM - 13:00 PM	2.31%	2.67%	2.10%	2.53%
13:00 PM - 14:00 PM	1.68%	2.35%	2.47%	2.74%
14:00 PM - 15:00 PM	1.37%	1.79%	-	-
15:00 PM - 16:00 PM	0.72%	1.31%	-	-
16:00 PM - 17:00 PM	0.42%	1.04%	0.99%	1.06%
17:00 PM - 18:00 PM	0.54%	0.75%	1.05%	0.87%
Average	1.58%	1.99%	1.80%	1.91%

Data Source: URS Corporation

Table 2-7: I-35W Bridge 9340 Five-Plus-Axle Heavy Vehicle Percentages – URS Manual Count

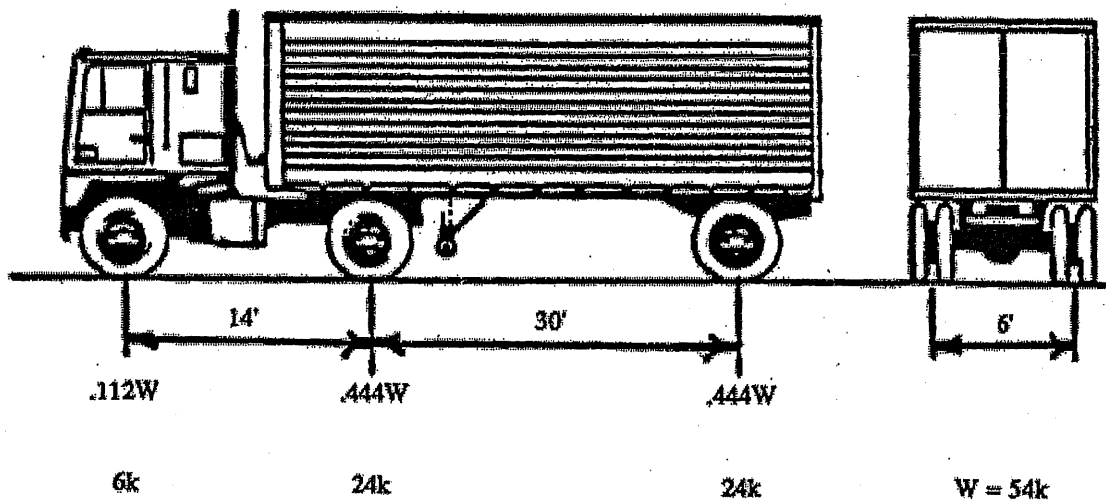
Time Period	5/23/2004		5/24/2004		5/25/2004		5/26/2004		5/27/2004		5/28/2004		5/29/2004		5/30/2004	
	NE	SB														
0:00 AM - 1:00 AM			1.63%	1.56%	0.72%	0.53%	0.40%	0.52%	1.21%	1.74%	1.51%	2.68%	1.95%	1.57%	1.50%	1.77%
1:00 AM - 2:00 AM			2.42%	2.23%	0.63%	0.98%	0.56%	0.53%	1.65%	2.42%	2.55%	3.69%	1.73%	1.34%	2.02%	3.04%
2:00 AM - 3:00 AM			2.74%	3.10%	0.64%	0.83%	0.69%	0.57%	2.07%	1.64%	3.03%	5.39%	3.53%	2.37%	3.39%	3.23%
3:00 AM - 4:00 AM			3.60%	4.01%	2.02%	1.91%	1.41%	0.60%	5.11%	5.40%	5.27%	7.95%	4.51%	5.90%	4.40%	4.17%
4:00 AM - 5:00 AM			3.67%	3.90%	1.65%	2.58%	1.77%	1.70%	3.60%	3.70%	4.49%	7.16%	4.11%	4.14%	3.85%	4.35%
5:00 AM - 6:00 AM			2.61%	2.33%	1.58%	2.58%	1.24%	1.44%	2.53%	2.26%	2.41%	2.91%	2.42%	2.13%	2.35%	2.21%
6:00 AM - 7:00 AM			2.33%	1.61%	1.93%	1.59%	1.07%	1.14%	2.37%	1.53%	2.31%	1.33%	2.33%	1.47%	2.36%	1.22%
7:00 AM - 8:00 AM			1.63%	1.51%	1.05%	1.37%	0.60%	1.02%	1.47%	1.60%	1.14%	1.31%	1.21%	1.35%	1.19%	1.38%
8:00 AM - 9:00 AM			1.99%	2.45%	1.02%	1.35%	0.48%	0.43%	1.90%	2.46%	1.43%	2.03%	1.53%	2.33%	1.72%	2.21%
9:00 AM - 10:00 AM			3.02%	2.97%	0.84%	0.85%	0.54%	0.54%	3.06%	3.12%	2.36%	2.69%	2.84%	2.71%	2.52%	2.66%
10:00 AM - 11:00 AM			3.06%	3.22%	0.73%	0.79%	0.34%	0.33%	3.14%	3.27%	3.27%	2.92%	3.34%	3.47%	3.10%	3.07%
11:00 AM - 12:00 PM			2.09%	3.00%	0.87%	0.47%	0.30%	0.33%	2.78%	3.18%	2.05%	2.71%	2.61%	3.22%	2.41%	2.60%
12:00 PM - 13:00 PM			2.41%	2.43%	0.52%	0.52%	0.22%	0.33%	2.56%	3.04%	1.96%	2.47%	2.44%	2.72%	2.40%	2.76%
13:00 PM - 14:00 PM			1.70%	2.15%	0.48%	0.49%	0.44%	0.37%	2.17%	2.44%	1.99%	2.52%	2.16%	2.58%	2.08%	2.27%
14:00 PM - 15:00 PM	1.32%	1.50%	1.13%	1.37%	0.42%	0.44%	0.44%	0.40%	1.43%	1.81%	1.37%	1.73%	1.33%	1.76%		
15:00 PM - 16:00 PM	0.63%	1.20%	0.67%	1.06%	0.42%	0.41%	0.27%	0.39%	0.81%	1.36%	0.72%	1.31%	0.70%	1.33%		
16:00 PM - 17:00 PM	0.57%	0.64%	0.56%	0.95%	0.54%	0.41%	0.21%	0.24%	0.64%	1.11%	0.70%	1.15%	0.72%	0.94%		
17:00 PM - 18:00 PM	0.70%	0.66%	0.77%	0.70%	0.37%	0.35%	0.28%	0.32%	0.62%	0.69%	0.78%	0.83%	0.82%	0.79%		
18:00 PM - 19:00 PM	0.75%	0.64%	0.65%	0.66%	0.30%	0.26%	0.36%	0.33%	0.94%	0.72%	0.83%	0.75%	1.07%	0.72%		
19:00 PM - 20:00 PM	0.64%	0.63%	0.71%	0.62%	0.39%	0.37%	0.23%	0.40%	1.06%	1.04%	0.63%	0.73%	0.92%	0.86%		
20:00 PM - 21:00 PM	0.70%	0.93%	0.71%	0.73%	0.35%	0.26%	0.36%	0.48%	0.92%	1.31%	0.51%	1.23%	0.71%	0.85%		
21:00 PM - 22:00 PM	0.57%	0.66%	0.57%	0.61%	0.34%	0.26%	0.49%	0.34%	0.70%	1.13%	0.67%	1.23%	0.65%	0.89%		
22:00 PM - 23:00 PM	0.69%	0.70%	0.39%	0.64%	0.11%	0.20%	0.42%	0.40%	0.90%	1.06%	0.81%	1.56%	0.92%	0.90%		
23:00 PM - 24:00 PM	0.81%	0.33%	0.53%	0.63%	0.18%	0.24%	0.66%	0.63%	1.35%	1.12%	1.23%	1.92%	1.23%	1.23%		
Daily Average	0.93%	0.90%	1.43%	1.59%	0.57%	0.56%	0.40%	0.43%	1.69%	1.80%	1.49%	1.75%	1.61%	1.68%	2.06%	2.07%

Data Source: URS Corporation

2.7 Review of Relevant Weigh-In-Motion Data

Weigh-in-motion data from 27 sites across the state was reviewed with particular emphasis on the sites on I-494, in an effort to refine the heavy truck volumes at Bridge No. 9340. The AASHTO fatigue truck is a three-axle, tractor-and-trailer type vehicle with a total weight of 54 kips, or 27 tons, as shown in Figure 2-6. The AASHTO fatigue truck is intended to represent the highway traffic load spectrum and is assumed to weigh approximately one half of the heaviest truck the bridge may experience in its design life. Mn/DOT categorizes all vehicles into fourteen categories (Figure 2-5) and truck categories 9 through 13 are considered to form the range of trucks the AASHTO fatigue truck is intended to represent.

From the review of the traffic video logs at the site for a seven-day period from September 23 to September 30, 2004 it was determined that the average daily traffic (ADT) was 78,500 northbound and 80,310 southbound. It was further determined that 5.58% of the ADT or about 8,860 vehicles were categorized as heavy commercial vehicles using the Mn/DOT definition of heavy commercial vehicles. This percentage is very similar to the weigh in motion data from the I-494 site, which shows that 5.37% of the ADT at that site was heavy commercial trucks in 2002.



Note: A Variable spacing of 14 to 30 feet can be used instead of the 30-foot main axle spacing, but this may significantly reduce the calculated remaining life.

Figure 2-6. The AASHTO Fatigue Truck

Based on the URS truck count data for the bridge site it was estimated that heavy trucks having five or more axles accounted for 1.61% of total vehicle volume in the weekdays and 0.53% on Saturday and 0.47% on Sunday. If an assumption of 1.6% of the ADT is used to estimate the number of heavy trucks on weekdays and 0.5% of the ADT on weekends the average daily number of heavy trucks the AASHTO fatigue truck represents would be about 2,000 per day for both directions.

A traffic growth rate of 2.4% was recently determined for traffic on I-35W just north of the bridge as reported in the "Statewide Planning Level Trunk Highway Traffic Projections" in March 25, 2004. In addition, an actual truck growth rate of 2% was reported as the rate between 1994 and 2000 in the "Minnesota Statewide Transportation Plan". Therefore an assumption of a 2% truck traffic growth rate for this segment of the interstate seems reasonable. With an assumption of 2,000 fatigue trucks per day in 2005 and assuming a 2% annual truck growth rate an average of approximately 1,260 fatigue trucks per day would have crossed the bridge in the past 37 years of its operation. This would equate to an assumption of approximately 17 million fatigue trucks that have used the bridge during its life. \

SECTION 3

3. COMPUTER MODELING OF TRUSS SPANS

3.1 Development of 3-D Finite Element Model

3.1.1 Overview

In order to analyze the behavior of Bridge 9340, a 3-D finite element computer model was created using the computer program GTSTRUDL. The model includes all structural components of the three-span deck truss and the supporting piers. The adjacent span of the approach span at each end, as well as the structural stiffness of the rest of the approach spans, was also included. **Figure 3-1** is an overview of the 3-D finite element model. **Figure 3-2** and **Figure 3-3** are closer views of the side span and center span of the model, respectively. It should be noted that **Figure 3-1** through **Figure 3-3** depict all members with solid views. The computer model is actually made of line members for all the steel components and planar elements for the deck, as shown in **Figure 3-4** and **Figure 3-5**.

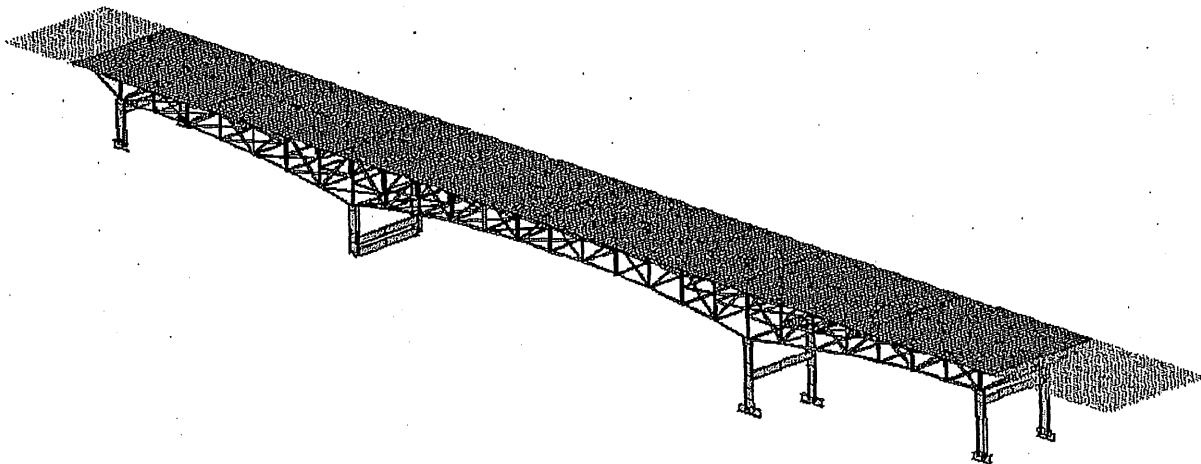


Figure 3-1. Overview of Bridge 9340 Computer Model

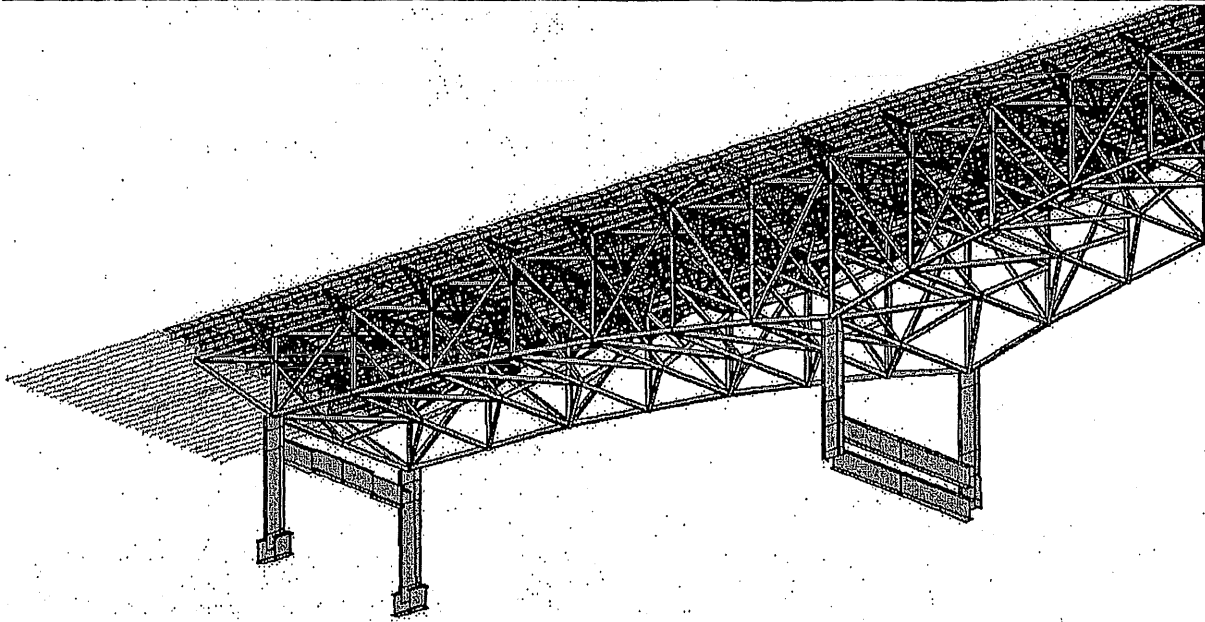


Figure 3-2. Side Span of Bridge 9340 Computer Model

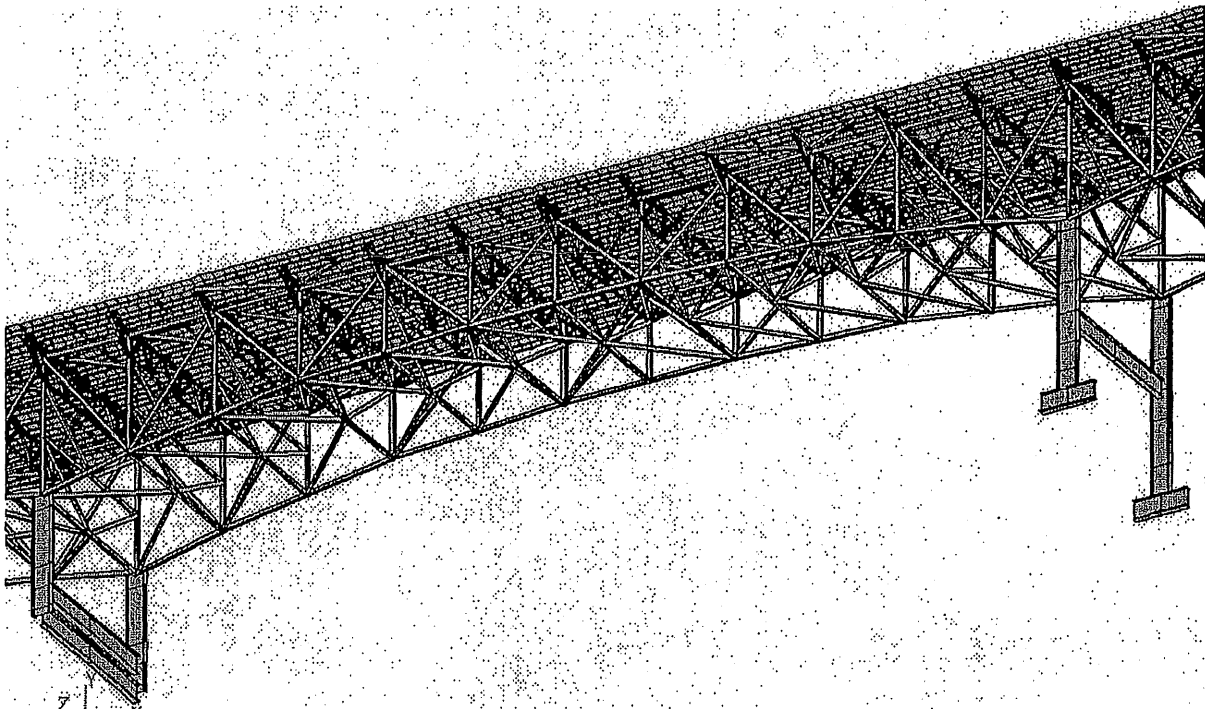


Figure 3-3. Center Span of Bridge 9340 Computer Model

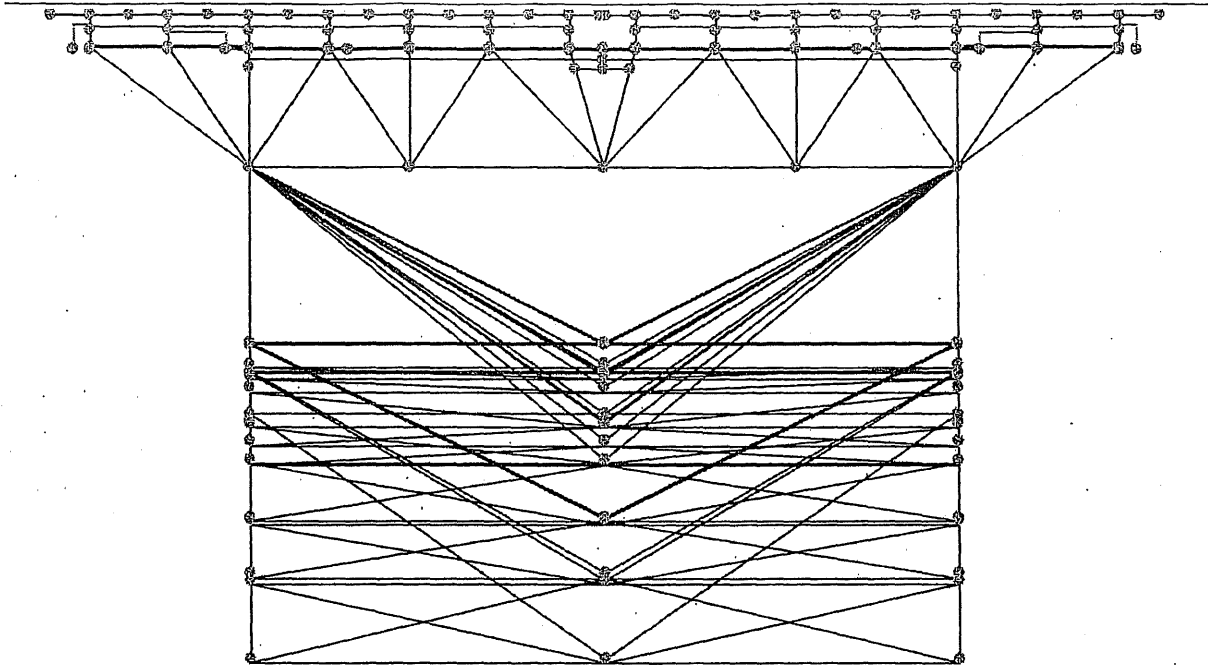


Figure 3-4. Cross Section of Bridge Model Presented by Line Members

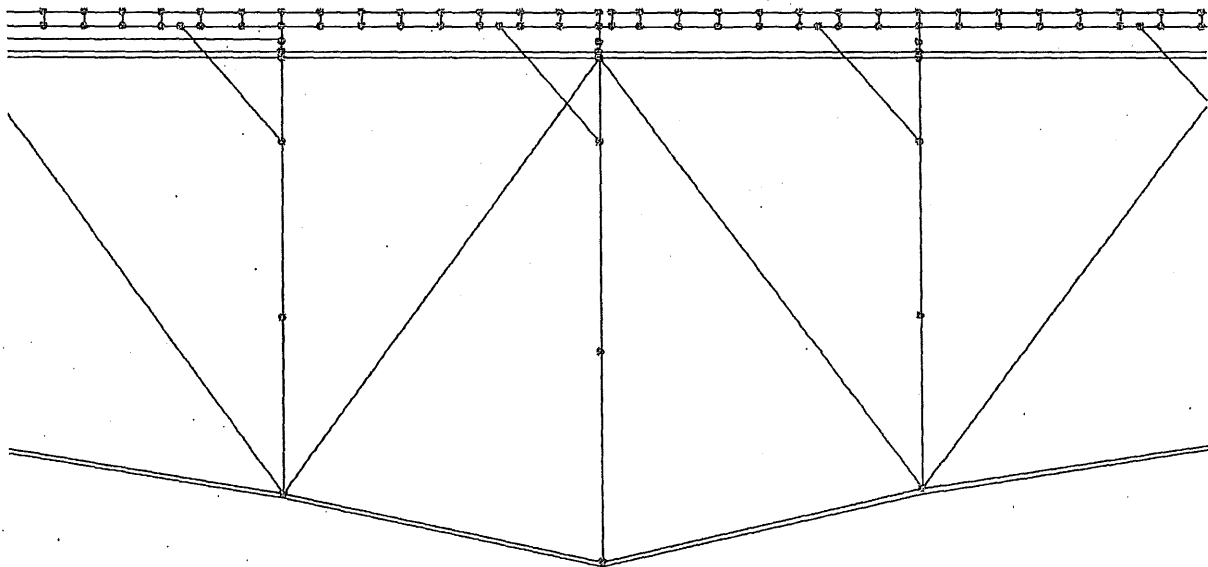


Figure 3-5. Elevation of a Portion of Bridge Model above a Pier Presented by Line Members

3.1.2 General Assumptions

The following assumptions were made in the development of the computer model:

- The vertical slope of the bridge and its impact on the structure geometry were neglected. Consequently, all truss upper chords, stringers and the deck are horizontal and all truss verticals are vertical.
- The small horizontal curvature of the structure at both the north and south ends was neglected.
- The two trusses (west and east) were assumed to be identical. In reality the trusses are the same except for Panel U0-U1 at the south end of the bridge where the horizontal curve caused the east truss to be slightly longer than the west truss. The average length at the bridge centerline for Panel U0-U1, however, is exactly 38'-0", which is the same as all other truss panels and is used in the model. The bridge horizontal curve at the north end only affects the approach spans, not the main trusses.
- The cross-slope of the structure was neglected and thus both trusses have the same elevation.
- All steel members (main trusses, floor trusses, stringers, bracing members, etc.) were modeled with "space frame" members that have six degrees of freedom at each joint. The beam members were placed along the centerlines of the actual members they represent between joints. The members are rigidly connected to the joints except where it is necessary to release certain forces per end support conditions.
- No adjustments have been made to account for member end conditions at truss joints. All truss members were modeled with prismatic beam members along their centerlines between joints. Local effects of gusset plated truss joints are not addressed in the model.
- The reinforced concrete deck was modeled with the GTSTRUDL plate elements which are shell elements in general terms. Quadrilateral elements were used in the model and each joint has six degrees of freedom. Linear elastic behavior was assumed and material properties were determined based on concrete strength specified in the original contract plans. The transverse and longitudinal deck joints were properly included in the model.

3.1.3 Main Trusses

The main truss members are comprised of the upper chords, lower chords, verticals, and diagonals. The cross section of the main truss members is either a box section, a box section with a center web, or an H section. The upper chords are all box sections with perforations in the bottom cover plate. The lower chords, verticals, and diagonals, which are either box sections or box sections with a center web, have perforations in both cover plates. These perforations are opposite in both cover plates and are spaced at a distance about the size of the perforation along the member. The section properties for all truss members were calculated assuming only one cover plate is perforated. Since the length of the member portion with two perforated cover plates is approximately equal to the length of the member portion with no perforated cover plates this method represents the average section properties along the entire member length. For the upper chord members, this calculation yields a section that is slightly less stiff than it actually is, but should not have a significant impact on the results.

The plate sizes used to determine the member properties were based mainly on the Truss Details shown on Sheets 28 through 31 of the original Contract B plans. The plate sizes were also listed in the Table of Truss Members and Stresses on Sheet 20 of the contract plans. In some cases where the plate sizes did not agree or were illegible, the values given on the shop drawings were used. In all cases that were checked, the shop drawings matched the Truss Details rather than the Table. The following members were verified using the shop drawings: U8-U10, U10'-U8', L1-L3, L7-L8, L8-L9, L9-L11, L11'-L9', L9'-L8', L8'-L7', U2-L3, U10-L11, and L11'-U10'.

3.1.4 Floor Trusses

The floor truss members are comprised of upper chords, lower chords, verticals, and diagonals. The floor trusses are symmetrical about the centerline of the bridge without the consideration of the cross slope. **Figure 3-6** shows one half of a representative floor truss, although certain details vary along the bridge due to the cross slope and flaring at the bridge ends. All floor truss members are rolled steel wide flange sections.

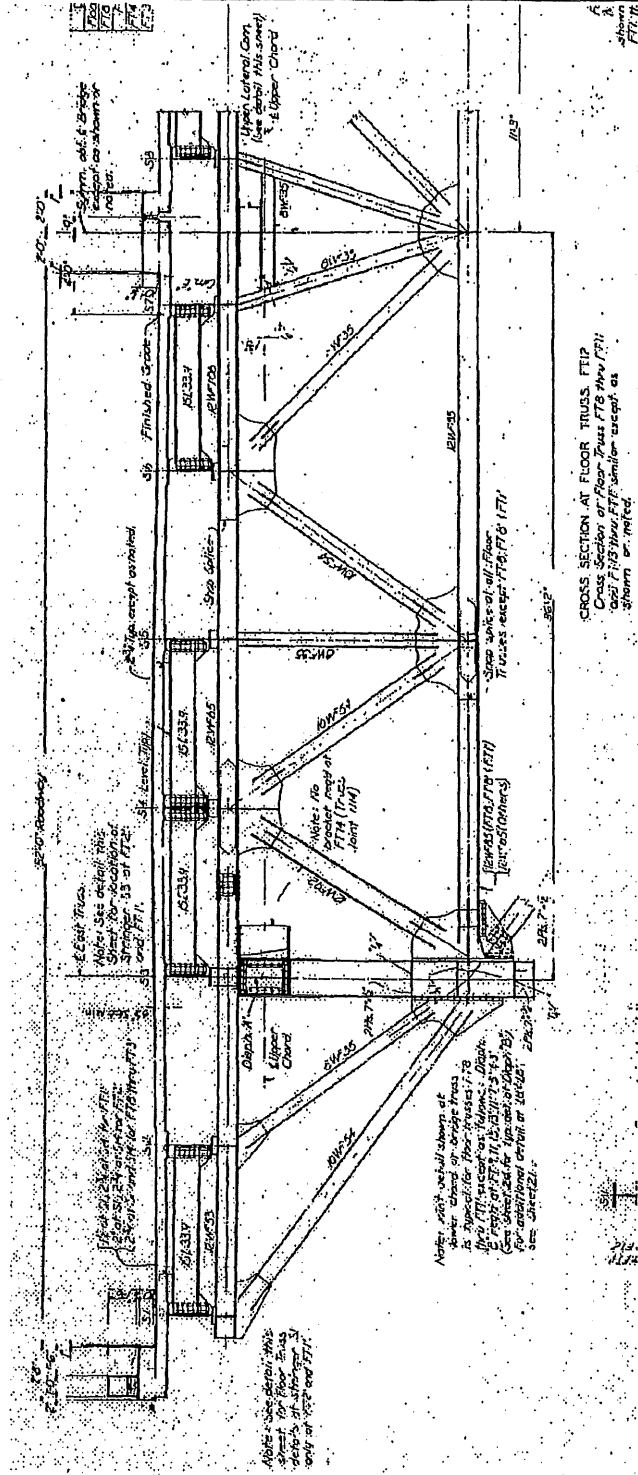


Figure 3-6: Typical Floor Truss (Half Shown)

BRIDGE 9340 STUDY

Near the centerline of the bridge, upper lateral braces are framed into the floor truss through a short horizontal member, named the “upper lateral bracing support member”, between the two floor truss diagonals nearest to the bridge centerline. **Figure 3-7** depicts the portion of the model for a partial floor truss near the bridge centerline with the upper lateral bracing support member labeled. The elevation of the upper lateral braces is usually between the floor truss upper chord and the upper lateral bracing support member, as shown in **Figure 3-7**. In the figure the yellow circles represent the joints and the red lines are for the floor truss members and the upper lateral bracing support member. The two blue lines, between the floor truss top chord and the upper lateral bracing support member, are rigid links used to form a joint at the proper elevation for the connection to the centerlines of the upper lateral braces. The rigid link is simply a very stiff beam member that has little relative displacements between the two joints under load.

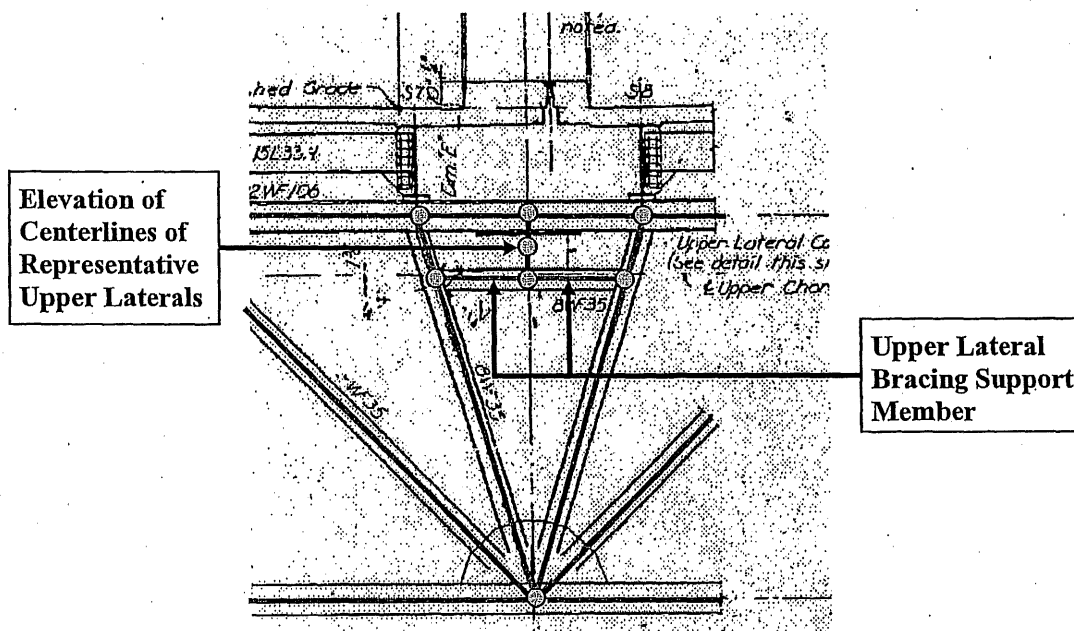


Figure 3-7: Partial Model for Floor Truss Members near Bridge Centerline

The following assumptions were made to simplify the computer model while not significantly affecting the analysis results:

- All floor truss top and bottom chords are assumed to be level. This is consistent with the general assumption to ignore the bridge cross-slope. In reality some floor trusses are actually sloped to follow the deck cross-slope (Sheets 24 and 25 of the Contract B plans).
- All floor trusses are assumed to have the same dimensions. The dimension variation, due to the actual structure flaring and curving at the bridge ends, is ignored. The floor truss dimensions used in the model represent typical floor trusses along the bridge length.

3.1.5 End Floor Beams

An end floor beam is located at each of the two ends (north and south) of the deck truss spans, next to the end cross girder of the approach span supported by the rocker bearings. Both floor beams are welded built-up plate girder sections with tapered web depths in the cantilevers outside the main trusses. Each end floor beam was modeled by a line of beam members placed at an elevation equal to the mid-depth at the center of the bridge. The cantilever portions were modeled by beam members of varying section properties with member eccentricities to adjust for the inclination of the section centerline due to the tapered web.

The following assumptions were made to simplify the model, which are consistent with the previously mentioned general assumptions:

- The top of both end floor beams was assumed to be level.
- The dimensions of the north end floor beam were used for both end floor beams. In reality the two beams are of slightly different dimensions due to the cross slope and flaring at the bridge ends.
- All stringers are assumed to be spaced at 8'-2" except S7 and S8 which are spaced at 7'-0". The stringer spacing actually varies at the north end due to the bridge flaring.
- A length of 18'-1" was used for all the floor beam cantilevers. This is taken from Sheet 27 of the Contract B plans for the west truss cantilever, which is shown under the typical 52'-0" roadway width rather than the flared width.

3.1.6 Portal and Sway Frames

Oriented in the vertical planes, the portal and sway frames connect between the two main trusses below the floor trusses. All the frame members are made of box cross-sections. Perforations were neglected for member properties since there are only a few. In the computer model, members for the intermediate horizontal strut and the diagonals were placed along their centerlines and connected to the main truss verticals on both sides, as shown in **Figure 3-8**. Since the centerline of the bottom strut is lower than the centerlines of the main truss lower chords, member eccentricities (materialized with rigid links) were defined in the model to keep the bottom strut members at the actual elevation. The space frame members for the bottom strut were also rotated as required to match the slope of the main truss lower chord.

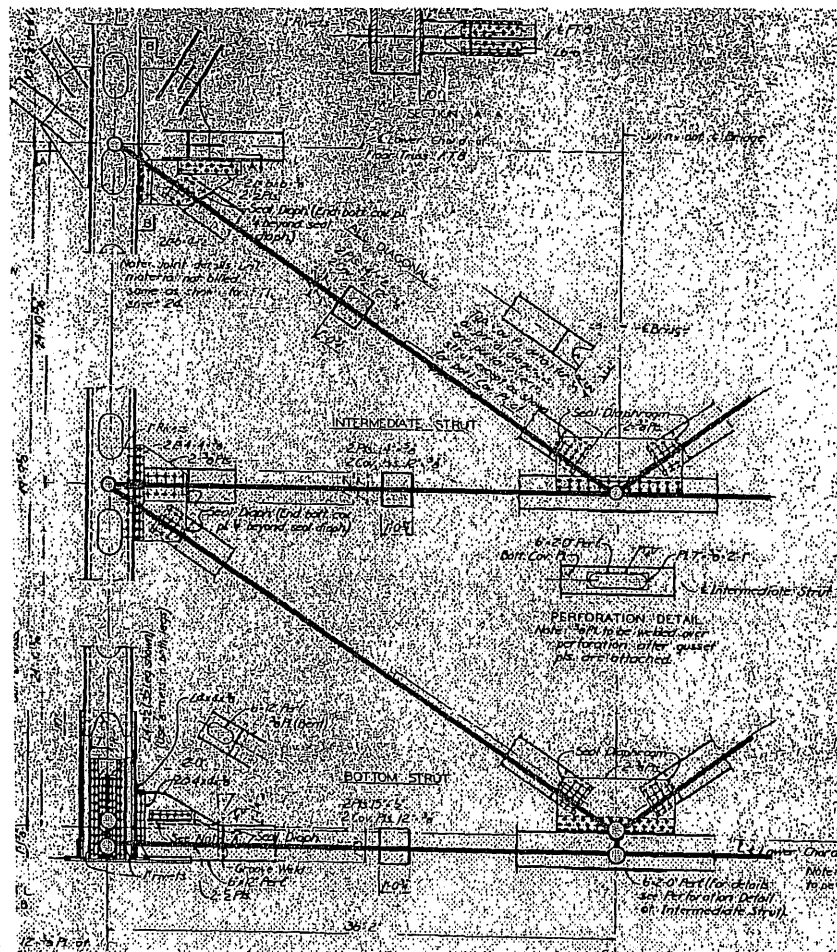


Figure 3-8: Partial Model for Portal/Sway Frame Members

3.1.7 Upper Lateral, Lower Lateral, and Cantilever Bracing Members

Three types of bracing are present on the structure: the upper lateral bracing for the upper chords of the main truss, the lower lateral bracing for the lower chords of the main truss, and the cantilever bracing for the cantilever portions of the floor beams outside the main trusses, as shown in the framing plan in **Figure 1-2**.

The upper lateral bracing members are box cross-sections without perforations, but with tapered section adjacent to the main truss upper chords. These members are connected between the gusset joints of the main truss upper chords and the center of the floor trusses at the bridge centerline. Member eccentricities were used in the model at the main truss ends of the members to shift the centerline up to coincide with the actual centerline of the upper lateral bracing at its minimum depth.

The lower lateral bracing members are also box cross-sections without perforations. These members are connected between the main truss lower chord joints and the center of the bottom strut of the portal or sway frame at the bridge centerline. In the computer model member eccentricities were used as necessary to match the actual centerline of the lower lateral bracing.

The cantilever bracing members are rolled steel ST6WF18 sections. These members are connected between the upper gusset joints of the main truss and the cantilever end of the floor truss. In the computer model vertical and horizontal member eccentricities were used as necessary at each end to match the actual centerline of the cantilever bracing to the member it is connected to.

There are also small hangers that connect the intermediate stringer diaphragms to the upper lateral and the cantilever bracing members, as shown in **Figure 3-9**. These members were omitted from the model since they were not expected to play measurable roles in the force distribution of the deck truss system.

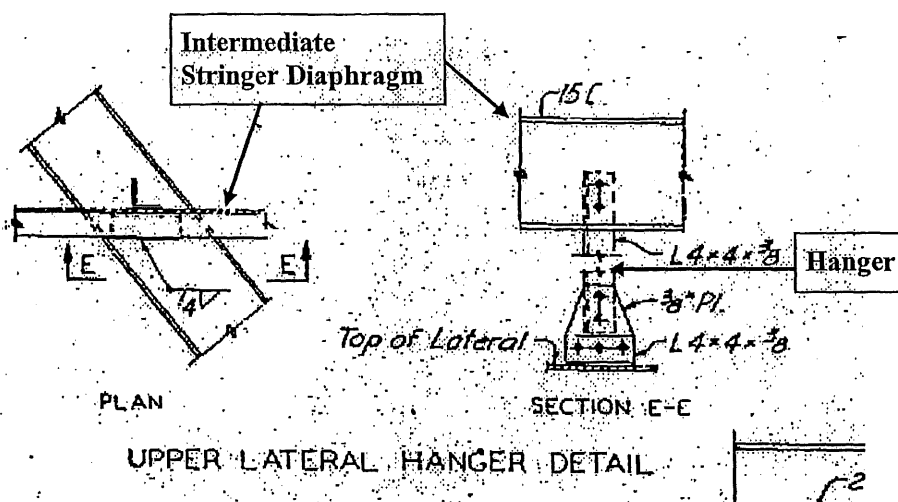


Figure 3-9: Hanger Detail between Intermediate Stringer Diaphragm and Upper Lateral Bracing

3.1.8 Stringers and Diaphragms

There are a total of fourteen lines of stringers across the width of the deck truss, all of which are 27WF94 wide flange sections. As shown in Figure 3-6, the stringers directly support the deck and are placed on top of the floor truss top chords. Stringer diaphragms exist at each floor truss location (panel point) and between each two adjacent floor trusses (mid-panel point). The stringer diaphragms are 16WF36 wide flange sections at deck expansion joint locations and 15C33.9 channel sections at all other locations. In the computer model member end eccentricities were used to properly locate the stringer-to-diaphragm connections. Figure 3-10 shows the layout of the stringers and diaphragms for the southern half of the bridge.

The stringers are continuous longitudinally except at panel points U4, U8, U14, U8', and U4', where there are expansion joints in the deck. Under the deck expansion joint, there is also a stringer expansion joint with one stringer end fixed to the floor truss top chord (the fixed side) and the other stringer end sits on an expansion bearing (the expansion side). The modeling of the deck and stringer expansion joint is illustrated in Figure 3-11 and the assumptions made are discussed in the following paragraphs.

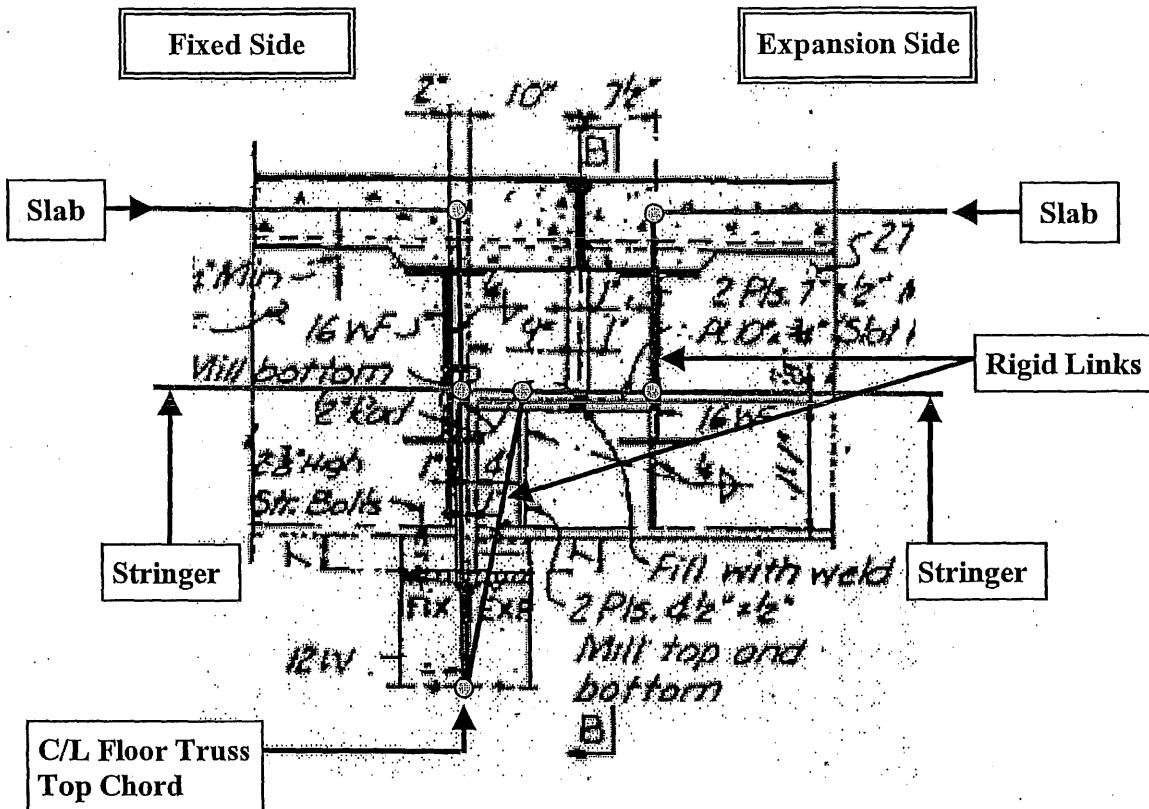


Figure 3-11: Stringer and Deck Expansion Joints

On the fixed side of the expansion joint, the stringer was assumed to end just above the centerline of the floor truss top chord although there is a small extension of the upper portion of the stringer, as shown in Figure 3-11. The stringer diaphragm was assumed to transversely frame into the fixed end of the stringer although in reality it is located about 2" from this position. Similarly the deck, modeled by shell elements at its mid-thickness, was also terminated just above the fixed end of the stringer although the actual deck joint is located a small distance away. Rigid links were used to connect between the deck and the stringers, and between the stringer ends and the floor truss top chord.

On the expansion side of the joint, the stringer was assumed to end directly above the centerline of the floor truss top chord, at the exact same location as the stringer end on the fixed side. The two coincidental ends of the stringers on both sides of the expansion joints, although not

connected to each other, are both connected to the same joint of the floor truss top chord underneath. **Figure 3-11** shows a small offset of the stringer end on the expansion side purely for illustration purposes. Member end releases were applied to the upper end of the rigid link between the floor truss and the stringer end on the expansion side to allow the longitudinal movement and rotation about the transverse axis. The stringer diaphragm on the expansion side of the joint was placed at the exact location in the model.

As shown in **Figure 3-11**, the deck slab expansion joint is exaggerated as a transverse opening of approximately 18" in the computer model. This is not expected to affect the results of structural analysis except the dead load of the transverse deck strip that was ignored.

The following assumptions were made in the model to the stringer members:

- All stringers were assumed to be spaced at 8'-2" except S7 and S8 which were spaced at 7'-0". The horizontal curve at the south end and the flaring of the bridge at the north end were neglected.
- All the stringers were placed at the same elevation, as a result of ignoring the bridge cross slope and profile grade.

3.1.9 Floor Truss Bracing Members

Floor truss bracing members are rolled steel 6WF25 sections connected between the bottom chord of the floor truss and the bottom flange of the stringer, as shown in **Figure 3-12**. There are two floor truss bracing members on each floor truss located at stringers S5 and S10. Although these members are actually pinned at both ends, they were modeled as space frame members with rigid end connections based on the assumption that the pins are likely frozen due to rust. Eccentricities between the actual connection and the member centerline were ignored at both ends due to the insignificance of these members in the force distribution of the deck truss structural system.

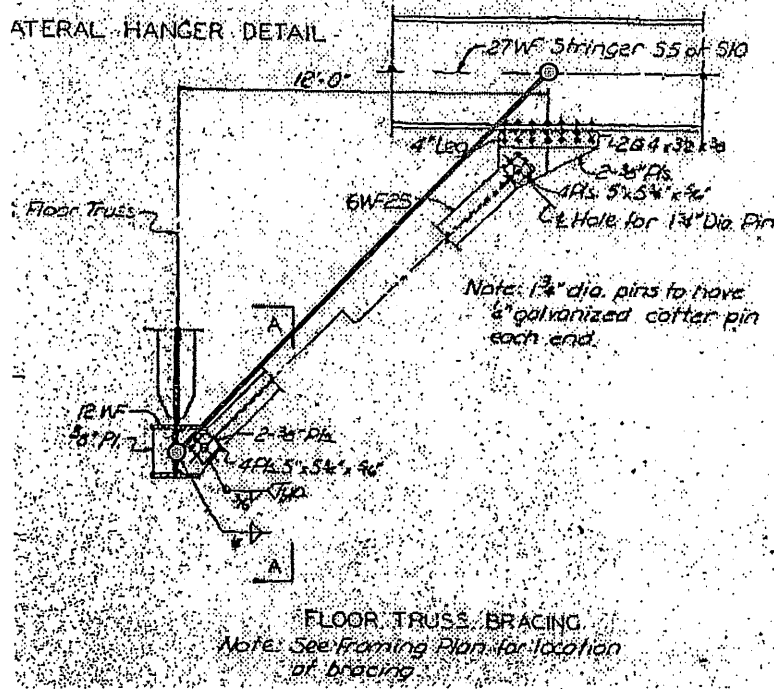


Figure 3-12: Typical Floor Truss Bracing Member

3.1.10 Deck and Barriers

The entire deck was modeled with four-node shell elements with six degrees of freedom at each node. All the deck expansion joints in the transverse and longitudinal directions were included in the model by leaving a gap between the elements on both sides. At least two elements were used between any two adjacent stringers in the transverse direction whereas at least eight elements were used longitudinally between any two floor trusses to keep the element aspect ratio approximately 1:1.

The bridge deck was assumed to be level throughout the model and all the deck elements were placed at the mid-thickness elevation of deck slab. In the original contract plans the deck thickness was specified as 6½" including a ½" integral wearing surface. In 1977, ¼" of the original deck was removed and a 2" low slump concrete overlay was placed, resulting in a total deck thickness of 8¼". In the computer model, the deck elements were assumed to be 6.0 inches

BRIDGE 9340 STUDY



in thickness to account for only the structural portion of the reinforced concrete deck. The shell elements have a linear elastic modulus of 3,605 ksi based on a 4,000 psi concrete compressive strength.

Bridge barriers were not included in the model as structural elements except for their dead loads. In 1998 multiple repairs were made including replacement of the edge and median barriers. **Figure 3-13** and **Figure 3-14** show the original and the 1998 replacement edge barriers, respectively. As shown in **Figure 3-14**, the 1998 work placed a new edge barrier on top of the existing curb adjacent to the original edge barrier. The new edge barrier is continuous only between cork joints in varying lengths up to a maximum length of 30-ft and is anchored to the exterior curb with drilled, epoxy anchors.

While the revised edge barriers did not affect the deck layout, the new median barrier changed the location of the longitudinal deck joint slightly. As shown in **Figure 3-15**, in 1998 portions of the deck on both sides of the longitudinal joint were removed and new longitudinal deck joint was placed exactly along the centerline of the bridge after the placement of new median barriers. This has been accounted for in the model.

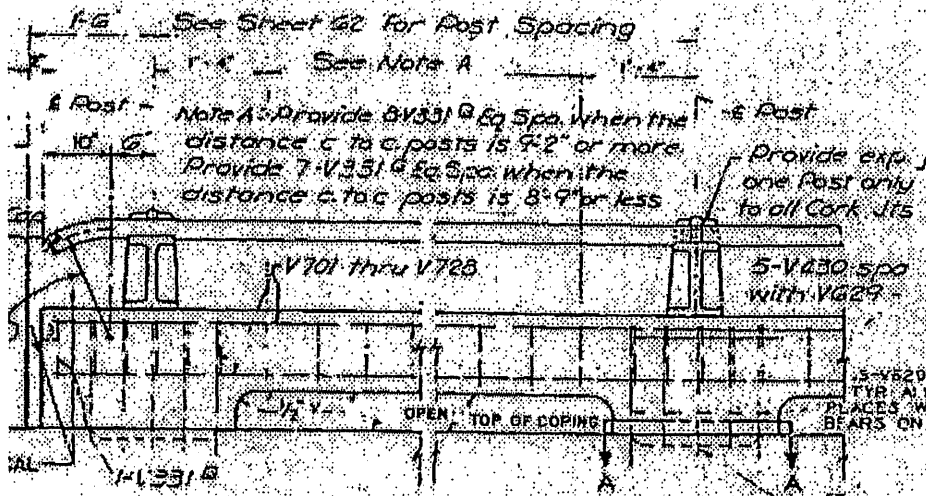


Figure 3-13: Original Edge Barrier

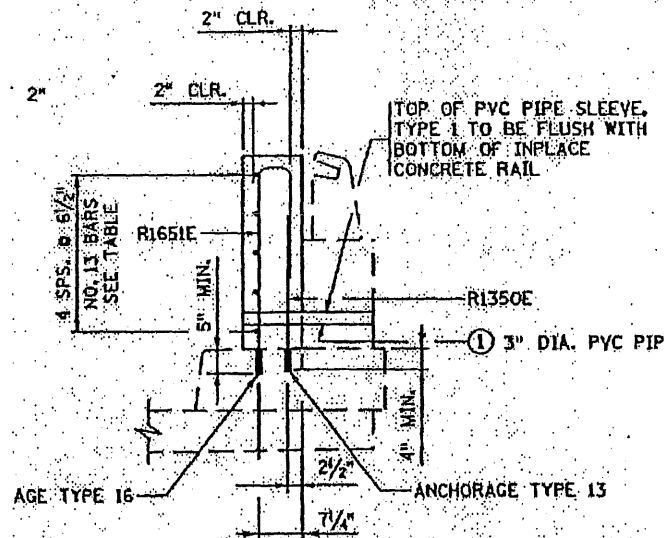


Figure 3-14: 1998 Replacement Edge Barrier

As shown in **Figure 3-15**, the original median barrier was a low curb with a guardrail and the 1998 replacement median barrier was comprised of two Jersey barriers with a precast concrete cap in between. The new median barrier is continuous only between cork joints in varying lengths up to a maximum length of approximately 20-ft and was anchored to the deck with dowel bars. Stay-in-place (SIP) forms were observed under the deck joint between the two stringers on both sides of the longitudinal joint, as shown in **Figure 3-16**, although not indicated in the plans. The existence of the longitudinal deck joint could not be verified from the top because of the precast cap between the median barriers. However, Mn/DOT confirmed that there is a longitudinal deck joint in the concrete and the SIP simply spans between the two stringers.

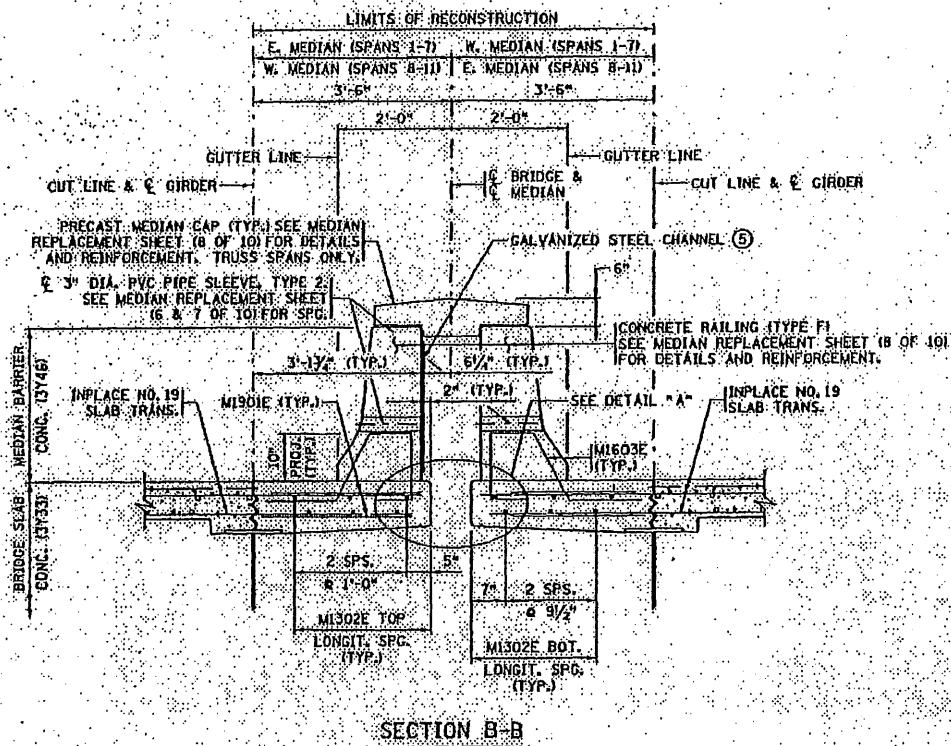
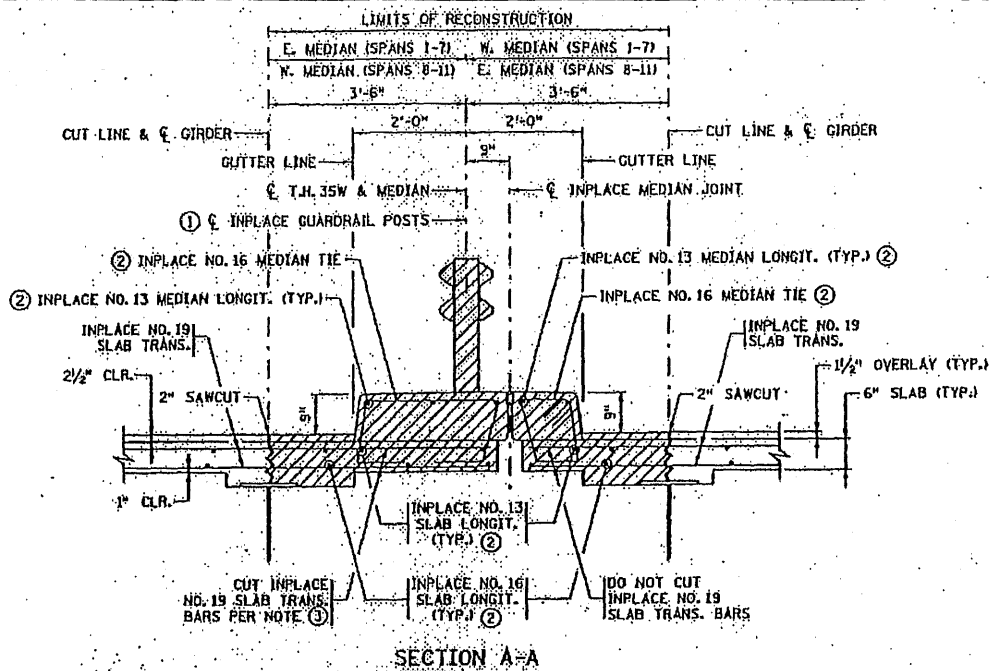


Figure 3-15: 1998 Median Barrier and Longitudinal Deck Joint Replacement

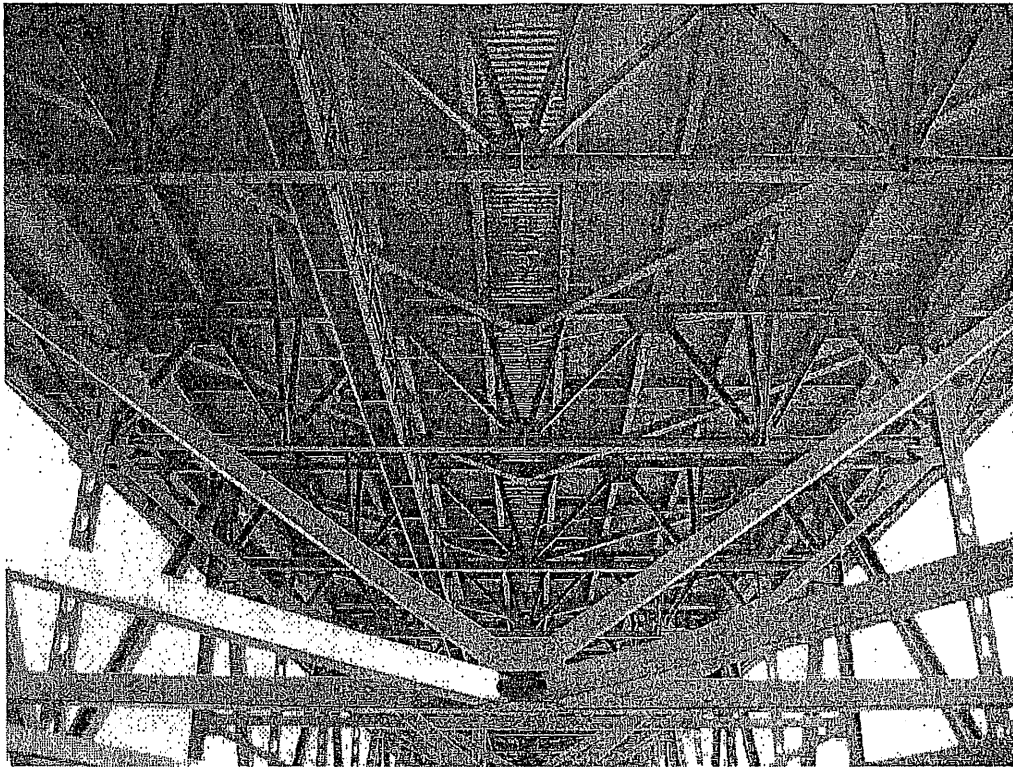


Figure 3-16: Under Side of Bridge Deck – SIP Forms Between S7 and S8

The following assumptions were made in the model in relation to the deck and barriers:

- All deck elements were set at the same elevation. In actuality, the bridge deck is sloped due to both the cross slope and the longitudinal profile grade.
- The vertical distance between the deck elements and the stringer members is comprised of half of the stringer member depth, half of the deck thickness and a concrete haunch between the stringer and the deck. A haunch thickness of 2" was assumed throughout because no information for the actual depth of the haunches was discovered on the plans.
- No structural participation was assumed for the edge and median barriers.

3.1.11 Connection between Deck and Stringers

The connection between the deck (shell elements) and the stringer (beam members) was modeled using rigid shear links for the composite action. The shear link consists of two segments of

different section properties, as shown in **Figure 3-17**. Segment 1 is for half-thickness of the deck plus the haunch between the stringer and the deck, and Segment 2 is for half-depth of the stringer. In regard to the stiffness for horizontal shear, Segment 1 is very stiff but Segment 2 is relatively flexible, especially in the direction for out-of-plane bending of the web. The section properties of Segment 2 were initially assumed to be stiff. These properties were then adjusted based on a contributory section of the web including the stiffener plate at the connection for better agreement with field testing results as discussed in Section 3.2 of the report.

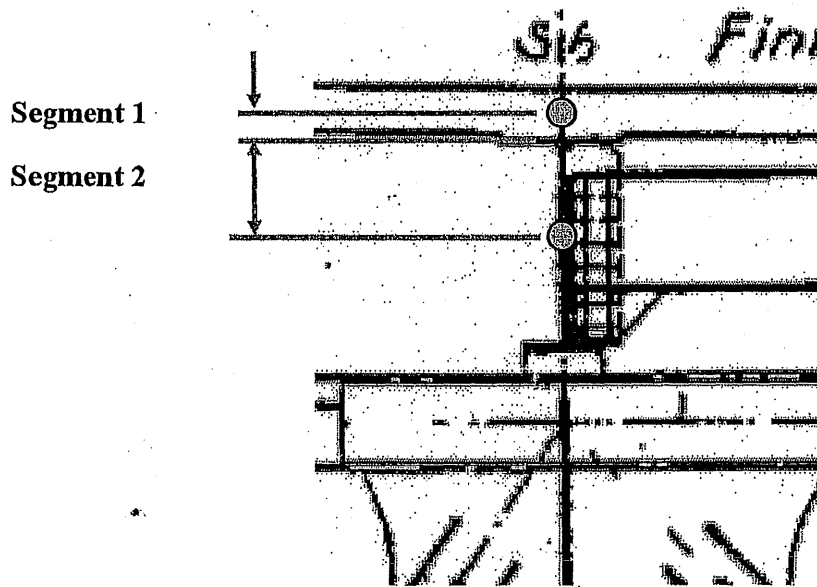


Figure 3-17: Modeling of Deck-to-Stringer Connection

3.1.12 Connection of Stringers to Floor Trusses and End Floor Beams

The connection of the stringer to the floor truss, and the connection of the stringer to the end floor beam, was also modeled using rigid shear links, respectively. The shear link between the stringer and the floor truss was comprised of three segments, as shown in **Figure 3-18**. Segment 1 was for half-depth of the stringer, Segment 2 for the bearing seat connected to the flanges, and Segment 3 for half-depth of the floor truss upper chord. While the stiffness of Segment 2 was very high, the shear stiffness of Segment 1 and Segment 3 was low in the directions for out-of-

plane bending of the webs of the stringer and the floor truss upper chord, respectively. The section properties of these members were also initially assumed to be stiff, and then adjusted based on a contributory section of the web including the stiffener plate at the connection for better agreement with field testing results as discussed in Section 3.2 of the report.

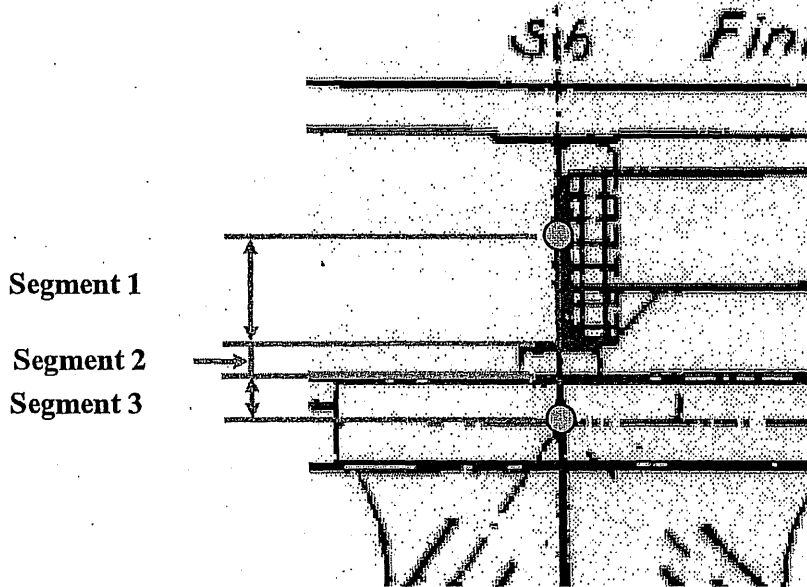


Figure 3-18: Modeling of Stringer-to-Floor-Truss Connection

At the connection between the stringer and the end floor beam, “rigid” shear links of high section properties were used because this connection was considered to be “stiff” due to the use of a stiffened knee-brace connection, as shown in **Figure 3-19**.

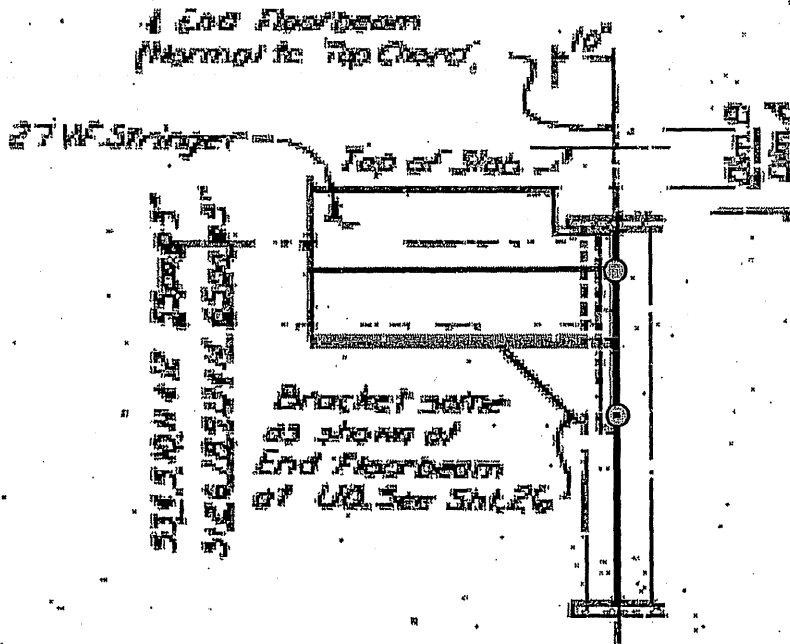


Figure 3-19: Modeling of Stringer-to-End-Floor-Beam Connection

3.1.13 Connection between Floor Trusses and Main Trusses

The connection between the floor truss and the main truss was also modeled using rigid shear links. The shear link was defined with two segments of different section properties, as shown in **Figure 3-20**. Segment 1, representing half-depth of the floor truss top chord, was given high stiffness initially in the direction for out-of-plane bending of the web, the same as the Segment 3 of the stringer-to-floor-truss shear link member (**Figure 3-18**). The section properties were adjusted in the model calibration process with field testing results. Segment 2, however, was assumed very “stiff” since it represents half-section of the box-shaped main truss upper chord.

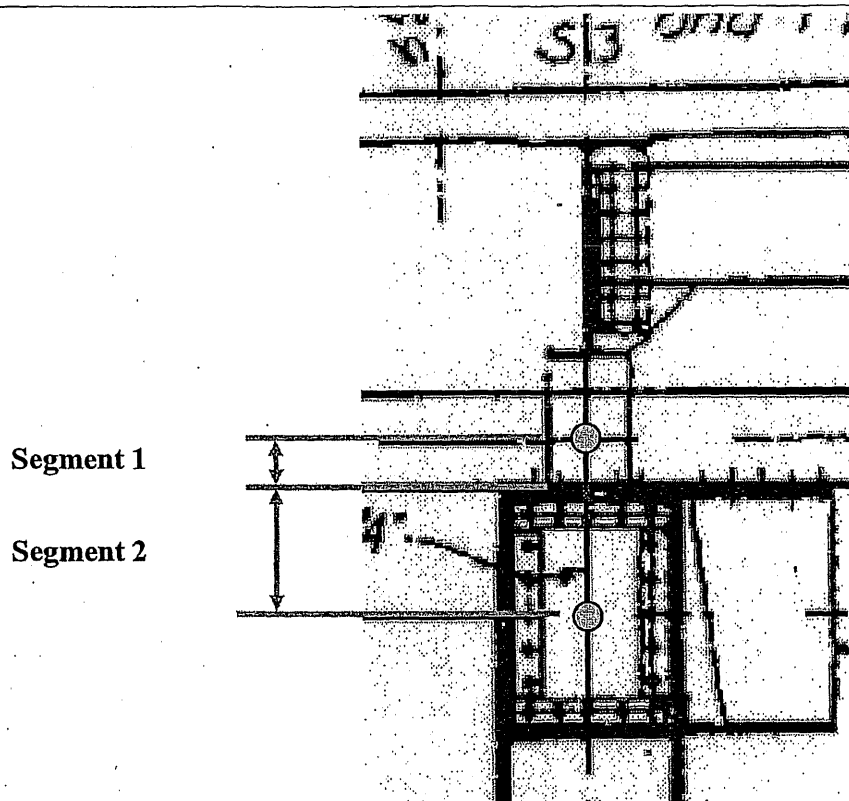


Figure 3-20: Modeling of Floor-Truss-to-Main-Truss Connection

3.1.14 Stringer Supports on Floor Trusses

As described previously in Section 3.1.8 and **Figure 3-11**, the stringers are supported on the floor truss upper chords by two types of supports: the fixed support and the expansion support. While the fixed supports were always treated as rigid connections in the model, two different conditions were investigated for the expansion supports: 1) the “as-designed” condition per original plans (**Figure 3-21** shows supports layout); and 2) the “locked” condition when all the connections become fixed.

For the “as-designed” condition, the expansion stringer-floor truss connections (the green dots in **Figure 3-21**) were released for longitudinal movement and rotation about the transverse axis while the fixed connections (the red dots in **Figure 3-21**) were rigid in the model. The layout of

BRIDGE 9340 STUDY



the stringer expansion supports is symmetric about the longitudinal centerline of the bridge and symmetric about the transverse centerline across the middle of the center span. An exception to the double symmetry occurs at Panel Point U14 where all north side connections are of expansion and the south side ones are fixed except two.

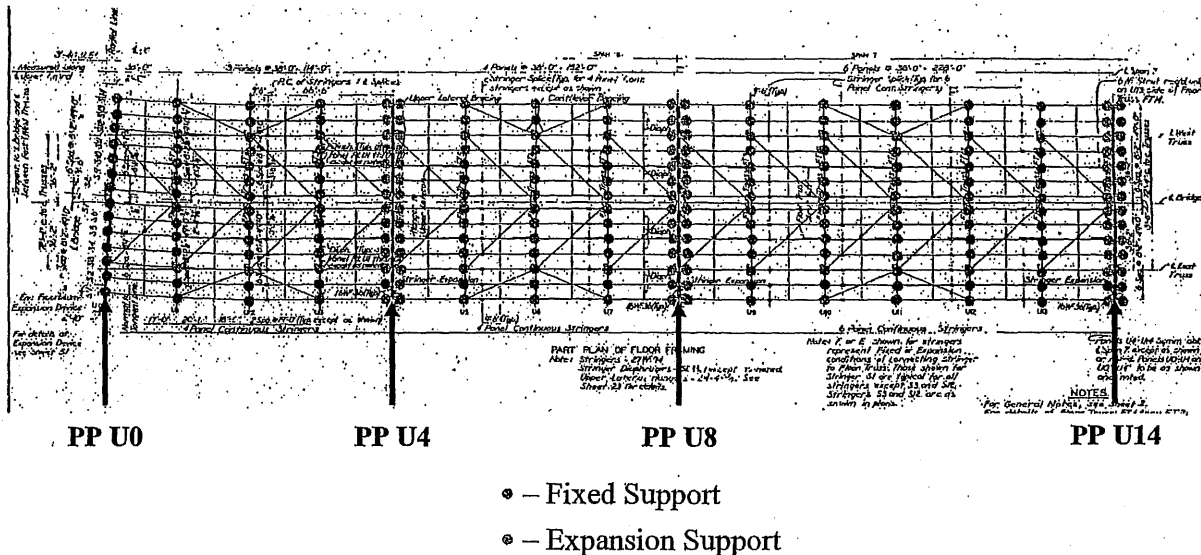


Figure 3-21: Half Stringer Support Layout at Floor Truss Locations (Symmetrical about PP 14)

The “locked” condition was based on the assumption that the stringer expansion bearings do not function as intended due to rust build-up over time. All the stringer-to-floor truss connections were defined as rigid in the model for this condition.

The fixity, or stiffness, of the stringer-floor truss connections is discussed in greater detail in Section 3.2 of the report.

3.1.15 Main Truss Bearings

As discussed in Section 2.2.3 and Section 2.5 previously, the main truss expansion bearings do not behave as intended in reality. Additionally, the actual force-displacement relationship of the bearings is nearly impossible to characterize. In the computer modeling, two extreme bearing

conditions were investigated for their impact: 1) the “as-designed” condition based on the plans; and 2) the fully “locked” condition.

For the “as-designed” condition in the computer model, the truss supports at Piers 5, 6, and 8 were released for longitudinal movement and rotation about the transverse axis and the supports at Pier 7 were fixed except for rotation about the transverse axis.

For the “locked” condition, all the truss supports were fixed for all translations and rotations based on the assumption that none of the main truss bearings would function as intended due to rust build-up. In this case, the piers were also included in the model for their contribution to the overall bridge system consisting of both the superstructure and the substructure.

The fixity, or stiffness, of the main truss bearings is discussed in greater detail in Section 3.2 of the report.

3.1.16 Piers

Piers were included in the model when the main truss expansion bearings were assumed to be fully locked. Piers 5 and 8 each consists of two columns supported on two separate footings with a strut connecting the top of the columns. Pier 6 is made of two columns supported by a pier wall, which in turn sits on top of a single footing that is supported by two rows of eleven battered caissons. Pier 7 is similar to Pier 6 except the individual footings are placed on concrete seals.

The piers were modeled with space frame members placed along the centerlines of the reinforced concrete columns and struts. Rigid link members were used as necessary, for example, to obtain the correct elevation of the truss bearings between the truss lower chords and the pier columns. Member and material properties were determined based on the original Contract A plans.

The support condition at the base of the piers varied with the location. Piers 5, 7, and 8 all have their footings founded directly on the bedrock. The model intended to correctly represent the actual support at the interface between the bottom of the footing and the bedrock. As shown in

Figure 3-22, the footing was also modeled with beam members in the longitudinal direction and the base support was defined with a pin at the center of the footing and two rollers at the heel and the toe, respectively.

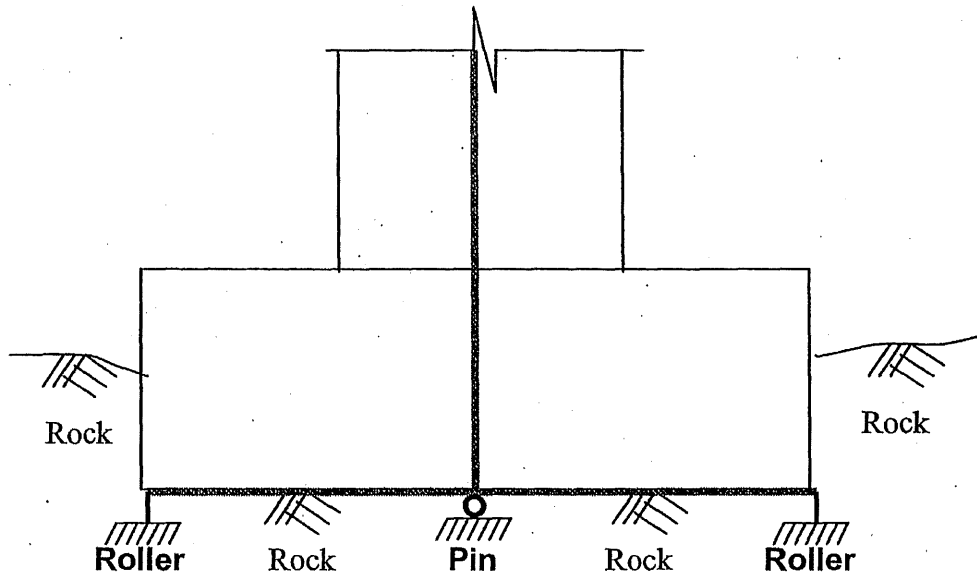


Figure 3-22: Modeling of Base Support of Piers 5, 7, and 8

At Pier 6, the footing is supported by two rows of eleven battered caissons which are embedded into the bedrock using sockets. In order to properly determine the support stiffness properties, the computer program FB-Pier was utilized for its ability to model the non-linear soil-caisson interaction. Figure 3-23 shows the FB-Pier model of Pier 6. The model includes two equivalent columns (each determined from the stiffness of a single column and half the wall), the footing, the battered piles, and the soil. The soil properties were determined from the boring logs per original plans and the soil model is shown in Figure 3-24. The top of soil elevation was assumed to be two feet above the top of the footing.

The purpose of the FB-Pier model was to determine stiffness properties of the caisson foundation, which would then be used to define the base support properties of Pier 6 in the GTSTRUDL model of the entire bridge. The model was also used to check the linearity of the foundation response to the loading forces applied at the top of the pier.

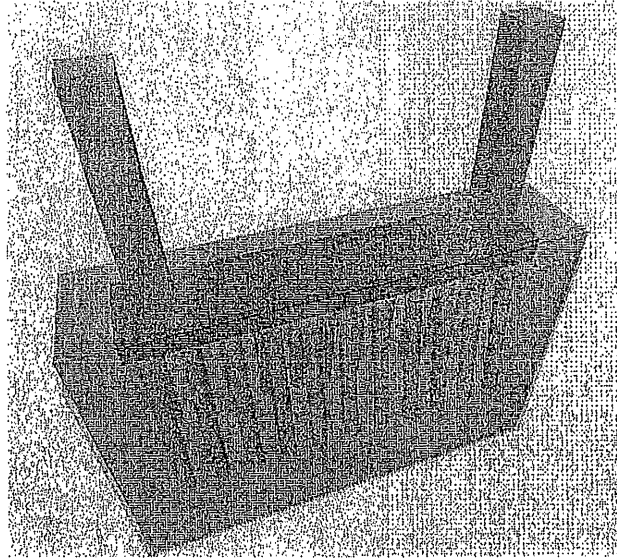


Figure 3-23: FB-Pier Model of Pier 6 Foundation



Figure 3-24: Soil Model of Pier 6 based on Boring Logs

Longitudinal forces of varying magnitude were applied at the top of the pier columns, as shown in **Figure 3-25**, and the response of the pier was studied in terms of translations and rotations at the top and the base.

The results of the FB-Pier model revealed that the displacement response of the foundation was linear to the longitudinal force applied at the top of the pier, up to 10% of the total vertical reaction force at Pier 6. It was also found that the translation at the base of the pier is negligible compared with that at the top of the pier. The rotation at the base of the pier, however, was found to make considerable contribution to the total translation at the pier top. As a result, a rotational stiffness about the transverse axis at the pier base was determined as the product of the total longitudinal force and the height of the column divided by the rotation at the column base. This rotational stiffness was assigned to the base support of Pier 6 in the global bridge model while all other degrees of freedom were assumed to be fixed at this support location.

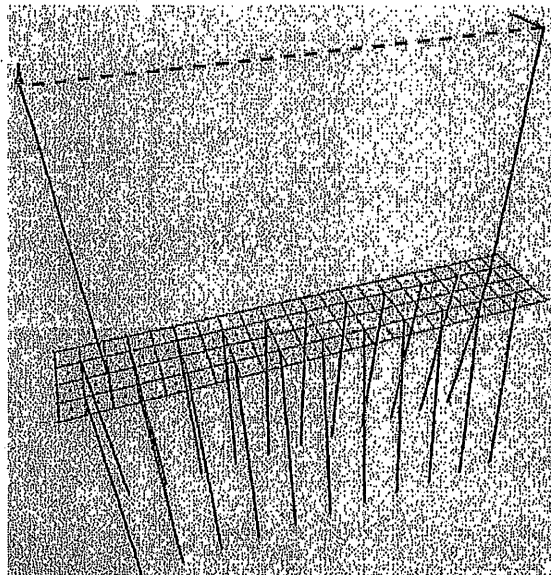


Figure 3-25: FB-Pier Model Loading - Longitudinal Forces at Top of Columns

3.1.17 Approach Spans

To properly consider the live load application onto the deck truss cantilever, the adjacent approach span was also included in the computer model at each end of the bridge, as shown in **Figure 3-1** and **Figure 3-2**. The approach span was modeled with space frame members for

longitudinal girders that frame into a cross girder at each end of the span. Each approach span was simply supported between the cantilever end of the truss and the next pier location, and was intended only for the purpose of live load transfer. The irregular geometric features due to the curvature and flaring at the ends of the bridge were ignored.

The weight of the approach spans was applied as concentrated forces at the truss cantilever end and is discussed further in Section 4.1 of the report.

3.2 Model Calibration per Field Testing Results

The computer model was compared with available strain gage test results of the bridge for truss member stresses under known loading conditions. Adjustments were made to the model for various support and connection stiffness properties to achieve a reasonable agreement with the test results.

The University of Minnesota (U/M), in conjunction with Mn/DOT, performed four separate strain gage tests, each with a unique tandem-axle dump-truck configuration. The live loads were applied, and strain gage data was recorded, for several bridge members. The test data from Test No. 4 was used for the computer model calibration because the University used this test in their model-test comparison. Test No. 4 was comprised of three groups of three trucks traveling side-by-side at highway speeds, in one direction at a time, along the centerlines of the three inside (fast) lanes. Each group of three trucks followed the previous group by no less than half a mile to ensure that only one group of trucks was on the bridge at a time. No lane closures were made, but the testing was conducted after midnight to minimize traffic interference. The truck weight and wheel configuration data were taken directly from U/M's report.

The model-test comparison was made for three main truss members in the west truss: lower chord L9-L10, upper chord U9-U10, and diagonal L9-U10, as highlighted in **Figure 3-26**. Three floor truss members were also used for the comparison: a lower chord, an upper chord, and a diagonal of Floor Truss No. 10, as highlighted in **Figure 3-27**.

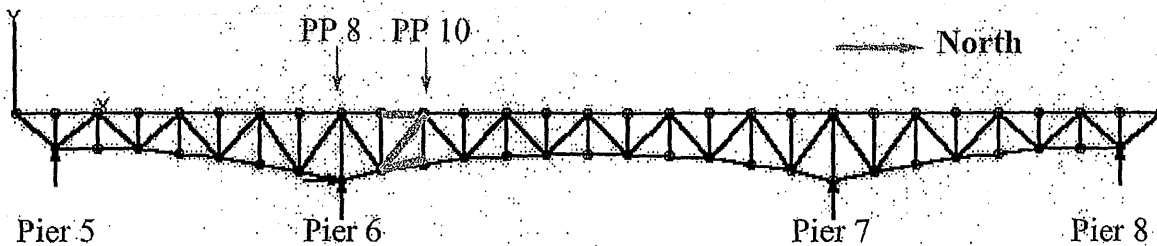


Figure 3-26: West Main Truss Members Used for Model-Test Comparison

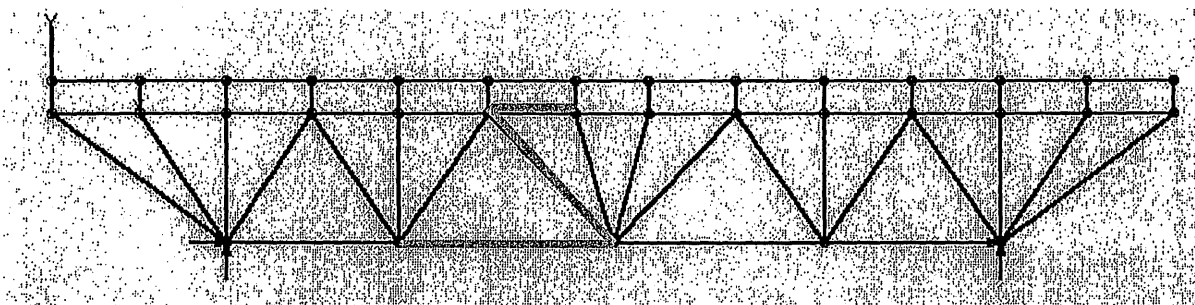


Figure 3-27: Members of Floor Truss No. 10 Used for Model-Test Comparison

To achieve the best agreement with the strain gage test results, the following properties of the computer model were adjusted systematically:

- Fixity of main-truss expansion bearings on piers
- Inclusion of piers in the model, when truss expansion bearings are fixed or pinned
- Fixity of stringer expansion bearings on floor trusses
- Stiffness of the shear links at the floor truss-to-main truss, stringer-to-floor truss, and stringer-to-deck connections

The University of Minnesota had previously developed relatively simplistic 2-D and 3-D computer models and compared with the strain gage test results. Those models, however, did not consider the longitudinal stiffness of the deck, and did not include stringers, sway bracing, lateral bracing, or substructure elements. The results of these models were also included in the comparison for reference purposes.

The model-test comparison was carried out in several progressive steps with varying combination of model properties. After each step, the model-test comparison results were reviewed and further adjustment made in the next step for improvement. The progressive model adjustments did result in improved agreement at each step and a reasonably good match at the end of the process. The model-test member axial stress comparison graphs of all steps of the comparison process are included in **Appendix I**. Key features of the comparison steps are described as follows.

Step 1: Superstructure-Only Model for Impact of Main Truss Bearing Condition (the results in this step are directly comparable with those of the U/M 2-D and 3-D models)

- Main truss expansion bearings varied between “roller” (as-designed) and “pinned” (translation locked) conditions
- Model included superstructure only
- All stringer expansion bearings on floor trusses were “rollers” (as-designed)
- All shear links were “rigid” (at the floor truss-to-main truss, stringer-to-floor truss, and stringer-to-deck connections)

Step 2: Superstructure-and-Substructure Model for Impact of Main Truss Bearing Condition

- Main truss expansion bearings varied between “pinned” and “fixed” conditions
- Model included superstructure and all piers
- All stringer expansion bearings on floor trusses were “fixed”
- All shear links were “rigid” (at the floor truss-to-main truss, stringer-to-floor truss, and stringer-to-deck connections)

Step 3: Superstructure-Only and Superstructure-and-Substructure Models for Impact of Longitudinal Shear Link Stiffness Affected by the Web of Floor Truss Top Chords

- Main truss expansion bearings varied between “roller” and “pinned” conditions for the Superstructure-Only model and “fixed” and “pinned” for the Superstructure-and-Substructure model

- Models included superstructure-only and superstructure-and-substructure
- All stringer expansion bearings on floor trusses were “fixed”
- The shear links at the stringer-to-floor truss (**Figure 3-18**) and floor truss-to-main truss (**Figure 3-20**) connections varied between “rigid” and longitudinally “softened” based on actual connection properties and web stiffness of the floor truss top chord. The shear links at the deck-to-stringer connections (**Figure 3-17**) were “rigid”.

Step 4: Superstructure-and-Substructure Model for Impact of Shear Link Stiffness Affected by the Web of Stringers and the Stringer Expansion Bearing Fixity

- Main truss expansion bearings varied between “pinned” and “fixed” conditions
- Models included superstructure-and-substructure
- Stringer expansion bearings on floor trusses varied between “fixed” and “released”
- The shear links at the stringer-to-floor truss and floor truss-to-main truss connections were longitudinally “softened” based on connection properties and web stiffness of the floor truss top chord. The shear links at the deck-to-stringer and stringer-to-floor truss connections were transversely “softened” based on connection properties and web stiffness of the stringer.

3.3 Summary

Based on the model-test comparison and calibration process described above, the following conditions of the computer model were determined to yield the best prediction of truss member forces for Bridge 9340:

- All main truss expansion bearings were completely fixed at the piers. This is different from the “as-designed” condition.
- The substructure was included for the stiffness of all piers and their foundations.
- All stringer expansion bearings were completely fixed at the floor truss and end floor beam locations. This is also different from the “as-designed” condition.

- The shear links at the stringer-to-floor truss and floor truss-to-main truss connections had a longitudinal stiffness that reflects the low out-of-plane web stiffness of the floor truss top chord and the actual connection properties.
- The shear links at the deck-to-stringer and stringer-to-floor truss connections had a transverse stiffness that reflects the low out-of-plane web stiffness of the stringer and the actual connection properties.

SECTION 4

4. STRENGTH EVALUATION OF TRUSS MEMBERS

4.1 Member Capacities

The member capacities are necessary to evaluate the effects of the loads on the structure. As a part of the overall analysis of Bridge 9340, URS determined the axial and moment capacity of the main truss, floor truss, portal and sway frame, upper lateral bracing, lower lateral bracing, and stringer members in the steel truss system. This task was approached using Excel spreadsheets to describe members, section properties, lengths, and to compute capacities in tension, compression, and bending. Data was compiled from a variety of sources including the original plan set, shop drawings, and photos of the existing bridge.

In traditional truss design the members are designed based on axial load without bending moment. For this assumption, only the axial capacity of the truss members would be required. This is how the original design of Bridge 9340 would have been done. In reality the connections of the main truss members are not "pinned" connections which means these members would in actuality be subjected to bending moments. This behavior has been neglected in the past by assuming that the bending caused by cambering the structure is completely counteracted by the moments caused by the application of the non-composite and the composite dead load. This may not necessarily be true, but can be investigated with the use of the 3-D computer model. In order to account for the bending in the truss members, an interaction equation was used that included the effects of axial load, in-plane bending, and out-of-plane bending. The interaction is discussed in more detail in the following sections.

4.1.1 Main Truss Members

The interaction equations are taken from the AASHTO *Guide Specifications for Strength Design of Truss Bridges (Load Factor Design)* (1985 with 1986 interims). Both ends of the members

were checked. The choice of which pair of interaction equations to use depends on whether the member is in tension or compression.

Various member properties are required for the interaction equations. These properties are based on the plate sizes and dimensions given on the original Contract B plan set. Sheet 20 includes a "Table of Truss Members and Stresses" which tabulates member plate sizes as well as some properties. Additional details are provided on sheets 28 through 31. Available shop drawings were used to verify some plate dimensions as noted in **Section 2.4**.

The interaction equations used for tension members are:

$$\frac{P}{(F_y)(A_n)} + \left[\frac{M}{(S_n)(F_y)(f)} \right]_{(in-plane)} + \left[\frac{M}{(S_n)(F_y)(f)} \right]_{(out-of-plane)} \leq 1.0 \quad (\text{Eq. 4-1})$$

$$\frac{P}{(F_u)(A_n)} + \left[\frac{M}{(S_n)(F_u)(f)} \right]_{(in-plane)} + \left[\frac{M}{(S_n)(F_u)(f)} \right]_{(out-of-plane)} \leq 1.0 \quad (\text{Eq. 4-2})$$

where, P = Axial Load in the Member determined from the computer models

F_y = Yield Point of Steel

Yield and Ultimate strength was determined from the original construction plans and varies based on plate thickness.

MHD 3306:	$F_s=20$ ksi	$F_y=36$ ksi	$F_u=58$ ksi
MHD 3309:	$F_s=27$ ksi	$F_y=50$ ksi	$F_u=70$ ksi
MHD 3310:	$F_s=27$ ksi	$F_y=50$ ksi	$F_u=70$ ksi (Thickness $\leq 3/4$ ")
	$F_s=24$ ksi	$F_y=45$ ksi	$F_u=60$ ksi ($3/4$ " < Thickness $\leq 1 1/2$ ")
	$F_s=22$ ksi	$F_y=40$ ksi	$F_u=58$ ksi ($1 1/2$ " < Thickness ≤ 4 ")

The members comprised of high strength structural steel plates are either MHD 3309 or MHD 3310. Any plate thicker than $\frac{3}{4}$ " is MHD 3309 and any plate $\frac{3}{4}$ " or thinner is MHD 3310. This means that all the high strength structural steel plates have the same F_s , F_y , and F_u values. All the remaining members are MHD 3306.

A_n = Net Area

The calculation of the net area for the capacity checks depends on the type of member that is being checked. The following paragraphs detail what was used in the capacity checks.

The main truss members have three different cross-sections: box without center web, box with center web, and H-section. Additionally, some of these members have perforations. As noted on Sheet 21 of 94 of the Contract B plans for the bridge, the upper chord box members have perforations in one cover plate only, and the lower chord, vertical, and diagonal box members have perforations in both cover plates. In members with two perforated cover plates, the perforations are aligned such that a section cut perpendicularly through the member will go through two perforations or no perforations. The net area for truss members is determined per Section 1.7 of the AASHTO *Guide Specifications for Strength Design of Truss Bridges*. This section states "The provisions of Articles 10.18 and 10.16.14 shall apply as amended herein. For built-up members, the determination of the amount of area to be deducted shall be made on each component part separately, and the net section of the whole member shall be the sum of the net sections of the separate parts, so calculated. Hand holes and perforations shall be deducted from the gross section in their entirety before applying the provisions of Articles 10.18 and 10.16.14 or this section". Section 10.18.4.1 of AASHTO *Standard Specifications for Highway Bridges (2002)* states that the net section of the members shall be computed as specified in Article 10.16.14. Article 10.16.14 .1 states "The net section of a riveted or high-strength bolted tension member is the sum of the net sections of its component parts. The net section of a part is the product of the thickness of the part multiplied by its least net width". Based on these provisions, the net area is determined

by calculating the gross area of the cross-section and subtracting the area of one (upper chord) or two (lower chord, vertical, and diagonal) perforations for the box truss members. For the H-sections, no perforations are present so the net area is equal to the gross area. For the box sections with center webs, the center webs are not perforated. The box member section properties are different than the section properties calculated for the computer model as discussed in Section 3. For the computer model, the box member properties were calculated based on removing a single perforation to create an average member property that would approximate the actual condition of alternating sections that have two and zero perforated cover plates. The length of each member that has two perforations and zero perforations is approximately equal, justifying the use of an average property. The capacity checks were done based on the worst possible case cross-section, which is taken at a location where two perforated cover plates are located. No deductions are made for the rivet holes because holes are only present at the gusset plate connections at the panel points. The strength of the connections will be checked separately.

M = Moment in member determined from the computer models, in-plane and out-of-plane considered separately.

$(S_n)(F_y)(f)$ = Product of the net section modulus, yield point of steel, and plastic shape factor. This product is equivalent to the product of the plastic section modulus (Z) and the yield point of steel (F_y). The plastic shape factor is equivalent to M_p/M_y which is equivalent to $(Z F_y)/(S_n F_y)$. Substituting $(Z F_y)/(S_n F_y)$ for f yields (Z) (F_y). Z is calculated with the perforations removed where appropriate for the main truss members and the rivet holes being partially accounted for in the portal frame, sway frame, upper lateral bracing, and lower lateral bracing member calculations.

F_u = Ultimate strength of steel

This has been discussed previously under F_y .

A_n = Net area with all holes removed. The net area with all holes removed is essentially A_n , with all the rivet holes removed. For consistency with the original design, this value was set equal to the net area listed in the "Table of Truss Members and Stresses" on sheet 20 of the Contract B plans.

$(S_n)(F_u)(f)$ = Product of the net section modulus with all holes removed, ultimate strength of steel, and plastic shape factor. This product will be assumed to be equivalent to the net section modulus with all holes removed (S_n), multiplied by the plastic section modulus (Z) and the ultimate strength of the steel (F_u), and divided by the net section modulus (S_n). In order to simplify the calculations, S_n is assumed to be equal to S_n , and Z is determined as discussed previously.

The interaction equations used for compression members are:

$$\frac{P}{0.85A_{ge}F_{cr}} + \left[\frac{MC}{M_u \left[1 - \frac{P}{A_{ge}F_e} \right]} \right]_{(in-plane)} + \left[\frac{MC}{M_u \left[1 - \frac{P}{A_{ge}F_e} \right]} \right]_{(out-of-plane)} \leq 1.0 \quad (\text{Eq. 4-3})$$

$$\frac{P}{0.85A_{ge}F_y} + \left[\frac{M}{M_p} \right]_{(in-plane)} + \left[\frac{M}{M_p} \right]_{(out-of-plane)} \leq 1.0 \quad (\text{Eq. 4-4})$$

where all repeated terms are as defined previously and,

A_{ge} = Gross effective area. For the main truss members, the perforation area where present, must be subtracted from the gross area to obtain the gross effective area. The area of the rivets should not be subtracted to determine this area.

F_{cr} = Critical load per AASHTO 10.54.1.1 with a suitable effective length factor, K .

$$\frac{K \cdot L_c}{r} > \sqrt{\frac{2 \cdot \pi^2 \cdot E}{F_y}} \quad F_{cr} = \frac{\pi^2 \cdot E}{\left(\frac{K \cdot L_c}{r}\right)^2}$$

$$\frac{K \cdot L_c}{r} \leq \sqrt{\frac{2 \cdot \pi^2 \cdot E}{F_y}} \quad F_{cr} = F_y \left[1 - \frac{F_y}{4 \cdot \pi^2 \cdot E} \cdot \left(\frac{K \cdot L_c}{r}\right)^2 \right]$$

$K = 0.75$ For riveted connection (Article 10.54.1.2(a) of Standard Specifications)

L_c = length of member from panel point to panel point

$r = \sqrt{\frac{I}{A_n}}$ where I is calculated with the perforations removed

C = Equivalent moment factor taken as 0.85 or 1.00 as appropriate. When a member is in single curvature 1.00 is used, and when a member is in double curvature 0.85 is used.

$$F_e = \frac{(0.85)(\pi^2)(E)}{\left(\frac{KL}{r}\right)^2}$$

$M_p = (F_y)(f)(S_{ge})$ which is equivalent to $(F_y)(Z)$ where (Z) has been calculated with the perforations removed where present.

M_u = Maximum Bending Strength Reduced for Lateral Buckling.

For Box Shaped Members:

$$M_u = F_y \cdot S_{ge} \cdot \left(1 - 0.0641 \cdot \frac{F_y \cdot S_{ge} \cdot L \cdot \sqrt{\sum \left(\frac{s}{t} \right)}}{E \cdot A \cdot \sqrt{I_y}} \right)$$

F_y = Steel yield strength

S_{ge} = Gross effective section modulus about bending axis

L = Length of member

s/t = Length of a side divided by its thickness

A = Area enclosed within centerlines of plates of the box member

For H-Shaped Members Bending About Minor Axis:

$$M_u = 1.5 F_y S_{ge}$$

For H-Shaped Members Bending About Major Axis:

$$\sigma_{cr} \leq 0.5 F_y, \quad M_u = \sigma_{cr} S_{ge}$$

$$\sigma_{cr} > 0.5 F_y, \quad M_u = F_y S_{ge} [1 - F_y / (4 \sigma_{cr})]$$

$$\sigma_{cr} = \frac{1}{S_{ge}} \cdot \sqrt{\frac{\pi^2 \cdot E \cdot I_y \cdot G \cdot J}{(K \cdot L)^2} + \frac{\pi^4 \cdot h^2 \cdot I_y^2 \cdot E^2}{4 \cdot (KL)^4}}$$

G = Shear modulus

J = St. Venant torsional constant, approximately $\Sigma bt^3/3$

K = Effective length factor for column buckling about weak axis

h = Depth of web plate plus flange thickness

4.1.2 Floor Truss Members

The interaction equations for the floor truss members were calculated in a similar manner as the main truss members. The floor truss member details are shown on sheets 24 and 25 of the Contract B plans. Important differences to note about the floor truss members are as follows:

A_n = Net Area

All of the floor truss members are wide-flange sections and have no perforations. Most of the connections between the floor truss members are welded, with the exception being the upper chord bolted splices where the section changes. The net area for the floor truss members equals the gross area. This matches the computer model section properties.

A_n^- = Net area with all holes removed. The net area with all holes removed is essentially A_n , with all the rivet holes removed. For the floor truss members, perforations and rivets are not present, so $A_n^- = A_n$.

A_{ge} = Gross effective area. For all members except the Main Truss members, this is equivalent to the gross area of the section. The area of the rivets should not be subtracted to determine this area.

4.1.3 Secondary Members

The interaction equations for the secondary members were calculated in a similar manner as the main truss members. The portal and sway frame member details are shown on sheets 32 and 33, the upper and lower lateral bracing member details are shown on sheets 20 and 28, and the stringer member details are shown on sheet 23 of the Contract B plans. Important differences to note about the secondary members are as follows:

A_n = Net Area

The portal and sway frame strut members are all box sections. The side plates have rivet holes where they are connected to the main truss members and at the center of the bridge. The rivet holes have been removed. This differs from the computer model where the gross area was used; however, for checking capacity, this is a more appropriate method. These members do have some perforations, but they have been ignored since they are only at select locations and used for drainage and access.

The upper and lower lateral bracing members are also all box sections. The top plates have rivet holes where they are connected to the main truss members and the floor trusses at the center of the bridge. These rivet holes have been removed. Again, this differs from the computer model where the gross area was used, but this is a more appropriate method for checking capacity. These members do have some perforations, but they have been ignored since they are only at select locations and used for drainage and access.

The stringers have no perforations or rivet holes, so no subtraction from the gross area is necessary. The net area for the stringers equals the gross area. This matches the computer model section properties.

A_n = Net area with all holes removed. For the portal and sway frame strut members, and the upper and lower lateral bracing members, this value has been set equal to the effective area calculated from AASHTO 10.18.2.2.4 for flange splices in flexural members. The effective area is the minimum of either the gross area, or the sum of the net area plus fifteen percent of the gross area. For the stringer members, perforations and rivets are not present, so $A_n = A_g$.

A_{ge} = Gross effective area. For all members except the main truss members, this is equivalent to the gross area of the section. The area of the rivets should not be subtracted to determine this area.

4.2 Truss Member Forces Under Camber and Dead Loads from 3-D Analysis

The camber and dead load forces included in the 3-D computer model were incorporated in such a way as to mimic the fabrication process of the bridge to give a realistic representation of the member forces in the truss. In design, the camber forces are typically neglected. Ideally, after the non-composite and composite dead loads are applied the bending moments would be zero. The cambering process does not induce significant axial forces in the members. However this cancellation effect may not actually occur to the full extent because of the nature of 3-D behavior. The camber and dead loads and forces are investigated in more detail in the following sections to determine how much force and moment the cambering process causes, whether or not the camber bending moments are counteracted by the dead load moments, and how the dead load interaction compares with the original design axial force to allowable load ratio.

It is important to note that the loads discussed in the following sections are based on the current existing condition. Additional dead load was added to the structure in 1977 and 1998 which is discussed in more detail in **Section 4.2.3**.

4.2.1 Camber Loads from 3-D Analysis

The cambering of the main trusses and floor trusses was included in the models as a load to account for the built-in forces this process would induce. To create the cambered shape, the main truss members were manufactured either too long or too short. These members were connected to the gusset plates by forcing the connections to align. The gusset plates are drilled based on the final geometry of the structure, not the cambered geometry. This force-fit creates the cambered shape of the structure and induces loads in the members. The main trusses, floor trusses, portal and sway frames, lower lateral bracing, upper lateral bracing, cantilever bracing, and end floorbeam members were all included in the model while the stringers, floor truss bracing, and deck were excluded. This is because the camber is induced into the structure prior to the placement of these members. The main truss bearings were assumed to function as-designed since the camber is applied during the construction phase when the bearings are most likely to behave as originally intended.

The theoretical main truss camber is shown on the "Dead Load Camber Diagram" on Sheet 21 of the Contract B plans (see **Figure 4-1**). Members are either lengthened or shortened to create the geometric shape of the main truss. The blocking dimensions are the positions of the upper chord joints above or below the geometric shape to provide for dead load deflections. When the truss members are manufactured with the length adjustments noted on the dead load camber diagram, and force-fit into the connections, the truss will take on the cambered shape which corresponds to the dead load blocking diagram values. The theoretical floor truss camber is noted on Sheet 22 as ½" parabolic camber at the centerline of each floor truss for a length between the center to center of the main trusses only.

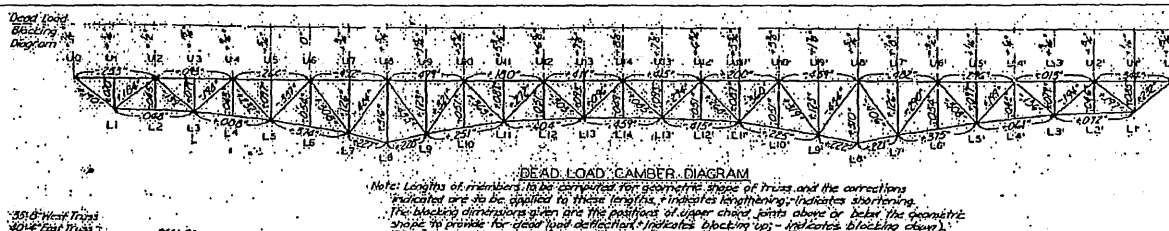
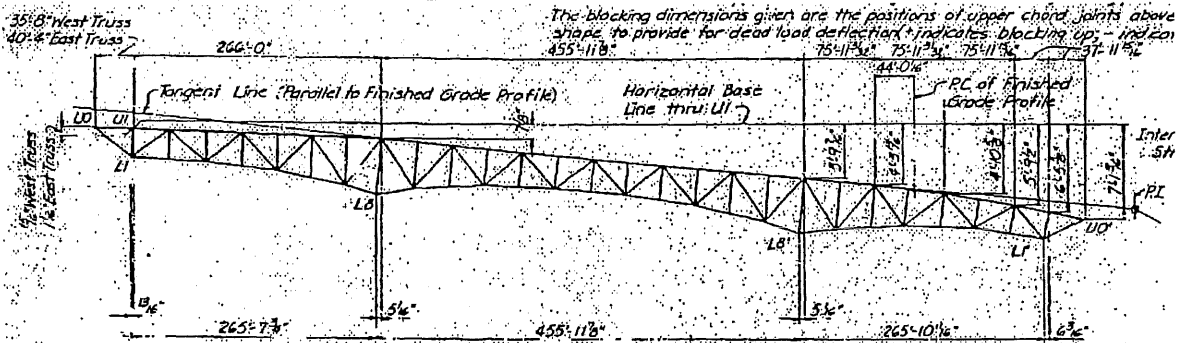


Figure 4-1: Dead Load Camber Diagram for Main Truss

Manufactured main truss camber values were determined from the available shop drawings (see Section 2.4). The shop drawings do not include camber diagrams, so the main truss manufactured camber was calculated as the difference between the manufactured length and the panel point to panel point length. Manufactured floor truss camber values were also determined from the available shop drawings (see Section 2.4). Camber diagrams are included on the shop drawings for these members.

Theoretical camber values were compared with manufactured values for the main truss and floor truss members to ensure that no significant differences were present. As noted in Section 2.4, some discrepancies were found for the following main truss members: L7-L8, L5'-L3', L3'-L1', U6'-L6', U4'-L4', and U2'-L2'. These discrepancies were determined to be due to adjustments from the leveled geometry to the final profile geometry (see Figure 4-2) and were verified by a geometric analysis. Since the slope of the bridge has previously been neglected, these discrepancies were also neglected. For all the floor trusses with available shop drawings, the theoretical geometry matched the manufactured geometry.



TRUSS LAYOUT

Note: Dimensions of truss shown for this layout and dimensions shown on Elevation of Truss, Sheet 20, are for the geometric shape after calculated deflection has occurred.

All chords are to be straight between splice points. The distance center to center of panel points measured along the \pm of upper chord to be 30'-0".

Posts, hangers and floor trusses from U1 thru U7 and at U5 are normal to upper chord; all others are normal to Finished Grade Profile.

Figure 4-2: Truss Layout

Shop drawings were not available for main truss members U12-U14, U14-U12', U6'-U4', U4'-U2', L13-L13', L7'-L5', and L3'-U2'. Manufactured camber values were estimated for all of these members except L3'-U2' using the laydown and reaming layout shop drawings (Sheets RA1 thru RA3 of Roll V-36). Shop drawings were not available for floor truss members FT12, FT13, FT14, FT15 (PP 13'), FT16 (PP 12'), FT18 (PP10'), FT19 (9'), FT23 (PP 5'), and FT24 (PP 4'). By inspection, the camber diagrams on the available shop drawings for FT8-FT14 and FT13'-FT1' are the same and the camber diagrams for FT1-FT7 are similar. Due to this similarity, it was assumed that the floor trusses with missing shop drawings were cambered in a similar manner.

The camber was included in the computer models as a uniform axial distortion load. This type of load models the initial strain in the members due to the lengthened or shortened members fit into the geometric layout. The load is applied uniformly to the entire length of the member and is equal to the change in the member length due to camber divided by the member panel point to panel point length. Since the theoretical camber was found to equal the manufactured camber for both the main truss and floor truss members, either set of values could have been used, but the theoretical values were chosen.

The unfactored member forces for the east main truss due to the camber are listed in **Table AII-1** in **Appendix II**. The values for the west truss are the same due to symmetry. The maximum axial load is about 80.8 kips (L13-L14), with the majority of members having axial forces less than 15 kips. The maximum out-of-plane bending moment is about 86.3 kip feet (U13-L13), with the majority of members having out-of-plane bending moments less than 20 kip feet. The vertical members tend to have higher out-of-plane bending moments between 30 and 40 kip feet. The maximum in-plane bending moment is about 480.0 kip-feet (L7-L8), with the majority of members having in-plane bending moments less than 50 kip feet. The upper and lower chord members tend to have higher in-plane bending moments with about seventy percent of the members having in-plane bending moments ranging between 50.0 and 480.0 kip feet. As predicted, the axial loads in the members due to camber are low, but the bending moments can be significant.

Both the main truss and floor truss camber application was checked using simplistic models. The main truss camber was checked using a model comprised of only a single plane of the truss and applying the theoretical camber. The application of this load resulted in joint deflections approximately equal to the ordinates of the dead load blocking diagram verifying the camber was applied correctly. The floor truss camber was verified in a similar manner using a model comprised of a single floor truss. The deflections due to the camber load approximated the camber diagram ordinates given on the shop drawings.

4.2.2 Non-Composite Dead Loads from 3-D Analysis

The non-composite portion of the dead load is the self-weight of the entire structure prior to the hardening of the deck concrete. At this stage, the deck concrete is present as a load only and does not contribute to the stiffness of the structure. The main truss bearings and the stringer bearings are assumed to act as-designed because the non-composite loads are applied during construction.

Member releases are applied to the rigid links connecting the deck to the stringers in the model to achieve the non-composite behavior of the deck. The longitudinal and transverse forces in the plane of the deck were released at deck level. Also released were the moments about the longitudinal and transverse axes in the plane of the deck. In order to maintain stability in the model, a single transverse line of rigid links in each continuous deck unit was left unreleased. The locations of these lines of fixity correspond to the panel points where stringers S3 and S12 are fixed: U0, U6, U11, U11', U6', and U0'.

The loads carried by the non-composite structure are the self-weight of the entire steel superstructure, the weight of the wet deck concrete, the ½" wearing surface which is cast integral with the deck but is not structural, and the weight of the approach spans based on the original plans and excluding any retrofits.

Based on an analysis of the deflection and member forces, as well as information on the shop drawings about the shipping sequence, it was determined the weight of the approach spans would be carried by the non-composite section. This seems likely because the approach spans could be used as a staging area to pour the main truss spans if they are poured first.

Some assumptions were made for the non-composite dead loads:

- The weight of the gusset plates, bolts, and nuts were assumed to be accounted for by the overlap of members since they are defined by joints at the centerlines of the members.
- A 1.02 detail factor was applied to all the members to account for miscellaneous items not directly included in the model such as the inspection walkways and the portions of the deck concrete discounted to model the transverse deck joints.
- For calculating the approach span load, the main trusses were assumed to carry the weight of the entire cross-girder and half of the approach span (including superimposed loads on approach spans) for each of the adjacent spans. The load is based on the original structure, not the retrofits.

The unfactored member forces for the east main truss due to the non-composite dead loads are listed in **Table AII-2** in **Appendix II**. The west main truss values are the same due to symmetry. The maximum axial load is about 2138.9 kips (L8-L9). The maximum out-of-plane bending moment is about 139.2 kip feet (U8'-L8'). The maximum in-plane bending moment is about 496.6 kip-feet (L7-L8).

4.2.3 Composite Dead Loads from 3-D Analysis

The composite portion of the dead load is all the superimposed dead load that is placed after the hardening of the deck concrete. At this stage, the deck concrete does contribute to the stiffness of the structure. The main truss bearings and the stringer bearings are again assumed to act as-designed because the composite loads are applied during construction. As previously noted in **Section 3.1.10** in the discussion of the deck elements, the deck is based on the 1998 retrofit configuration rather than the original deck.

The loads carried by the composite structure are the weight of the existing wearing surface after the 1977 repairs, the weight of the existing curb and barrier including the additional barrier added during the 1998 repairs, the weight of the existing center median and precast median cap that were added during the 1998 repairs, and the additional weight on the approach spans that was added during the 1998 repairs. The effects of the original curb and barrier weight and original median and guardrail weight were also considered to check the behavior of the model.

The unfactored member forces for the east main truss due to the non-composite dead loads are listed in **Table AII-3** in **Appendix II**. The west main truss values are the same due to symmetry. The maximum axial load is about 768.7 kips (L8-L9). The maximum out-of-plane bending moment is about 46.8 kip feet (U13'-L13'). The maximum in-plane bending moment is about 149.6 kip-feet (L7-L8).

4.2.4 Total Dead Loads from 3-D Analysis

The total dead load was obtained by summing the values from the camber loads, non-composite dead loads, and composite dead loads. As noted previously, the total dead load is based on the current existing condition which includes the additional weight placed during the 1977 and 1998 repairs. This means that the dead loads on the structure in the current condition are greater than the design dead load forces shown on Sheet 20 of the Contract B plans.

In order to check the behavior of the model under total dead load, the dead load reactions were investigated for three cases: 1) the design dead load reactions specified on Sheet 20 of the Contract B plans; 2) the dead load reactions from the 3-D model assuming the original dead loads based on the Contract B plans; and 3) the dead load reactions from the 3-D model assuming the existing dead load based on the current in-service condition. The results are summarized in **Table 4-1**. The results indicate that the 3-D model is predicting the total dead load rather well for the original design condition, with the 3-D model results between 5% and 7% less than the design reactions. The sum of the total dead loads in the 3-D model is about 6% less than the sum of the total design dead loads. As expected, the 3-D model results based on the current existing condition are greater than both the original design results and the 3-D model results based on the original design dead loads. The results from the 3-D model based on the existing conditions are between 14% and 18% greater than the results from the original design dead load. The total dead load predicted by the 3-D existing condition model is about 15% larger than the total dead load from the original plans. The final comparison in the table is between the results from the two different 3-D models. The results from the 3-D model based on the existing condition are between 22% and 25% greater than the results from the 3-D model based on the original condition. Based on these findings, the 3-D model appears to be predicting the total dead load behavior accurately.

Table 4-1: Summary of Total Dead Load Reactions

Summary of Total Dead Load Reactions							
Truss	Pier	Design Reactions From Plans	3D Model Reactions Based On Plans	Ratio: 3D Model / Plans	3D Model Reactions Based On Existing Conditions	Ratio: 3D Model / Plans	Ratio: 3D Model Exist. / 3D Model Plans
		(kips)	(kips)		(kips)		
East	5	1098.00	1038.99	0.946	1298.12	1.182	1.249
	6	3660.00	3428.59	0.937	4181.54	1.142	1.220
	7	3589.00	3363.18	0.937	4104.05	1.144	1.220
	8	1446.00	1383.91	0.957	1706.79	1.180	1.233
West	5	1098.00	1038.78	0.946	1298.12	1.182	1.250
	6	3660.00	3427.60	0.937	4181.54	1.142	1.220
	7	3589.00	3362.42	0.937	4104.05	1.144	1.221
	8	1446.00	1383.68	0.957	1706.79	1.180	1.234
Total		19586.00	18427.16	0.941	22580.98	1.153	1.225

The unfactored member forces for the east main truss due to total dead loads are listed in **Table AII-4** in **Appendix II**. The west main truss values are the same due to symmetry. The maximum axial loads for the upper chords, lower chords, diagonals, and verticals are 2172.7 kips (U13'-U12'), 2923.3 kips (L8-L9), 2000.2 kips (L9-U10), and 2898.9 kips (U8-L8) respectively. The maximum out-of-plane bending moments for the upper chords, lower chords, diagonals, and verticals are 67.0 kip feet (U1'-U0'), 8.3 kip feet (L8-L9), 59.7 kip feet (L9-U10), and 163.3 kip feet (U8'-L8') respectively. The maximum in-plane bending moments for the upper chords, lower chords, diagonals, and verticals are 504.5 kip feet (U1'-U0'), 166.3 kip feet (L7-L8), 251.5 kip feet (L1'-U0'), and 42.9 kip feet (U14-L14) respectively. **Tables AII-5** thru **AII-7** in **Appendix II** respectively include breakdowns of the axial load, out-of-plane bending moment, and in-plane bending moment for camber, non-composite dead load, and composite dead load.

For axial load, the non-composite dead load is the primary contributor as shown in **Table AII-5**. The camber load does not contribute much to the axial load except in the upper and lower chords

near the midspan; however, at these locations the camber axial load is insignificant when compared to the non-composite axial dead load.

For the out-of-plane bending moment either the camber or the non-composite dead load is the primary contributor as shown in **Table AII-6**. In a few random upper and lower chord members the composite dead load is the primary contributor; however, for these members the total out-of-plane bending moment is negligible. The out-of-plane bending moment due to camber is not always counteracted by the dead load moments. This can be seen in member U8'-L8' where the maximum out-of-plane bending moment occurs. At this joint of this member all three components are additive and camber accounts for almost 30% of the total out-of-plane bending moment.

For the in-plane bending moment either the camber or the non-composite dead load is the primary contributor as shown in **Table AII-7**. In a few random vertical members the composite dead load is the primary contributor; however, for these members the total out-of-plane bending moment is negligible. For the maximum values that occur for each of the member types, two conditions apply: 1) the moment due to camber is small relative to the total moment (U1'-U0', L1'-U0', and U14-L14); or 2) the moment due to camber and the moment due to non-composite dead load are almost equal and opposite and effectively cancel each other out.

Based on the results in **Tables AII-5** thru **AII-7**, the 3-D analysis indicated that after applying all the dead loads the member end moments due to camber were not always counteracted by the dead load effects, and sometimes significant bending moments may still remain. This indicates that the bending effect cannot be neglected and the members should be investigated utilizing the force interaction ratio.

The force interaction ratio for the total dead load was calculated for three cases:

- Case 1 unfactored load and ultimate capacity
- Case 2 LFD factored load and ultimate capacity
- Case 3 LRFD factored load and capacity

Case 1 has no load or resistance factors applied in order to evaluate the actual loads versus the actual capacity. The capacities were determined as discussed in Section 4.1 and the interaction is the higher of the two values determined from the equation pairs of Equation 4-1 and 4-2 or Equation 4-3 and 4-4.

Case 2 has the Load Factor design method load factors applied, which yields a value of 1.3 applied to the camber, non-composite dead load, and composite dead load. This method is consistent with the AASHTO *Guide Specifications for Strength Design of Truss Bridges (Load Factor Design)* (1985 with 1986 interims). The capacities were determined as discussed in Section 4.1 and the interaction is the higher of the two values determined from the equation pairs of Equation 4-1 and 4-2 or Equation 4-3 and 4-4.

Case 3 has the Load and Resistance Factor Design method load and resistance factors applied. This method is consistent with the current design philosophy in the state of Minnesota. Any redecking design would most likely be done utilizing this method. The basic equation of the LRFD method is:

$$\sum \eta_i \gamma_i Q_i \leq \phi R_n = R_r \quad (\text{Eq. 4-5})$$

where $\eta_i = \eta_D \eta_R \eta_I \geq 0.95$ for loads for which a maximum γ_i is appropriate

or $\eta_i = \frac{1}{\eta_D \eta_R \eta_I} \leq 1.0$ for loads for which a minimum γ_i is appropriate

γ_i = load factor

ϕ = resistance factor

η_i = load modifier relating to ductility, redundancy, and operational importance.

A value of $\eta_i = 1.05$ was determined assuming a maximum γ_i to maximize dead load, $\eta_D = 1.00$ for conventional designs, $\eta_R = 1.05$ for nonredundant members, and $\eta_I = 1.00$ for typical bridges. According to the LRFD method, the permanent load factor, γ_p , varies based on the portion

considered. The camber loads are considered to be “locked-in erection stresses”, therefore $\gamma_p = 1.0$. All the dead load excluding the wearing surface is considered as “components and attachments”, therefore $\gamma_p = 1.25$ or 0.90 . The maximum value of 1.25 was chosen in order to maximize the dead load effect. The wearing surface is considered as separate permanent load with $\gamma_p = 1.50$ or 0.65 . This is most likely due to the fact that it is difficult to know the thickness of the eventual wearing surface on a bridge. Since the thickness for this structure is fairly well known a value of $\gamma_p = 1.25$ was used for the wearing surface. The total factors for the camber, non-composite, and composite dead loads are 1.05 , 1.3125 , and 1.3125 respectively.

The resistance factors vary depending on the type of loading. The following are the resistance values that were used:

Flexure:	$\phi = 1.00$
Axial Compression:	$\phi = 0.90$
Tension, fracture in the net section:	$\phi = 0.80$
Tension, yielding in the gross section:	$\phi = 0.95$

These values were inserted into the denominators of **Equations 4-1** thru **4-4** to yield the following:

The interaction equations used for tension members are:

$$\frac{P}{0.95(F_y)(A_n)} + \left[\frac{M}{1.00(S_n)(F_y)(f)} \right]_{(in-plane)} + \left[\frac{M}{1.00(S_n)(F_y)(f)} \right]_{(out-of-plane)} \leq 1.0 \quad (\text{Eq. 4-6})$$

$$\frac{P}{0.80(F_u)(A_n)} + \left[\frac{M}{1.00(S_n)(F_u)(f)} \right]_{(in-plane)} + \left[\frac{M}{1.00(S_n)(F_u)(f)} \right]_{(out-of-plane)} \leq 1.0 \quad (\text{Eq. 4-7})$$

The interaction equations used for compression members are:

$$\frac{P}{(0.90)0.85A_{ge}F_{cr}} + \left[\frac{MC}{1.00M_u \left[1 - \frac{P}{(0.90)A_{ge}F_e} \right]} \right]_{(in)} + \left[\frac{MC}{1.00M_u \left[1 - \frac{P}{(0.90)A_{ge}F_e} \right]} \right]_{(out)} \leq 1.0$$

(Eq. 4-8)

$$\frac{P}{(0.90)0.85A_{ge}F_y} + \left[\frac{M}{1.00M_p} \right]_{(in-plane)} + \left[\frac{M}{1.00M_p} \right]_{(out-of-plane)} \leq 1.0$$

(Eq. 4-9)

The force interaction ratio results for the total dead load for these three cases are presented in **Tables AII-8** thru **AII-10**. The tables list the total interaction ratio, the type of member stress, the components of the interaction ratio, and the percentage of the total interaction due to each of the components.

For Case 1 the maximum interaction ratio is 0.639 (U1'-U0'). For Case 2 the maximum interaction ratio is 0.831 (U1'-U0'). For Case 3 the maximum interaction ratio is 0.858 (U1'-U0'). For all three cases axial load is the primary contributor to the interaction ratios for the majority of the members contributing a maximum of 99.59% (U5'-U4') for Case 1 and Case 2 and 99.71% (U8-U9) for Case 3. In-plane bending can be a significant percentage of the interaction ratio, but only for members that have low total interaction ratios: Case 1 and Case 2 86.36% (U4'-U3') with total interactions of 0.032 and 0.041 respectively; Case 3 88.28% (U4'-U3') with a total interaction of 0.050. Out-of-plane bending can also be a significant percentage of the interaction ratio, but only for members that have low total interaction ratios: Case 1 and Case 2 79.49% (U2-L2) with total interactions of 0.045 and 0.058 respectively; Case 3 74.87% (U2-L2) with a total interaction of 0.065.

4.2.5 Dead Load Member Forces from Original Contract B Plans

The design dead load member forces are shown on sheet 20 of the original contract plans. In order to evaluate the differences between the traditional planar analysis that was done when Bridge 9340 was designed and the 3-D analysis done for this investigation, the original design forces were compared to the forces obtained from the 3-D computer models. These two methods can be compared by calculating the design ratio which is defined as the design axial dead load divided by the design axial capacity and comparing that to the interaction ratios from Section 4.2.4.

The original design axial capacities were not available on the plans and were calculated for each main truss member based on the provisions of AASHTO *Standard Specifications for Highway Bridges* (1961 Edition and 1961 and 1962 Interim Specifications). For tension members, the axial capacity is the product of the allowable steel stress and the area of the net section. The allowable stress is provided on sheet 2, and is $f_s = 27$ ksi for high strength steel (MHD 3310 $\leq \frac{3}{4}$ " ; MHD $> \frac{3}{4}$ ") and $f_s = 20$ ksi for all the other material (MHD 3306). The net areas are provided on sheet 20 and are based on all the holes removed from the cross section. For compression members, the axial capacity is the product of the allowable steel stress and the area of the gross section. The allowable stress is determined from the following equation:

$$\left(\frac{f_s}{18000} \right) 15,000 - \frac{1}{4} \left(\frac{L^2}{r^2} \right) \quad (\text{Eq. 4-10})$$

This is based on the equation from AASHTO for concentrically loaded columns with riveted ends having values of L/r not greater than 140. The ratio of $f_s / 18000$ was added because the 1961 AASHTO code is based on steel with a yield of 33 ksi and not the 36 ksi or 50 ksi present in this bridge. The ratio of L/r is included on sheet 20 of the Contract B plans.

Table AII-11 in **Appendix II** is a comparison between the design ratio and the interaction ratio and components based on the dead loads obtained from the 3-D models. The last three columns

in the table are the comparisons between the two methods of analysis. The "Same Type of Force" column indicates whether or not a member is in tension or compression for both analysis methods, or whether it is in tension for one and compression for the other. The next column is the interaction ratio over the design ratio. A value greater than 1.0 indicates that the 3-D model produces a tighter design where the member is more fully loaded and closer to capacity. Any values greater than or equal to 1.0 in this column are indicated with a bold number. The last column is the ratio of the axial component of the interaction ratio over the ratio of the axial load to the axial capacity. A value greater than 1.0 indicates the 3-D analysis produces a larger axial load to capacity ratio than the original design loads and capacities. Any values greater than or equal to 1.0 in this column are indicated with a bold number.

The original design load values in **Table AII-11** are based on the Group I loading only. The Group I loads govern over Group III because of the 125% reduction for Group III. For each member, the interaction ratios were calculated for all possible combinations and the governing value is presented in the table. For the members with alternating stresses, additional load has been included per section 1.6.5 of AASHTO *Standard Specifications for Highway Bridges* (1961 Edition and 1961 and 1962 Interim Specifications). The additional load is determined by taking 50% of the absolute value of the smaller of the tension or the compression load. This load is then added to both the tension and the compression load and the member must be proportioned to resist both the increased tension and compression load. The provisions of AASHTO do not address how much of the additional load should be applied to the dead load and live load portion of the load. For simplicity half of the additional load was assumed to be applied to the dead load and half to the live load. For members where the dead and live load are not the same stress type the entire additional load was applied to the portion of the load with the larger absolute value. This occurs for members L3-L4 and L4-L5 where the live load is significantly larger than the dead load so the entire additional load was applied to the live load. This is necessary because the value of half of the additional load exceeds the dead load value, which means the dead load would be in tension rather than compression.

For every member except U4'-U3', both methods of analysis produce the same type of stress. In other words, if a member was in tension under the design loads, it is also in tension in the 3-D

analysis. Member U4'-U3' is at an area of stress reversal and has a low ratio for both methods of analysis: 0.134 based on original design loads and 0.032 based on 3-D analysis.

For all the members except U0-U1, L3-L4, L4-L5, and U14-L14 the original design ratio is higher than the force interaction ratio. This means that for the majority of the members, the original design forces are much closer to the original design capacity than the 3-D analysis forces are to the ultimate capacity. For the members where the 3-D analysis interaction ratio exceeds the original design axial load to capacity ratio the interaction ratio tends to be much smaller than 1.0 with a maximum value of 0.518 (U0-U1). These findings indicate that for most members the original design is tighter than if the members had been designed based on 3-D analysis with unfactored loads, even though the 3-D analysis is based on the force interaction ratio rather than just the axial load.

For all the members except L3-L4 and L4-L5 the axial component of the interaction ratio is less than the original design ratio. This means that for the majority of the members, the original design loads are much closer to the original design capacity than the 3-D analysis axial loads are to the ultimate capacity. For members L3-L4 and L4-L5 the axial component of the interaction ratio is less than 0.030. This behavior is expected because the original design was based on the analysis of a single plane of truss and an assumed distribution of load. In the 3-D analysis the dead load is distributed in a more realistic way and the composite deck is included which was neglected in the original design. These findings indicate that if the truss were evaluated based on axial load alone, the unfactored forces from the 3-D analysis would generally not produce as tight of results as the original design forces.

4.3 Truss Member Forces Under Live Loads

Various types of live load were investigated for this analysis based on Cases 1 thru 3 as discussed in Section 4.2.4. The following live load cases were investigated:

Case 1 7 trucks or 7 lanes – unfactored load and ultimate capacity

Case 2 7 trucks or 7 lanes – LFD factored load and ultimate capacity

In addition to these live loads, the original live loads from the Contract B plans were also investigated for comparison purposes.

4.3.1 From Original Contract B Plans

As specified on sheet 2 of the Contract B Plans, the original design live load is H20-S16-44 Loading and alternate loading designated in P.P.M. 20-4, Section 4C. The H20-S16-44 loading is equivalent to the HS20-44 loading in the current AASHTO Specifications. The live loads and impact loads for each member are listed on sheet 20.

Table AII-12 in Appendix II summarizes the design ratio based on the original design live load, and the tension and compression axial live and impact loads for each member as taken from sheet 20. The impact factor is the impact load divided by the axial load. The live load axial load to capacity ratio was determined in a similar manner as for the dead load as discussed in **Section 4.2.5**. Because the ratios include the additional loads due to alternating stresses where present and the loads included in the table are raw loads taken directly from the plans, the ratios may not be directly determined from the loads in the table. The loads are included for informational purposes and to illustrate how the impact factor was calculated.

4.3.2 Lateral Live Load Distribution

In order to properly model the live load, the number of trucks and lateral positioning was investigated. Various truck positions and number of trucks were considered. **Table 4-2** is a summary of the truck number and positions that were investigated. The values were determined by simple span analysis assuming that the deck is simply supported at the locations of the trusses. Values are listed with no reduction factors applied, with the reduction in load intensity factors applied as per the AASHTO Standard Specifications, and with the multiple presence

factors applied as per the AASHTO LRFD Specifications. The current AASHTO Standard Specification reduction in load intensity factors are the same as when the bridge was designed.

From **Table 4-2**, the live loading that produces the maximum affect in one truss is seven trucks pushed to the east as far possible. This is true for all three of the sets of reduction factors that were investigated. **Figure 4-1** shows the governing live load position for strength design.

Table 4-2: Summary of Lateral Load Distribution

Summary of Live Load Reactions on Main Trusses In Terms of Multiples of a Single Wheel Load - East Truss Maximized						
Load Cases	No Reduction Factors Applied		Standard Specifications Reduction in Load Intensity		LRFD Multiple Presence Factors	
	East Truss Reaction	West Truss Reaction	East Truss Reaction	West Truss Reaction	East Truss Reaction	West Truss Reaction
1 Truck 2' from East Curb	2.36	-0.36	2.36	-0.36	2.83	-0.43
1 Truck Along CL East Lane	2.27	-0.27	2.27	-0.27	2.72	-0.32
2 Trucks Pushed to East	4.38	-0.38	4.38	-0.38	4.38	-0.38
3 Trucks Pushed to East	6.07	-0.07	5.46	-0.06	5.16	-0.06
4 Trucks Pushed to East	7.43	0.57	5.57	0.43	4.83	0.37
5 Trucks Pushed to East	8.24	1.76	6.18	1.32	5.36	1.14
6 Trucks Pushed to East	8.71	3.29	6.53	2.47	5.66	2.14
7 Trucks Pushed to East	8.85	5.15	6.64	3.86	5.75	3.35
8 Trucks Pushed to East	8.66	7.34	6.50	5.51	5.63	4.77
8 Trucks Centered in Each Lane	8.00	8.00	6.00	6.00	5.20	5.20

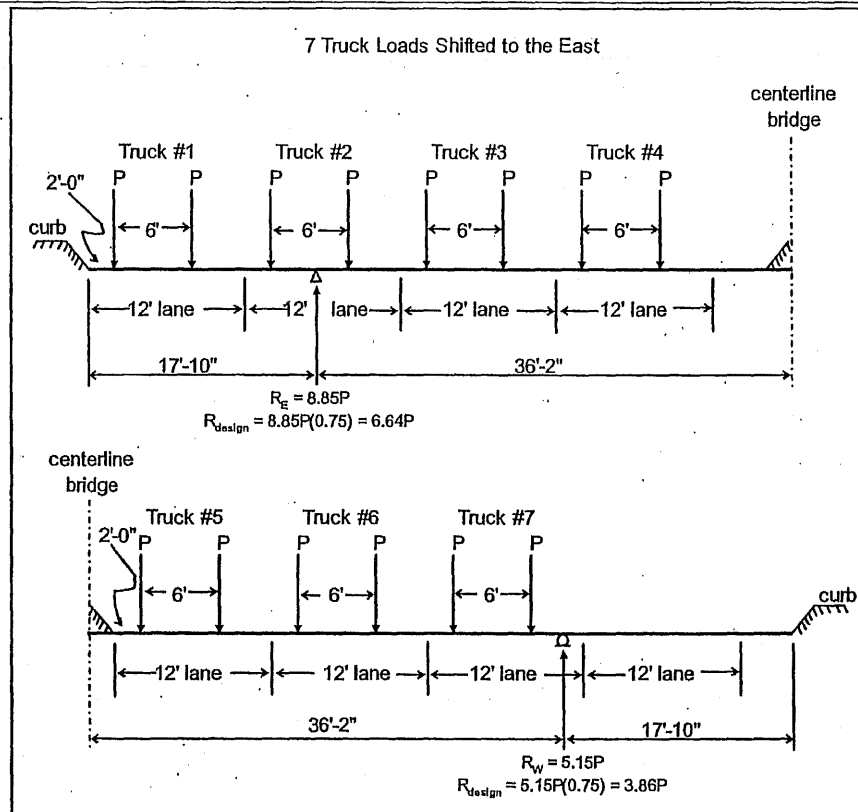


Figure 4-1: Governing Live Load for Strength Design

4.3.3 3-D Analysis – Unfactored Live Load and Ultimate Capacity

Live Load Case 1 consists of the unfactored live load compared to the ultimate capacity. The live load is based on the current AASHTO Standard Specifications and is seven HS20 trucks or seven HS20 lanes pushed as far to the east as possible. The lane load is comprised of a uniform load portion and a concentrated load portion placed as required to maximize the axial force in the members. All three concentrated load conditions specified by AASHTO (1-18 kip load 2-18 kip loads or 1 26 kip load) were investigated in order to determine the worst case forces in the member. No load, impact, or multi-presence factors are applied. Both the “as-designed” and “locked” bearing conditions were considered for the main truss and stringer bearings.

Tables AII-13 and AII-14 in Appendix II summarize the “as-designed” bearings and “locked” bearings results of this analysis respectively. For both bearing conditions, the HS20 lane load of the uniform load combined with one 26 kip concentrated load is the governing lane load for

every member. For about 75% of the joints the lane loading produces a higher interaction ratio than the truck loading.

Table AII-15 in **Appendix II** is a comparison of the governing interaction ratios for the two bearing conditions. The governing interaction ratio, load, stress type, and bearing condition is listed for each member. The difference between the interaction ratios is also listed and is the maximum interaction ratio minus the minimum interaction ratio. For approximately 70% of the members the "as-designed" bearing conditions produces higher interaction ratios. The difference in the interaction ratio can be as high as 0.215 (U4'-U3'), but typically it is much less. Only about 25% of the members have a difference in interaction ratios greater than 0.05 and less than 10% have a difference greater than 0.10. The same member may be in tension for one bearing condition and compression for the other (U4-U5). Also, the same member may have a truck controlled live load for one bearing condition and a lane controlled for the other (U3-U4). Based on this comparison it can be concluded that the bearing conditions will affect the results of the analysis but for the majority of the members this effect is minimal.

4.3.4 3-D Analysis – LFD Factored Live Load and Ultimate Capacity

Live Load Case 2 consists of the LFD factored live load compared to the ultimate capacity. The live load is based on the current AASHTO Standard Specifications and is seven HS20 trucks or seven HS20 lanes pushed as far to the east as possible. The lane load is comprised of a uniform load portion and a concentrated load portion placed as required to maximize the axial force in the members. All three concentrated load conditions specified by AASHTO (1-18 kip load 2-18 kip loads or 1 26 kip load) were investigated in order to determine the worst case forces in the member. A 2.171 load factor, 0.75 load reduction factor, and impact, are applied. The impact factor is determined from the original design values which are summarized in **Table AII-12**. In the original design, impact was only calculated for the type of stress that a member experienced under total dead and live load, or both if the member was in reversal. The results from the 3-D live load analysis typically yielded a tension and compression force. Since live load alone is being investigated at this step, an impact value was needed for all the members for both types of

stress. These impact values were not needed in the original design because the combined dead plus live load may not necessarily cause reversal even though the live load causes reversal; hence only one type of stress is present and impact was calculated accordingly. If an original design impact value was not available, a value of 1.21 was used. This is based on the impact note on sheet 20 of the Contract B plans which lists the maximum value of impact as 21% excluding the verticals. This was selected as a reasonable and conservative assumption. Both the "as-designed" and "locked" bearing conditions were considered for the main truss and stringer bearings.

Tables AII-16 and AII-17 in Appendix II summarize the "as-designed" bearings and "locked" bearings results of this analysis respectively. For both bearing conditions, the HS20 lane load of the uniform load combined with one 26 kip concentrated load is the governing lane load for every member. For about 75% of the joints the lane loading produces a higher interaction ratio than the truck loading.

Table AII-18 in Appendix II is a comparison of the governing interaction ratios for the two bearing conditions. The governing interaction ratio, load, stress type, and bearing condition is listed for each member. The difference between the interaction ratios is also listed and is the maximum interaction ratio minus the minimum interaction ratio. For approximately 70% of the members the "as-designed" bearing conditions produces higher interaction ratios. The difference in the interaction ratio can be as high as 0.399 (U4'-U3'), but typically it is much less. Only about 25% of the members have a difference in interaction ratios greater than 0.10 and less than 10% have a difference greater than 0.20. The same member may be in tension for one bearing condition and compression for the other (U4-U5). Also, the same member may have a truck controlled live load for one bearing condition and a lane controlled for the other (U3-U4). Based on this comparison it can be concluded that the bearing conditions will affect the results of the analysis but for the majority of the members this effect is minimal. The difference in the results between this live load case and the previous live load case is entirely due to the use of the live load, impact, and load reduction factors. Nothing else is different.

4.3.5 3-D Analysis – LRFD Factored Load and Capacity

Live Load Case 3 consists of the LRFD factored live load compared to the LRFD factored capacity. The live load is based on the current AASHTO LRFD Specifications and is seven HS20 trucks combined with seven HS20 lanes pushed as far to the east as possible. The lane load is comprised of a uniform load portion only with the truck load acting as the concentrated load portion placed as required to maximize the axial force in the members. A 1.05 load modifier, 1.75 live load factor, 0.65 multi-presence factor, and 1.33 impact factor are applied. Both the “as-designed” and “locked” bearing conditions were considered for the main truss and stringer bearings.

Tables AII-19 and AII-20 in Appendix II summarize the “as-designed” bearings and “locked” bearings results of this analysis respectively.

Table AII-21 -in Appendix II is a comparison of the governing interaction ratios for the two bearing conditions. The governing interaction ratio, load, stress type, and bearing condition is listed for each member. The difference between the interaction ratios is also listed and is the maximum interaction ratio minus the minimum interaction ratio. For approximately 70% of the members the “as-designed” bearing conditions produces higher interaction ratios. The difference in the interaction ratio can be as high as 0.454 (U4'-U3'), but typically it is much less. Only about 26% of the members have a difference in interaction ratios greater than 0.10 and less than 10% have a difference greater than 0.20. The same member may be in tension for one bearing condition and compression for the other (U8-U9). Based on this comparison it can be concluded that the bearing conditions will affect the results of the analysis but for the majority of the members this effect is minimal.

4.3.6 Summary and Comparison

The design ratios and total interaction ratios for the various live loads investigated are summarized in **Table AII-22** and **AII-23** for the “as-designed” and “locked” bearings

respectively. The tables also list the overall maximum ratio as well as the live loading that caused it.

From **Table AII-22**, the design ratio and the LRFD interaction ratio are typically the larger values for the "as-designed" bearing condition. About 42% of the joints have the highest ratio due to the design load, and about 46% have the highest ratio due to the LRFD load. The remaining 12% of the joints have the highest ratio due to the LFD Lane ratio. The unfactored truck, unfactored lane, and LFD Truck do not produce the largest interaction ratio for any joints. Additional finds from **Table AII-22** are described in the following paragraphs.

For the "as-designed" bearing condition the governing unfactored interaction ratio, defined as the larger of the two interaction ratios produced by the truck or lane loading, is almost always less than the original design live load ratio. The unfactored interaction ratio exceeds the design ratio at only two joints (U0-U1 and L1'-U0') and only by a factor of 1.10. This indicates that for the majority of the members the original design loads are more severe than the unfactored loads even though the unfactored loads include axial and bending components rather than just axial as was the case for the original design.

The governing LFD factored interaction ratio always exceeds the governing unfactored interaction ratio by a factor of at least 1.78 and at most 2.19 (U7-L7 and U7'-L7'). This indicates that the LFD loads are more severe than the unfactored loads. This is expected because the LFD loads are the same as the unfactored but with the LFD factors applied. The ultimate capacity is used for both methods in determining the interaction ratios. The reason the LFD interactions are not all simply equal to the unfactored interactions multiplied by a constant value is because the impact factor varies by member. The LFD interaction ratio exceeds the design ratio at about half of the joints. The LFD interaction ratio can exceed the design ratio by as much as a factor of 2.17 (U0-U1). The design ratio can exceed the LFD interaction ratio by as much as a factor of 17.0 (U6'-L6'), but for this member the design ratio is 0.492 and the LFD interaction ratio is only 0.029. This disparity is present because the design ratio is the maximum value for a member whereas the LFD interaction ratio for the 3-D models was taken at multiple computer joints on the member. In the computer model three members with six joints comprise U6'-L6' which

yields six interaction ratios which are all compared to the same design ratio. These findings indicate that the LFD factored loads are more severe than the design loads for about half of the joints.

For about 77% of the joints, the LRFD interaction ratio exceeds the governing LFD interaction ratio by as much as a factor of 1.29 (U11-U12). For the remaining members the LFD interaction ratio exceeds the LRFD interaction ratio by as much as a factor of 1.18 (U8-U9 and U8'-U9'). These findings indicate that for the majority of the members the LRFD load is more severe than the LFD loads. The governing LRFD factored interaction ratio always exceeds the governing unfactored interaction ratio by a factor of at least 1.53 and at most 2.58 (U0-L1). This indicates that the LRFD loads are more severe than the unfactored loads. The LRFD interaction ratio exceeds the design ratio for about 56% of the joints. The LRFD interaction ratio can exceed the design ratio by as much as a factor of 2.34 (U0-U1). The design ratio can exceed the LRFD interaction ratio by as much as a factor of 14.5 (U6-L6, U14-L14, and U6'-L6'), but for this member the design ratio is 0.492 and the LRFD interaction ratio is only 0.034. This disparity is present for the same reason as discussed for the LFD interaction ratios. These findings indicate that the LRFD factored loads are more severe than the design loads for about half of the joints.

From **Table AII-23**, the design ratio and the LRFD interaction ratio are typically the larger values for the "locked" bearing condition. About 59% of the joints have the highest ratio due to the design load, and about 32% have the highest ratio due to the LRFD load. The remaining 9% of the joints have the highest ratio due to the LFD Lane ratio. The unfactored truck, unfactored lane, and LFD truck do not produce the largest interaction ratio for any joints. Additional finds from **Table AII-23** are described in the following paragraphs.

For the "locked" bearing condition the governing unfactored interaction ratio is almost always less than the original design live load ratio. The unfactored interaction ratio exceeds the design ratio at only three joints (U0-U1, L8-L9, and L9'-L8') and only by a factor of 1.18. This indicates that for the majority of the members the original design loads are more severe than the unfactored loads even though the unfactored loads include axial and bending components rather than just axial as was the case for the original design.

The governing LFD factored interaction ratio always exceeds the governing unfactored interaction ratio by a factor of at least 1.77 and at most 2.19 (U9'-L9'). This indicates that the LFD loads are more severe than the unfactored loads. This is expected because the LFD loads are the same as the unfactored but with the LFD factors applied. As noted for the "as-designed" bearings condition, the reason the LFD interactions are not all simply equal to the unfactored interactions multiplied by a constant value is because the impact factor varies by member. The design ratio exceeds the LFD interaction ratio at about 66% of the joints. The LFD interaction ratio can exceed the design ratio by as much as a factor of 2.33 (U0-U1). The design ratio can exceed the LFD interaction ratio by as much as a factor of 22.4 (U4-L4), but for this member the design ratio is 0.492 and the LFD interaction ratio is only 0.022. As noted previously for the "as-designed" bearing condition, this disparity is present because the design ratio is the maximum value for a member whereas the LFD interaction ratio for the 3-D models was taken at multiple computer joints on the member. These findings indicate that the design loads are more severe than the LFD factored loads for about two-thirds of the joints.

For about 81% of the joints, the LRFD interaction ratio exceeds the governing LFD interaction ratio by as much as a factor of 1.32 (U4-U5). For the remaining members the LFD interaction ratio exceeds the LRFD interaction ratio by as much as a factor of 1.23 (U2'-U1'). These findings indicate that for the majority of the members the LRFD load is more severe than the LFD loads. The governing LRFD factored interaction ratio always exceeds the governing unfactored interaction ratio by a factor of at least 1.48 and at most 2.63 (U0-L1). This indicates that the LRFD loads are more severe than the unfactored loads. The design ratio exceeds the LRFD interaction ratio for about 60% of the joints. The LRFD interaction ratio can exceed the design ratio by as much as a factor of 2.48 (U0-U1). The design ratio can exceed the LRFD interaction ratio by as much as a factor of 18.5 (U4-L4), but for this member the design ratio is 0.492 and the LRFD interaction ratio is only 0.026. This disparity is present for the same reason as discussed for the LFD interaction ratios. These findings indicate that the design loads are more severe than the LRFD factored loads for more than half of the joints.

In summary for the “as-designed” bearing case no single loading produces the most severe interactions for all the members. The design loads (42% of the joints), LRFD loads (46% of the joints), and LFD Lane loads (12% of the joints) can all produce the most severe design ratio or interaction ratio at the joints. The unfactored loads never produce the most severe interaction and are almost always exceeded by the design ratio.

In summary for the “locked” bearing case no single loading produces the most severe interactions for all the members. The design loads (59% of the joints), LRFD loads (32% of the joints), and LFD Lane loads (9% of the joints) can all produce the most severe design ratio or interaction ratio at the joints. The unfactored loads never produce the most severe interaction and are almost always exceeded by the design ratio.

4.4 Truss Member Forces Under Combined Dead and Live Loads

The truss member forces and interaction ratios were investigated under combined dead plus live loading. The dead load from the previous sections was combined with the three live load cases previously investigated and the total was analyzed for live loads applied with the “as-designed” and the “locked” bearing conditions. As noted previously, the dead load portion of the load was analyzed with the “as-designed” bearing conditions. In addition to these total loads, the original total loads from the Contract B plans were also investigated for comparison purposes.

4.4.1 From Original Contract B Plans

Table AII-24 in Appendix II summarizes the design ratio based on the Group I total original design load, and the tension and compression axial loads for each member as taken from sheet 20. The Group I loads almost always govern over the Group III loads for the upper chord members once the 125% stress reduction has been applied. The values in the table on sheet 20 are raw numbers only with the stress reduction. For a few reversal members, the Group III loads do control, but only where the compressive force is negligible compared to the tension force.

The total load axial load to capacity ratio was determined in a similar manner as for the dead load as discussed in **Section 4.2.5**.

Based on the information in the original contract plans as shown on Table AII-24, the design ratio was found to range between 0.730 and 1.004 for all the main truss members. This indicates that some of the members were sized very tightly in terms of the axial capacity and any bending moments would likely cause an overstress in relation to the design criteria.

4.4.2 3-D Analysis Unfactored Dead and Live Load and Ultimate Capacity

The results for the 3-D analysis of the unfactored dead and live load were determined by combining the unfactored dead load forces from **Section 4.2.4** with the unfactored live load forces from **Section 4.3.3**. The interaction ratio was then calculated based on the combined dead plus live force.

Tables AII-25 and AII-26 in Appendix II summarize the “as-designed” bearings and “locked” bearings results of this analysis respectively. For both bearing conditions, the HS20 lane load of the uniform load combined with one 26 kip concentrated load is the typically governing lane load for every member. For about 75% of the joints the lane loading produces a higher interaction ratio than the truck loading. For the “as-designed” bearing condition, the maximum force interaction ratio is 0.929 (U1'-U0'). For the “locked” bearing condition, the maximum force interaction ratio is 0.930 (U1'-U0'). These findings indicate that the maximum interaction ratio occurs in U1'-U0' for both bearing conditions and that no members have an interaction ratio exceeding the limiting value of 1.0.

Table AII-27 in Appendix II is a comparison of the governing interaction ratios for the two bearing conditions. The governing interaction ratio, load, stress type, and bearing condition is listed for each member. The difference between the interaction ratios is also listed and is the maximum interaction ratio minus the minimum interaction ratio. For approximately 70% of the members the “as-designed” live load bearing condition produces higher interaction ratios. The

difference in the interaction ratio can be as high as 0.202 (U4'-U3'), but typically it is much less. Only about 30% of the members have a difference in interaction ratios greater than 0.05 and less than 10% have a difference greater than 0.10. The same member may be in tension for one bearing condition and compression for the other (L3-L4), but this is not typical. Also, the same member may have a truck controlled live load for one bearing condition and a lane controlled for the other (U3-U4). Based on this comparison it can be concluded that the bearing conditions for the live loads will affect the results of the analysis but for the majority of the members this effect is minimal.

4.4.3 3-D Analysis LFD Factored Dead and Live Load and Ultimate Capacity

The results for the 3-D analysis of the LFD factored dead and live load were determined by combining the LFD factored dead load forces from **Section 4.2.4** with the LFD factored live load forces from **Section 4.3.4**. The interaction ratio was then calculated based on the combined dead plus live force.

Tables AII-28 and AII-29 in Appendix II summarize the “as-designed” bearings and “locked” bearings results of this analysis respectively. For both bearing conditions, the HS20 lane load of the uniform load combined with one 26 kip concentrated load is the typically governing lane load for every member. For about 75% of the joints the lane loading produces a higher interaction ratio than the truck loading. For the “as-designed” bearing condition, the maximum force interaction ratio is 1.501 (L1'-U0'). Twenty-four joints, about 8%, have force interaction ratios greater than 1.0. For the “locked” bearing condition, the maximum force interaction ratio is 1.464 (U0-L1). Twenty joints, about 7%, have force interaction ratios greater than 1.0. These findings indicate that for LFD factored loading there are members with force interactions greater than 1.0 for both bearing conditions. These members are investigated in more detail in **Section 4.4.5**.

Table AII-30 in Appendix II is a comparison of the governing interaction ratios for the two bearing conditions. The governing interaction ratio, load, stress type, and bearing condition is

listed for each member. The difference between the interaction ratios is also listed and is the maximum interaction ratio minus the minimum interaction ratio. For approximately 70% of the members the "as-designed" live load bearing condition produces higher interaction ratios. The difference in the interaction ratio can be as high as 0.397 (U4'-U3'), but typically it is much less. About 50% of the members have a difference in interaction ratios greater than 0.05 and about 30% have a difference greater than 0.10. The same member may be in tension for one bearing condition and compression for the other (L3-L4), but this is not typical. Also, the same member may have a truck controlled live load for one bearing condition and a lane controlled for the other (U3-U4). Based on this comparison it can be concluded that the bearing conditions for the live loads will affect the results of the analysis but for the majority of the members this effect is minimal.

4.4.4 3-D Analysis LRFD Factored Dead and Live Load and Capacity

The results for the 3-D analysis of the LRFD factored dead and live load were determined by combining the LRFD factored dead load forces from **Section 4.2.4** with the LRFD factored live load forces from **Section 4.3.5**. The interaction ratio was then calculated based on the combined dead plus live force.

Tables AII-31 and AII-32 in Appendix II summarize the "as-designed" bearings and "locked" bearings results of this analysis respectively. For the "as-designed" bearing condition, the maximum force interaction ratio is 1.773 (U0-L1). Sixty-eight joints, about 23%, have force interaction ratios greater than 1.0. For the "locked" bearing condition, the maximum force interaction ratio is 1.858 (U0-L1). Fifty-six joints, about 19%, have force interaction ratios greater than 1.0. These findings indicate that for LRFD factored loading there are members with force interactions greater than 1.0 for both bearing conditions. These members are investigated in more detail in **Section 4.4.5**.

Table AII-33 in Appendix II is a comparison of the governing interaction ratios for the two bearing conditions. The governing interaction ratio, load, stress type, and bearing condition is

listed for each member. The difference between the interaction ratios is also listed and is the maximum interaction ratio minus the minimum interaction ratio. For approximately 73% of the members the “as-designed” live load bearing condition produces higher interaction ratios. The difference in the interaction ratio can be as high as 0.458 (U4'-U3'), but typically it is much less. About 45% of the members have a difference in interaction ratios greater than 0.05 and about 30% have a difference greater than 0.10. The same member may be in tension for one bearing condition and compression for the other (L3-L4), but this is not typical. Based on this comparison it can be concluded that the bearing conditions for the live loads will affect the results of the analysis but for the majority of the members this effect is minimal.

4.4.5 Summary and Comparison

Tables AII-34 and AII-35 in Appendix II summarize the total force interaction ratios for the various loads for the “as-designed” live load bearing condition and “locked” live load bearing condition results of this analysis respectively. The tables also list the overall maximum interaction ratio, as well as the load which caused the maximum ratio.

For all the truss members, the LRFD loading was found to produce the highest magnitudes of the force interaction ratio. For the “as-designed” truss bearing condition, the maximum values of the interaction ratio are: upper chords 1.452 (U1'-U0'), lower chords 1.120 (L8-L9), diagonals 1.773 (U0-L1), and verticals 1.321 (U1'-L1'). The maximum values for the “locked” bearing condition are: upper chords 1.504 (U1'-U0'), lower chords 1.264 (L8-L9), diagonals 1.827 (U0-L1), and verticals 1.310 (U1'-L1). One distinct feature of the LRFD loading is the inclusion of both truck and lane load as compared with the LFD loading that uses the higher of truck or lane loading. As noted previously, the analysis indicated that under the unfactored loads no truss member has a force interaction ratio exceeding 1.0 and under LFD and LRFD factored loads some members have a force interaction ratios exceeding 1.0.

The overall governing value for the members is either the design ratio or the LRFD force interaction ratio. For the “as-designed” live load bearing conditions about 62% of the joints are

governed by the design ratio with the remaining 38% being governed by the LRFD force interaction ratio. For the “locked” live load bearing conditions about 68% of the joints are governed by the design ratio with the remaining 32% being governed by the LRFD force interaction ratio. This indicates that although the original design was based on axial load only and the 3-D results on combined force interaction, the original design ratio still governs for the majority of the joints.

The various live load results were discussed in detail in **Section 4.3** with various comparisons made. The behavior of the members under total load is similar and the same type of comparisons are made in the following paragraphs.

For both bearing conditions the design ratio always exceeds the governing unfactored interaction ratio. This indicates that for the majority of the members the original design loads are more severe than the unfactored loads even though the unfactored loads include axial and bending components rather than just axial as was the case for the original design.

The governing LFD factored interaction ratio always exceeds the governing unfactored interaction ratio for both bearing conditions. For the “as-designed” live load bearing condition the factor is at least 1.43 and at most 1.87 (U4'-U3'). For the “locked” live load bearing condition the factor is at least 1.33 and at most 2.22 (U2-L2). This indicates that the LFD loads are more severe than the unfactored loads. This is expected because the LFD loads are the same as the unfactored but with the LFD factors applied. The design ratio exceeds the LFD interaction ratio for about 73% and 77% of the joints for the “as-designed” and “locked” live load bearing conditions respectively. The LFD interaction ratio can exceed the design ratio by as much as a factor of 1.70 (L1'-U0') for the “as-designed” bearing condition and 1.69 (U0-L1) for the “locked” bearing condition. The design ratio can exceed the LFD interaction ratio by as much as a factor of 18.2 for both bearing conditions (U10-L10 “as-designed”, U14-L14 “locked”), but for these members the design ratio is close to 1.0 and the LFD interaction ratio is less than 0.10. This disparity is present because the design ratio is the maximum value for a member whereas the LFD interaction ratio for the 3-D models was taken at multiple computer joints on the

member. These findings indicate that the design loads are more severe than the LFD factored loads for about three quarters of the joints.

The LRFD interaction ratio almost always exceeds the governing LFD interaction ratio. For about 92% of the joints for the "as-designed" live load bearing condition, the LRFD interaction ratio exceeds the governing LFD interaction ratio by as much as a factor of 1.25 (U0-L1). For about 96% of the joints for the "locked" live load bearing condition, the LRFD interaction ratio exceeds the governing LFD interaction ratio by as much as a factor of 1.31 (U4'-U3'). These findings indicate that for the majority of the members the LRFD load is more severe than the LFD loads. The governing LRFD factored interaction ratio always exceeds the governing unfactored interaction ratio for both bearing conditions. For the "as-designed" live load bearing condition the factor is at least 1.40 and at most 2.26 (U4'-U3'). For the "locked" live load bearing condition the factor is at least 1.35 and at most 2.29 (U0-L1). This indicates that the LRFD loads are more severe than the unfactored loads. The design ratio exceeds the LRFD interaction ratio for about 62% and 68% of the joints for the "as-designed" and "locked" live load bearing conditions respectively. The LRFD interaction ratio can exceed the design ratio by as much as a factor of 2.04 (U0-L1) for the "as-designed" bearing condition and 2.14 (U0-L1) for the "locked" bearing condition. The design ratio can exceed the LRFD interaction ratio by as much as a factor of 18.9 (U14-L14) for the "as-designed" bearing condition and 17.9 (U14-L14) for the "locked" bearing condition, but for these members the design ratio is close to 1.0 and the LRFD interaction ratio is less than 0.10. This disparity is present for the same reason as discussed for the LFD interaction ratios. These findings indicate that the design loads are more severe than the LRFD factored loads for more than half of the joints.

In summary for the "as-designed" bearing case no single loading produces the most severe interactions for all the members. The design loads (62% of the joints) and the LRFD loads (38% of the joints) produce the most severe design ratio or interaction ratio at the joints. The unfactored loads and the LFD loads never produce the most severe interaction and are almost always exceeded by the design ratio. The LRFD load is almost always more severe than the LFD load, and it is always more severe than the unfactored load.

In summary for the "locked" bearing case no single loading produces the most severe interactions for all the members. The design loads (68% of the joints) and the LRFD loads (32% of the joints) produce the most severe design ratio or interaction ratio at the joints. The unfactored loads and the LFD loads never produce the most severe interaction and are almost always exceeded by the design ratio. The LRFD load is almost always more severe than the LFD load, and it is always more severe than the unfactored load.

Further investigation was made for truss members with force interaction ratios greater than 1.0 for the "locked" live load bearing condition. This bearing condition was selected because it was determined to be the actual in-service condition based on the model calibration with the field data and the maximum values are typically greater for this condition. (except for the verticals). The results are presented in **Appendix II**. **Table AII-36** shows a comparison of the design ratio and the various force interaction ratios for all the members that were investigated. A member was investigated if one or more interaction ratios exceeded 1.0. **Tables AII-37 through AII-41** lists the force interaction breakdowns into axial, in-plane bending, and out-of-plane bending for the unfactored total load with the truck live load, the unfactored total load with the lane live load, the LFD factored total load with the truck live load, the LFD factored total load with the lane live load, and the LRFD factored total load.

It was found that for all the cases considered, the axial component of the force interaction ratio is either less than 1.0 or slightly above 1.0 (1.039 maximum). This indicates that if the truss were evaluated based on the design assumption that the members take axial load only, the members would be okay. A comparison between the force interaction ratios of the same members under the LRFD and the LFD loads indicates that the LRFD loading produces higher interaction ratios for all but two of the joints, or 98% of the joints. The LRFD loading can produce interaction ratios as much as almost 30% greater than the LFD loading (L1'-U0'). For the members where the LFD produces a higher interaction ratio, the value is only about 5% greater than the LRFD interaction ratio (U1-L1). This indicates the impact of the heavier LRFD loading. The overall highest force interaction ratio occurred in member U0-L1, the diagonal supporting the truss cantilever at the end of the truss spans. Under the LRFD loading the total interaction ratio is 1.858 with 1.038 from axial, 0.819 from in-plane bending, and essentially zero from out-of-plane

bending. A large portion of this axial load and in-plane bending can be directly attributed to the approach span loads that are applied at U0. Under the LFD loading the governing total interaction ratio for U0-L1 is 1.464 with 0.871 from axial, 0.590 from in-plane bending, and essentially zero from out-of-plane bending. U0-L1 is also the member with the highest force interaction ratio due to LFD factored loading.

In general, the highest force interaction ratios occur in the members located near the cantilevered ends of the truss. This behavior is consistent for the upper chord, diagonal, and vertical members. For the upper chord members, U0-U1 and U1'-U0' have the highest force interaction ratios of the members investigated while U10-U11 and U11'-U10' have force interaction ratios between 1.10 and 1.0. The values greater than 1.0 for U10-U11 and U11'-U10' can be attributed to the more severe LRFD loading because the LFD loading does not produce interaction ratios greater than 1.0 for these members. For the diagonal members, U0-L1, L1-U2, U2'-L1', and L1'-U0' have the highest force interaction ratios while the remaining investigated members have force interaction ratios between 1.10 and 1.0. The values greater than 1.0 for the members away from the cantilevers can be attributed to the more severe LRFD loading because the LFD loading does not produce interaction ratios greater than 1.0 for these members. For the vertical members, U1-L1 and U1'-L1' have the highest force interaction ratios while the remaining investigated members have force interaction ratios between 1.22 and 1.0. The values greater than 1.0 for the members away from the cantilevers can be attributed to the more severe LRFD loading because the LFD loading does not produce interaction ratios greater than 1.0 for these members.

The lower chord members behave differently. For the lower chord members, the members adjacent to piers 6 and 7 (L7-L8, L8-L9, L9'-L8', and L8'-L7') have force interaction ratios greater than 1.0 with L8-L9 and L9'-L8' having the highest values. These members also have interaction ratios greater than 1.0 due to LFD loading. No lower chord members adjacent to the cantilevers have force interaction ratios greater than 1.0. From **Table AII-40** and **AII-41**, for member L8-L9 which has the largest LFD and LRFD interaction ratio, the ratio is due primarily to axial load (LFD: 0.877; LRFD: 0.932) with a significant contribution from in-plane bending (LFD: 0.290; LRFD: 0.323). The axial load in the member is due primarily to the dead load (72%) with the live load also making a contribution (28%). A further breakdown of the dead

load portion of the axial load indicates that the non-composite dead load is the primary contributor to the axial dead load. About half of the in-plane bending moment is due to the dead load (55%) with the live load making an almost equal contribution (45%). A further breakdown of the dead load portion of the in-plane bending indicates that the value is due primarily to the combined non-composite and composite dead load which largely, but not completely counteract the in-plane bending caused by the cambering process. The design ratio for this member was 0.946 indicating that the member was loaded very close to capacity considering axial load alone. The large interaction ratios for the lower chord members can be attributed to the unexpected bending that is present in the member due to the combined non-composite and composite dead load in-plane bending exceeding the camber in-plane bending.

A force interaction ratio greater than or equal to 1.0 for the existing structure does not necessarily indicate a member "failure", but rather a localized overstress beyond the elastic limit under the factored design load and section capacities. Besides, the occurrence of a local yielding in an indeterminate system typically results in a load redistribution, and thus a reduction of loading forces at the overstressed section, based on the change of member/connection stiffness properties. It is important to note that no interaction ratios greater than 1.0 were observed in the analysis using the unfactored load and the ultimate capacity. This indicates that the actual design load should not cause overstress in any truss members. No signs of overstress have been reported in the service history of the bridge for more than 40 years. Although some members exhibited large interaction ratios using the LRFD criteria, this is mainly because the LRFD loading can be significantly greater than the original design load for some members. Another difference between the current analysis and the original design is the assumption that the truss member end connections are rigid rather than "pinned". This assumption of rigid connections, although tending to maximize bending moments in the truss members, should better represent the actual truss joint condition.

In summary, a close examination of the force interaction ratios indicates that bending effects may not be negligible in truss members when the members are assembled with moment connections. Such bending effects may become significant when there are special sources for concentrated forces, such as the truss span ends that serve as supports to the approach spans.

BRIDGE 9340 STUDY



Additionally, the LRFD loading was also found to produce more severe load effects than the traditional ASD and LFD design load, due to the use of combined truck and lane load as well as a greater vehicle impact. The 3-D analysis showed force interaction ratios greater than 1.0 in some member sections using the LRFD and LFD criteria. However, a force interaction ratio exceeding 1.0 does not necessarily indicate a section failure but rather a localized overstress under the factored load which should result in a consequent load reduction at the overstressed section due to a load redistribution.

SECTION 5

5. FATIGUE EVALUATION OF TRUSS MEMBERS

5.1 AASHTO Fatigue Specifications

AASHTO currently has four methods available for fatigue design and/or evaluation of steel bridges as follows:

1. *Standard Specifications for Highway Bridges* (Standard Specifications), 17th Edition, 2002
2. *AASHTO LRFD Bridge Design Specifications* (LRFD Specifications), 3rd Edition, 2004
3. *Guide Specifications for Fatigue Evaluation of Existing Steel Bridges* (Guide Specifications), 1990, with interim revisions through 1995
4. *Guide Manual for Condition Evaluation and Load and Resistance Factor Rating (LRFR) of Highway Bridges* (LRFR Manual), 2003

All these fatigue specification documents are based on the same experimentally derived S-N curves. The primary difference among them lies on the fatigue load, the method for determining the nominal stress range and the corresponding stress cycles, as well as the reliability factors or safety margin.

The Standard Specifications were developed primarily for the design of new bridges and are usually not suitable for fatigue evaluation of existing bridges. The fatigue load utilizes the same live load configurations used for strength design, considering both the truck and lane loads applied over multiple lanes with full impact. Therefore, this specification was not considered for the fatigue evaluation of Bridge 9340.

The LRFD Specifications can be used for both new bridge design and for existing bridge fatigue evaluation. The LRFD fatigue provisions removed the lane load and the multiple-lane loading, and require the use of a single design truck, which is equivalent to the HS-20 truck in the

Standard Specifications but with a constant spacing of 30.0 ft between the rear axles. For the fatigue and fracture limit state, a load factor of 0.75 is applied along with a dynamic load allowance of 15%, as opposed to 33% for the strength design load. The single fatigue truck is to be positioned both transversely and longitudinally to maximize the stress range in the detail under consideration regardless of the position of traffic or design lanes on the deck.

The Guide Specifications, released in 1990, and the LRFR Manual, released in 2003, were developed for the purpose of evaluating existing bridges only and both allow several alternative methods that are not available in the Standard Specifications or the LRFD Specifications. These methods include field strain measurements, fatigue load adjusted by weigh station measurements or weigh-in-motion measurements at the bridge site, etc. Both specifications follow similar procedures that first check the satisfaction of infinite fatigue life then an estimate of finite life.

The fatigue load in the Guide Specifications is the same as that in the LRFD except with an impact of 10%. When the finite element method is used for stress analysis, the fatigue truck is to be placed in the center of the outer lane. The fatigue load in the LRFR Manual is also the same as that in the Guide Specifications and the LRFD. The primary difference is the use of different reliability factors for the assessment of both infinite and finite fatigue lives.

For the fatigue evaluation of Bridge 9340, the provisions of the Guide Specifications and the LRFR Manual were used. The primary fatigue susceptible detail in the main truss members is the welded tabs at the intermediate diaphragms, a Category D detail, as discussed in Section 1.1. These details exist in the tension and stress reversal members, as illustrated in Figure 5-1.

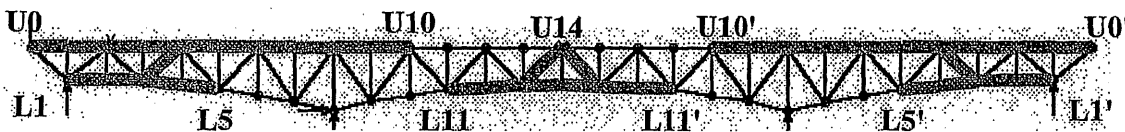


Figure 5-1: Main Truss Members with Fatigue Susceptible Details

5.2 Truss Member Fatigue Evaluation per AASHTO LRFR Manual

According to the LRFR Manual, the live load induced fluctuating stresses at a fatigue prone detail are represented by:

$$(\Delta f)_{\text{eff}} = R_s \Delta f$$

where, $(\Delta f)_{\text{eff}}$ = effective nominal stress range at a fatigue detail

Δf = stress range calculated from the factored (0.75 times) LRFD fatigue truck;
 stress range calculated using the actual truck weight based on traffic data or weight-in-motion study; or actual root-mean-cube stress range determined from a field strain measurement.

$R_s = R_{sa} R_{st}$ = stress range estimate partial load factor, varying with the method for determining Δf , as listed in **Table 5-1** (Table 7-1 of the LRFR Manual)

As shown in **Table 5-1**, for a refined analysis method using the LRFD fatigue truck, the value of the stress range estimate partial load factor (R_s) is suggested to be 0.95. **Table 5-2** and **Table 5-3** list the stress range analysis results for the “as-designed” and “locked” live load bearing conditions respectively in descending order for all tension and stress reversal main truss members that have the concerned fatigue details. Compression members are also listed if the unfactored dead load compressive stress is less than twice the maximum tensile live load stress. A table listing the stress values and ranges for all the members is listed in **Table AIII-1** and **Table AIII-2** in **Appendix III** for the “as-designed” and “locked” live load bearing conditions respectively.

According to the LRFR Manual, the fatigue life of a fatigue-prone detail is considered infinite if the maximum stress range the detail is expected to experience in its entire life is less than the constant amplitude fatigue threshold, or:

$$(\Delta f)_{\text{max}} \leq (\Delta F)_{\text{TH}}$$

where, $(\Delta f)_{max}$ = maximum stress range expected at the detail, may be taken as $2.0(\Delta f)_{eff}$
 $(\Delta F)_{TH}$ = constant amplitude fatigue threshold, 7.0 ksi for Category D detail, as listed in Table 6.6.1.2.5-3 of the LRFD

As shown in Table 5-2 and Table 5-3, the estimated maximum live load stress range, $(\Delta f)_{max} = 2.0R_s\Delta f$, in all truss members are well below the constant amplitude fatigue threshold $(\Delta F)_{TH}=7.0$ ksi. Therefore, the truss members are expected to have infinite fatigue life per AASHTO LRFR Manual.

Table 5-1. Stress Range Estimate Partial Load Factors in the LRFR Manual

Table 7-1 Partial Load Factors: R_{sa} , R_{st} , and R_s .

Fatigue-Life Evaluation Methods	Analysis Partial Load Factor, R_{sa}	Truck-Weight Partial Load Factor, R_{st}	Stress-Range Estimate Partial Load Factor, R_s (In general, R_s equals R_{sa} times R_{st})
For Evaluation or Minimum Fatigue Life			
Stress range by simplified analysis, and truck weight per Article 3.6.1.4 of the LRFD Specifications	1.0	1.0	1.0
Stress range by simplified analysis, and truck weight estimated through weight-in-motion study	1.0	0.95	0.95
Stress range by refined analysis, and truck weight per Article 3.6.1.4 of the LRFD Specifications	0.95	1.0	0.95
Stress range by refined analysis, and truck weight by weight-in-motion study	0.95	0.95	0.90
Stress range by field-measured strains	NA	NA	0.85
For Mean Fatigue Life			
All methods	NA	NA	1.00

BRIDGE 9340 STUDY



Table 5-2: Infinite Fatigue Life Check per LRFR Manual for Category D Detail
Main Truss and Stringer Bearings "As-Designed"

Member	Dead Load Stress	Max Live Load + Impact Stress	Min Live Load + Impact Stress	Stress Range Δf $w/I = .15$	Member Stress Type	$(\Delta\sigma)_{max} =$ $2.0 R_s \Delta f'$	$(\Delta F)_{TH} =$ 7.0
	(ksi)	(ksi)	(ksi)	(ksi)		(ksi)	(ksi)
L1-L2	1.50	0.80	-0.84	1.63	T	3.10	7.00
L3-U4	11.09	0.91	-0.67	1.58	T	3.01	7.00
U4'-L3'	7.46	0.87	-0.67	1.54	T	2.92	7.00
L2-L3	1.50	0.74	-0.77	1.51	T	2.86	7.00
U0-U1	9.76	1.25	-0.05	1.30	T	2.48	7.00
U5'-U4'	11.61	0.48	-0.76	1.25	T	2.37	7.00
U6'-U5'	10.95	0.48	-0.76	1.24	T	2.35	7.00
U4-U5	10.04	0.46	-0.75	1.21	T	2.29	7.00
U5-U6	9.42	0.44	-0.74	1.18	T	2.25	7.00
U4'-U3'	0.14	0.35	-0.76	1.11	T/C	2.10	7.00
L4-L5	-0.63	0.80	-0.30	1.10	T/C	2.09	7.00
L3-L4	-0.62	0.75	-0.30	1.05	T/C	1.99	7.00
U3'-U2'	-0.24	0.30	-0.74	1.04	T/C	1.98	7.00
U1'-U0'	13.21	0.99	-0.04	1.03	T	1.95	7.00
L11-L12	15.73	0.57	-0.18	0.75	T	1.42	7.00
L12-L13	15.73	0.57	-0.18	0.75	T	1.42	7.00
U1-U2	8.54	0.72	-0.02	0.74	T	1.41	7.00
L13'-L12'	16.18	0.54	-0.15	0.69	T	1.31	7.00
L12'-L11'	16.19	0.54	-0.14	0.68	T	1.30	7.00
U2'-U1'	11.42	0.64	0.00	0.64	T	1.22	7.00
L13-L14	17.54	0.53	-0.08	0.61	T	1.16	7.00
L14-L13'	17.54	0.53	-0.08	0.61	T	1.16	7.00
U8'-U7'	18.58	0.37	-0.09	0.46	T	0.88	7.00
U7-U8	18.80	0.36	-0.09	0.45	T	0.85	7.00
U7'-U6'	18.06	0.33	-0.08	0.41	T	0.78	7.00
U6-U7	18.30	0.33	-0.08	0.40	T	0.77	7.00
U9'-U8'	17.45	0.30	-0.09	0.39	T	0.74	7.00
U8-U9	18.15	0.29	-0.08	0.37	T	0.71	7.00
U10'-U9'	17.33	0.29	-0.07	0.36	T	0.69	7.00
U9-U10	18.13	0.29	-0.07	0.36	T	0.68	7.00

Table 5-3: Infinite Fatigue Life Check per LRFR Manual for Category D Detail
Main Truss and Stringer Bearings "Locked"

Member	Dead Load Stress	Max Live Load + Impact Stress	Min Live Load + Impact Stress	Stress Range Δf w/ I = .15	Member Stress Type	$(\Delta\sigma)_{max} =$ 2.0 $R_s \Delta f$	$(\Delta F)_{TR} =$ 7.0
	(ksi)	(ksi)	(ksi)	(ksi)		(ksi)	(ksi)
L3-U4	11.09	0.78	-0.72	1.50	T	2.86	7.00
U4'-L3'	7.46	0.76	-0.68	1.45	T	2.75	7.00
U0-U1	9.76	1.21	-0.05	1.26	T	2.40	7.00
L1-L2	1.50	0.59	-0.63	1.22	T	2.31	7.00
L2-L3	1.50	0.54	-0.59	1.13	T	2.14	7.00
U1'-U0'	13.21	0.95	-0.04	0.99	T	1.87	7.00
L4-L5	-0.63	0.62	-0.18	0.80	C	1.52	7.00
L3-L4	-0.62	0.60	-0.18	0.77	C	1.47	7.00
L13'-L12'	16.18	0.45	-0.09	0.54	T	1.03	7.00
L12-L13	15.73	0.45	-0.09	0.53	T	1.01	7.00
L12'-L11'	16.19	0.44	-0.09	0.53	T	1.01	7.00
L11-L12	15.73	0.44	-0.09	0.53	T	1.00	7.00
L14-L13'	17.54	0.44	-0.03	0.47	T	0.90	7.00
L13-L14	17.54	0.44	-0.03	0.47	T	0.90	7.00
U4'-U3'	0.14	0.11	-0.26	0.37	T/C	0.71	7.00
U5'-U4'	11.61	0.14	-0.22	0.36	T	0.68	7.00
U5-U6	9.42	0.05	-0.29	0.35	T	0.66	7.00
U6'-U5'	10.95	0.05	-0.29	0.34	T	0.64	7.00
U4-U5	10.04	0.10	-0.23	0.32	T	0.62	7.00
U1-U2	8.54	0.27	-0.04	0.31	T	0.59	7.00
U2'-U1'	11.42	0.25	-0.03	0.29	T	0.54	7.00
U9-U10	18.13	0.24	-0.01	0.25	T	0.47	7.00
U10'-U9'	17.33	0.24	-0.01	0.24	T	0.46	7.00
U7'-U6'	18.06	0.21	-0.03	0.24	T	0.45	7.00
U6-U7	18.30	0.20	-0.02	0.22	T	0.42	7.00
U9'-U8'	17.45	0.15	-0.03	0.18	T	0.35	7.00
U7-U8	18.80	0.15	-0.02	0.18	T	0.33	7.00
U8-U9	18.15	0.15	-0.03	0.17	T	0.33	7.00
U8'-U7'	18.58	0.15	-0.02	0.17	T	0.32	7.00

5.3 Truss Member Fatigue Evaluation per AASHTO Fatigue Guide Specifications

Based on the belief that the fatigue truck is expected to produce one half of an extreme stress range in the bridge service life, the Guide Specifications consider a fatigue detail to have infinite safe life and no further analysis required if:

$$R_s S_r < S_{FL}, \text{ or, } 2R_s S_t < S_c$$

where, S_r = nominal stress range calculated using the fatigue truck; adjusted using the actual truck weight based on traffic data or weight-in-motion study; or the root-mean-cube stress range determined from a field strain measurement.

S_{FL} = limiting stress range for infinite life, 2.6 ksi for Category D details, as listed in **Table 5-4**.

S_t = maximum tension portion of live load stress range S_r

S_c = compressive dead load stress at the fatigue detail

R_s = reliability factor associated with calculation of stress range, defined as

$$R_s = R_{SO} (F_{S1})(F_{S2})(F_{S3})$$

where, R_{SO} = basic reliability factor, 1.35 for redundant members and 1.75 for non-redundant members.

$(F_{S1})(F_{S2})(F_{S3})$ = reliability factors for method used to determine the nominal stress range, as listed in **Table 5-5**.

Table 5-4. Detail Constant and Limiting Stress Range in the Guide Specifications

Detail Category	Detail Constant K	Limiting Stress Range, ksi S_{FL}
A	68	8.8
B	33	5.9
B'	17	4.4
C	12	3.7*
D	6.0	2.6
E	2.9	1.6
E'	1.1	0.9
F	2.9	2.9

* Use 4.4 ksi for stiffeners.

Table 5-5. Reliability Factors in the Guide Specifications

Method for Nominal Stress Range S_r		F_{S1}	F_{S2}	F_{S3}
Field measurement for stress range histograms under normal traffic		0.85	1.0	1.0
Simplified analysis with live load distribution factor	Use of the fatigue truck	1.0	1.0	1.0
	Fatigue truck weight adjusted by truck traffic or weight station data		1.0	
	Fatigue truck weight adjusted by weigh-in-motion measurement		0.95	
Rigorous analysis such as finite element method	Use of the fatigue truck	1.0	1.0	0.96
	Fatigue truck weight adjusted by truck traffic or weight station data		1.0	
	Fatigue truck weight adjusted by weigh-in-motion measurement		0.95	

As shown in Table 5-5, for a rigorous analysis method using the fatigue truck, the final value of the reliability factors for non-redundant members is: $R_s = R_{SO} (F_{S1})(F_{S2})(F_{S3}) = (1.75)(1.0)(1.0)(0.96)=1.68$. Table 5-6 and Table 5-7 list the stress range analysis results in descending order for the “as-designed” and “locked” live load bearing conditions respectively for all tension and stress reversal main truss members that have the concerned fatigue details. Compression members are also listed if the unfactored dead load compressive stress is less than twice the maximum tensile live load stress. A table listing the stress values and ranges for all the members is listed in Table AIII-3 and Table AIII-4 in Appendix III for the “as-designed” and “locked” live load bearing conditions respectively.

Table 5-6: Infinite Fatigue Life Check per Guide Specifications for Category D Detail
Main Truss and Stringer Bearings "As-Designed"

Member	Dead Load Stress	Max Live Load + Impact Stress	Min Live Load + Impact Stress	Stress Range Sr w/ I = .10	Member Stress Type	$R_s S_r =$ 1.68 Sr	S_{FL}
	(ksi)	(ksi)	(ksi)	(ksi)		(ksi)	(ksi)
L1-L2	1.50	0.76	-0.78	1.53	T	2.58	2.60
L3-U4	11.09	0.85	-0.63	1.49	T	2.50	2.60
U4'-L3'	7.46	0.82	-0.63	1.45	T	2.43	2.60
L2-L3	1.50	0.70	-0.72	1.42	T	2.38	2.60
U0-U1	9.76	1.15	-0.04	1.19	T	2.00	2.60
U5'-U4'	11.61	0.46	-0.71	1.17	T	1.97	2.60
U6'-U5'	10.95	0.45	-0.71	1.16	T	1.95	2.60
U4-U5	10.04	0.43	-0.70	1.13	T	1.91	2.60
U5-U6	9.42	0.42	-0.69	1.11	T	1.86	2.60
U4'-U3'	0.14	0.33	-0.71	1.04	T/C	1.75	2.60
L4-L5	-0.63	0.75	-0.30	1.04	T/C	1.75	2.60
L3-L4	-0.62	0.71	-0.30	0.99	T/C	1.67	2.60
U3'-U2'	-0.24	0.28	-0.70	0.98	T/C	1.65	2.60
U1'-U0'	13.21	0.90	-0.04	0.94	T	1.58	2.60
L11-L12	15.73	0.54	-0.17	0.71	T	1.20	2.60
L12-L13	15.73	0.54	-0.17	0.71	T	1.19	2.60
U1-U2	8.54	0.67	-0.02	0.68	T	1.15	2.60
L13'-L12'	16.18	0.52	-0.14	0.66	T	1.11	2.60
L12'-L11'	16.19	0.51	-0.14	0.65	T	1.10	2.60
U2'-U1'	11.42	0.60	0.00	0.60	T	1.01	2.60
L13-L14	17.54	0.50	-0.08	0.58	T	0.97	2.60
L14-L13'	17.54	0.50	-0.08	0.58	T	0.97	2.60
U8'-U7'	18.58	0.35	-0.09	0.43	T	0.73	2.60
U7-U8	18.80	0.34	-0.09	0.42	T	0.71	2.60
U7'-U6'	18.06	0.31	-0.07	0.38	T	0.65	2.60
U6-U7	18.30	0.31	-0.07	0.38	T	0.63	2.60
U9'-U8'	17.45	0.28	-0.09	0.36	T	0.61	2.60
U8-U9	18.15	0.27	-0.08	0.35	T	0.59	2.60
U10'-U9'	17.33	0.27	-0.07	0.34	T	0.58	2.60
U9-U10	18.13	0.27	-0.07	0.34	T	0.57	2.60

Table 5-7: Infinite Fatigue Life Check per Guide Specifications for Category D Detail
Main Truss and Stringer Bearings "Locked"

Member	Dead Load Stress	Max Live Load + Impact Stress	Min Live Load + Impact Stress	Stress Range Sr w/ I = .10	Member Stress Type	$R_s S_r =$ 1.68 Sr	S_{FL}
	(ksi)	(ksi)	(ksi)	(ksi)		(ksi)	(ksi)
L3-U4	11.09	0.73	-0.67	1.41	T	2.36	2.60
U4'-L3'	7.46	0.71	-0.64	1.36	T	2.28	2.60
U0-U1	9.76	1.11	-0.04	1.15	T	1.94	2.60
L1-L2	1.50	0.55	-0.59	1.14	T	1.91	2.60
L2-L3	1.50	0.51	-0.55	1.06	T	1.77	2.60
U1'-U0'	13.21	0.87	-0.03	0.90	T	1.52	2.60
L4-L5	-0.63	0.58	-0.17	0.75	C	1.26	2.60
L3-L4	-0.62	0.56	-0.17	0.73	C	1.23	2.60
L13'-L12'	16.18	0.42	-0.09	0.51	T	0.86	2.60
L12'-L11'	16.19	0.42	-0.09	0.50	T	0.85	2.60
L12-L13	15.73	0.42	-0.08	0.50	T	0.84	2.60
L11-L12	15.73	0.42	-0.08	0.50	T	0.84	2.60
L14-L13'	17.54	0.41	-0.03	0.45	T	0.75	2.60
L13-L14	17.54	0.41	-0.03	0.45	T	0.75	2.60
U4'-U3'	0.14	0.10	-0.25	0.36	T/C	0.60	2.60
U5'-U4'	11.61	0.14	-0.22	0.36	T	0.60	2.60
U6'-U5'	10.95	0.05	-0.28	0.33	T	0.56	2.60
U5-U6	9.42	0.05	-0.27	0.32	T	0.54	2.60
U4-U5	10.04	0.09	-0.22	0.31	T	0.52	2.60
U1-U2	8.54	0.25	-0.04	0.29	T	0.48	2.60
U2'-U1'	11.42	0.23	-0.03	0.26	T	0.44	2.60
U9-U10	18.13	0.22	-0.01	0.22	T	0.38	2.60
U10'-U9'	17.33	0.21	-0.01	0.22	T	0.37	2.60
U7'-U6'	18.06	0.19	-0.03	0.22	T	0.36	2.60
U6-U7	18.30	0.18	-0.02	0.21	T	0.35	2.60
U9'-U8'	17.45	0.14	-0.04	0.18	T	0.30	2.60
U7-U8	18.80	0.14	-0.03	0.17	T	0.29	2.60
U8-U9	18.15	0.14	-0.03	0.17	T	0.28	2.60
U8'-U7'	18.58	0.14	-0.03	0.16	T	0.28	2.60

As shown in Table 5-6 and Table 5-6, the estimated effective live load stress range, $R_s S_r$, in all truss members are below the limiting stress range for infinite fatigue life, which is 0.375 times the constant amplitude fatigue threshold (7.0 ksi for Category D). Therefore, the truss members are expected to have infinite fatigue life per AASHTO Fatigue Guide Specifications.

5.4 Truss Member Fatigue Evaluation per Field Strain Measurements

The University of Minnesota conducted field strain measurements and load tests in 2001 for fatigue evaluation of Bridge 9340. The study concluded that fatigue cracking is not expected in the deck truss of this bridge.

5.5 Fatigue Evaluation Summary

Using the 3-D computer model and the fatigue truck for live load stress analysis, the truss members were determined to have infinite fatigue life in accordance with the AASHTO *Guide Manual for Condition Evaluation and Load and Resistance Factor Rating (LRFR) of Highway Bridges* (LRFR Manual) and the *Guide Specifications for Fatigue Evaluation of Existing Steel Bridges* (Guide Specifications). The University of Minnesota also concluded that fatigue cracking is not expected in the deck truss of this bridge based on field strain measurements and load tests in 2001. Therefore, it can be concluded that the probability for fatigue crack development at the concerned Category D details is remote.

However, the fatigue concern should not be completely discounted for the following reasons: (1) the access to the fatigue susceptible details inside the truss sections is very limited for crack inspection at the weld toes and therefore a timely discovery is unlikely to happen should a crack occur for some unusual causes; (2) the length of the welded tabs at the box section diaphragms was specified 3.5" in length in the original contract plans, which is very close to the lower limit of 4" for the Category E detail. The infinite fatigue life requirement would not be satisfied per the AASHTO Fatigue Guide Specifications if fabrication errors or poor workmanship causes the detail to have the fatigue resistance of a Category E detail; (3) the traffic on the bridge is heavy compared with the average highway bridge and therefore the use of a single fatigue truck may be underestimating the repetitive load effects on the structure. Based on discussions with Mn/DOT, a load case with three side-by-side fatigue trucks was investigated and the results will be discussed in Section 6.1.

SECTION 6

6. STRUCTURAL REDUNDANCY ANALYSIS

6.1 Identification of Eight Critical Truss Members

Eight critical main truss members were selected from one half of each truss for the investigation of structural redundancy and retrofit need. The eight members actually represent thirty-two main truss members due to the nearly double symmetry of the trusses.

Using the 3-D computer model calibrated with field testing results, the selection of the eight truss members was based on the following criteria:

- Subject to tension under combined dead load and live load
- Containing the fatigue susceptible welded details at the interior diaphragm as depicted in **Figure 1-5** and **Figure 1-6**
- Among members subject to the highest magnitude of fatigue load stress range (stress analysis results as discussed in Section 5.1)

The eight truss members selected based on these criteria are: L3-U4, L1-L2, U0-U1, U4-U5, U3-U4, L4-L5, L12-L13, and L13-L14, as shown in **Figure 6-1**. They cover all truss member types except the vertical, because the verticals are either compression members or do not have the fatigue susceptible detail.

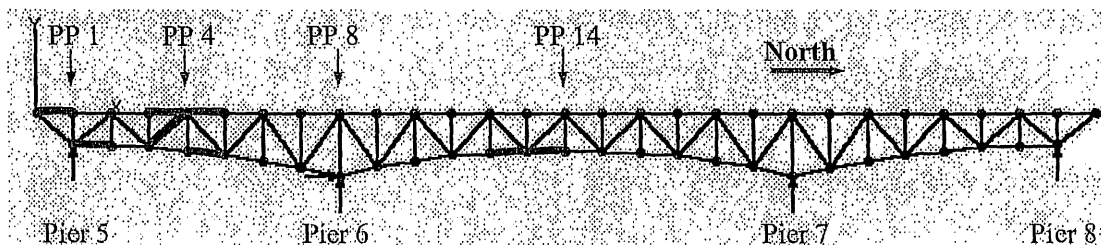


Figure 6-1: Eight Most Critical Truss Members

These eight members are considered most susceptible to fatigue-induced fracture among all truss members since they all have the same fatigue susceptible detail and are subject to the highest live load stress ranges. Stress ranges of the eight members under the 3-truck fatigue load are summarized in Table 6-1.

Table 6-1: Stress Summary of Eight Most Critical Truss Members
(Three side-by-side fatigue trucks in centerlines of outer lanes with 15% impact)

Member	DL Stress	Max LL+I	Min LL+I	Stress Range	Member	Cat. D	Cat. E
	(ksi)	Stress	Stress	$I = 0.15$ (ksi)		Stress	CAFL
		(ksi)	(ksi)		Type	(ksi)	(ksi)
L3-U4	11.09	2.05	-1.91	3.96	T	7.00	4.50
L1-L2	1.50	1.61	-1.61	3.22	T/C	7.00	4.50
U0-U1	9.76	2.89	-0.09	2.98	T	7.00	4.50
U4-U5	10.04	0.25	-0.67	0.92	T	7.00	4.50
U4'-U3'	0.14	0.29	-0.74	1.03	T/C	7.00	4.50
L4-L5	-0.63	1.68	-0.47	2.15	T/C	7.00	4.50
L12-L13	15.73	1.22	-0.25	1.47	T	7.00	4.50
L13-L14	17.54	1.18	-0.09	1.27	T	7.00	4.50

6.2 Objective and Key Issues of Bridge Redundancy Analysis

The redundancy analysis was to evaluate the structural consequence for the sudden failure of each of the eight critical truss members, using the 3-D computer model calibrated with field testing results. Based on the conventional planar analysis method used in truss bridge design, most tension truss members would be classified as fracture critical for statically determinant trusses. The primary objective of the redundancy analysis was to assess the three-dimensional bridge structural system's ability to redistribute the load upon failure of a main truss member, considering the participation of all structural components. The force effects of load redistribution after a sudden member failure were to be calculated and compared with load carrying capacities of the remaining members.

The following key issues were identified for the bridge redundancy analysis:

- Structural analysis procedure for a sudden member failure

- Live Load for redundancy analysis
- Criteria for evaluating capacities of remaining members

In order to properly address these issues, a redundancy analysis procedure was proposed to Mn/DOT after a literature review. The procedure was finalized after incorporating comments from Mn/DOT. Findings of the literature review, details of the procedure, and the results of the redundancy analysis are discussed in the subsequent sections of the report.

6.3 Literature Review on Bridge Redundancy Analysis

A literature review was conducted to investigate current status and available methods on the subject of bridge redundancy analysis. The following relevant AASHTO/NCHRP documents were found:

- AASHTO *LRFD Bridge Design Specifications*, 3rd Edition, 2004
- AASHTO *Guide Manual for Condition Evaluation and Load and Resistance Factor Rating (LRFR) of Highway Bridges*, 2003
- NCHRP Report 406, *Redundancy in Highway Bridge Superstructures*, 1998
- NCHRP Report 319, *Recommended Guidelines for Redundancy Design and Rating of Two-Girder Steel Bridges*, 1989
- NCHRP Synthesis 354, *Inspection and Management of Bridges with Fracture Critical Details*, 2005

6.3.1 AASHTO LRFD Bridge Design Specifications

The AASHTO LRFD Bridge Design Specifications have the following definitions for fracture critical members: “Main elements and components whose failure is expected to cause the collapse of the bridge or the inability of the bridge to perform its function shall be designated as failure-critical and the associated structural system as non-redundant.” “Alternatively, failure-critical members in tension may be designated fracture-critical.” Additionally, bridge

redundancy is defined as: “the quality of a bridge that enables it to perform its design function in the damaged state.”

The LRFD considers structural redundancy in its general design criterion:

$$\Sigma \eta_i \gamma_i Q_i \leq \phi R_n \quad (\text{Eq. 6-1})$$

where $\eta_i = \eta_D \eta_R \eta_I$ = load modifier, a factor relating to ductility, redundancy, and operational importance, respectively.

γ_i = load factor, a statistically determined multiplier on loading effects.

Q_i = nominal load effect, such as moment, shear, stress, displacement, etc.

ϕ = resistance factor, a statistically based multiplier applied to nominal resistance.

R_n = nominal resistance corresponding to the loading effect, based on nominal dimensions of the member and specified strength of the material.

The value of load modifier η_i in Equation (6-1) is affected by its component η_R , which is a function of member redundancy:

For the strength limit state:

$$\begin{aligned} \eta_R &\geq 1.05 \text{ for non-redundant members} \\ &= 1.00 \text{ for members of conventional redundancy} \\ &\geq 0.95 \text{ for members of exceptional level of redundancy} \end{aligned}$$

For all other limit states:

$$\eta_R = 1.00$$

As shown above, the quantification of redundancy consideration in the LRFD design is not clearly specified. The “1.05 or higher” allowance of load modifier for member redundancy is approximate and may be quite subjective in actual applications. Additionally, no detailed guidelines are provided in the LRFD for the evaluation of “collapse” in terms of damage types, loading, member failure criteria, and analysis procedure for load redistribution in the damaged structure including dynamic amplification.

6.3.2 AASHTO LRFR Manual

The AASHTO *Guide Manual for Condition Evaluation and Load and Resistance Factor Rating (LRFR) of Highway Bridges* was published in 2003 to serve as a standard for existing bridge evaluation using the reliability based methods that are consistent with the LRFD. In the LRFR Manual, considerations for the level of redundancy of superstructure system are reflected in the system factor (ϕ_s) in load and resistance factor rating. The system factor is used as a multiplier for reducing the nominal member capacity in non-redundant bridges, only for checking the flexural and axial effects at the strength limit state. For two-girder/truss/arch bridges of typical spans and geometries, for example, $\phi_s = 0.85$ for welded members, and $\phi_s = 0.90$ for riveted members, respectively. Additionally, $\phi_s = 0.85$ for three-girder bridges with girder spacing less than or equal to 6-ft; $\phi_s = 0.95$ for four-girder bridges with girder spacing less than or equal to 4-ft; and $\phi_s = 1.00$ for all other girder bridges and slab bridges, respectively.

The use of the system factor is to maintain an adequate level of safety of the complete bridge superstructure system. Non-redundant bridges are penalized by requiring their members to provide higher safety levels than those of similar bridges with redundant configurations. The system factor in the LRFR rating corresponds to, and is more conservative than, the load modifier in the LRFD design for non-redundant bridges. The aim of the LRFR system factor is to add a reserve capacity such that the overall system reliability is increased from approximately an Operating level (for redundant systems) to a more realistic target for non-redundant systems corresponding to the Inventory level.

The LRFR Manual noted that if the Engineer can demonstrate the presence of adequate redundancy in a bridge superstructure system following the procedures of NCHRP Report 406, the system factor may be taken as $\phi_s = 1.0$. No quantitative criteria, however, have been provided.

6.3.3 NCHRP Report 406

The NCHRP Report 406, *Redundancy in Highway Bridge Superstructures*, was published in 1998 to serve as a guide to bridge redundancy analysis. The objective of the document was to develop a framework for considering redundancy in design and evaluation of highway bridge superstructures. Its definition of redundancy is “*the capacity of a bridge superstructure to continue to carry loads after the failure of one of its members*”. The report emphasizes structural system behavior by introducing system factors for safety and redundancy of the entire bridge system rather than the individual bridge members.

Four limit states were defined: (1) the Member Failure Limit State for individual members; (2) the Ultimate/Collapse Limit State for system capacity under extreme loading; (3) the Functionality Limit State for excessive deformations for traffic; and (4) the Damaged Condition Limit State for load carrying capacity after the loss of a main member. The structural capacity for each limit state is measured by a load factor, which was defined as the ratio of the bridge capacity subtracting the dead load effect to the maximum live load effect:

$$LF = \frac{R - D}{L} \quad (\text{Eq. 6-2})$$

where LF = load factor for a limit state

R = bridge resistance, or capacity, for a limit state

D = dead load effect

L = maximum live load effect

For live load analysis, a set of two side-by-side HS-20 trucks were specified to be placed across the bridge for maximum effects of each limit state. This live load is to be increased incrementally until a limit state is reached, independent of the actual number of lanes on the bridge. Therefore, the structural capacity, or load factor, for each limit state is a multiplier of two HS-20 trucks the bridge can carry before the limit state is reached. The member failure limit state was defined as the yielding or ultimate failure of the first member, under unfactored load, based on a linear elastic analysis of the intact structure. The ultimate/collapse limit state was defined as the

formation of a collapse mechanism or loss of load-carrying capacity of main member(s), based on a non-linear analysis of the intact structure under unfactored load. The functionality limit state was defined as a permanent deformation of one hundredth of span length, based on a non-linear analysis of the intact structure under unfactored load. Lastly the damaged condition limit state was defined as the collapse of the damaged structure (loss of a main load-carrying component due to fracture or an accident), based on a non-linear analysis of the damaged condition under unfactored load.

In NCHRP Report 406, structural redundancy was defined as the capacity of structure to continue to carry load after the first failure of a main member. The level of bridge redundancy is measured by system reserve ratios for each of the latter three limit states:

$$\begin{aligned}R_u &= \frac{LF_u}{LF_1} \\R_f &= \frac{LF_f}{LF_1} \\R_d &= \frac{LF_d}{LF_1}\end{aligned}\tag{Eq. 6-3}$$

where, R_u , R_f and R_d = system reserve ratios for ultimate, functionality and damaged condition limit states, respectively.

LF_u , LF_f and LF_d = load factors, or multipliers of two HS-20 trucks, for ultimate, functionality and damaged condition limit states, respectively.

LF_1 = load factor for member failure limit state

For example, if $R_u = 1.0$, or $LF_u = LF_1$, the bridge is non-redundant since the failure of the most critical member would result in a collapse of the system.

Bridge redundancy check per the NCHRP 406 procedure requires the calculation of load factors for all the limit states and system reserve ratios. The adequacy of the system reserve ratios are then verified in accordance with the specified minimum acceptable values developed upon structural reliabilities to account for load and resistance uncertainties as well as the redundancy

level of AASHTO designs of four-beam simple span bridges. The required system reserve ratios for adequate bridge redundancy are summarized in Table 6-2.

Table 6-2: Required System Reserve Ratios for Adequate Redundancy (NCHRP Report 406)

Ultimate/Collapse Limit State	$R_{u \text{ req}} = (LF_u / LF_l)_{\text{req}}$	1.30
Functionality Limit State	$R_{f \text{ req}} = (LF_f / LF_l)_{\text{req}}$	1.10
Damaged Condition Limit State	$R_{d \text{ req}} = (LF_d / LF_l)_{\text{req}}$	0.50

It should be indicated that check of structural redundancy based on system reserve ratios is only for the redundancy of the structural system. Non-redundant bridges may still provide high levels of system safety if members are over-designed. Therefore, redundancy check should be performed in conjunction with member safety check.

6.3.4 NCHRP Report 319

The NCHRP Report 319, Recommended Guidelines for Redundancy Design and Rating of Two-Girder Steel Bridges, was published in 1989. This document was primarily focused on load redistribution in the two-girder steel bridge system. Its application for general bridge redundancy analysis was limited and had been largely superseded by the much more extensive NCHRP Report 406.

6.3.5 NCHRP Synthesis 354

The NCHRP Synthesis 354, Inspection and Management of Bridges with Fracture Critical Details, was published in 2005. It focuses on the inspection and maintenance of bridges with fracture-critical members (FCMs), as defined in the AASHTO LRFD specifications. The objectives of this report were to survey and identify gaps in literature; determine practices and problems with FCMs; and identify specific research needs. Based on a survey responded by thirty-four US states and three Canadian provinces, information was gathered regarding how

bridge owners define, identify, document, inspect, and manage bridges with fracture-critical details.

The NCHRP Synthesis 354 provides no details in regard to bridge redundancy analysis. One of its findings was that NCHRP Report 406 was at the time the most comprehensive document available for quantitative bridge redundancy analysis.

6.4 Proposed Procedure for Redundancy Analysis

The redundancy analysis procedure proposed in NCHRP Report 406 was reviewed and discussed with Mn/DOT. It was determined that it did not exactly fit the specific needs of Bridge 9340 evaluation in terms of loading conditions and the perspectives of examining the structural consequence in case of a main truss member failure. The NCHRP Report 406 procedure is for general quantification of bridge superstructure redundancy based on structural reliabilities. For Bridge 9340, the primary objective is to evaluate the probability of a structural failure caused by a sudden member failure of the main truss, and to establish most efficient retrofit measures to minimize such failure. Therefore, the general approach should be to evaluate the force effects of the member failure and compare them with the load carrying capacities of the remaining members.

The statics for a truss member failure occurring under the combined dead load and a specific live load is illustrated in **Figure 6-2**. Truss member forces at the failed state (Condition A) is a result of the superposition of the intact structure under the total load (Condition B) and the failed structure with the total member forces of the failed member prior to the failure applied to both ends in the opposite directions (Condition C), i.e., $\text{Condition A} = \text{Condition B} + \text{Condition C}$. In Condition B, the original state, the role of the to-be-removed member in the structural system may be physically replaced by its member forces applied at its both ends. The superposition of Condition C to Condition B, therefore, cancels out the member end forces and is equivalent to removing the member from the structural system.

Statics for Loss of a Truss Member (Linear Elastic Stiffness Analysis)

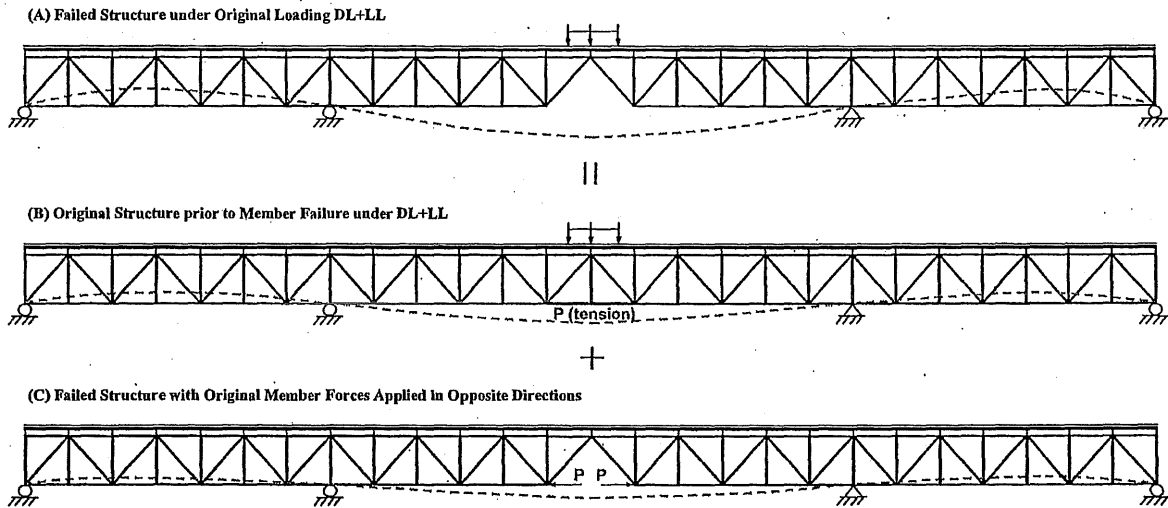


Figure 6-2: Superposition Process for Truss Member Forces Caused by a Member Failure

The dynamic effect due to a sudden member failure also needs to be considered to account for the magnified member forces in the rest of the structure. This happens when the final stage of the member failure is a result of a brittle fracture, although likely preceded by a relatively slow fatigue crack propagation process. The failed structure with the original member forces applied in the opposite directions (Figure 6-3) can be idealized as a single-degree-of-freedom (SDOF) system composed of a mass with certain stiffness and damping (Figure 6-4). The sudden member failure acts like the application of a step load that instantly increases from zero to its full magnitude (Figure 6-4). The normalized displacement of the SDOF system, which is the ratio of the dynamic displacement to the static displacement, is illustrated in the graph in Figure 6-4 and is based on the equation $u(t)$ known as the Duhamel's Integral. This graph shows the normalized displacement for three different levels of damping (ζ): $\zeta = 0$ (no damping), $\zeta = 0.05$ (5% damping), and $\zeta = 0.2$ (20% damping). A damping value of 5%, which is typically acceptable for most bridge applications, yields a dynamic-to-static behavior ratio of 1.854. This value was used throughout the redundancy analysis of Bridge 9340 to magnify the static results to account for the dynamic effects caused by a sudden member failure.

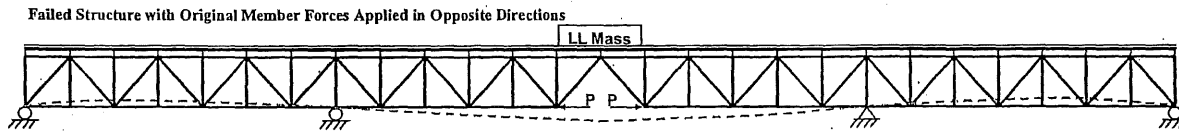


Figure 6-3: Sudden Member Failure as a Dynamic Step Load Consisting of a Pair of Forces

$$u(t) = (u_{st})_o \left[1 - e^{-\zeta \omega_n t} \left(\cos \omega_D t + \frac{\zeta}{\sqrt{1-\zeta^2}} \sin \omega_D t \right) \right]$$

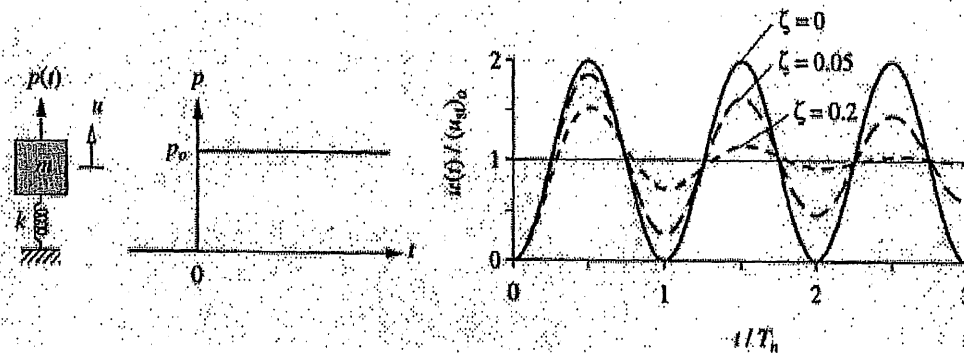


Figure 6-4: Dynamic Response of a Single-Degree-Of-Freedom System to a Step Load
(Courtesy of *Dynamics of Structures* by Anil K. Chopra)

A procedure for truss bridge redundancy analysis was developed and performed for each of the eight critical members for various load cases. Only one member failure was assumed to occur at a time. The analysis was performed using the 3-D computer model calibrated with field testing results. The procedure has eight steps and is described in detail as follows.

Step 1: Analysis of Intact Structure for Dead Load Effects. The cumulative dead load effects in member forces were analyzed following a step-wise procedure to account for the varying structural configuration during the construction stages from cambering, non-composite dead load, to composite dead load, as described in Section 4.1. For dead load analysis, the main truss bearings and the stringer bearings were all assumed to behave “as-designed” in the model because the expansion bearings should have functioned properly at the bridge construction phase.

Step 2: Analysis of Intact Structure for Live Load Effects at Failure. The failure of each critical member was assumed to occur at the live load position that induces the maximum axial force in the member under investigation. The live load, to be discussed in detail in Section 6.5, was moved across the bridge longitudinally for maximum axial force in the member under investigation and member forces of the intact structure were solved. In the live load analysis, the main truss bearings were assumed to be “locked” based on findings from the model calibration with field testing data. The stringer bearings were assumed to behave as-designed since the model calibration indicated that the stringer expansion bearing condition did not affect live load force effects significantly and a truss member failure would likely force the stringer bearings to move.

Step 3: Total Member Forces in Intact Structure just before Failure. Total member forces from the dead and live loads in the intact structure just before a member failure were determined by summing the member forces obtained from Step 1 and Step 2. This corresponds to Condition (B) in Figure 6-2.

Step 4: Model of “Failed” Structure with a Main Truss Member Failure. The computer model for the “failed” structure was formed by removing one main truss member at a time. This was done for each of the eight critical truss members so that eight models of the failed structure were established.

Step 5: Analysis of “Failed” Structure for Original Member Forces Applied in Opposite Directions. Each “failed” structure was analyzed for the static loading of the original member forces of the removed member just before failure (from Step 4) applied in the opposite directions, corresponding to Condition (C) in Figure 6-2. Loads were applied to the two joints where the critical member under investigation had been removed and the forces at each joint include three forces and three moments.

Step 6: Dynamic Impact of Sudden Member Failure. The static member forces obtained in Step 5 were multiplied by the step-load dynamic factor of 1.854 with an assumed 5% damping. The dynamic magnification only applies to the force results from Step 5, not those from Step 3.

Step 7: Total Member Forces Resulted from Sudden Member Failure. The total member forces in the failed structure, including the dynamic impact of sudden member failure, were obtained by summing the force results from Step 3 with those from Step 6. This is the structural consequence of a sudden failure of a main truss member.

Step 8: Structural Stability Check of Remaining Members. The stability of the bridge superstructure after a truss member failure was checked by comparing the total member forces from Step 7 with their corresponding capacities, for tension and compression, respectively. This was to determine if any additional member failure may be possible. Since all steel members were modeled with space frame members, the capacity check was performed at both ends of each member utilizing the force interaction equation that takes into account axial force and both in-plane and out-of-plane bending moments. Shear forces were ignored in the capacity check. Failure for any member was defined as an interaction ratio greater than or equal to 1.0 at either end of the member. The capacity check was performed both with and without the 1.854 dynamic impact factor. All members of the main truss, the floor truss, the portal and sway truss, and the upper and lower lateral bracing were checked for the failure of each of the eight critical members and for each live load case. Details of the member capacity check are discussed in the next section.

6.5 Live Load for Redundancy Analysis

Four live load cases were used for the redundancy analysis. The load cases were chosen to represent conditions that are likely to occur on Bridge 9340.

BRIDGE 9340 STUDY

URS

Case 1: Dead Load Only without Live Load - This load case represented the bridge being closed to traffic. The results of this load case were used to determine if the self-weight of the structure would cause any additional member failures if a main truss member failed.

Case 2: Eight Lanes of Slow Moving HS-20 Truck Load - Each of the eight lanes was loaded with an HS-20 truck. The eight HS-20 trucks were placed side-by-side transversely, centered in each lane, and placed longitudinally to maximize the axial force in the critical member under investigation. No multiple presence factor or vehicle impact was applied.

Case 3: Eight Lanes of Standstill HS-20 Truck and Lane Load - This load case represented the "parking lot" condition of bumper to bumper traffic during rush hour. The eight HS-20 trucks were placed side-by-side transversely, centered in each lane, and placed longitudinally to maximize the axial force in the critical member under investigation. The lane load was placed over the full length of the bridge for each lane, instead of only in areas for maximum load effect, to represent the more realistic parking lot situation. Similar to Case 2, no multiple presence factor or vehicle impact was applied.

Case 4: LRFD Design Load - A transverse load distribution determined that seven lanes of load induce the maximum load effect to the main truss due to the transverse cantilever at each side. As a result, seven of the eight lanes were loaded with a full length lane load combined with an HS-20 truck. The seven side-by-side HS-20 trucks were pushed as close to the east edge as possible in each lane, and placed longitudinally to maximize the axial force in the critical member under investigation. This load case is consistent with the LRFD design load, which is the current design code used by Mn/DOT, except that the lane load was used as full length for simplification purposes. In accordance with the LRFD specifications, a multiple presence factor of 0.65 and a dynamic load allowance of 33% were used in this load case.

6.6 Criteria for Capacity Check of Remaining Bridge System

After the force effects were calculated using the analysis procedure and live load discussed in the previous sections, the remaining bridge system (members and connections) were checked for their structural capacities against the consequent forces resulting from the sudden loss of each of the eight critical truss members under investigation.

6.6.1 Member Capacity Check

Since space frame members were used in the model for all steel components (main trusses, floor trusses, portal and sway frames, lateral bracings, and stringers), their capacities were checked using the force interaction ratio as discussed in Section 4.1, including the effects of axial force and in-plane and out-of-plane bending moments. Both end sections of each member were checked. The general expression for a member section capacity check using the force interaction ratio is:

$$R = \frac{P}{P_u} + \left[\frac{M}{M_u} \right]_{(in-plane)} + \left[\frac{M}{M_u} \right]_{(out-of-plane)} \quad (\text{Eq. 6-4})$$

where, R = force interaction ratio, when > 1.0, indicating section capacity exceeded by force effects, or a section failure

P = axial force resulting from a member failure

M = bending moment resulting from a member failure

P_u = ultimate axial capacity of member section

M_u = ultimate bending capacity of member section

The calculation of member section capacities, for tension or compression members, was based on the AASHTO *Guide Specifications for Strength Design of Truss Bridges (Load Factor Design)* (1985 with 1986 interims), as discussed in Section 4.1. It should be noted that the capacity criteria in the Truss Bridge Guide Specifications are based on the Load Factor Design

method. As a result, the member design forces are based on factored loads and the section capacities represent the ultimate section strength.

For redundancy analysis of Bridge 9340, the actual member forces, under unfactored load, resulting from a sudden member failure were used in Eq. 6-4 for the force interaction ratio, along with the actual section capacity at the ultimate state. The force interaction ratio, therefore, presents an actual measurement of the load effects in terms the member section capacity, or the probability of section failure.

6.6.2 Connection Capacity Check

Another consideration in the capacity check is the connections, such as the gusset joints of truss members. For connection design using the Allowable Stress Design method, the basic AASHTO criterion is: "Connections for main members shall be designed for a capacity based on the average of the calculated design stress in the member and the allowable stress of the member at the point of connection, but in any event, not less than 75% of the capacity of the member." This is a general requirement that applies to tension, compression, bending, or shear. In the original design of Bridge 9340 that followed the 1961 AASHTO *Standard Specifications for Highway Bridges*, the general requirement for connection design was the same. An examination of the plans indicated the likelihood of the use of the 75% member capacity rule in the truss connection design, since relatively less connection bolts were used for lightly loaded truss members compared with more heavily loaded members of comparable section dimensions.

The connection capacities were not calculated based on the actual dimensions of the gusset plates and the rivets/bolts because of the complexities and uncertainties in possible failure sections of the gusset plates and in ultimate capacities of rivets and bolts. Instead, the calculated member capacities as discussed in Section 4.3 were adjusted to consider the truss connection capacities per the following:

- A member design force (P) was determined in accordance with the stress table in the original design sheet for each member at the service load level

- A member ultimate axial capacity (C) was determined based on its actual plate dimensions
- For truss members with a design force less than 75% of its capacity, i.e., $P/C < 0.75$, the connection capacity is assumed to be 75% of member capacity
- For truss members with a design force greater than 75% of its capacity, i.e., $P/C \geq 0.75$, the connection capacity is assumed to be $(r_{conn})C$, where $r_{conn} = [(P+C)/2]/(C)$, which should vary between 0.75 and 0.99.
- In member capacity check using Eq. (6-4), the calculated member force interaction ratio (R) is divided by r_{conn} to consider a reduction of the member capacity due to the relatively weaker connection.

For example, a truss member has: $P = 100$ kips, $C = 120$ kips, and thus $r_{conn} = [(P+C)/2]/(C) = 0.92$. If the force interaction ratio using Eq. (6-4) is calculated as $R = 0.90$ considering the axial and in-plane and out-of-plane bending effects, the adjusted interaction ratio considering the relatively weaker connection capacity is $R/r_{conn} = 0.90/0.92 = 0.98$.

Table 6-3 summarizes the connection capacity adjustment factors for each of the main truss members. Due to symmetry about the longitudinal centerline, the factors for the east truss members are equivalent to the factors for the west truss members.

Table 6-3: Connection Capacity Adjustment Factors for Main Truss Members

Connection Capacity Adjustment Factors for Main Truss Members East and West Truss Values are the Same					
Bridge Component Member Type	Member	Connection Capacity Adjustment Factor	Bridge Component Member Type	Member	Connection Capacity Adjustment Factor
Upper Chord Members	U0-U1	0.914	Diagonals	U0-L1	0.934
	U1-U2	0.914		L1-U2	0.937
	U2-U3	0.750		U2-L3	0.750
	U3-U4	0.750		L3-U4	0.993
	U4-U5	0.990		U4-L5	0.939
	U5-U6	0.990		L5-U6	0.992
	U6-U7	0.994		U6-L7	0.931
	U7-U8	0.994		L7-U8	0.995
	U8-U9	0.982		U8-L9	1.000
	U9-U10	0.982		L9-U10	0.940
	U10-U11	0.905		U10-L11	0.999
	U11-U12	0.905		L11-U12	0.944
	U12-U13	0.969		U12-L13	0.989
	U13-U14	0.969		L13-U14	0.924
	U14-U13'	0.969		U14-L13'	0.924
	U13'-U12'	0.969		L13'-U12'	0.989
	U12'-U11'	0.905		U12'-L11'	0.944
	U11'-U10'	0.905		L11'-U10'	0.999
	U10'-U9'	0.982		U10'-L9'	0.940
	U9'-U8'	0.982		L9'-U8'	1.000
	U8'-U7'	0.994		U8'-L7'	0.995
	U7'-U6'	0.994		L7'-U6'	0.931
	U6'-U5'	0.990		U6'-L5'	0.992
	U5'-U4'	0.990		L5'-U4'	0.939
U4'-U3'	0.750	U4'-L3'	0.910		
U3'-U2'	0.750	L3'-U2'	0.964		
U2'-U1'	0.990	U2'-L1'	0.944		
U1'-U0'	0.990	L1'-U0'	0.941		
Lower Chord Members	L1-L2	0.750	Verticals	U1-L1	0.924
	L2-L3	0.750		U2-L2	0.989
	L3-L4	0.750		U3-L3	0.925
	L4-L5	0.750		U4-L4	0.960
	L5-L6	0.965		U5-L5	0.919
	L6-L7	0.965		U6-L6	0.997
	L7-L8	0.971		U7-L7	0.889
	L8-L9	0.973		U8-L8	0.938
	L9-L10	0.958		U9-L9	0.886
	L10-L11	0.958		U10-L10	0.994
	L11-L12	0.980		U11-L11	0.900
	L12-L13	0.980		U12-L12	0.993
	L13-L14	1.000		U13-L13	0.938
	L14-L13'	1.000		U14-L14	0.969
	L13'-L12'	0.980		U13'-L13'	0.938
	L12'-L11'	0.980		U12'-L12'	0.993
	L11'-L10'	0.958		U11'-L11'	0.900
	L10'-L9'	0.958		U10'-L10'	0.994
	L9'-L8'	0.973		U9'-L9'	0.886
	L8'-L7'	0.971		U8'-L8'	0.938
	L7'-L6'	0.965		U7'-L7'	0.889
	L6'-L5'	0.965		U6'-L6'	0.997
	L5'-L4'	0.750		U5'-L5'	0.919
	L4'-L3'	0.750		U4'-L4'	0.960
L3'-L2'	0.750	U3'-L3'	0.925		
L2'-L1'	0.750	U2'-L2'	0.989		
			U1'-L1'	0.924	

6.7 Results Summary of Redundancy Analysis

This section presents the results of the redundancy analysis using the procedure described previously. The results are grouped by live load cases and the critical truss members under investigation. As structural consequences of a critical truss member failure, all members of the main trusses, floor trusses, portal and sway frames, and upper lateral and lower lateral bracings were investigated for possible failures. Detailed tables for the main truss and floor truss member results are included in **Appendix IV** and are referenced in the report text as necessary. The deck and stringers were also investigated for possible consequent failures but only for selected load cases and critical truss members under investigation. Details are discussed in the following sections.

6.7.1 Member Failures of Intact Structure under Dead Load

Prior to the assumed failure of any of the main truss members, some floor truss members were determined to have force interaction ratios greater than 1.0 under the dead load only. These floor trusses were typically located at the location of the deck expansion joints, as shown in **Figure 6-5**. Upon further investigation, it was determined that the dominate contributor to the total interaction ratio for these floor truss members was the out-of-plane bending. For those members the effects of the axial force and the in-plane bending were negligible compared with that of the out-of-plane bending in terms of the force to capacity ratio. These greater than 1.0 interaction ratios were caused by the out-of-plane distortion of the floor truss due to the asymmetry of the as-designed stringer bearing releases, as shown in **Figure 3-21**. At the deck expansion joint locations the stringer releases are mostly fixed on one side and expansion on the other. Since the stringer-floor truss-main truss system tends to act as a composite structure, the global bending of the superstructure under the vertical load induces longitudinal shear at the connections. The asymmetric layout of stringer bearing release causes the fixed stringers to exert a longitudinal load to the floor truss while the expansion stringers move longitudinally with much smaller forces depending on the friction. The unbalanced longitudinal load causes the floor truss to bend

out-of-plane. This behavior would not have been considered in a planar analysis in the conventional truss bridge design.

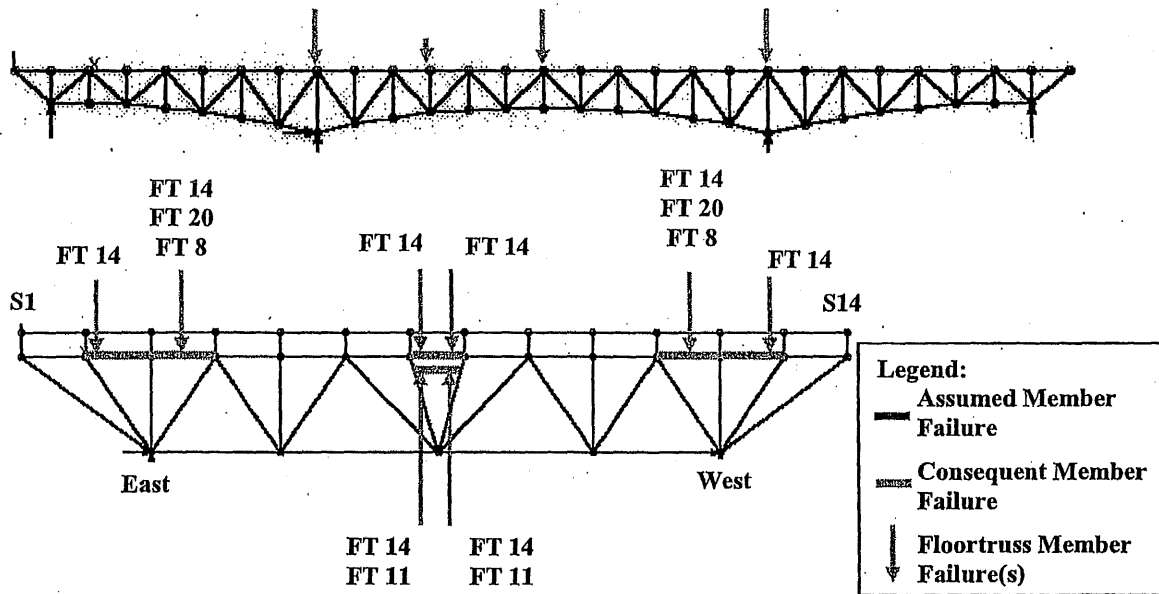


Figure 6-5: Floor Truss Member “Failures” of Intact Structure under Dead Load Only

The interaction ratios greater than 1.0 for the floor truss members of the intact structure under the dead load are not considered serious since no signs of overstress have been reported for these members in the bridge history. Additionally, the out-of-plane bending effects of the floor truss at the deck expansion joint may likely have been overestimated due to the complete ignorance of the friction of the stringer expansion bearing.

6.7.2 Member Failures of Intact Structure under Combined Dead and Live Load

For the live load cases (discussed in Section 6.5) for redundancy analysis, some floor truss members were found to produce force interaction ratios exceeding 1.0 under the combined dead and live load in the intact condition prior to the removal of the critical truss member under investigation. Most of these members had relatively high (close to 1.0) force interaction ratios under the dead load, caused by the out-of-plane distortion of the floor truss due to the asymmetry

of the as-designed stringer bearing releases as discussed in Section 6.7.1. This behavior is discussed in the subsequent sections of the report where applicable.

6.7.3 Deformed Shapes of Failed Structure

The redundancy analysis was to determine member forces of the remaining structure after the failure of each of the eight critical truss members, for the four live load cases as discussed in Section 6.5. The deformed shapes of the structure after the failure of each critical member under investigation are shown in Figures 6-6 through 6-13, respectively. The deformed shapes remain essentially the same for all four live load cases used in the study.

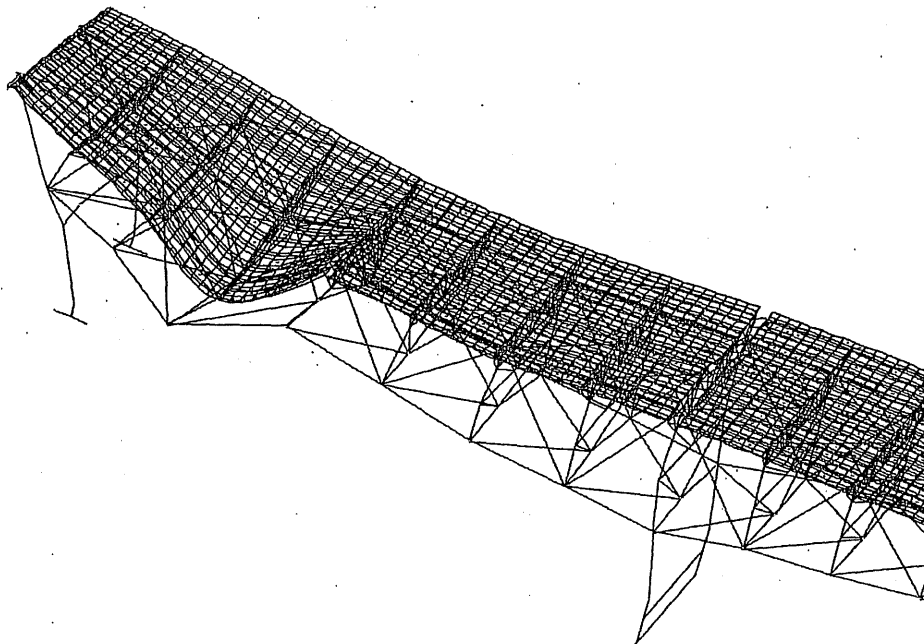


Figure 6-6: Deformed Shape after Failure of East Truss Diagonal L3-U4

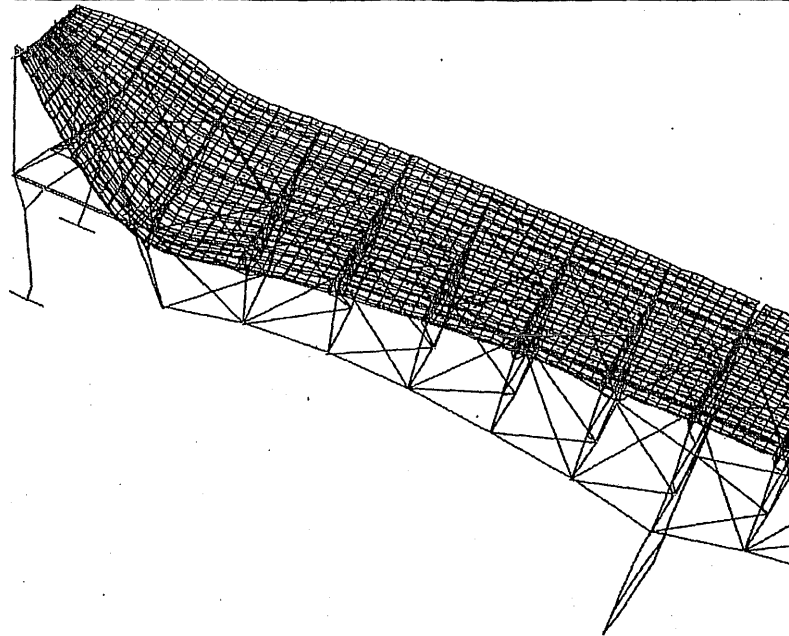


Figure 6-7: Deformed Shape after Failure of East Truss Lower Chord L1-L2

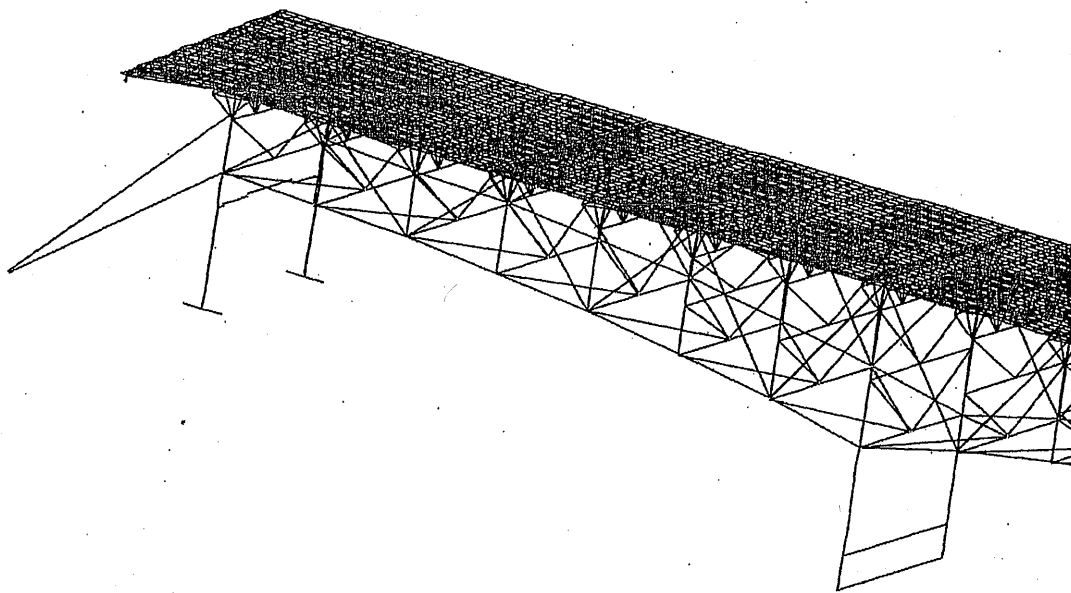


Figure 6-8: Deformed Shape after Failure of East Truss Upper Chord U0-U1

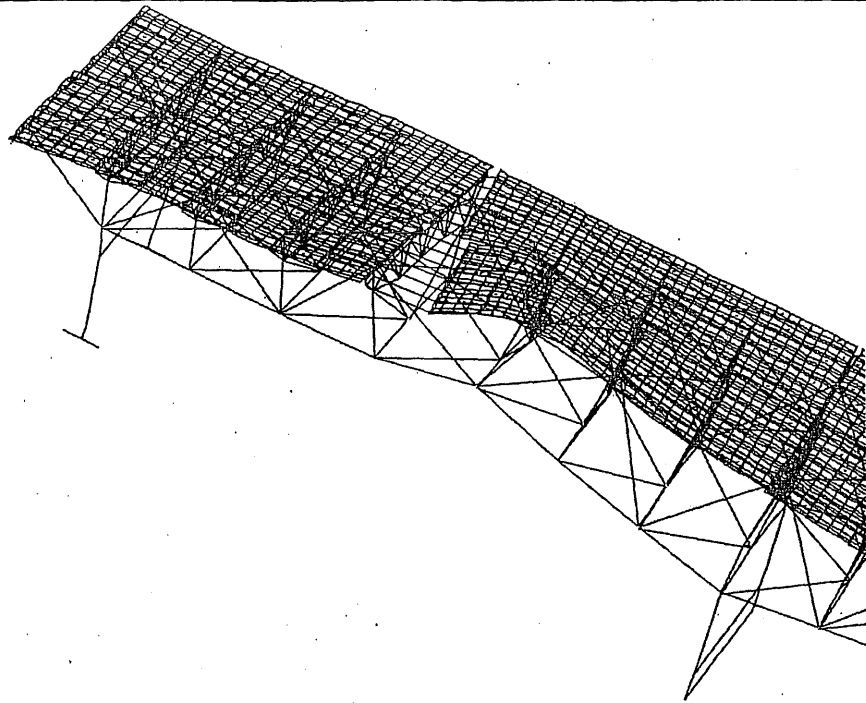


Figure 6-9: Deformed Shape after Failure of East Truss Upper Chord U4-U5

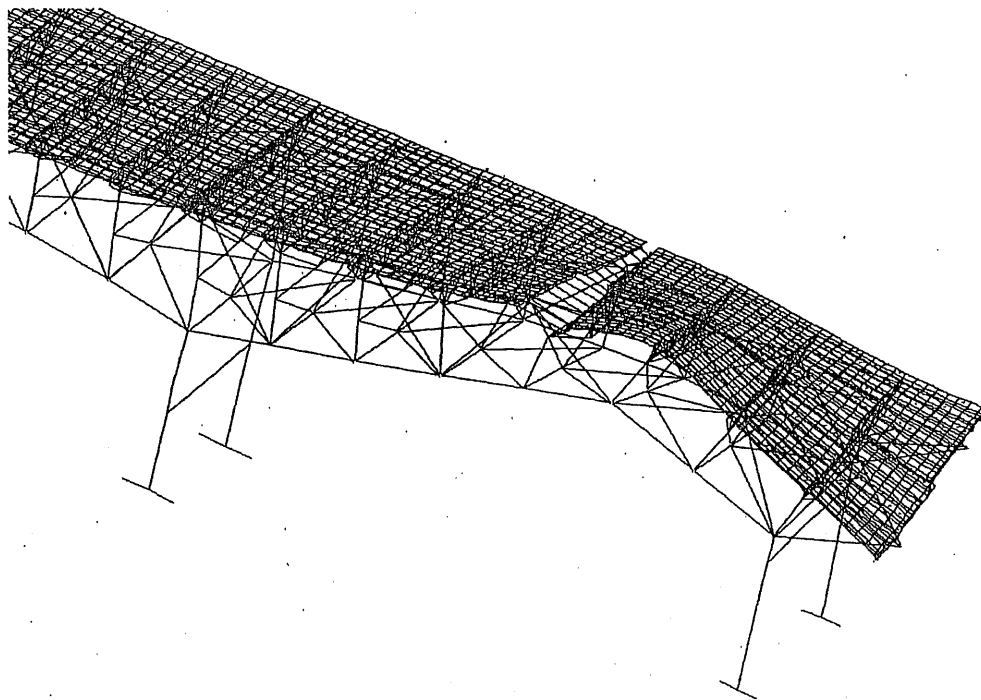


Figure 6-10: Deformed Shape after Failure of East Truss Upper Chord U4'-U3'

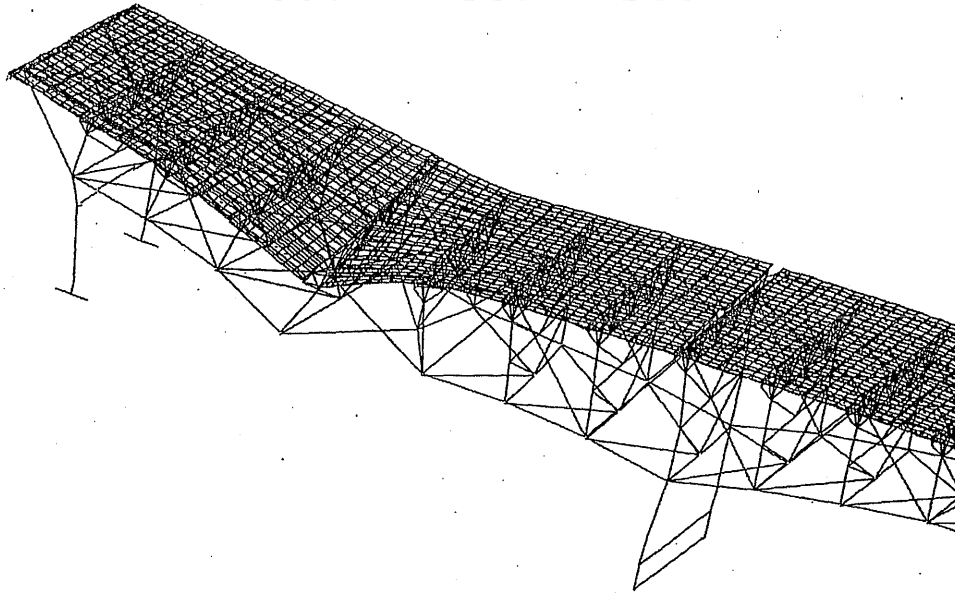


Figure 6-11: Deformed Shape after Failure of East Truss Lower Chord L4-L5

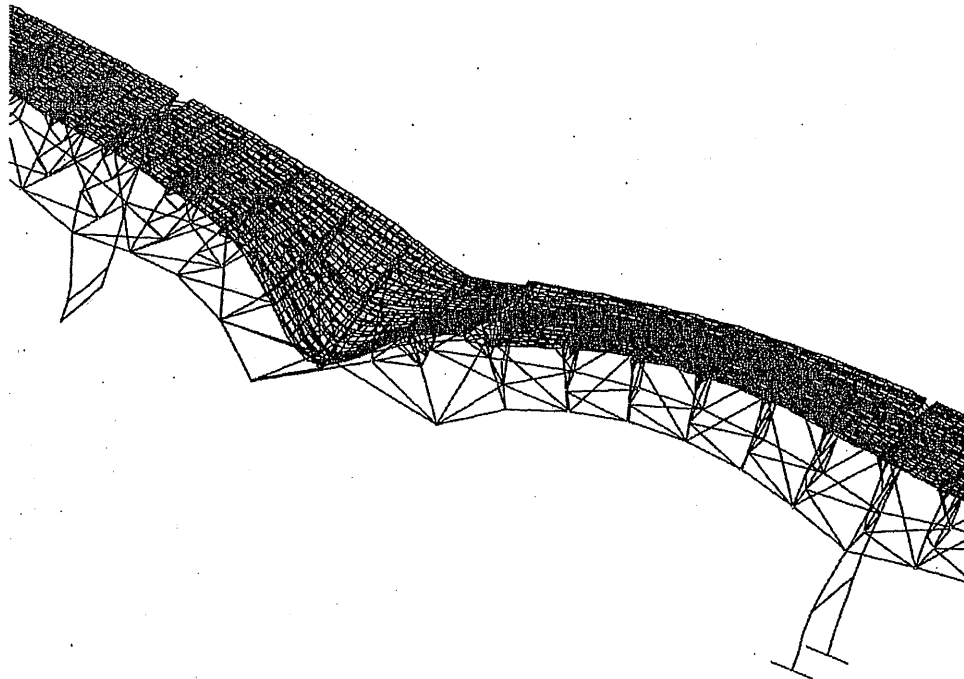


Figure 6-12: Deformed Shape after Failure of East Truss Lower Chord L12-L13

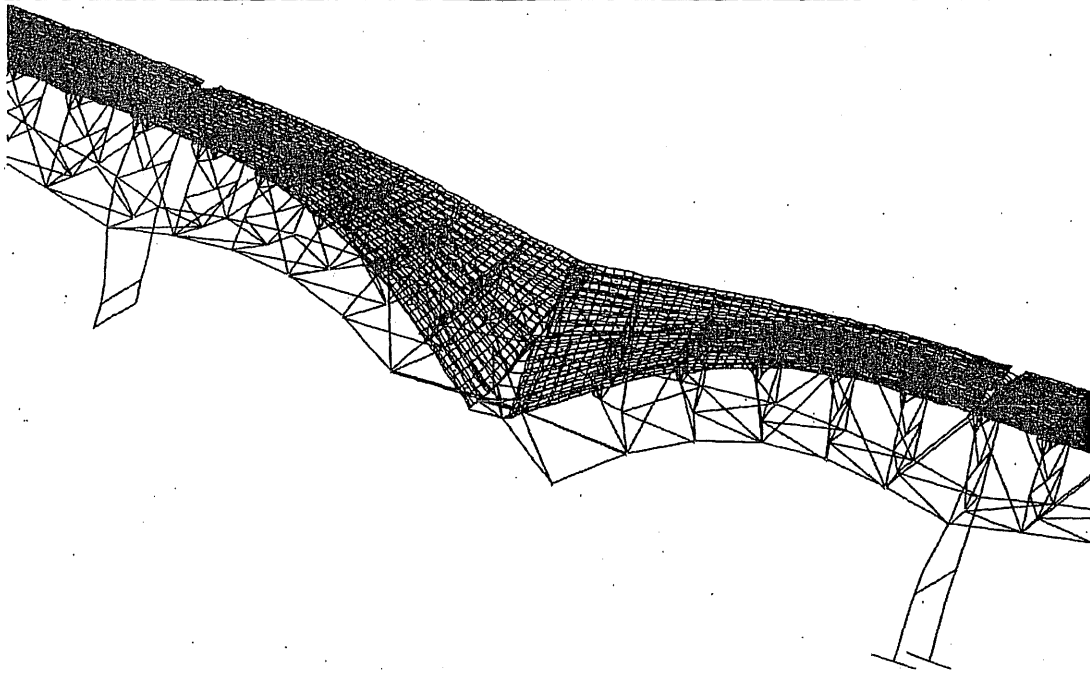


Figure 6-13: Deformed Shape after Failure of East Truss Lower Chord L13-L14

6.7.4 General Summary of Redundancy Analysis Results

Results of the redundancy analysis are discussed in **Table 6-4** for each of the four load cases due to the sudden failure of each of the eight critical main truss members. The results include the following items, with details discussed in the subsequent sections:

- Number of consequent main truss member failures
- Number of consequent floor truss member failures
- Impact on the floor truss members that “failed” in the intact structural condition
- Consequent impact on reactions at the expansion bearings
- Consequent maximum bridge deflections

Table 6-4: General Summary of Structural Consequences Resulting from Failure of a Main Truss Member (1 of 2)

General Summary of Structural Consequences Resulting from Failure of a Main Truss Member

Notes:

1. All failures reported in this table are member failures, which may include either or both section failure(s) of the member.
2. For floor trusses, the number is new failures of members that did not fail in the intact condition under combined dead and live load
3. All truss expansion bearings are in "as-designed" condition for dead load analysis, and "locked" condition for live load analysis.

Member for Failure Investigation	Load Case	Dynamic Impact of Sudden Failure	No. of Consequent Member Failures					Expansion Bearing Reactions			Max Displacements	
			Main Trusses (Members)	Main Trusses (Connections)	Floor Trusses	Sway Portal Frames	Top/Bott Lateral Bracings	Max R(long) kips	Max Ratio of (Rl/Rv)	Bearing Location	Max Disp(vert) inch	Joint Location
L3-U4 (Diagonal)	Load 1	x 1.0	0	0	0	0	0	92.19	0.04	P5-E	-0.20	L3-East
		x 1.854	0	0	0	0	0	170.93	0.08	P5-E	-0.38	L3-East
	Load 2	x 1.0	0	0	0	0	0	97.94	0.07	P5-E	-0.38	L3-East
		x 1.854	0	0	0	0	0	127.16	0.09	P5-E	-0.71	L3-East
	Load 3	x 1.0	0	0	0	0	0	143.28	0.08	P5-E	-0.44	L3-East
		x 1.854	0	0	0	0	0	177.12	0.10	P5-E	-0.82	L3-East
	Load 4	x 1.0	0	0	0	0	0	115.71	0.07	P5-E	-0.41	L3-East
		x 1.854	0	0	0	0	0	146.78	0.09	P5-E	-0.76	L3-East
L1-L2 (Lower Chord)	Load 1	x 1.0	0	0	0	0	0	34.49	0.03	P5-E	0.11	U0-East
		x 1.854	0	0	0	0	0	63.95	0.05	P5-E	0.20	U0-East
	Load 2	x 1.0	0	0	0	0	0	182.60	0.12	P5-E	0.39	U0-East
		x 1.854	0	0	0	0	0	287.88	0.20	P5-E	0.72	U0-East
	Load 3	x 1.0	0	0	0	0	0	267.86	0.15	P5-E	0.53	U0-East
		x 1.854	1	2	0	0	0	411.85	0.24	P5-E	0.99	U0-East
	Load 4	x 1.0	0	0	0	0	0	215.90	0.13	P5-E	0.44	U0-East
		x 1.854	0	1	2	0	0	334.86	0.20	P5-E	0.82	U0-East
U0-U1 (Upper Chord)	Load 1	x 1.0	2	2	5	0	0	35.13	0.11	P5-E	-71.14	U0-East
		x 1.854	3	4	15	0	2	65.13	0.20	P5-E	-131.90	U0-East
	Load 2	x 1.0	2	2	12	0	2	109.35	0.17	P5-E	-108.75	U0-East
		x 1.854	4	5	17	0	4	155.00	0.28	P5-E	-201.62	U0-East
	Load 3	x 1.0	2	3	13	0	2	300.34	0.12	P5-E	-109.98	U0-East
		x 1.854	6	6	20	0	3	347.37	0.22	P5-E	-203.91	U0-East
	Load 4	x 1.0	2	2	14	0	2	193.72	0.13	P5-E	-108.05	U0-East
		x 1.854	4	5	23	0	3	239.66	0.24	P5-E	-200.32	U0-East
U4-U5 (Upper Chord)	Load 1	x 1.0	0	0	4	0	0	69.02	0.04	P5-E	0.63	L5-East
		x 1.854	0	0	6	0	1	127.97	0.07	P5-E	1.17	L5-East
	Load 2	x 1.0	0	0	3	0	0	267.60	0.06	P6-W	0.79	L5-East
		x 1.854	0	0	8	0	1	340.97	0.08	P6-W	1.46	L5-East
	Load 3	x 1.0	0	0	7	0	2	457.35	0.08	P6-W	0.79	L5-East
		x 1.854	0	1	11	0	3	531.01	0.10	P6-W	1.46	L5-East
	Load 4	x 1.0	0	0	4	0	0	305.52	0.06	P6-W	0.75	L5-East
		x 1.854	0	0	10	0	2	375.80	0.08	P6-W	1.40	L5-East

Table 6-4: General Summary of Structural Consequences Resulting from Failure of a Main Truss Member (2 of 2)

General Summary of Structural Consequences Resulting from Failure of a Main Truss Member

Notes:

1. All failures reported in this table are member failures, which may include either or both section failure(s) of the member.
2. For floor trusses, the number is new failures of members that did not fail in the intact condition under combined dead and live load
3. All truss expansion bearings are in "as-designed" condition for dead load analysis, and "locked" condition for live load analysis.

Member for Failure Investigation	Load Case	Dynamic Impact of Sudden Failure	No. of Consequent Member Failures					Expansion Bearing Reactions			Max Displacements	
			Main Trusses (Members)	Main Trusses (Connections)	Floor Trusses	Sway Portal Frames	Top/Bott Lateral Bracings	Max R(long) kips	Max Ratio of (Rl/Rv)	Bearing Location	Max Disp(vert) inch	Joint Location
U4'-U3' (Upper Chord)	Load 1	x 1.0	0	0	0	0	0	2.65	0.00	P5-E	0.06	L3'-East
		x 1.854	0	0	0	0	0	4.92	0.00	P5-E	0.11	L3'-East
	Load 2	x 1.0	0	0	2	0	0	32.69	0.01	P6-E	0.42	L3'-East
		x 1.854	0	0	3	0	0	47.55	0.01	P8-W	0.79	L3'-East
	Load 3	x 1.0	0	0	0	0	0	205.83	0.04	P6-E	0.02	U4'-East
		x 1.854	0	0	0	0	0	206.80	0.04	P6-E	0.04	U4'-East
	Load 4	x 1.0	0	0	0	0	0	131.93	0.03	P6-E	0.11	L3'-East
		x 1.854	0	0	0	0	0	135.62	0.03	P6-E	0.21	L3'-East
L4-L5 (Lower Chord)	Load 1	x 1.0	0	0	0	0	0	24.92	0.01	P5-E	0.10	L4-East
		x 1.854	0	0	0	0	0	46.21	0.02	P5-E	0.19	L4-East
	Load 2	x 1.0	0	0	0	0	0	134.16	0.10	P5-E	-0.38	L4-East
		x 1.854	0	0	0	0	0	191.74	0.14	P5-E	-0.70	L4-East
	Load 3	x 1.0	0	0	0	0	0	200.92	0.12	P5-E	-0.54	L4-East
		x 1.854	0	0	0	0	0	281.43	0.17	P5-E	-1.00	L4-East
	Load 4	x 1.0	0	0	1	0	0	152.67	0.10	P5-E	-0.40	L4-East
		x 1.854	0	0	1	0	0	213.48	0.14	P5-E	-0.75	L4-East
L12-L13 (Lower Chord)	Load 1	x 1.0	0	1	4	0	0	481.21	0.11	P6-E	-1.50	U12-East
		x 1.854	2	3	6	0	0	892.17	0.20	P6-E	-2.78	U12-East
	Load 2	x 1.0	2	2	3	0	0	740.81	0.16	P6-E	-1.77	U12-East
		x 1.854	3	5	5	1	0	1225.59	0.26	P6-E	-3.28	U12-East
	Load 3	x 1.0	4	5	5	0	1	991.36	0.18	P6-E	-1.97	U12-East
		x 1.854	7	9	11	2	1	1529.41	0.26	P6-E	-3.64	U12-East
	Load 4	x 1.0	3	3	3	0	0	850.38	0.16	P6-E	-1.84	U12-East
		x 1.854	5	6	5	1	0	1354.35	0.25	P6-E	-3.41	U12-East
L13-L14 (Lower Chord)	Load 1	x 1.0	0	0	4	0	0	631.56	0.15	P6-E	-2.95	U14-East
		x 1.854	6	6	7	4	3	1170.91	0.27	P6-E	-5.47	U14-East
	Load 2	x 1.0	4	4	6	1	3	911.53	0.21	P6-E	-3.40	U14-East
		x 1.854	7	7	12	4	6	1531.64	0.34	P6-E	-6.29	U14-East
	Load 3	x 1.0	7	9	8	3	3	1203.19	0.22	P6-E	-3.88	U14-East
		x 1.854	10	11	24	4	6	1911.69	0.34	P6-E	-7.20	U14-East
	Load 4	x 1.0	6	6	5	1	3	1044.36	0.20	P6-E	-3.63	U14-East
		x 1.854	7	7	15	4	6	1706.45	0.33	P6-E	-6.72	U14-East

6.7.5 Load Case 1: Dead Load Only (Bridge Closed to Traffic)**1. Failure of East Truss Diagonal L3-U4**

The calculated force interaction ratios indicated no consequent failures of any structural members as a result of the failure of east truss diagonal L3-L4, without or with the dynamic impact factor of 1.854. This is true for the investigation of the member capacities as well as the investigation of the connection capacities which were evaluated by applying the connection capacity adjustment factor to the member capacities, as discussed in **Section 6.6.2**. The results of calculated force interaction ratios are summarized in **Table AIV-1A** (member capacities) and **Table AIV-1B** (connection capacities) for main truss members and **Table AIV-2** and **Table AIV-3** for floor truss members. Floor truss members that had interaction ratios greater than 1.0 under dead load in the intact condition were listed separately (**Table AIV-3**). As seen in these tables, the sudden member failure does not cause significant force changes in most members of the main trusses and the floor trusses. This may be partly due to the assumed "locked" bearing condition that creates an arch effect.

Table AIV-4 and **Table AIV-5** list support reactions and maximum joint displacements and corresponding locations, respectively, induced from the failure of east truss diagonal L3-L4. As indicated in **Table AIV-4**, longitudinal bearing reactions are induced by the member failure. The ratio of the longitudinal force to the dead load vertical reaction at each pier, however, is very low, with the highest value of approximately 0.08 at the east bearing of Pier 5 with a dynamic impact factor of 1.854. The low longitudinal forces are not expected to overcome the frictional resistance at the steel roller bearings and therefore the expansion bearings should remain "locked". The maximum joint displacements resulting from the member failure, as indicated in **Table AIV-5**, were very low.

2. Failure of East Truss Lower Chord L1-L2

The calculated force interaction ratios indicated no consequent failures of any structural members as a result of the failure of east truss lower chord L1-L2, without or with the dynamic impact factor of 1.854. This is true for the investigation of the member capacities as well as the investigation of the connection capacities. The results of calculated force interaction ratios are summarized in **Table AIV-6A** (member capacities) and **Table AIV-6B** (connection capacities) for main truss members and **Table AIV-7** and **Table AIV-8** for floor truss members. For those floor truss members that have interaction ratios greater than 1.0 under dead load in the intact condition, the failure of east truss lower chord L1-L2 did not cause significant changes to the force interaction ratio, as shown in **Table AIV-8**.

Table AIV-9 and **Table AIV-10** list support reactions and maximum joint displacements and corresponding locations, respectively. The induced longitudinal reactions at the "locked" expansion bearings are low (a maximum longitudinal to vertical force ratio of 0.05 at the east bearing of Pier 5 with a dynamic impact factor of 1.854), and are not expected to change the existing bearing condition. The maximum joint displacements resulting from the member failure were very low.

3. Failure of East Truss Upper Chord U0-U1

The calculated force interaction ratios indicated that two consequent main truss member failures and five consequent floor truss member failures would result from the failure of east truss upper chord U0-U1, when dynamic impact was not included (**Figure 6-14**). No portal and sway frame members or upper lateral and lower lateral bracing members would fail. When a dynamic impact factor of 1.854 was included, three consequent main truss member failures and fifteen consequent floor truss member failures would occur (**Figure 6-15**). No portal and sway frame members would fail but two upper lateral and lower lateral bracing members would fail. When the connection capacities are

considered, two (U0-L1 and U1-L1) and four (U0-L1, U1-L1, U0-U1, and L1-L2) consequent main truss member failures would occur without and with the 1.854 dynamic impact factor respectively. The results of the calculated force interaction ratios are summarized in Table AIV-11A (member capacities) and Table AIV-11B (connection capacities) for main truss members and Table AIV-12 and Table AIV-13 for floor truss members. For those floor truss members that have interaction ratios greater than 1.0 under dead load in the intact condition, the sudden member failure did not cause significant changes to the force interaction ratio.

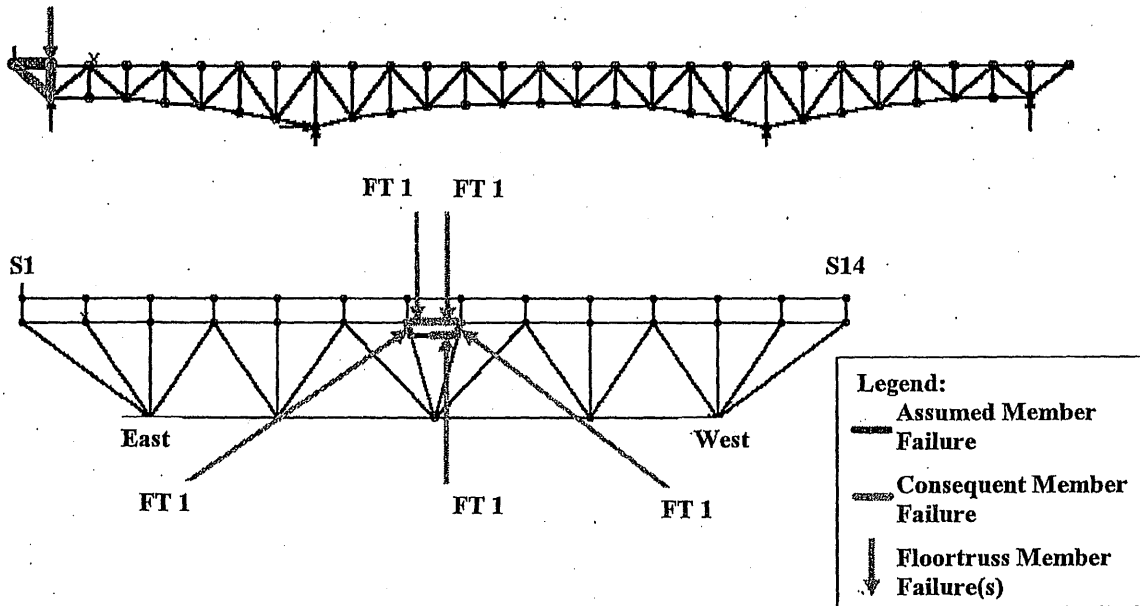


Figure 6-14: Load Case 1 – Failure of East Truss Upper Chord U0-U1
Consequent Member Failures without Dynamic Impact

Table AIV-14 and Table AIV-15 list support reactions and maximum joint displacements and corresponding locations, respectively. The induced longitudinal reactions at the “locked” expansion bearings are relatively low (a maximum longitudinal to vertical force ratio of 0.20 at the east bearing of Pier 5 with a dynamic impact factor of 1.854), and are not expected to change the existing “locked” condition of the steel roller bearing. The displacements of the east truss upper joint U0 resulting from the member

failure were extremely high, which indicated the instability of diagonal U0-L1 for supporting the weight of the approach span without the upper chord U0-U1.

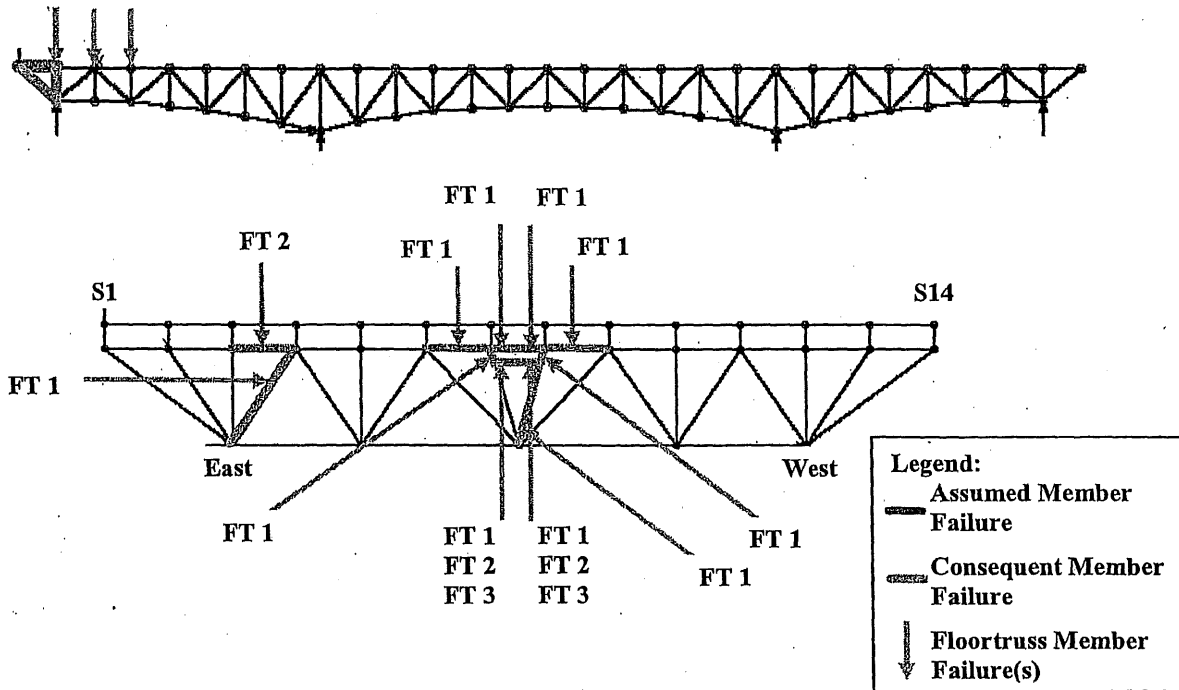


Figure 6-15: Load Case 1 – Failure of East Truss Upper Chord U0-U1 Consequent Member Failures with a Dynamic Impact Factor of 1.854

4. Failure of East Truss Upper Chord U4-U5

The calculated force interaction ratios indicated no consequent main truss member failures as a result of the failure of east truss upper chord U4-U5, without or with the dynamic impact factor of 1.854. This is true for the investigation of the member capacities as well as the investigation of the connection capacities. When no dynamic impact was included, four consequent floor truss member failures were determined to occur (Figure 6-16) and no portal and sway frame members or upper lateral and lower lateral bracing members would fail. When a dynamic impact factor of 1.854 was included, six consequent floor truss member failures were found to occur (see Figure 6-17) and no portal and sway frame members would fail. In addition one upper lateral

bracing consequent member failure would occur. The results of calculated force interaction ratios are summarized in Table AIV-16A (member capacities) and Table AIV-16B (connection capacities) for main truss members and Table AIV-17 and Table AIV-18 for floor truss members. For those floor truss members that have interaction ratios greater than 1.0 under dead load in the intact condition, the sudden member failure did not cause significant changes to the force interaction ratio.

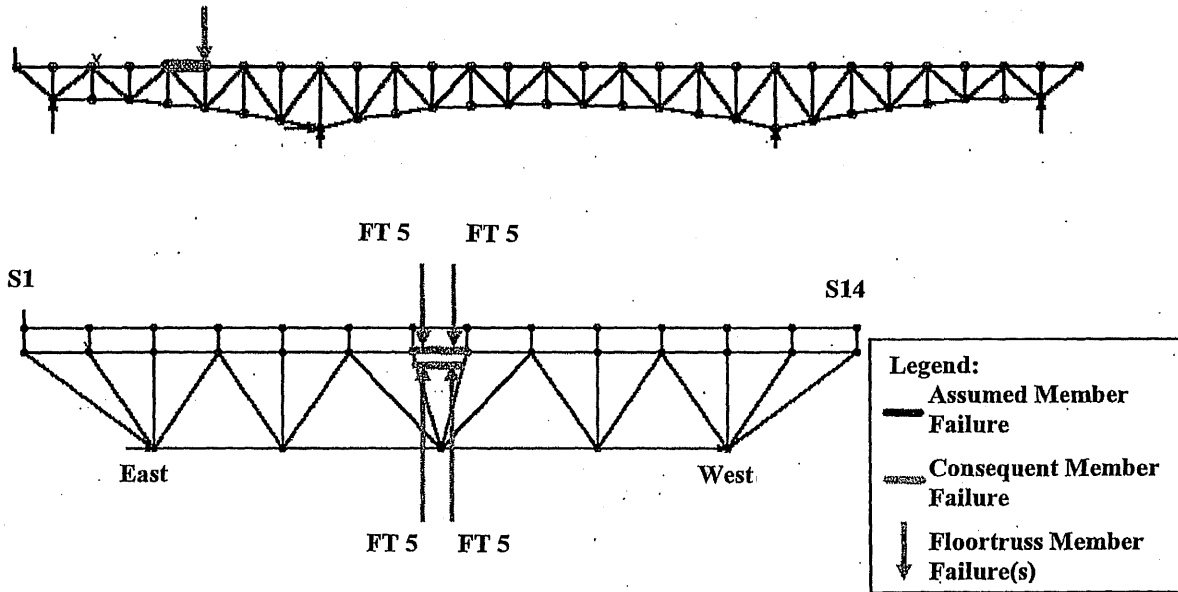


Figure 6-16: Load Case 1 – Failure of East Truss Upper Chord U4-U5
Consequent Member Failures without Dynamic Impact

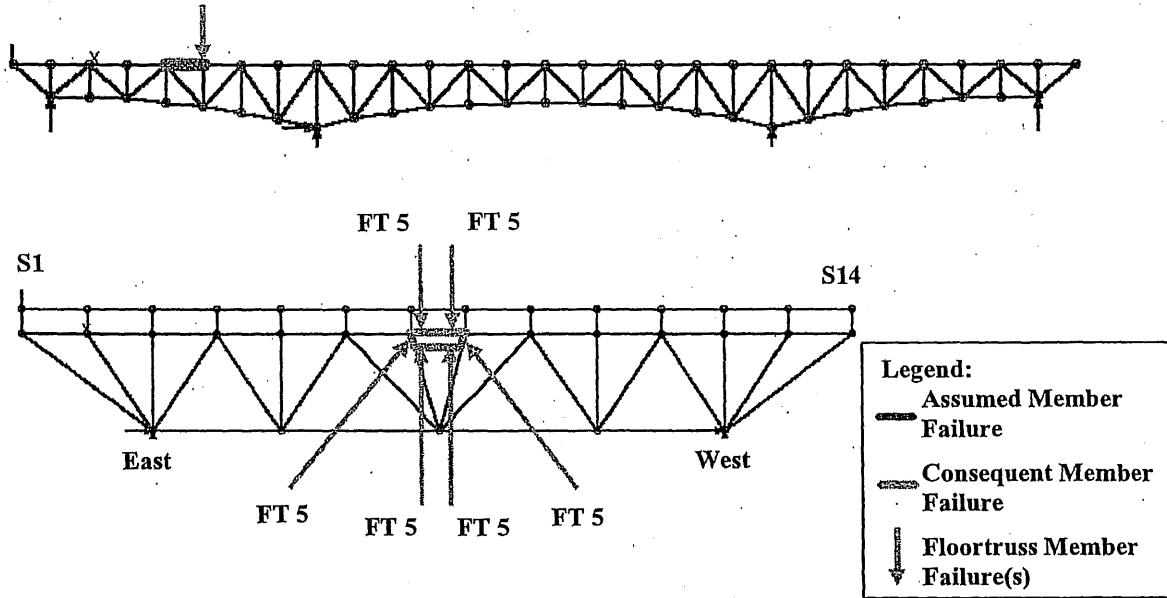


Figure 6-17: Load Case 1 – Failure of East Truss Upper Chord U4-U5
Consequent Member Failures with a Dynamic Impact Factor of 1.854

Table AIV-19 and Table AIV-20 list support reactions and maximum joint displacements and corresponding locations, respectively. The induced longitudinal reactions at the “locked” expansion bearings were low (a maximum longitudinal to vertical force ratio of 0.08 at the west bearing of Pier 6 with a dynamic impact factor of 1.854), and are not expected to change the existing bearing condition. The maximum joint displacements resulting from the member failure were found low.

5. Failure of East Truss Upper Chord U4'-U3'

Member U4'-U3' was found to be subject to slightly higher forces than its counterpart U3-U4 due to different section properties and therefore used for the redundancy analysis. The calculated force interaction ratios indicated no consequent failures of any structural members as a result of the failure of east truss upper chord U4'-U3', without or with the dynamic impact factor of 1.854. This is true for the investigation of the member capacities as well as the investigation of the connection capacities. The results of calculated force interaction ratios are summarized in Table AIV-21A (member

capacities) and **Table AIV-21B** (connection capacities) for main truss members and **Table AIV-22** and **Table AIV-23** for floor truss members. For those floor truss members that have interaction ratios greater than 1.0 under dead load in the intact condition, the sudden member failure did not cause significant changes to the force interaction ratio.

Table AIV-24 and **Table AIV-25** list support reactions and maximum joint displacements and corresponding locations, respectively. The induced longitudinal reactions at the "locked" expansion bearings were low (a maximum longitudinal to vertical force ratio of less than 0.01 at the east bearing of Pier 5 with a dynamic impact factor of 1.854), and are not expected to change the existing bearing condition. The maximum joint displacements resulting from the member failure were very low.

6. Failure of East Truss Lower Chord L4-L5

The calculated force interaction ratios indicated no consequent failures of any structural members as a result of the failure of east truss lower chord L4-L5, without or with the dynamic impact factor of 1.854. This is true for the investigation of the member capacities as well as the investigation of the connection capacities. The results of calculated force interaction ratios are summarized in **Table AIV-26A** (member capacities) and **Table AIV-26B** (connection capacities) for main truss members and **Table AIV-27** and **Table AIV-28** for floor truss members. For those floor truss members that have interaction ratios greater than 1.0 under dead load in the intact condition, the sudden member failure did not cause significant changes to the force interaction ratio.

Table AIV-29 and **Table AIV-30** list support reactions and maximum joint displacements and corresponding locations, respectively. The induced longitudinal reactions at the "locked" expansion bearings were very low (a maximum longitudinal to vertical force ratio of 0.02 at the east bearing of Pier 5 with a dynamic impact factor of 1.854), and are not expected to change the existing bearing condition. The maximum joint displacements resulting from the member failure were very low.

7. Failure of East Truss Lower Chord L12-L13

When dynamic impact was not included, the calculated force interaction ratios indicated no consequent main truss member failures but four consequent floor truss member failures resulting from the failure of east truss lower chord L12-L13 (Figure 6-18). When a dynamic impact factor of 1.854 was included, however, two consequent main truss member failures and six consequent floor truss member failures would occur (Figure 6-19). No portal and sway frame members or upper lateral and lower lateral bracing members would fail. When the connection capacities are considered, one (L10-L11) and three (L10-L11, L9-L10, and L8-L9) consequent main truss member failures would occur without and with the 1.854 dynamic impact factor respectively. The results of calculated force interaction ratios are summarized in Table AIV-31A (member capacities) and Table AIV-31B (connection capacities) for main truss members and Table AIV-32 and Table AIV-33 for floor truss members. For those floor truss members that have interaction ratios greater than 1.0 under dead load in the intact condition, the sudden member failure did not cause significant changes to the force interaction ratio, as shown in Table AIV-33.

Table AIV-34 and Table AIV-35 list support reactions and maximum joint deflections and locations respectively. The induced longitudinal reactions at the "locked" expansion bearings were relatively low (a maximum longitudinal to vertical force ratio of 0.20 at the east bearing of Pier 6 with a dynamic impact factor of 1.854), and are not expected to change the existing bearing condition. The maximum joint displacements resulting from the member failure were low (a maximum vertical deflection of 2.8 inches at panel point U12 with a dynamic impact factor of 1.854).

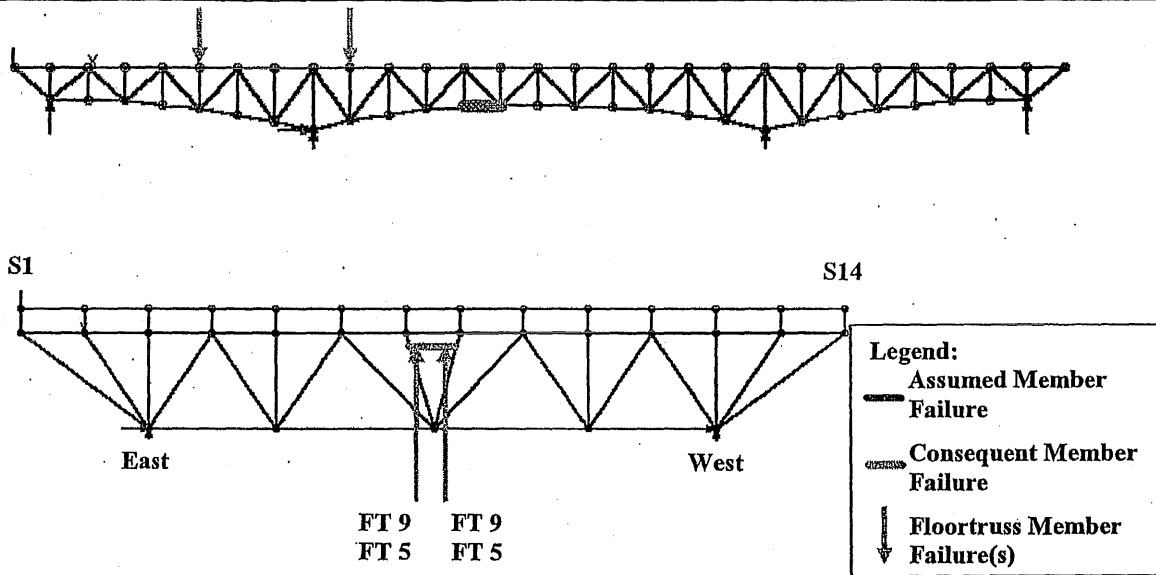


Figure 6-18: Load Case 1 – Failure of East Truss Lower Chord L12-L13
Consequent Member Failures without Dynamic Impact

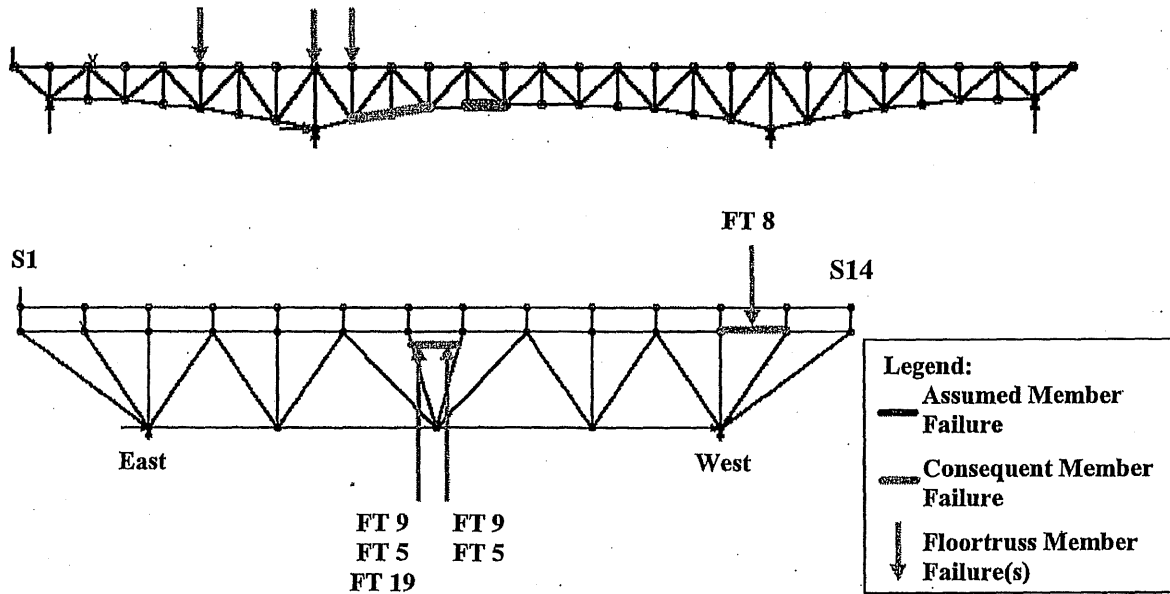


Figure 6-19: Load Case 1 – Failure of East Truss Lower Chord L12-L13
Consequent Member Failures with a Dynamic Impact Factor of 1.854

8. Failure of Critical Member L13-L14

When dynamic impact was not included, the calculated force interaction ratios indicated no consequent main truss member failures but four consequent floor truss member failures resulting from the failure of east truss lower chord L13-L14 (Figure 6-20). No portal and sway frame members or upper lateral and lower lateral bracing members would fail. When a dynamic impact factor of 1.854 was included, however, six consequent main truss members and seven consequent floor truss members would occur (Figure 6-21). Four portal and sway frame consequent member failures and three upper lateral and lower lateral bracing consequent member failures would occur. When the connection capacities are considered six (L10-L11, L11'-L10', L9-L10, L10'-L9', L8-L9, and L9'-L8') consequent main truss member failures would occur with the 1.854 dynamic impact factor. The results of calculated force interaction ratios are summarized in Table AIV-36A (member capacities) and Table AIV-36B (connection capacities) for main truss members and Table AIV-37 and Table AIV-38 for floor truss members. Some of the floor truss members that have interaction ratios greater than 1.0 under dead load in the intact condition exhibited a significant increase of the force interaction ratio due to the sudden member failure, as shown in Table AIV-38.

Table AIV-39 and Table AIV-40 list the support reactions and maximum joint deflections and locations respectively. The induced longitudinal reactions at the "locked" expansion bearings were relatively high, a maximum longitudinal to vertical force ratio of 0.27 at the east bearing of Pier 6 with a dynamic impact factor of 1.854, but are not expected to change the existing "locked" condition of the steel roller bearing. The maximum joint displacements resulting from the member failure were also relatively high, with a maximum vertical deflection of 5.5 inches at panel point U14 with a dynamic impact factor of 1.854.

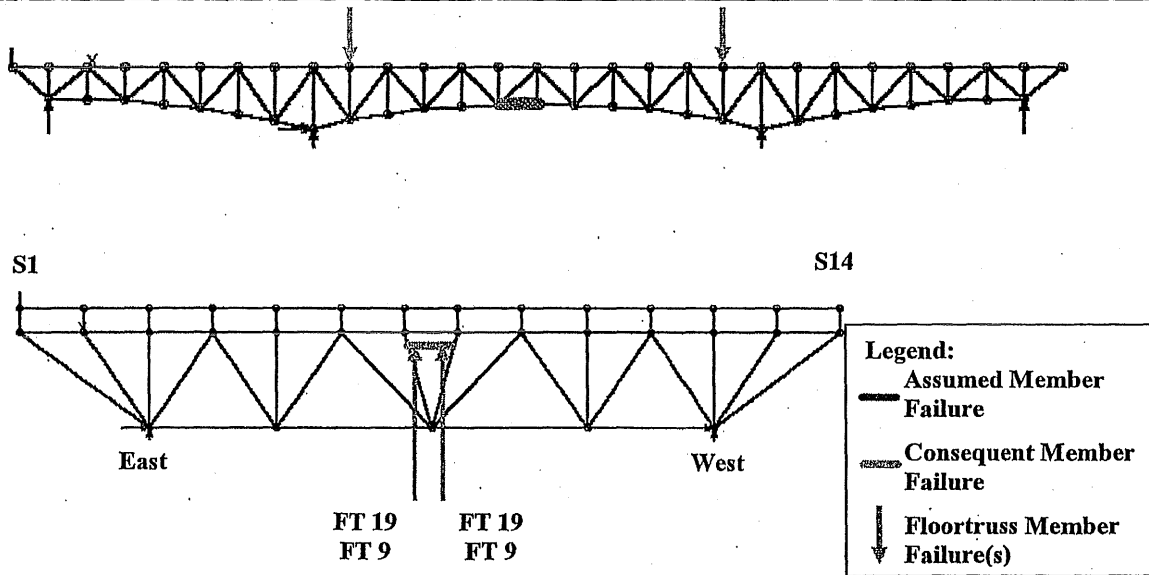


Figure 6-20: Load Case 1 – Failure of East Truss Lower Chord L13-L14
Consequent Member Failures without Dynamic Impact

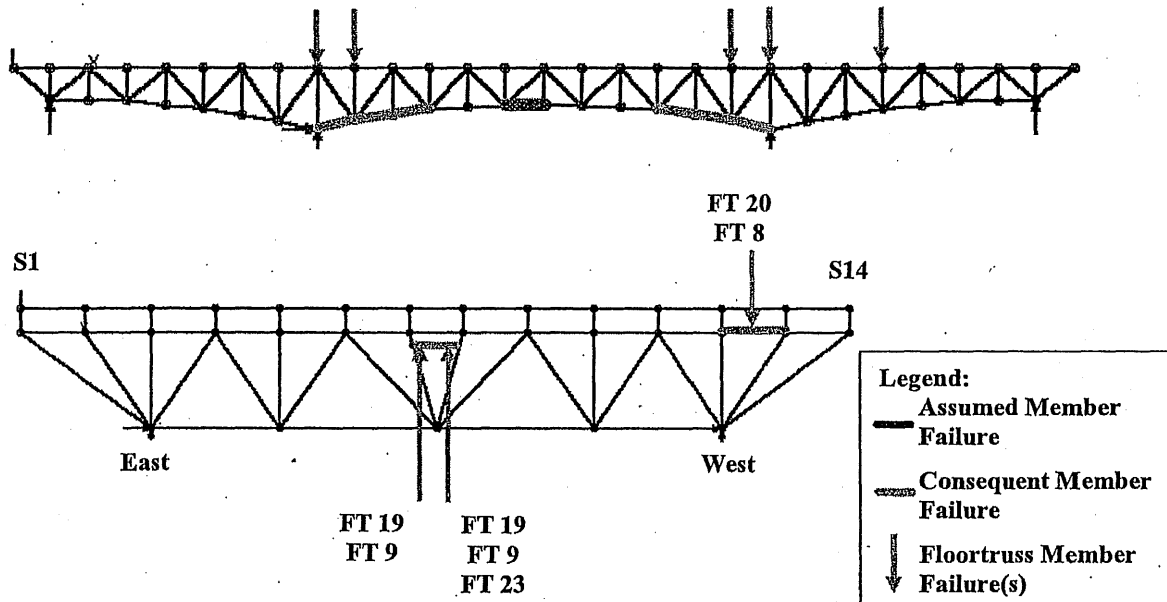


Figure 6-21: Load Case 1 – Failure of East Truss Lower Chord L13-L14
Consequent Member Failures with a Dynamic Impact Factor of 1.854

6.7.6 Load Case 2: Eight HS-20 Trucks at Slow Speed (MPF=1.0; IM=1.0)

Some floor truss members were found to have force interaction ratios exceeding 1.0 under the combined dead load and live load in the intact condition prior to the removal of the critical truss member under investigation. This behavior is discussed where applicable.

1. Failure of East Truss Diagonal L3-U4

The calculated force interaction ratios indicated no consequent failures of any structural members would occur as a result of the failure of east truss diagonal L3-U4, without or with the dynamic impact factor of 1.854. This is true for the investigation of the member capacities as well as the investigation of the connection capacities. The results of calculated force interaction ratios are summarized in **Table AIV-41A** (member capacities) and **Table AIV-41B** (connection capacities) for main truss members and **Table AIV-42** and **Table AIV-43** for floor truss members. For those floor truss members that have interaction ratios greater than 1.0 under the combined dead and live load in the intact condition, the sudden member failure did not cause significant changes to the force interaction ratio.

Table AIV-44 and **Table AIV-45** list support reactions and maximum joint displacements and corresponding locations, respectively. The induced longitudinal reactions at the "locked" expansion bearings were very low (a maximum longitudinal to vertical force ratio of 0.09 at the east bearing of Pier 5 with a dynamic impact factor of 1.854), and are not expected to change the existing bearing condition. The maximum joint displacements resulting from the member failure were very low.

2. Failure of East Truss Lower Chord L1-L2

The calculated force interaction ratios indicated no consequent failures of any structural members as a result of the failure of east truss lower chord L1-L2, without or with the

dynamic impact factor of 1.854. This is true for the investigation of the member capacities as well as the investigation of the connection capacities. The results of calculated force interaction ratios are summarized in **Table AIV-46A** (member capacities) and **Table AIV-46B** (connection capacities) for main truss members and **Table AIV-47** and **Table AIV-48** for floor truss members. For those floor truss members that have interaction ratios greater than 1.0 under the combined dead and live load in the intact condition, the sudden member failure did not cause significant changes to the force interaction ratio.

Table AIV-49 and **Table AIV-50** list support reactions and maximum joint displacements and corresponding locations, respectively. The induced longitudinal reactions at the "locked" expansion bearings were low (a maximum longitudinal to vertical force ratio of 0.20 at the east bearing of Pier 5 with a dynamic impact factor of 1.854), and are not expected to change the existing bearing condition. The maximum joint displacements resulting from the member failure were very low.

3. Failure of East Truss Upper Chord U0-U1

Calculated force interaction ratios indicated that two consequent main truss member failures and twelve consequent floor truss member failures would result from the failure of east truss upper chord U0-U1, when dynamic impact was not included (**Figure 6-22**). No consequent portal and sway frame member failures would occur but two upper lateral and lower lateral bracing consequent member failures would occur. When a dynamic impact factor of 1.854 was included, four consequent main truss member failures and seventeen consequent floor truss member failures would occur (**Figure 6-23**). No consequent portal and sway frame member failures would occur but four consequent upper lateral and lower lateral bracing member failures would occur. When the connection capacities are considered, two (U0-L1 and U1-L1) and five (U0-L1, U1-L1, L1-L2, U0-U1, and U0-L1 West) consequent main truss member failures would occur without and with the 1.854 dynamic impact factor respectively. The results of calculated

force interaction ratios are summarized in Table AIV-51A (member capacities) and Table AIV-51B (connection capacities) for main truss members and Table AIV-52 and Table AIV-53 for floor truss members. For those floor truss members that have interaction ratios greater than 1.0 under the combined dead and live load in the intact condition, the sudden member failure did not cause significant changes to the force interaction ratio.

Table AIV-54 and Table AIV-55 list support reactions and maximum joint displacements and corresponding locations, respectively. The induced longitudinal reactions at the “locked” expansion bearings are relatively high (a maximum longitudinal to vertical force ratio of 0.28 at the east bearing of Pier 5 with a dynamic impact factor of 1.854), and are not expected to change the existing “locked” condition of the steel roller bearing. The displacements of the east truss upper joint U0 resulting from the member failure were extremely high, which indicated the instability of diagonal U0-L1 for supporting the weight of the approach span without the upper chord U0-U1.

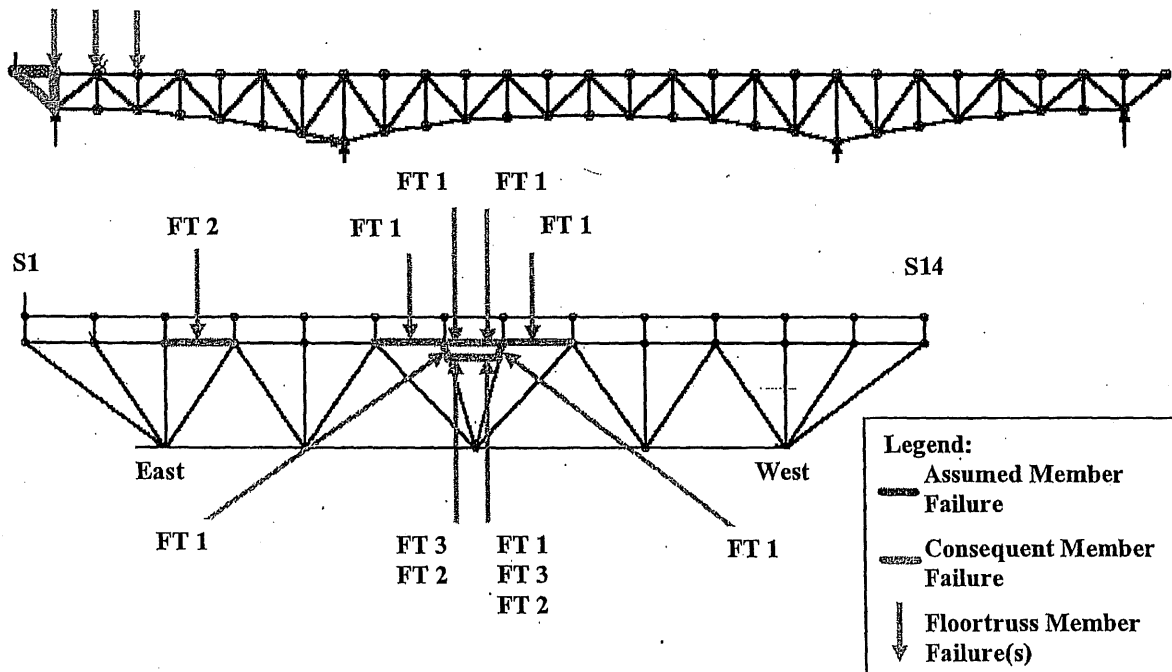
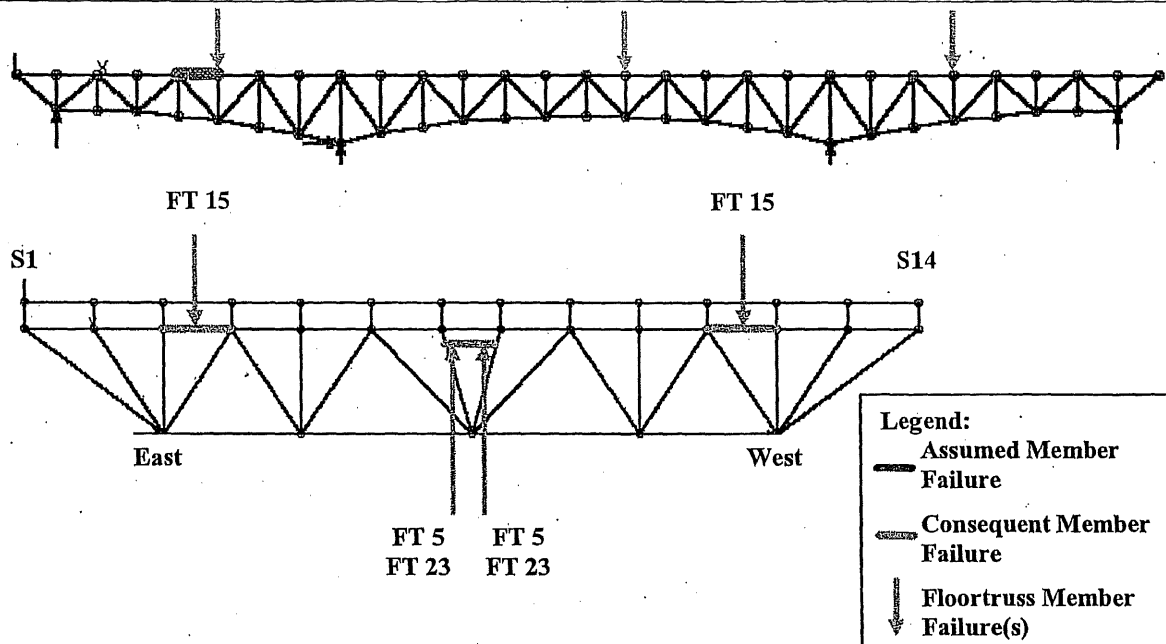


Figure 6-22: Load Case 2 – Failure of East Truss Upper Chord U0-U1
Consequent Member Failures without Dynamic Impact



**Figure 6-24: Load Case 2 – Failure of East Truss Upper Chord U4-U5
Additional Member Failures Due To DL+LL on Intact Structure**

As a result of the failure of east truss upper chord U4-U5, calculated force interaction ratios indicated no consequent failures of any main truss members, without or with the dynamic impact factor of 1.854. This is true for the investigation of the member capacities as well as the investigation of the connection capacities. Without the dynamic impact, three consequent floor truss member failures were found to occur (Figure 6-25) but no consequent failures of any portal/sway frame or upper/lower lateral bracing members were found to occur. When a dynamic impact factor of 1.854 was included, eight consequent floor truss member failures were found to occur (Figure 6-26). No consequent portal/sway frame member failures would occur but one consequent upper/lower lateral bracing member failure would occur.

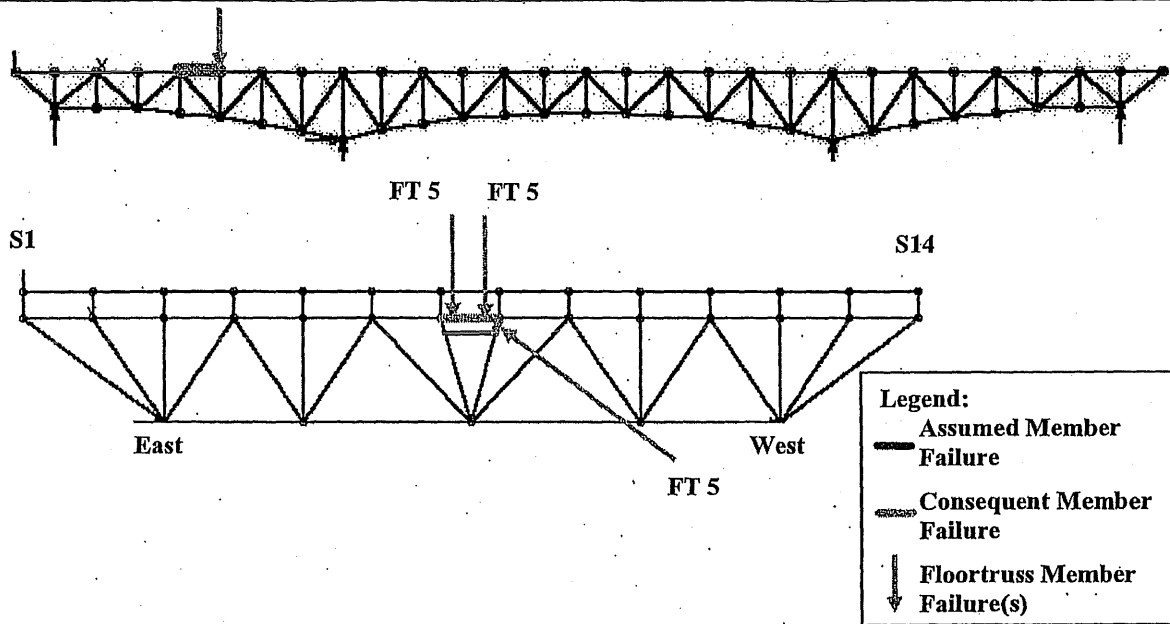


Figure 6-25: Load Case 2 – Failure of East Truss Upper Chord U4-U5
Consequent Member Failures without Dynamic Impact

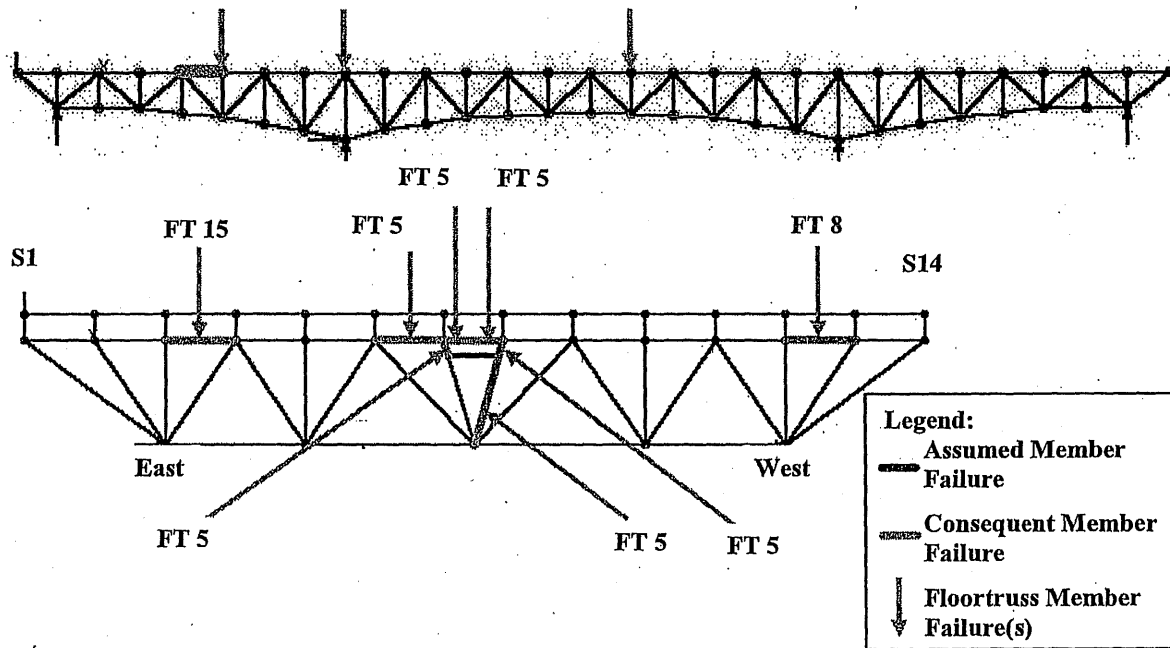


Figure 6-26: Load Case 2 – Failure of East Truss Upper Chord U4-U5
Consequent Member Failures with a Dynamic Impact Factor of 1.875

The results of calculated force interaction ratios are summarized in **Table AIV-56A** (member capacities) and **Table AIV-56B** (connection capacities) for main truss members and **Tables AIV-57** through **AIV-59** for floor truss members. For some floor truss members that have interaction ratios greater than 1.0 under the dead load or the combined dead and live load in the intact condition, the sudden member failure caused significant changes to the force interaction ratio.

Table AIV-60 and **Table AIV-61** list the support reactions and maximum joint displacements and corresponding locations, respectively. The induced longitudinal reactions at the "locked" expansion bearings are very low (a maximum longitudinal to vertical force ratio of 0.08 at the east bearing of Pier 6 with a dynamic impact factor of 1.854), and are not expected to change the existing "locked" condition of the steel roller bearing. The maximum joint displacements resulting from the member failure were low, a maximum of 1.5 inches of vertical deflection at panel point L5 with a dynamic impact factor of 1.854.

5. Failure of East Truss Upper Chord U4'-U3'

Member U4'-U3' was found to be subject to slightly higher forces than its counterpart U3-U4 due to different section properties and therefore used for the redundancy analysis. Under the combined dead and live load on the intact structure prior to the removal of east truss upper chord U4'-U3', four additional floor truss members were found to have interaction ratios greater than 1.0 compared to the dead load only condition, as shown in **Figure 6-27**. All of these members are located adjacent to a floor truss that support the stringers with the asymmetric expansion joint (**Sections 6.7.1** and **6.7.2** and **Figure 3-21**), and the failures were attributed primarily to the out-of-plane bending.

As a result of the failure of east truss upper chord U4'-U3', calculated force interaction ratios indicated no consequent failures of any main truss members, without or with the dynamic impact factor of 1.854. This is true for the investigation of the member

capacities as well as the investigation of the connection capacities. Without the dynamic impact, two consequent floor truss member failures were found to occur (Figure 6-28) but no consequent failures of any portal/sway frame or upper/lower lateral bracing members would occur. When a dynamic impact factor of 1.854 was included, three consequent floor truss member failures were found to occur (Figure 6-29). No portal/sway frame or upper/lower lateral bracing members would fail. The results of calculated force interaction ratios are summarized in Table AIV-62A (member capacities) and Table AIV-62B (connection capacities) for main truss members and Tables AIV-63 through AIV-65 for floor truss members. For those floor truss members that have interaction ratios greater than 1.0 under the dead load only in the intact condition (Table AIV-64), the sudden member failure did not cause significant changes to the force interaction ratio.

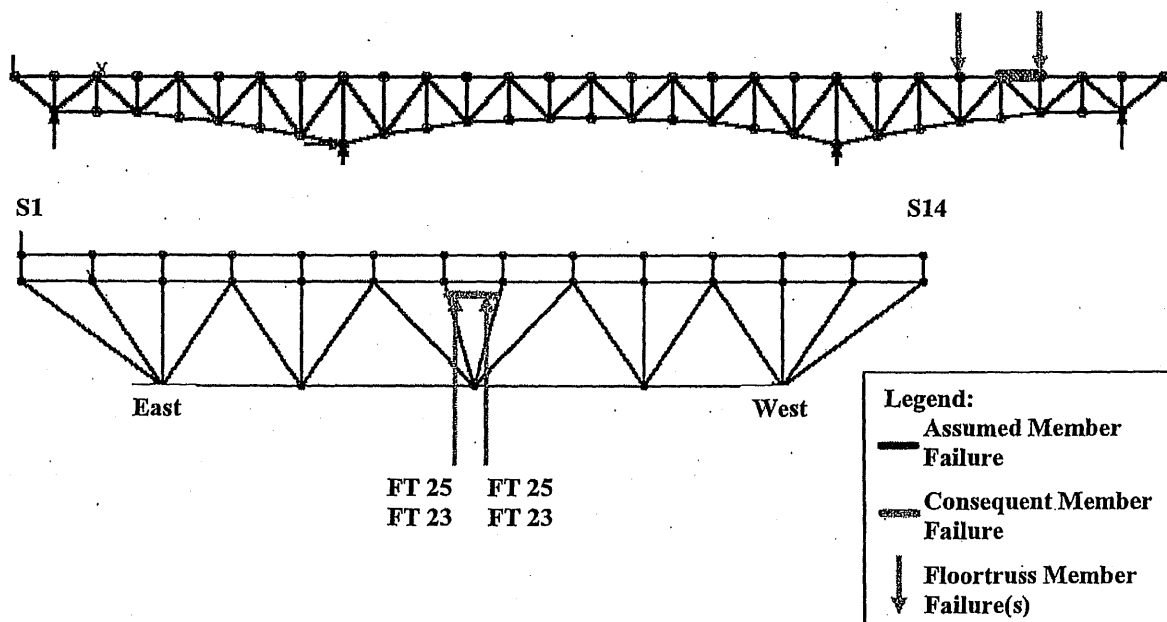


**Figure 6-27: Load Case 2 – Failure of East Truss Upper Chord U4'-U3'
Additional Member Failures Due To DL+LL on Intact Structure**

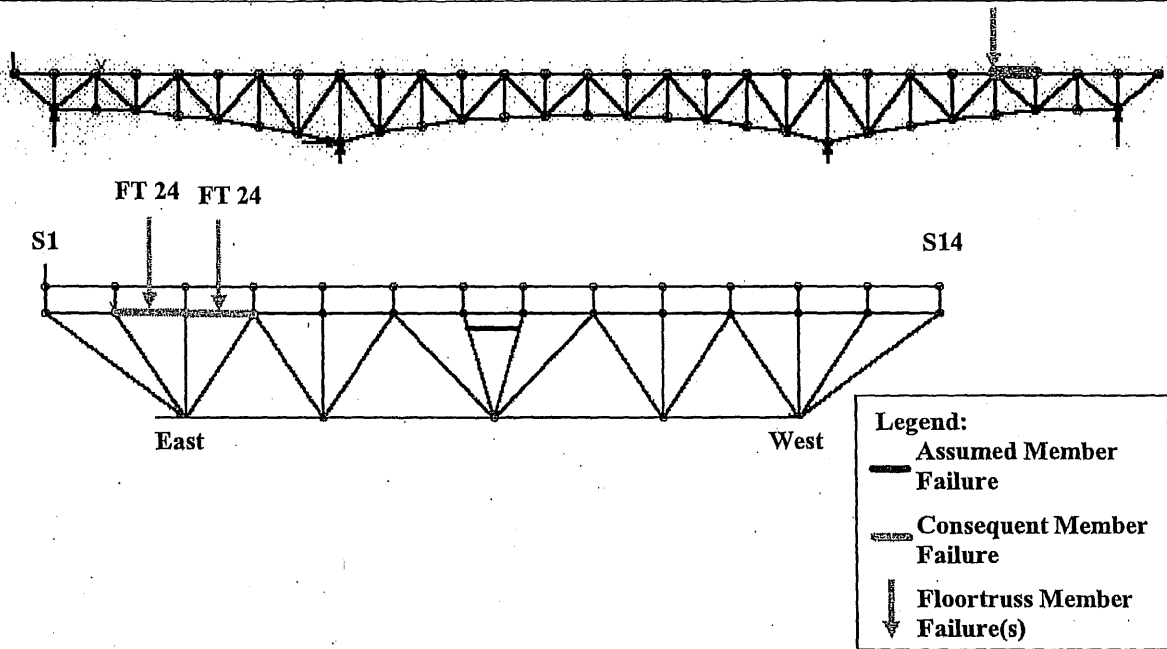


Figure 6-28: Load Case 2 – Failure of East Truss Upper Chord U4'-U3' Consequent Member Failures without Dynamic Impact

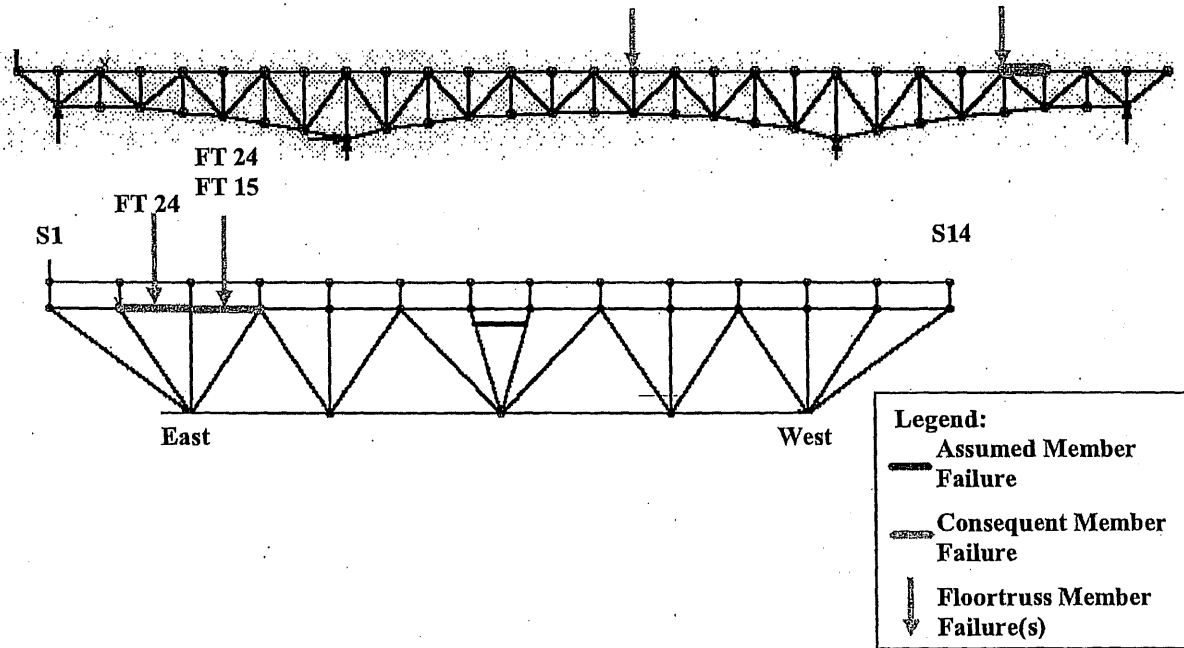


Figure 6-29: Load Case 2 – Failure of East Truss Upper Chord U4'-U3' Consequent Member Failures with a Dynamic Impact Factor of 1.854

Table AIV-66 and Table AIV-67 list the support reactions and maximum joint displacements and corresponding locations, respectively. The induced longitudinal reactions at the “locked” expansion bearings are very low (a maximum longitudinal to vertical force ratio of 0.01 at the west bearing of Pier 8 with a dynamic impact factor of 1.854), and are not expected to change the existing “locked” condition of the steel roller bearing. The maximum joint displacements resulting from the member failure were very low.

6. Failure of East Truss Lower Chord L4-L5

Under the combined dead and live load on the intact structure prior to the removal of east truss lower chord L4-L5, two additional floor truss members were found to have interaction ratios greater than 1.0 compared to the dead load only condition, as shown in **Figure 6-30**. All of these members are located adjacent to a floor truss that support the stringers with the asymmetric expansion joint (**Sections 6.7.1 and 6.7.2 and Figure 3-21**), and the failures were attributed primarily to the out-of-plane bending.

The calculated force interaction ratios indicated no consequent failures of any structural members as a result of the failure of east truss lower chord L4-L5, without or with the dynamic impact factor of 1.854. This is true for the investigation of the member capacities as well as the investigation of the connection capacities. The results of calculated force interaction ratios are summarized in **Table AIV-68A** (member capacities) and **Table AIV-68B** (connection capacities) for main truss members and **Tables AIV-69 through AIV-71** for floor truss members. For those floor truss members that have interaction ratios greater than 1.0 under the combined dead and live load in the intact condition, the sudden member failure did not cause significant changes to the force interaction ratio.

Table AIV-72 and Table AIV-73 list the support reactions and maximum joint deflections and locations respectively. The induced longitudinal reactions at the “locked”

expansion bearings are low (a maximum longitudinal to vertical force ratio of 0.14 at the east bearing of Pier 5 with a dynamic impact factor of 1.854), and are not expected to change the existing “locked” condition of the steel roller bearing. The maximum joint displacements resulting from the member failure were very low.

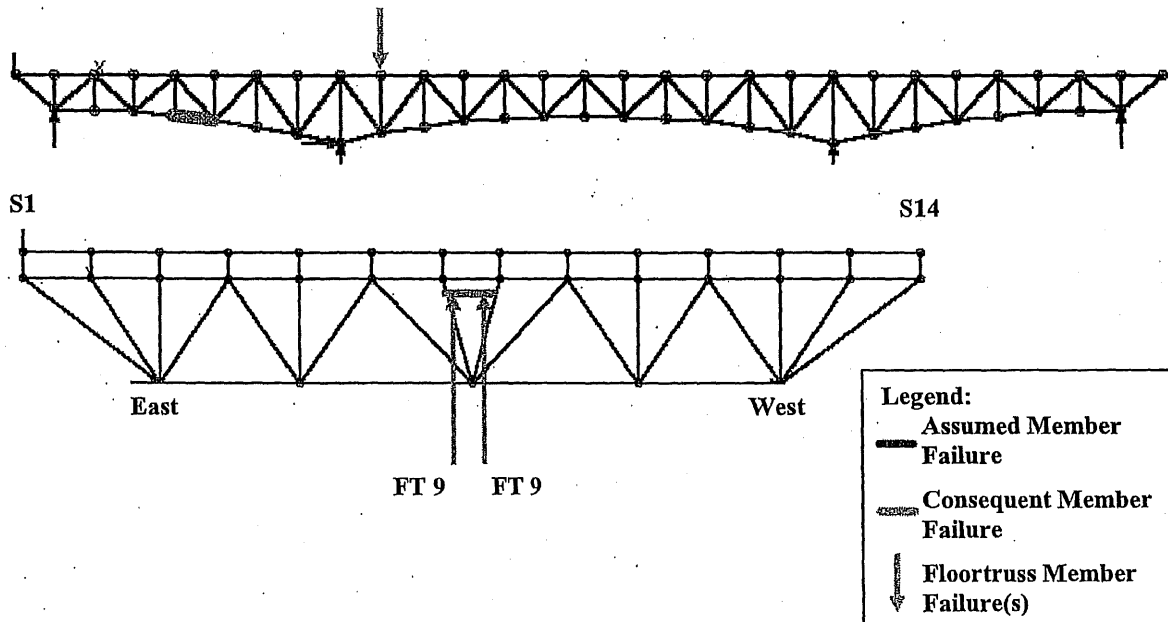


**Figure 6-30: Load Case 2 – Failure of East Truss Lower Chord L4-L5
Additional Member Failures Due To DL+LL on Intact Structure**

7. Failure of East Truss Lower Chord L12-L13

Under the combined dead and live load on the intact structure prior to the removal of east truss lower chord L12-L13, six additional floor truss members were found to have interaction ratios greater than 1.0 compared to the dead load only condition, as shown in **Figure 6-31**. All of these members are located adjacent to a floor truss that support the stringers with the asymmetric expansion joint (**Sections 6.7.1 and 6.7.2 and Figure 3-21**), and the failures were attributed primarily to the out-of-plane bending.

Calculated force interaction ratios indicated that two consequent main truss member failures and three consequent floor truss member failures would occur resulting from the failure of east truss upper chord L12-L13, when dynamic impact was not included (Figure 6-32). No portal/sway frame or upper/lower lateral bracing members would fail. When a dynamic impact factor of 1.854 was included, three consequent main truss member failures and five consequent floor truss member failures would occur (Figure 6-33). One portal/sway frame member would fail but no upper/lower lateral bracing members would fail. When the connection capacities are considered, two (L10-L11 and L9-L10) and five (L10-L11, L9-L10, L8-L9, L10'-L9', and L11'-L10') consequent main truss member failures would occur without and with the 1.854 dynamic impact factor respectively. The results of calculated force interaction ratios are summarized in Table AIV-74A (member capacities) and Table AIV-74B (connection capacities) for main truss members and Tables AIV-75 through AIV-77 for floor truss members. For most floor truss members that have interaction ratios greater than 1.0 under the combined dead and live load in the intact condition, the sudden member failure did not cause significant changes to the force interaction ratio.

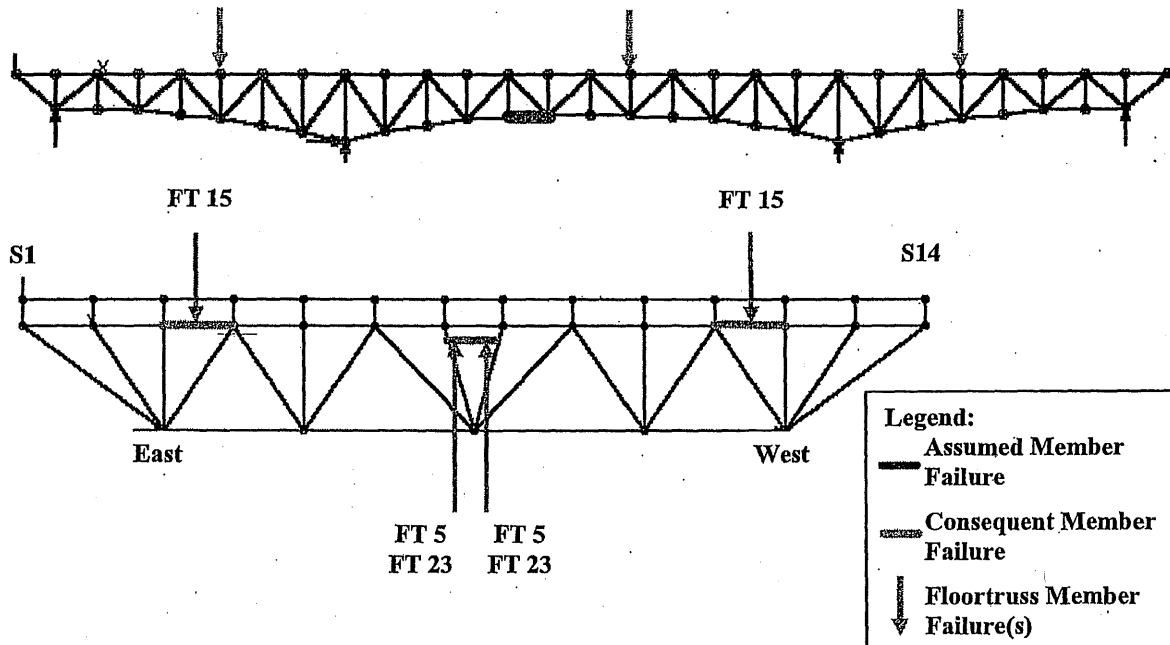


Figure 6-31: Load Case 2 – Failure of East Truss Lower Chord L12-L13
Additional Member Failures Due To DL+LL on Intact Structure

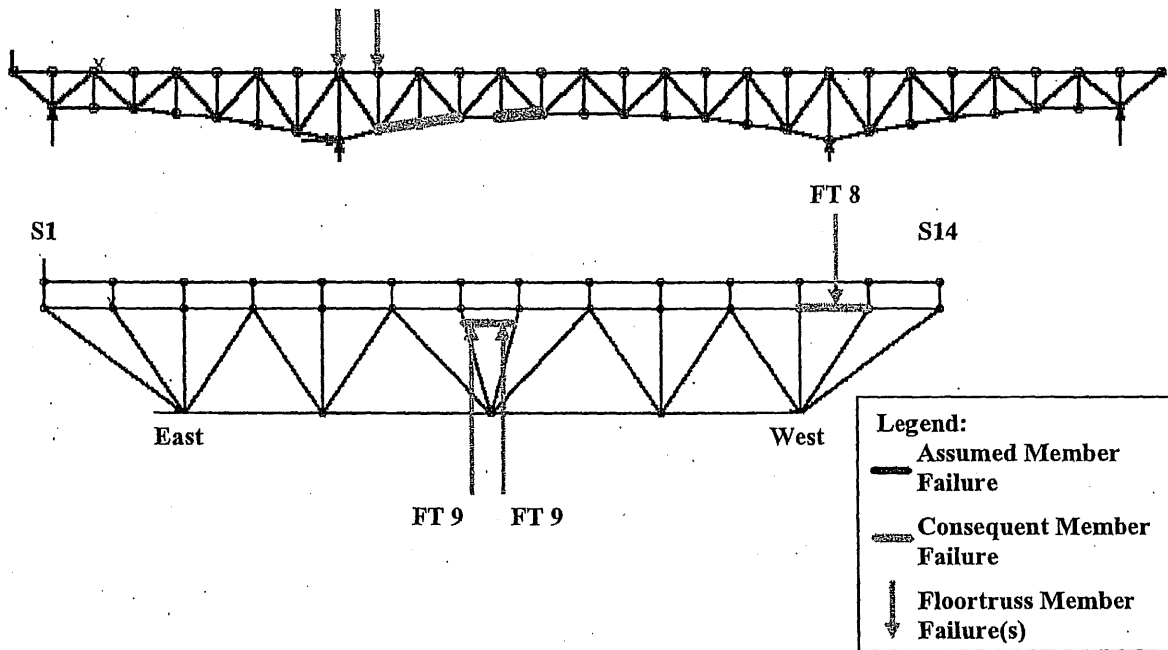


Figure 6-32: Load Case 2 – Failure of East Truss Lower Chord L12-L13
Consequent Member Failures without Dynamic Impact

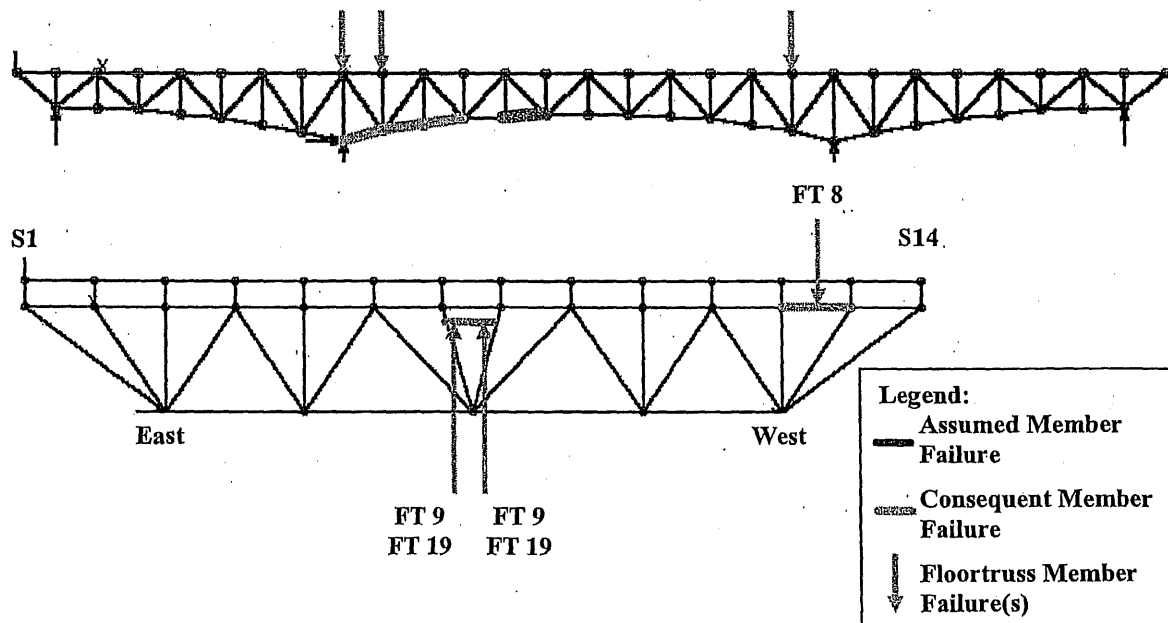


Figure 6-33: Load Case 2 – Failure of East Truss Lower Chord L12-L13
Consequent Member Failures with a Dynamic Impact Factor of 1.854

Table AIV-78 and Table AIV-79 list the support reactions and maximum joint deflections and locations respectively. The induced longitudinal reactions at the “locked” expansion bearings were relatively low (a maximum longitudinal to vertical force ratio of 0.26 at the east bearing of Pier 6 with a dynamic impact factor of 1.854), and are not expected to change the existing “locked” condition of the steel roller bearing. The maximum joint displacements resulting from the member failure were not very high (a maximum vertical deflection of 3.3 inches at panel point U12 with a dynamic impact factor of 1.854).

8. Failure of East Truss Lower Chord L13-L14

Under the combined dead and live load on the intact structure prior to the removal of east truss lower chord L13-L14, six additional floor truss members were found to have interaction ratios greater than 1.0 compared to the dead load only condition, as shown in Figure 6-34. All of these members are located adjacent to floor trusses that support the stringers with the asymmetric expansion joint (Sections 6.7.1 and 6.7.2 and Figure 3-21), and the failures were attributed primarily to the out-of-plane bending.

Calculated force interaction ratios indicated that four consequent main truss member failures and six consequent floor truss member failures would occur resulting from the failure of east truss upper chord L13-L14, when dynamic impact was not included (Figure 6-35). One portal/sway frame member and three upper/lower lateral bracing members would fail. When a dynamic impact factor of 1.854 was included, seven consequent main truss member failures and twelve consequent floor truss member failures would occur (Figure 6-36). Four portal/sway frame members and six upper/lower lateral bracing members would fail. When the connection capacities are considered, four (L10-L11, L11'-L10', L9-L10, and L10'-L9') and seven (L10-L11, L11'-L10', L9-L10, L10'-L9', L8-L9, L9'-L8' and U14-L14 West) consequent main truss member failures would occur without and with the 1.854 dynamic impact factor respectively. The results of calculated force interaction ratios are summarized in Table

AIV-80A (member capacities) and Table AIV-80B (connection capacities) for main truss members and Tables AIV-81 through AIV-83 for floor truss members. For those floor truss members that have interaction ratios greater than 1.0 under dead load or combined dead and live load in the intact condition, the sudden member failure caused significant changes to the force interaction ratio in some of them.

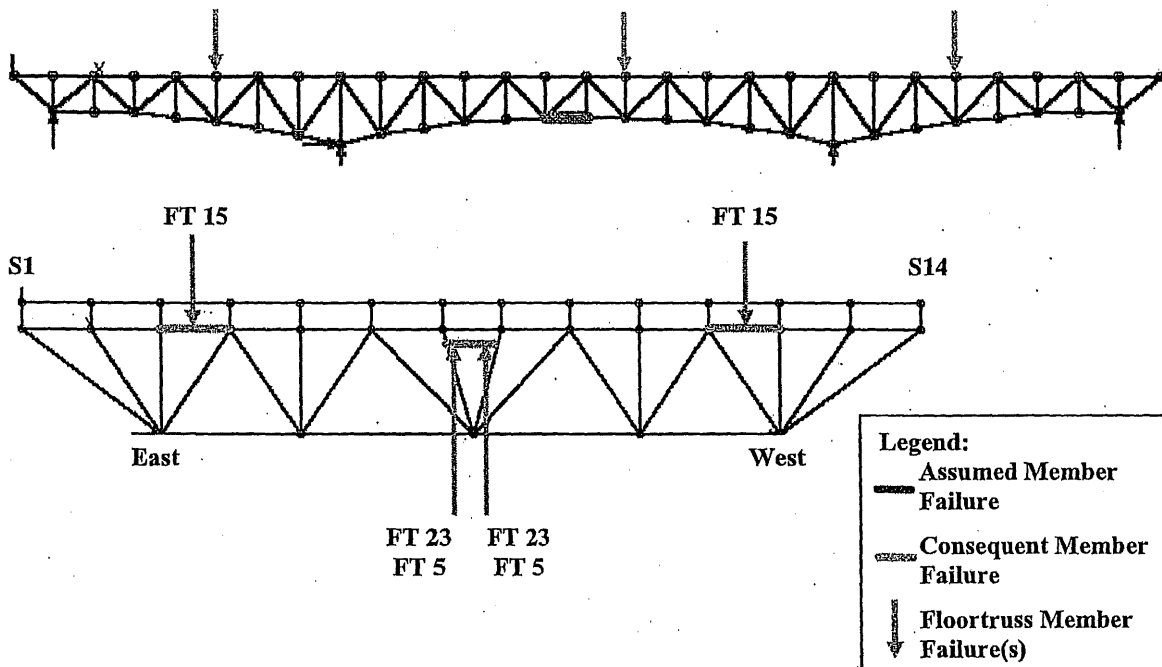


**Figure 6-34: Load Case 2 – Failure of East Truss Lower Chord L13-L14
Additional Member Failures Due to DL+LL on Intact Structure**

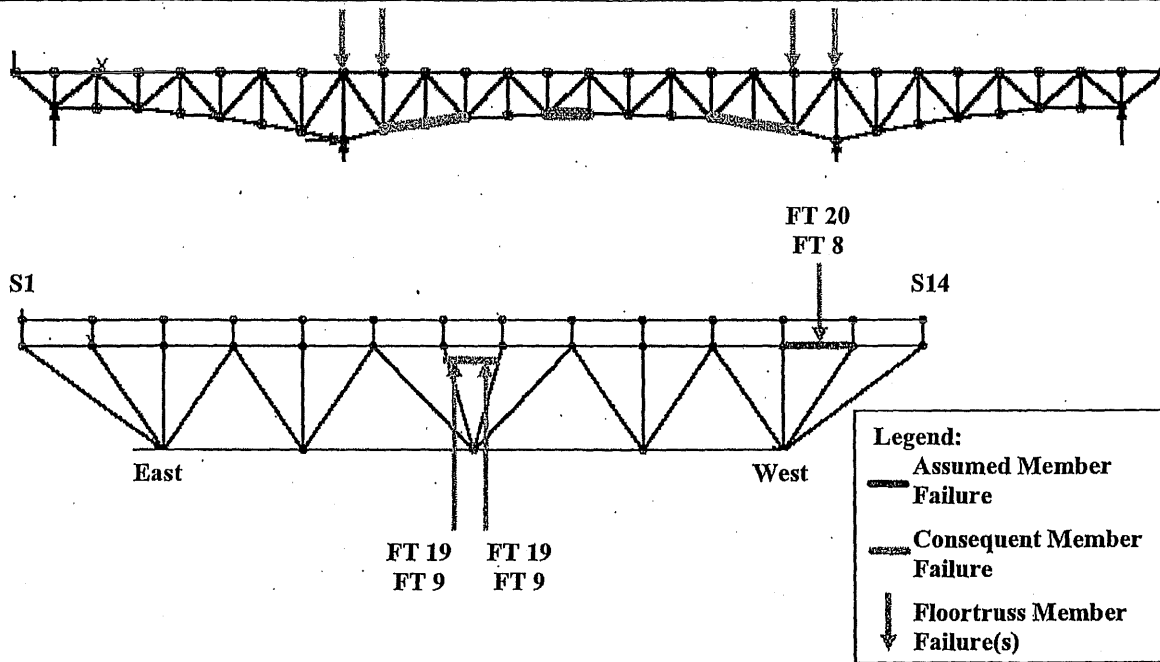


Figure 6-35: Load Case 2 – Failure of East Truss Lower Chord L13-L14
 Consequent Member Failures without Dynamic Impact

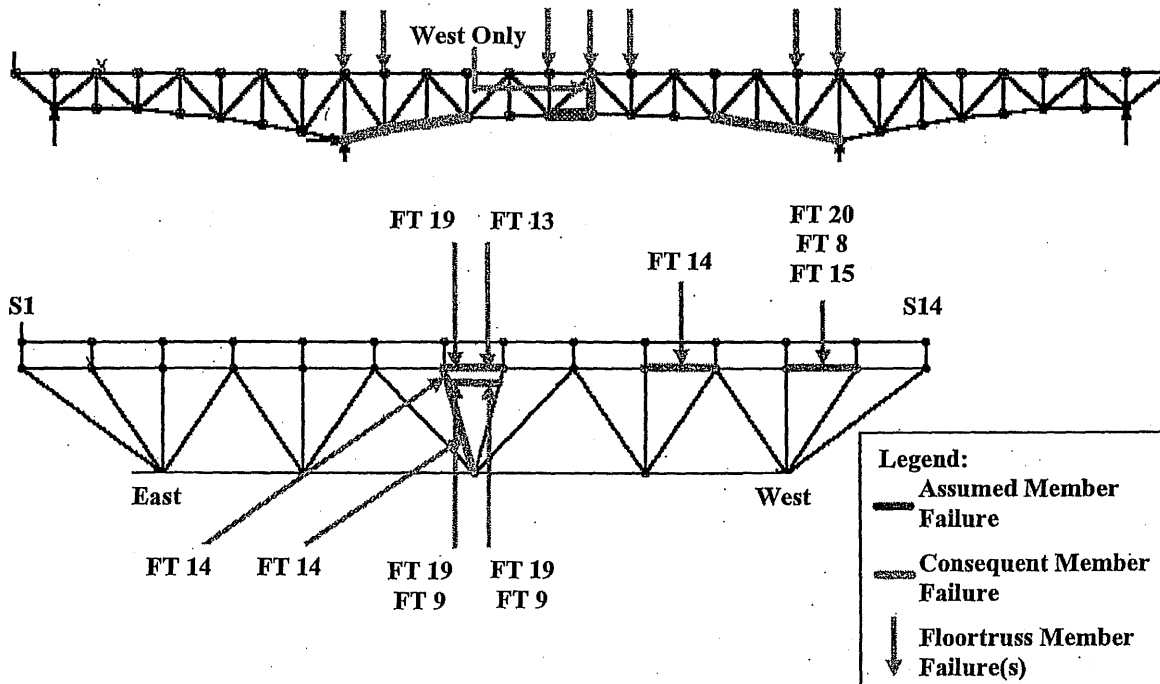


Figure 6-37: Load Case 2 – Failure of East Truss Lower Chord L13-L14
 Consequent Member Failures with a Dynamic Impact Factor of 1.854

Table AIV-84 and Table AIV-85 list the support reactions and maximum joint deflections and locations respectively. The induced longitudinal reactions at the “locked” expansion bearings were relatively high, a maximum longitudinal to vertical force ratio of 0.34 at the east bearing of Pier 6 with a dynamic impact factor of 1.854. This level of longitudinal force may not change the existing “locked” condition of the steel roller bearing, depending on the surface condition, since a frictional coefficient of 0.40 is generally accepted for steel. The maximum joint displacements resulting from the member failure were also relatively high, a maximum vertical deflection of 6.3 inches at panel point U14 with a dynamic impact factor of 1.854.

6.7.7 Load Case 3: Eight Lanes of Standstill HS-20 Truck & Lane Load (Rush Hour “Parking Lot”) (MPF=1.0; IM=1.0)

Some floor truss members were found to have force interaction ratios exceeding 1.0 under the combined dead load and live load in the intact condition prior to the removal of the critical truss member under investigation. This behavior is discussed where applicable.

1. Failure of East Truss Diagonal L3-U4

Under the combined dead and live load on the intact structure prior to the removal of east truss diagonal chord L3-U4, sixteen additional floor truss members were found to have interaction ratios greater than 1.0 compared to the dead load only condition, as shown in **Figure 6-38**. All of these members are located adjacent to floor trusses that support the stringers with the asymmetric expansion joint (**Sections 6.7.1 and 6.7.2 and Figure 3-21**), and the failures were attributed primarily to the out-of-plane bending.

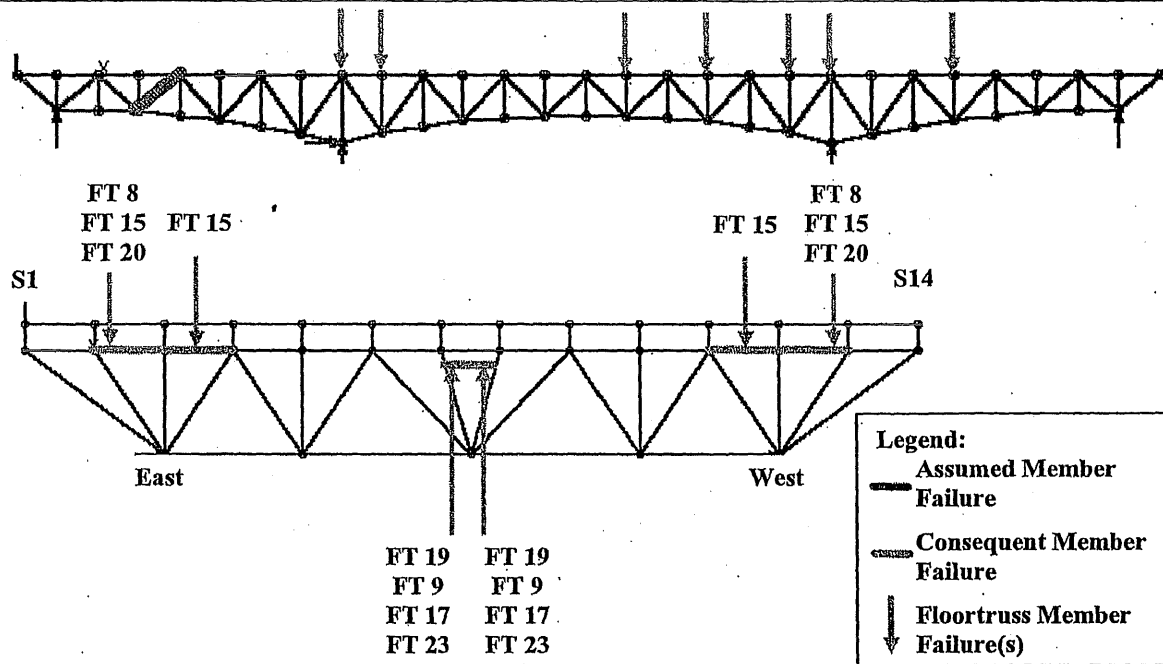


**Figure 6-38: Load Case 3 – Failure of East Truss Diagonal L3-U4
Additional Member Failures Due to DL+LL on Intact Structure**

The calculated force interaction ratios indicated no consequent failures of any structural members would occur as a result of the failure of east truss diagonal L3-U4, without or with the dynamic impact factor of 1.854. This is true for the investigation of the member capacities as well as the investigation of the connection capacities. The results of calculated force interaction ratios are summarized in **Table AIV-86A** (member capacities) and **Table AIV-86B** (connection capacities) for main truss members and **Table AIV-87** and **Table AIV-88** for floor truss members. For those floor truss members that have interaction ratios greater than 1.0 under the combined dead and live load in the intact condition, the sudden member failure did not cause significant changes to the force interaction ratio.

Table AIV-89 and **Table AIV-90** list support reactions and maximum joint displacements and corresponding locations, respectively. The induced longitudinal reactions at the “locked” expansion bearings were very low (a maximum longitudinal to vertical force ratio of 0.10 at the east bearing of Pier 5 with a dynamic impact factor of

1.854), and are not expected to change the existing bearing condition. The maximum joint displacements resulting from the member failure were very low.

2. Failure of East Truss Lower Chord L1-L2

Under the combined dead and live load on the intact structure prior to the removal of east truss upper chord L1-L2, sixteen additional floor truss members were found to have interaction ratios greater than 1.0 compared to the dead load only condition, as shown in **Figure 6-39**. All of these members are located adjacent to floor trusses that support the stringers with the asymmetric expansion joint (**Sections 6.7.1 and 6.7.2 and Figure 3-21**), and the failures were attributed primarily to the out-of-plane bending.

The calculated force interaction ratios indicated no consequent failures of any structural members as a result of the failure of east truss lower chord L1-L2, without the dynamic impact factor. When a dynamic impact factor of 1.854 was included, one consequent main truss member failure and no consequent floor truss member failures would occur (**Figure 6-40**). No portal/sway frame members or upper/lower lateral bracing members would fail. When the connection capacities are considered two (U1-L1 and L1-U2) consequent main truss member failures would occur with the 1.854 dynamic impact factor. The results of calculated force interaction ratios are summarized in **Table AIV-92A** (member capacities) and **Table AIV-92B** (connection capacities) for main truss members and **Tables AIV-93 through AIV-95** for floor truss members. For those floor truss members that have interaction ratios greater than 1.0 under dead load or combined dead and live load in the intact condition, the sudden member failure did not cause significant changes to the force interaction ratio.

Table AIV-96 and **Table AIV-97** list the support reactions and maximum joint deflections and locations respectively. The induced longitudinal reactions at the "locked" expansion bearings were relatively low (a maximum longitudinal to vertical force ratio of

0.24 at the east bearing of Pier 5 with a dynamic impact factor of 1.854), and are not expected to change the existing "locked" condition of the steel roller bearing. The maximum joint displacements resulting from the member failure were not very high (a maximum vertical deflection of 0.99 inches at panel point U0 with a dynamic impact factor of 1.854).

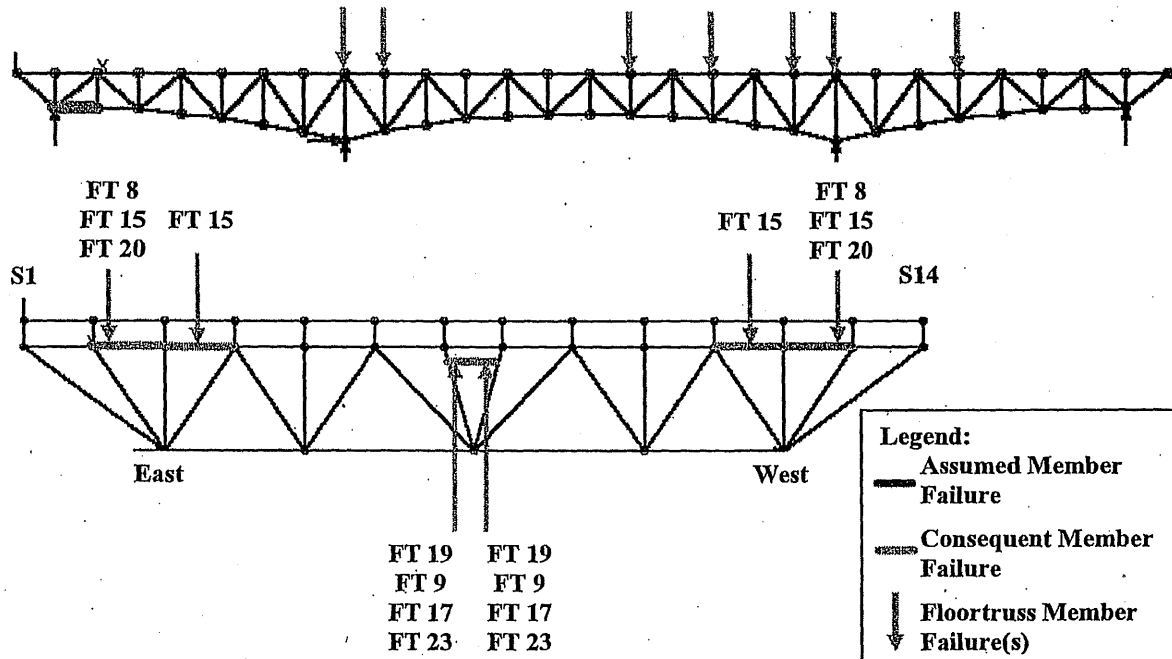
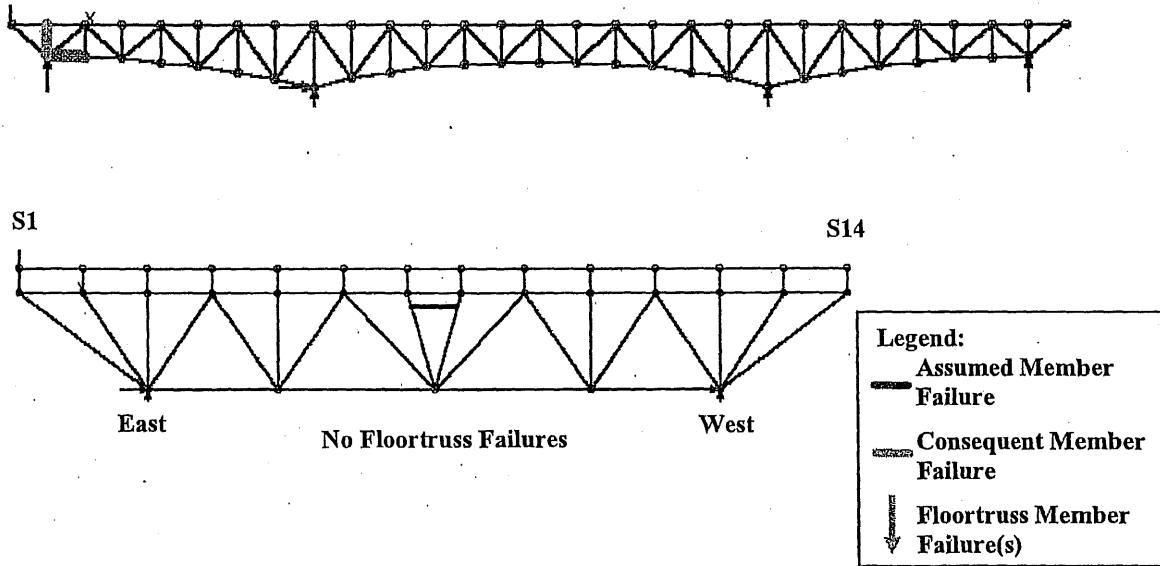


Figure 6-39: Load Case 3 – Failure of East Truss Lower Chord L1-L2
Additional Member Failures Due to DL+LL on Intact Structure



**Figure 6-40: Load Case 3 – Failure of East Truss Lower Chord L1-L2
Consequent Member Failures with a Dynamic Impact Factor of 1.854**

3. Failure of East Truss Upper Chord U0-U1

Under the combined dead and live load on the intact structure prior to the removal of east truss upper chord U0-U1, eighteen additional floor truss members were found to have interaction ratios greater than 1.0 compared to the dead load only condition, as shown in **Figure 6-41**. All of these members are located adjacent to floor trusses that support the stringers with the asymmetric expansion joint (**Sections 6.7.1 and 6.7.2 and Figure 3-21**), and the failures were attributed primarily to the out-of-plane bending.

Calculated force interaction ratios indicated that two consequent main truss member failures and thirteen consequent floor truss member failures would result from the failure of east truss upper chord U0-U1, when dynamic impact was not included (**Figure 6-42**). No consequent portal and sway frame member failures would occur but two upper lateral and lower lateral bracing consequent member failures would occur. When a dynamic impact factor of 1.854 was included, six consequent main truss member failures and twenty consequent floor truss member failures would occur (**Figure 6-43**). No

consequent portal and sway frame member failures would occur but four consequent upper lateral and lower lateral bracing member failures would occur. When the connection capacities are considered, three (U0-L1, U1-L1 and U0-L1 West) and six (U0-L1, U1-L1, L1-L2, SFB-U1, U1-U2 and U0-L1 West) consequent main truss member failures would occur without and with the 1.854 dynamic impact factor respectively. The results of calculated force interaction ratios are summarized in **Table AIV-98A** (member capacities) and **Table AIV-98B** (connection capacities) for main truss members and **Table AIV-99** thru **Table AIV-101** for floor truss members. For those floor truss members that have interaction ratios greater than 1.0 under the combined dead and live load in the intact condition, the sudden member failure does not cause significant changes to the force interaction ratio.

Table AIV-102 and **Table AIV-103** list support reactions and maximum joint displacements and corresponding locations, respectively. The induced longitudinal reactions at the "locked" expansion bearings are relatively high (a maximum longitudinal to vertical force ratio of 0.22 at the east bearing of Pier 5 with a dynamic impact factor of 1.854), and are not expected to change the existing "locked" condition of the steel roller bearing. The displacements of the east truss upper joint U0 resulting from the member failure were extremely high, which indicated the instability of diagonal U0-L1 for supporting the weight of the approach span without the upper chord U0-U1.

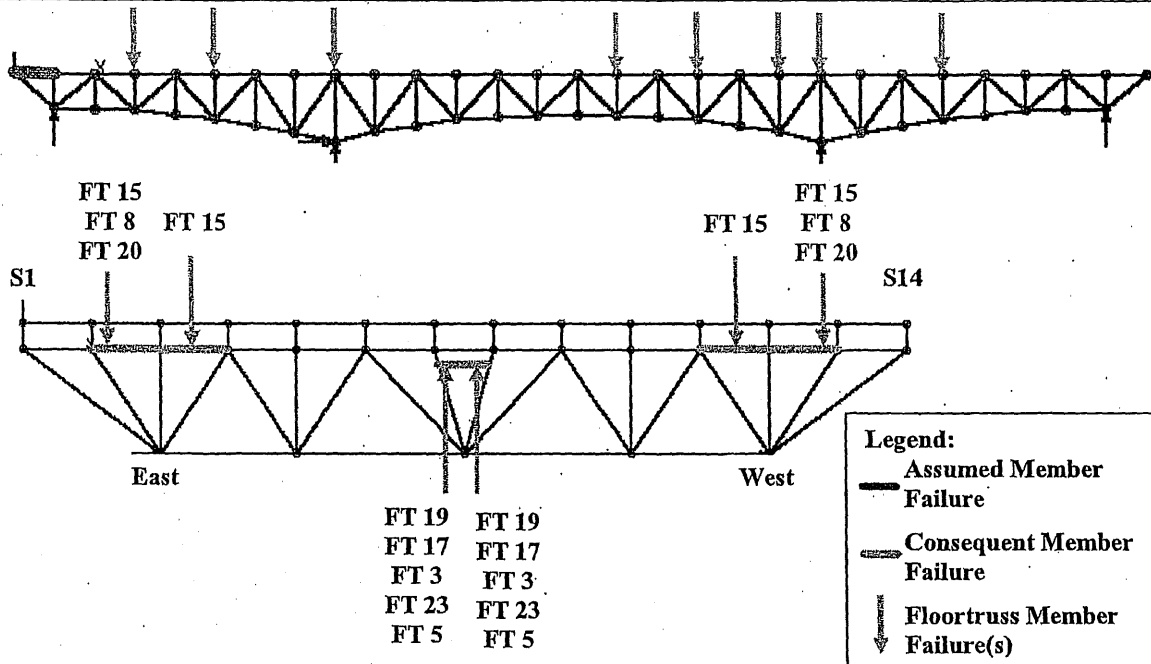


Figure 6-41: Load Case 3 – Failure of East Truss Upper Chord U0-U1
 Additional Member Failures Due to DL+LL on Intact Structure

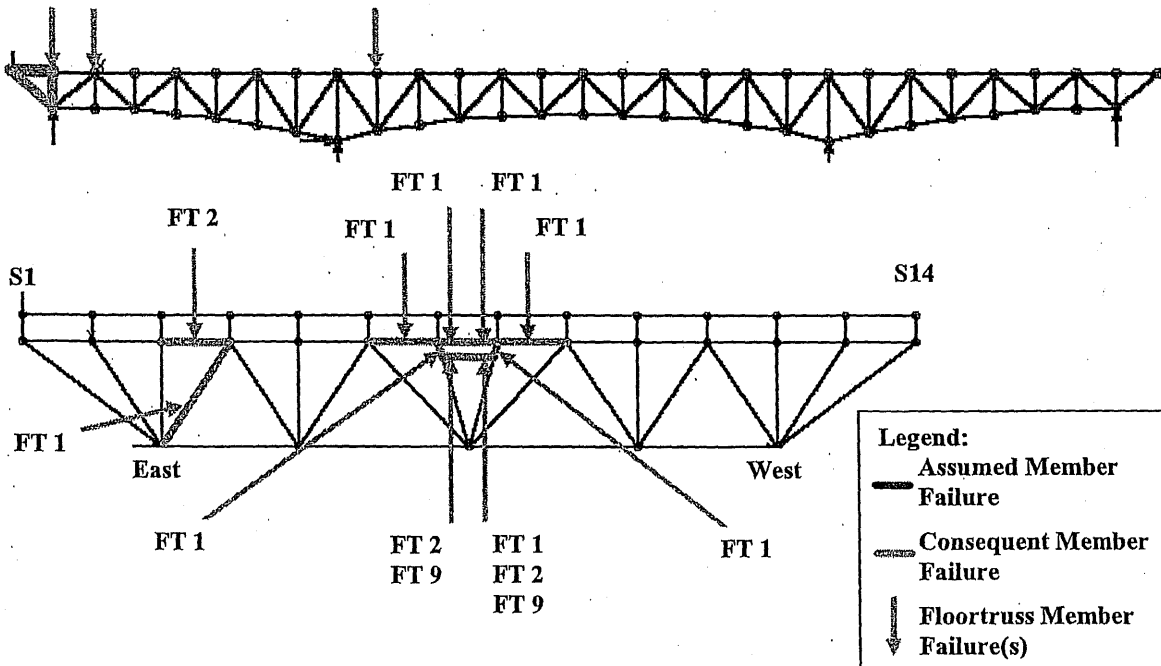


Figure 6-42: Load Case 3 – Failure of East Truss Upper Chord U0-U1 –
 Consequent Member Failures without Dynamic Impact

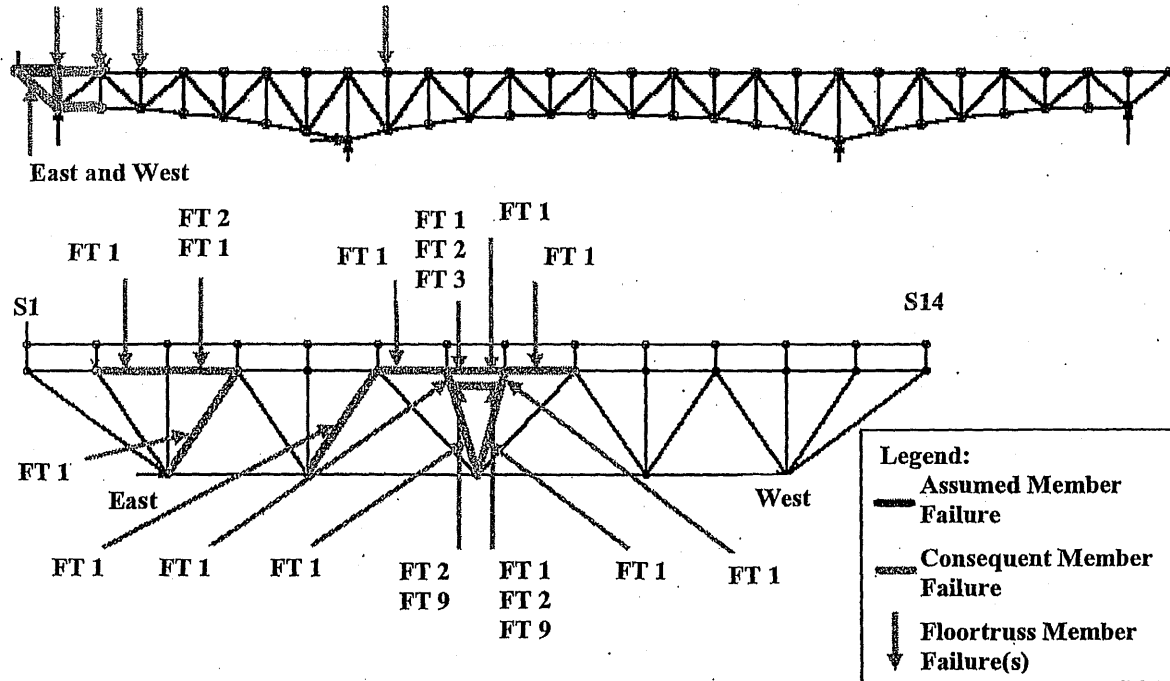


Figure 6-43: Load Case 3 – Failure of East Truss Upper Chord U0-U1 – Consequent Member Failures with a Dynamic Impact Factor of 1.854

4. Failure of East Truss Upper Chord U4-U5

Under the combined dead and live load on the intact structure prior to the removal of east truss upper chord U4-U5, eighteen additional floor truss members were found to have interaction ratios greater than 1.0 compared to the dead load only condition, as shown in Figure 6-44. All of these members are located adjacent to the floor trusses that support the stringers with the asymmetric expansion joint (Sections 6.7.1 and 6.7.2 and Figure 3-21), and the high interaction ratios were attributed primarily to the out-of-plane bending.

As a result of the failure of east truss upper chord U4-U5, calculated force interaction ratios indicated no consequent failures of any main truss members, without or with the dynamic impact factor of 1.854. Without the dynamic impact, seven consequent floor truss member failures were found to occur (Figure 6-45), No consequent portal/sway frame member failures would occur but two consequent upper/lower lateral bracing

member failure would occur. When a dynamic impact factor of 1.854 was included, eleven consequent floor truss member failures were found to occur (**Figure 6-46**). No consequent portal/sway frame member failures would occur but three consequent upper/lower lateral bracing member failure would occur. When the connection capacities are considered, one (L8-L9 West) consequent main truss member failures would occur with the 1.854 dynamic impact factor. The results of calculated force interaction ratios are summarized in **Table AIV-104A** (member capacities) and **Table AIV-104B** (connection capacities) for main truss members and **Tables AIV-105** through **AIV-107** for floor truss members. For some floor truss members that have interaction ratios greater than 1.0 under the dead load or the combined dead and live load in the intact condition, the sudden member failure did cause significant changes to the force interaction ratio.

Table AIV-108 and **Table AIV-109** list the support reactions and maximum joint displacements and corresponding locations, respectively. The induced longitudinal reactions at the "locked" expansion bearings are very low (a maximum longitudinal to vertical force ratio of 0.10 at the west bearing of Pier 6 with a dynamic impact factor of 1.854), and are not expected to change the existing "locked" condition of the steel roller bearing. The maximum joint displacements resulting from the member failure were low, a maximum of 1.5 inches of vertical deflection at panel point L5 with a dynamic impact factor of 1.854.

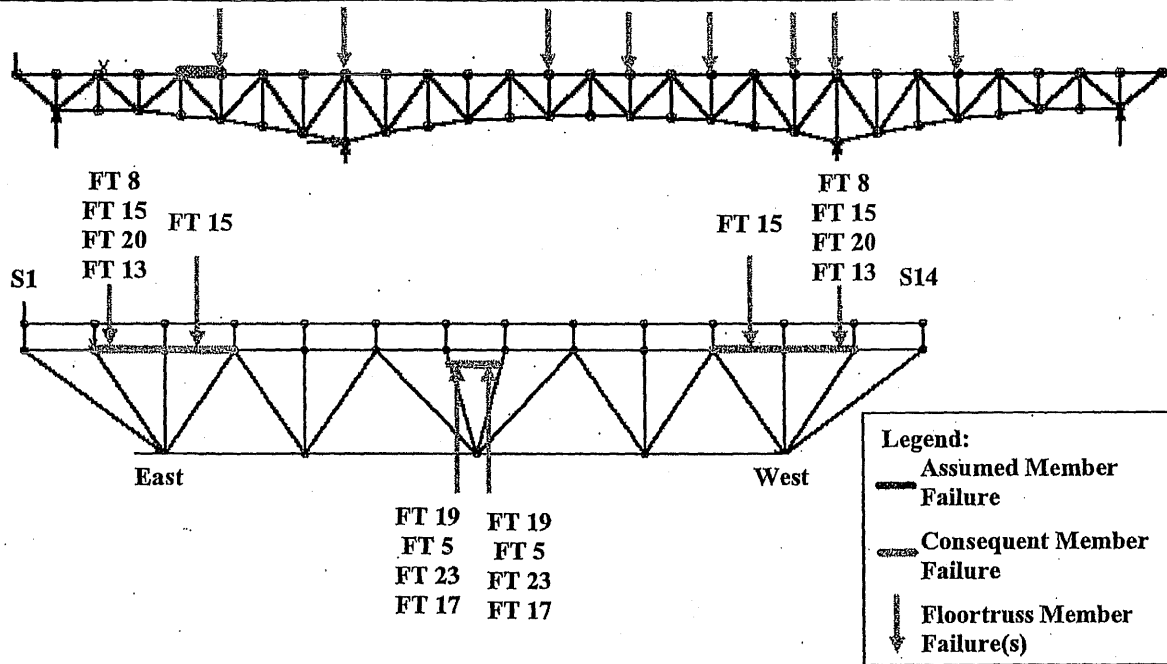


Figure 6-44: Load Case 3 – Failure of East Truss Upper Chord U4-U5
 Additional Member Failures Due to DL+LL on Intact Structure

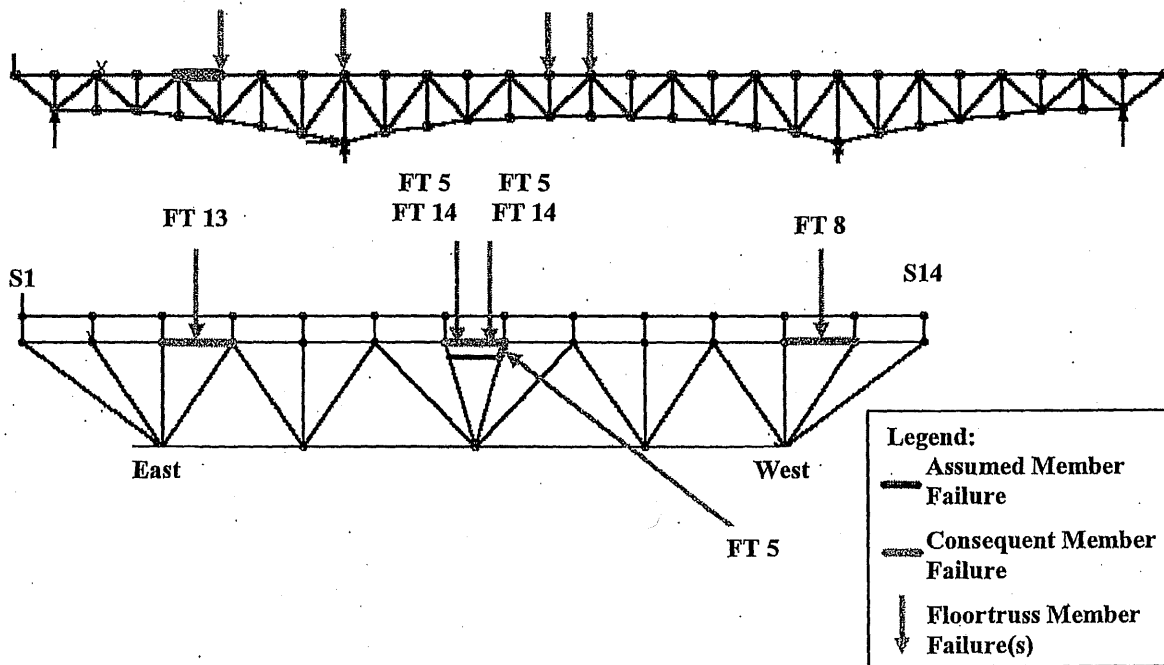


Figure 6-45: Load Case 3 – Failure of East Truss Upper Chord U4-U5
 Consequent Member Failures without Dynamic Impact

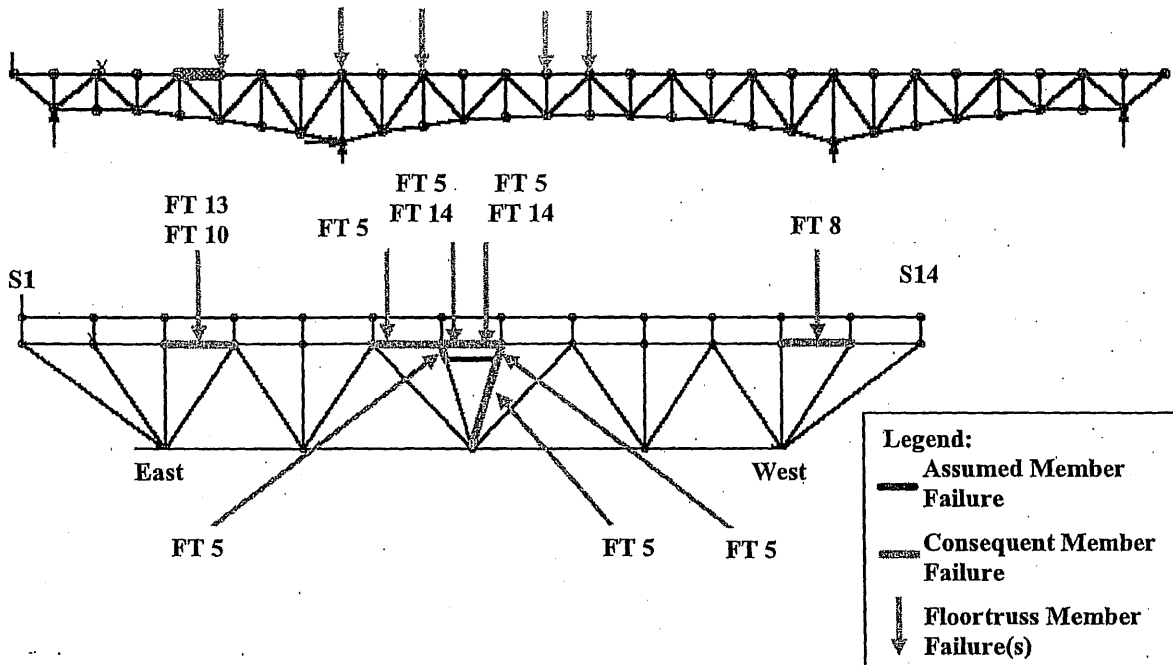


Figure 6-46: Load Case 3 – Failure of East Truss Upper Chord U4-U5
Consequent Member Failures with a Dynamic Impact Factor of 1.854

5. Failure of East Truss Upper Chord U4'-U3'

Member U4'-U3' was found to be subject to slightly higher forces than its counterpart U3-U4 due to different section properties and therefore used for the redundancy analysis. Under the combined dead and live load on the intact structure prior to the removal of east truss upper chord U4'-U3', sixteen additional floor truss members were found to have interaction ratios greater than 1.0 compared to the dead load only condition, as shown in Figure 6-47. All of these members are located adjacent to a floor truss that support the stringers with the asymmetric expansion joint (Sections 6.7.1 and 6.7.2 and Figure 3-21), and the failures were attributed primarily to the out-of-plane bending.

As a result of the failure of east truss upper chord U4'-U3', calculated force interaction ratios indicated no consequent failures of any structural members, without or with the dynamic impact factor of 1.854. This is true for the investigation of the member

capacities as well as the investigation of the connection capacities. The results of calculated force interaction ratios are summarized in Table AIV-110A (member capacities) and Table AIV-110B (connection capacities) for main truss members and Tables AIV-111 through AIV-113 for floor truss members. For those floor truss members that have interaction ratios greater than 1.0 under the dead load only in the intact condition (Table AIV-113), the sudden member failure did not cause significant changes to the force interaction ratio.

Table AIV-114 and Table AIV-115 list the support reactions and maximum joint displacements and corresponding locations, respectively. The induced longitudinal reactions at the "locked" expansion bearings are very low (a maximum longitudinal to vertical force ratio of 0.04 at the east bearing of Pier 6 with a dynamic impact factor of 1.854), and are not expected to change the existing "locked" condition of the steel roller bearing. The maximum joint displacements resulting from the member failure were very low.

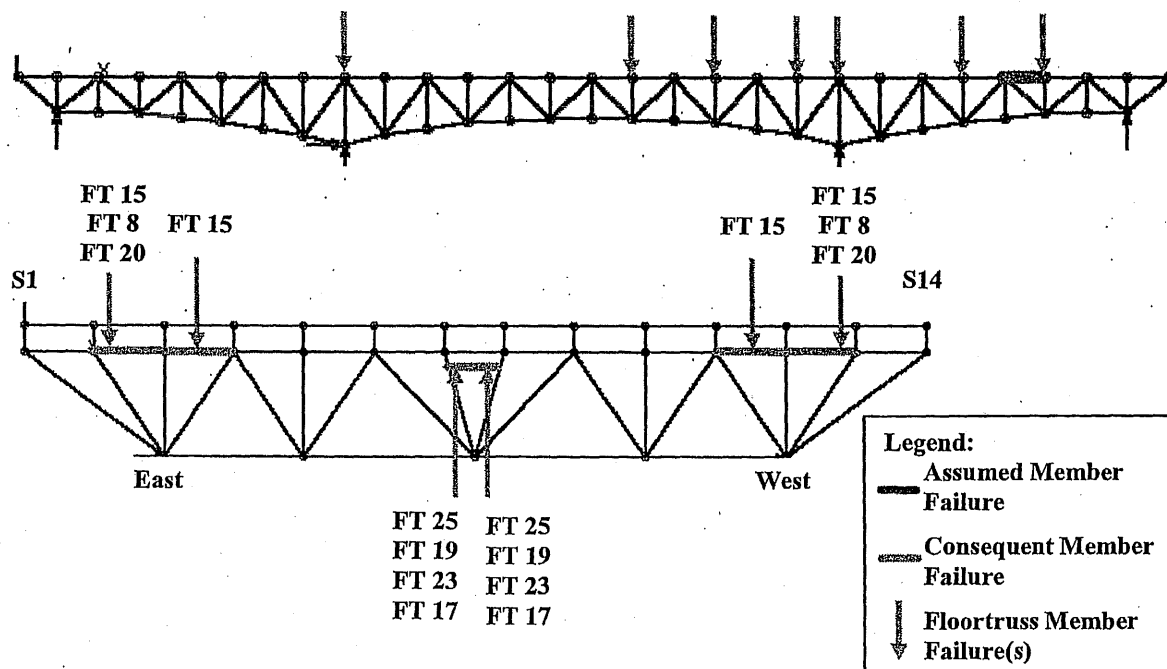


Figure 6-47: Load Case 3 – Failure of East Truss Upper Chord U4'-U3'
Additional Member Failures Due to DL+LL on Intact Structure

6. Failure of East Truss Lower Chord L4-L5

Under the combined dead and live load on the intact structure prior to the removal of east truss lower chord L4-L5, sixteen additional floor truss members were found to have interaction ratios greater than 1.0 compared to the dead load only condition, as shown in **Figure 6-48**. All of these members are located adjacent to a floor truss that support the stringers with the asymmetric expansion joint (**Sections 6.7.1 and 6.7.2 and Figure 3-21**), and the failures were attributed primarily to the out-of-plane bending.

The calculated force interaction ratios indicated no consequent failures of any structural members as a result of the failure of east truss lower chord L4-L5, without or with the dynamic impact factor of 1.854. This is true for the investigation of the member capacities as well as the investigation of the connection capacities. The results of calculated force interaction ratios are summarized in **Table AIV-116A** (member capacities) and **Table AIV-116B** (connection capacities) for main truss members and **Tables AIV-117 through AIV-119** for floor truss members. For those floor truss members that have interaction ratios greater than 1.0 under the combined dead and live load in the intact condition, the sudden member failure did not cause significant changes to the force interaction ratio.

Table AIV-120 and **Table AIV-121** list the support reactions and maximum joint deflections and locations respectively. The induced longitudinal reactions at the “locked” expansion bearings are low (a maximum longitudinal to vertical force ratio of 0.17 at the east bearing of Pier 5 with a dynamic impact factor of 1.854), and are not expected to change the existing “locked” condition of the steel roller bearing. The maximum joint displacements resulting from the member failure were very low.

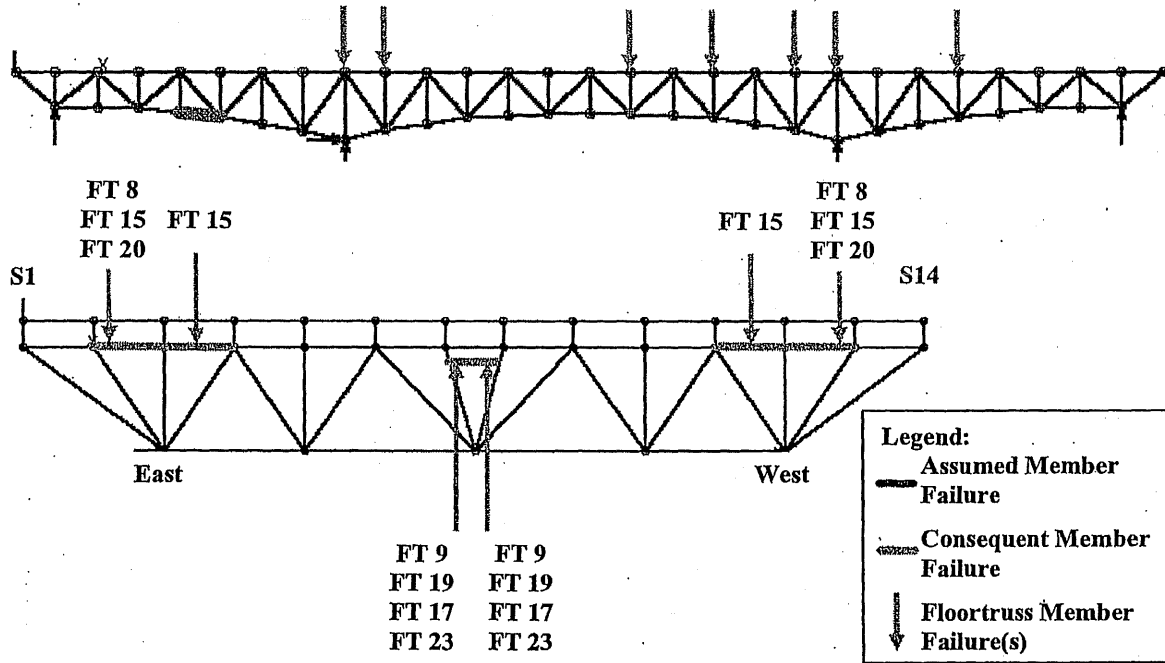


**Figure 6-48: Load Case 3 – Failure of East Truss Lower Chord L4-L5
Additional Member Failures Due to DL+LL on Intact Structure**

7. Failure of East Truss Lower Chord L12-L13

Under the combined dead and live load on the intact structure prior to the removal of east truss lower chord L12-L13, sixteen additional floor truss members were found to have interaction ratios greater than 1.0 compared to the dead load only condition, as shown in **Figure 6-49**. All of these members are located adjacent to a floor truss that support the stringers with the asymmetric expansion joint (**Sections 6.7.1 and 6.7.2 and Figure 3-21**), and the failures were attributed primarily to the out-of-plane bending.

Calculated force interaction ratios indicated that four consequent main truss member failures and five consequent floor truss member failures would occur resulting from the failure of east truss upper chord L12-L13, when dynamic impact was not included (**Figure 6-50**). No portal/sway frame members would fail, but one upper/lower lateral

bracing member would fail. When a dynamic impact factor of 1.854 was included, seven consequent main truss member failures and eleven consequent floor truss member failures would occur (**Figure 6-51**). Two portal/sway frame members would fail and one upper/lower lateral bracing member would fail. When the connection capacities are considered, five (L10-L11, L9-L10, L8-L9, L9'-L8' and L8-L9 West) and nine (L10-L11, L9-L10, L8-L9, L10'-L9', L11'-L10', L9'-L8', L8-L9 West, L9'-L8' West, and U8-L8) consequent main truss member failures would occur without and with the 1.854 dynamic impact factor respectively. The results of calculated force interaction ratios are summarized in **Table AIV-122A** (member capacities) and **Table AIV-122B** (connection capacities) for main truss members and **Tables AIV-123** through **AIV-125** for floor truss members. For some of the floor truss members that have interaction ratios greater than 1.0 under the combined dead and live load in the intact condition, the sudden member failure did cause significant changes to the force interaction ratio.

Table AIV-126 and **Table AIV-127** list the support reactions and maximum joint deflections and locations respectively. The induced longitudinal reactions at the "locked" expansion bearings were relatively low (a maximum longitudinal to vertical force ratio of 0.26 at the east bearing of Pier 6 with a dynamic impact factor of 1.854), and are not expected to change the existing "locked" condition of the steel roller bearing. The maximum joint displacements resulting from the member failure were not very high (a maximum vertical deflection of 3.6 inches at panel point U12 with a dynamic impact factor of 1.854).

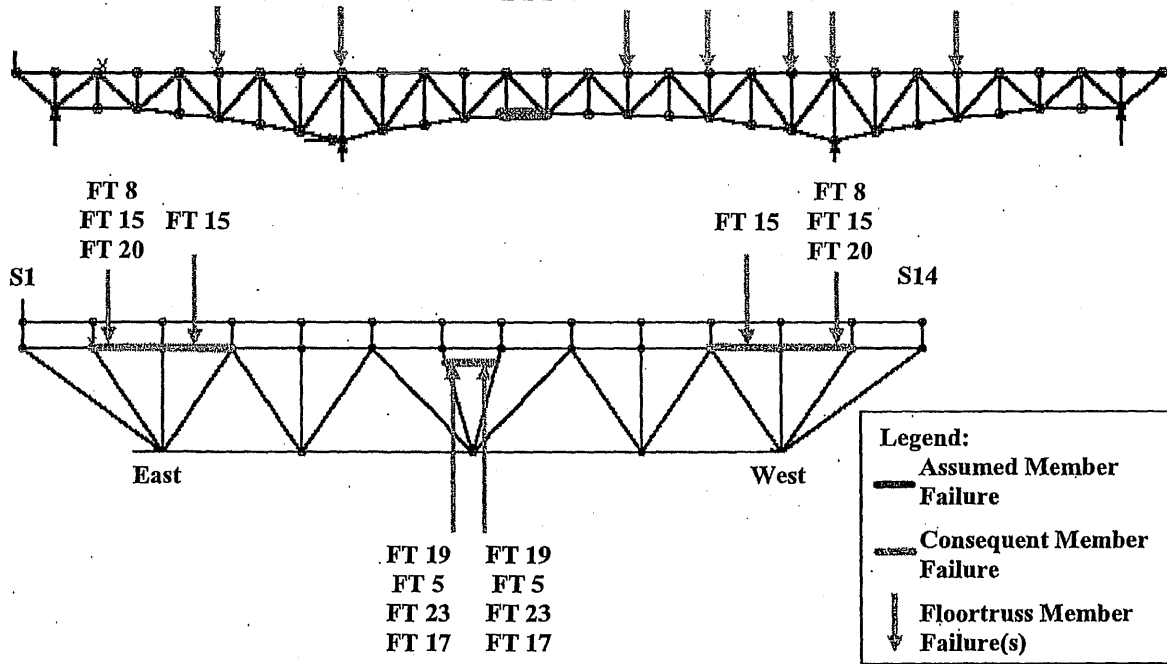


Figure 6-49: Load Case 3 – Failure of East Truss Lower Chord L12-L13
 Additional Member Failures Due to DL+LL on Intact Structure

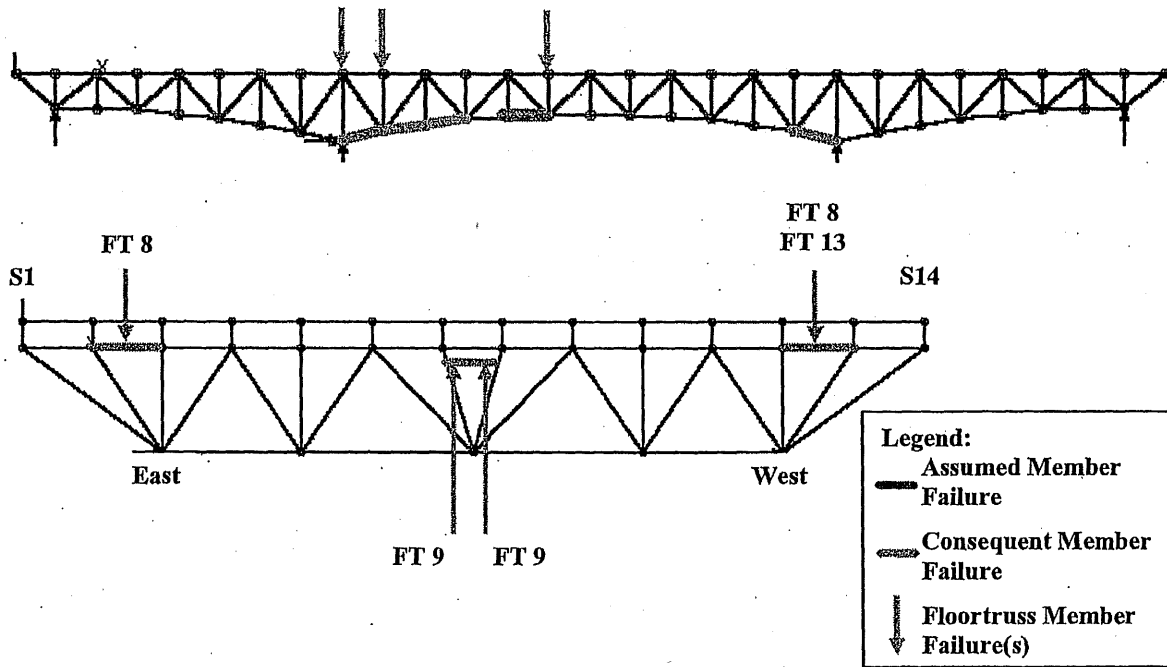
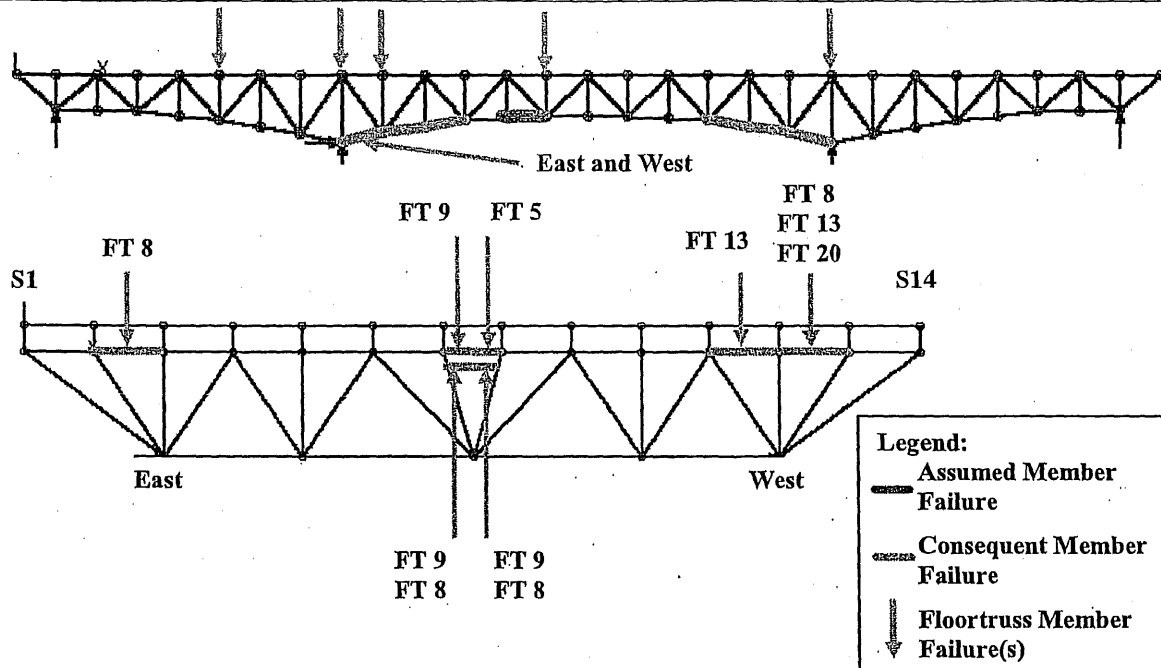


Figure 6-50: Load Case 3 – Failure of East Truss Lower Chord L12-L13
 Consequent Member Failures without Dynamic Impact



**Figure 6-51: Load Case 3 – Failure of East Truss Lower Chord L12-L13
Consequent Member Failures with a Dynamic Impact Factor of 1.854**

8. Failure of East Truss Lower Chord L13-L14

Under the combined dead and live load on the intact structure prior to the removal of east truss lower chord L13-L14, sixteen additional floor truss members were found to have interaction ratios greater than 1.0 compared to the dead load only condition, as shown in **Figure 6-52**. All of these members are located adjacent to floor trusses that support the stringers with the asymmetric expansion joint (Sections 6.7.1 and 6.7.2 and **Figure 3-21**), and the failures were attributed primarily to the out-of-plane bending.

Calculated force interaction ratios indicated that seven consequent main truss member failures and eight consequent floor truss member failures would occur resulting from the failure of east truss upper chord L13-L14, when dynamic impact was not included (**Figure 6-53**). Three portal/sway frame member and three upper/lower lateral bracing members would fail. When a dynamic impact factor of 1.854 was included, ten consequent main truss member failures and twenty-four consequent floor truss member

failures would occur (Figure 6-54). Four portal/sway frame members and six upper/lower lateral bracing members would fail. When the connection capacities are considered, nine (L10-L11, L11'-L10', L9-L10, L10'-L9', L8-L9, L9'-L8', U14-L14 West, L8-L9 West, and L9'-L8' West) and eleven (L10-L11, L11'-L10', L9-L10, L10'-L9', L9'-L8', L8-L9, U14-L14 West, L9'-L8' West, L8-L9 West, U14-U13' West and U13-U14 West) consequent main truss member failures would occur without and with the 1.854 dynamic impact factor respectively. The results of calculated force interaction ratios are summarized in Table AIV-128A (member capacities) and Table AIV-128B (connection capacities) for main truss members and Tables AIV-129 through AIV-131 for floor truss members. For those floor truss members that have interaction ratios greater than 1.0 under dead load or combined dead and live load in the intact condition, the sudden member failure caused significant changes to the force interaction ratio in some of them.

Table AIV-132 and Table AIV-133 list the support reactions and maximum joint deflections and locations respectively. The induced longitudinal reactions at the "locked" expansion bearings were relatively high, a maximum longitudinal to vertical force ratio of 0.34 at the east bearing of Pier 6 with a dynamic impact factor of 1.854. This level of longitudinal force may not change the existing "locked" condition of the steel roller bearing, depending on the surface condition, since a frictional coefficient of 0.40 is generally accepted for steel. The maximum joint displacements resulting from the member failure were also relatively high, a maximum vertical deflection of 7.2 inches at panel point U14 with a dynamic impact factor of 1.854.

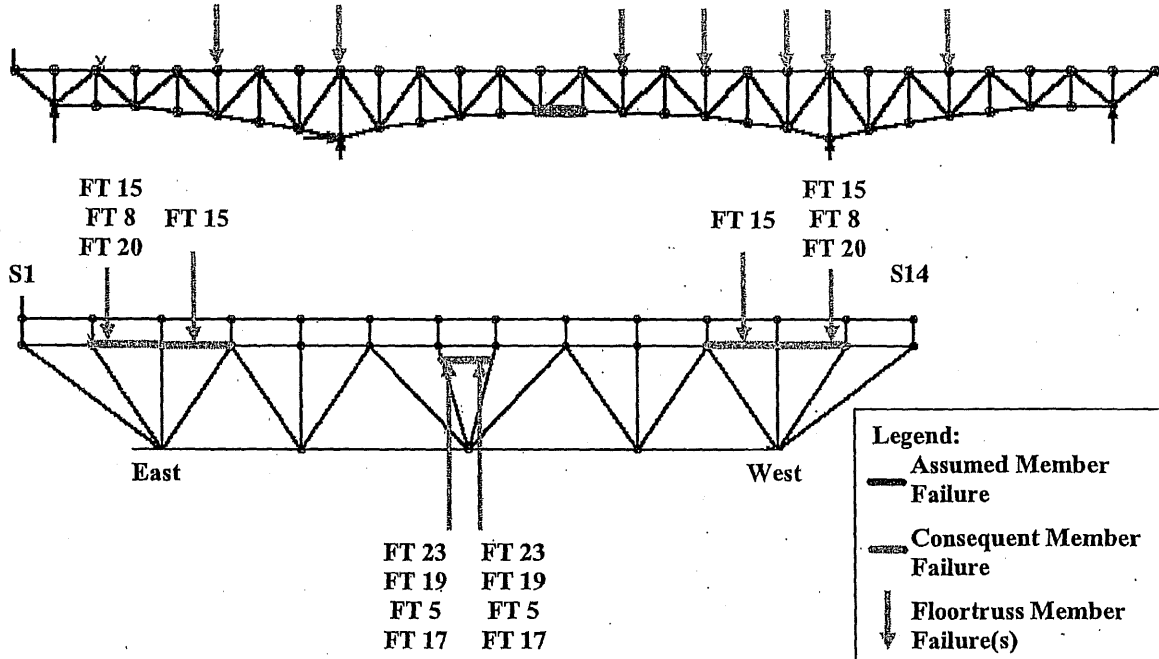


Figure 6-52: Load Case 3 – Failure of East Truss Lower Chord L13-L14
 Additional Member Failures Due to DL+LL on Intact Structure

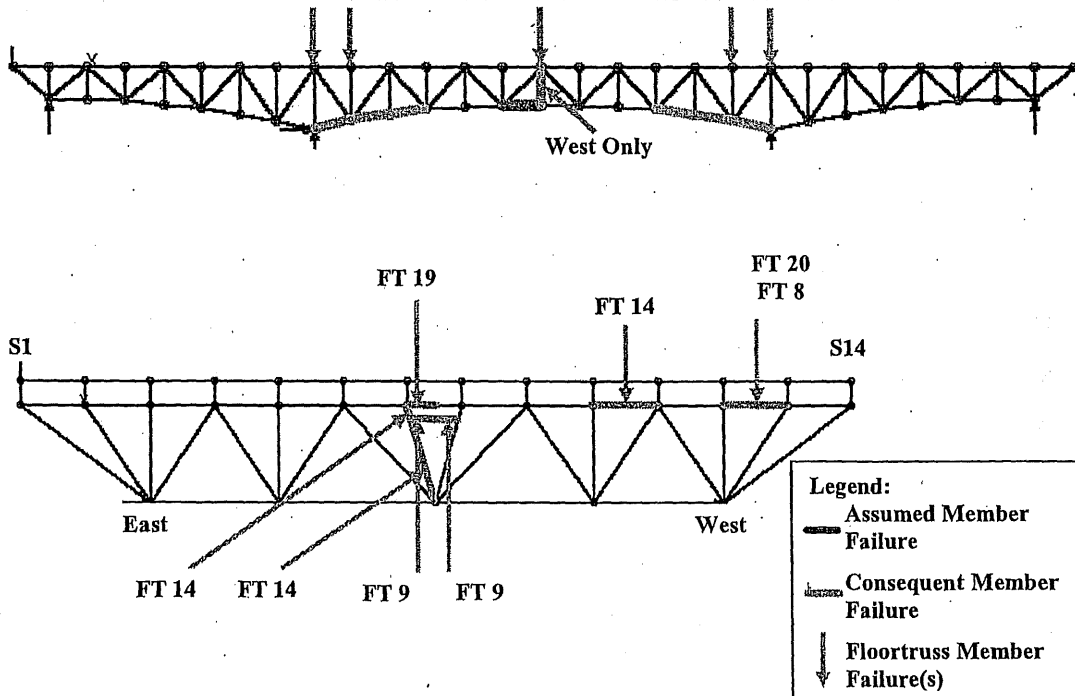


Figure 6-53: Load Case 3 – Failure of East Truss Lower Chord L13-L14
 Consequent Member Failures without Dynamic Impact

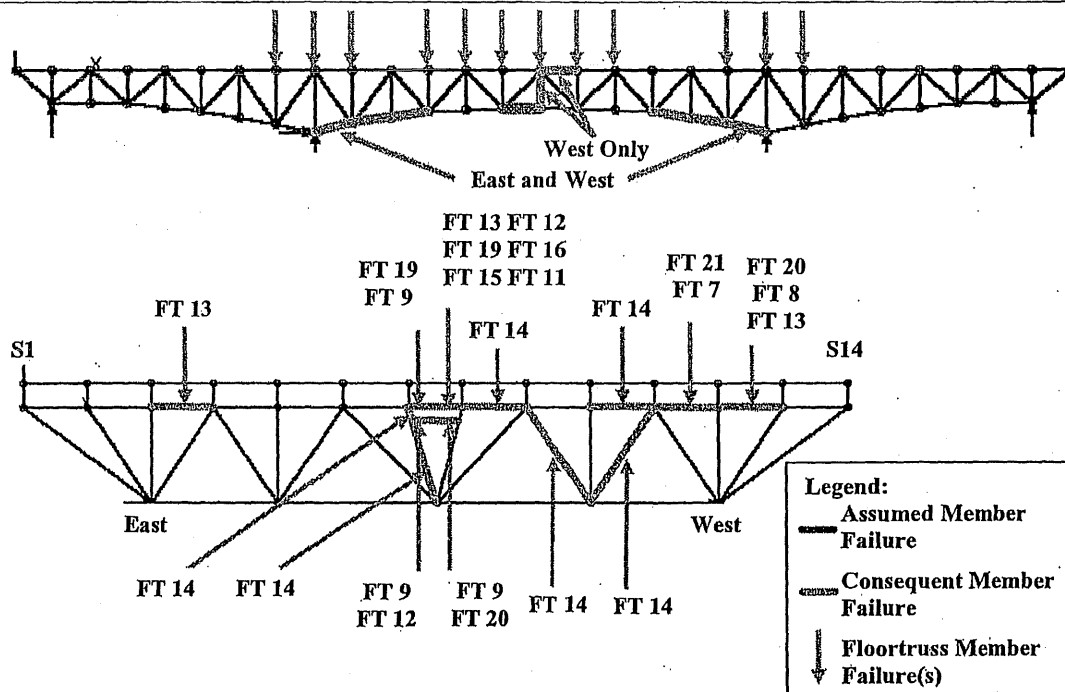


Figure 6-54: Load Case 3 – Failure of East Truss Lower Chord L13-L14
Consequent Member Failures with a Dynamic Impact Factor of 1.854

6.7.8 Load Case 4: LRFD Design Load – Seven HS-20 Truck & Lane Load Lopsided (MPF=0.65; IM=1.33)

Some floor truss members were found to have force interaction ratios exceeding 1.0 under the combined dead load and live load in the intact condition prior to the removal of the critical truss member under investigation. This behavior is discussed where applicable.

1. Failure of East Truss Diagonal L3-U4

Under the combined dead and live load on the intact structure prior to the removal of east truss diagonal chord L3-U4, six additional floor truss members were found to have interaction ratios greater than 1.0 compared to the dead load only condition, as shown in Figure 6-55. All of these members are located adjacent to floor trusses that support the

stringers with the asymmetric expansion joint (Sections 6.7.1 and 6.7.2 and Figure 3-21), and the failures were attributed primarily to the out-of-plane bending.

The calculated force interaction ratios indicated no consequent failures of any structural members would occur as a result of the failure of east truss diagonal L3-U4, without or with the dynamic impact factor of 1.854. This is true for the investigation of the member capacities as well as the investigation of the connection capacities. The results of calculated force interaction ratios are summarized in **Table AIV-134A** (member capacities) and **Table AIV-134B** (connection capacities) for main truss members and **Table AIV-135** thru **Table AIV-137** for floor truss members. For those floor truss members that have interaction ratios greater than 1.0 under the combined dead and live load in the intact condition, the sudden member failure did not cause significant changes to the force interaction ratio.

Table AIV-138 and **Table AIV-139** list support reactions and maximum joint displacements and corresponding locations, respectively. The induced longitudinal reactions at the "locked" expansion bearings were very low (a maximum longitudinal to vertical force ratio of 0.09 at the east bearing of Pier 5 with a dynamic impact factor of 1.854), and are not expected to change the existing bearing condition. The maximum joint displacements resulting from the member failure were very low.

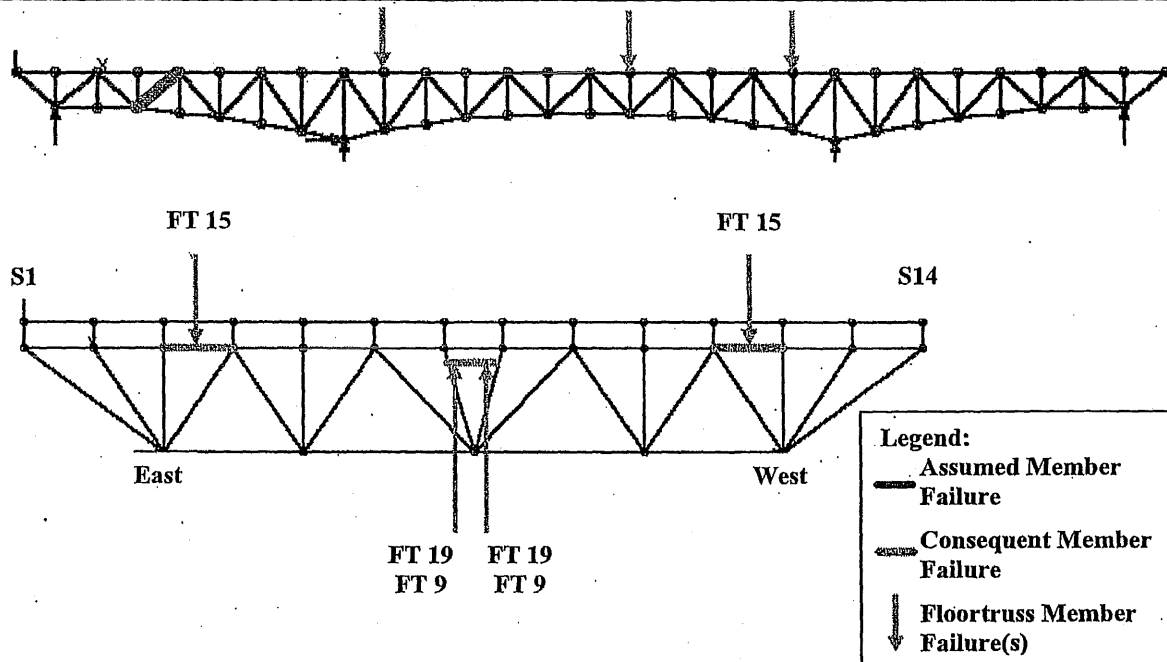


**Figure 6-55: Load Case 4 – Failure of East Truss Diagonal L3-U4
Additional Member Failures Due to DL+LL on Intact Structure**

2. Failure of East Truss Lower Chord L1-L2

Under the combined dead and live load on the intact structure prior to the removal of east truss upper chord L1-L2, four additional floor truss members were found to have interaction ratios greater than 1.0 compared to the dead load only condition, as shown in **Figure 6-56**. All of these members are located adjacent to floor trusses that support the stringers with the asymmetric expansion joint (**Sections 6.7.1 and 6.7.2 and Figure 3-21**), and the failures were attributed primarily to the out-of-plane bending.

The calculated force interaction ratios indicated no consequent failures of any structural members as a result of the failure of east truss lower chord L1-L2, without the dynamic impact factor. When a dynamic impact factor of 1.854 was included, two consequent floor truss member failures would occur (**Figure 6-57**). No portal/sway frame members or upper/lower lateral bracing members would fail. When the connection capacities are considered one (U1-L1) consequent main truss member failure would occur with the

1.854 dynamic impact factor. The results of calculated force interaction ratios are summarized in **Table AIV-140A** (member capacities) and **Table AIV-140B** (connection capacities) for main truss members and **Tables AIV-141** through **AIV-143** for floor truss members. For those floor truss members that have interaction ratios greater than 1.0 under dead load or combined dead and live load in the intact condition, the sudden member failure did not cause significant changes to the force interaction ratio.

Table AIV-144 and **Table AIV-145** list the support reactions and maximum joint deflections and locations respectively. The induced longitudinal reactions at the “locked” expansion bearings were relatively low (a maximum longitudinal to vertical force ratio of 0.20 at the east bearing of Pier 5 with a dynamic impact factor of 1.854), and are not expected to change the existing “locked” condition of the steel roller bearing. The maximum joint displacements resulting from the member failure were not very high (a maximum vertical deflection of 0.82 inches at panel point U0 with a dynamic impact factor of 1.854).

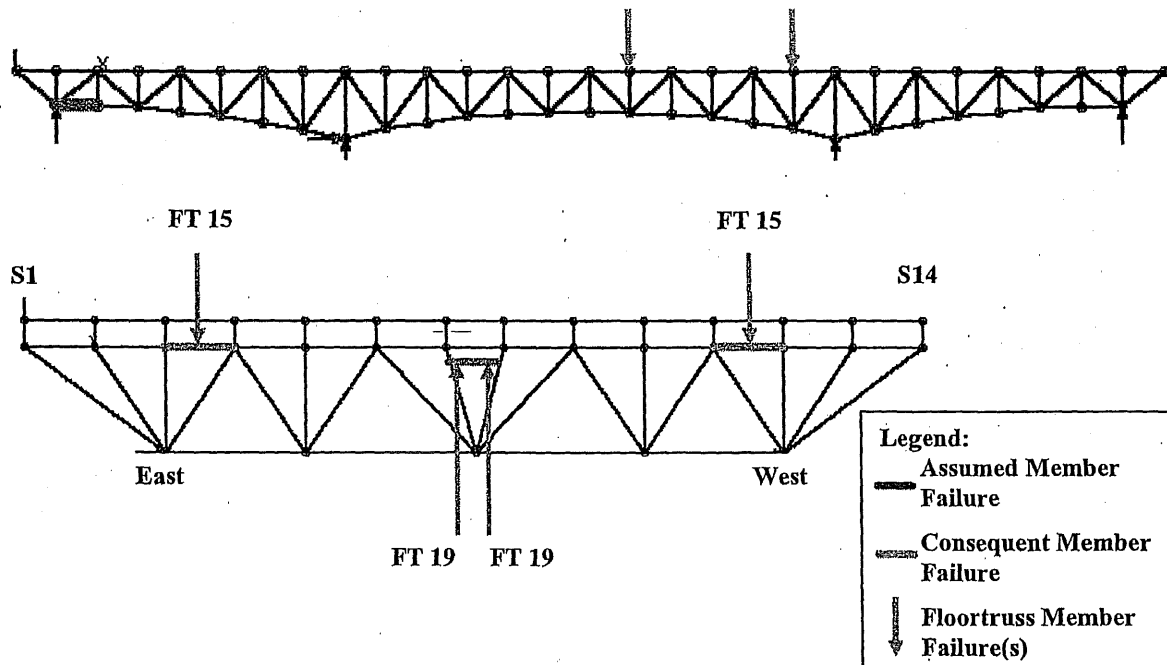


Figure 6-56: Load Case 4 – Failure of East Truss Lower Chord L1-L2

Additional Member Failures Due to DL+LL on Intact Structure

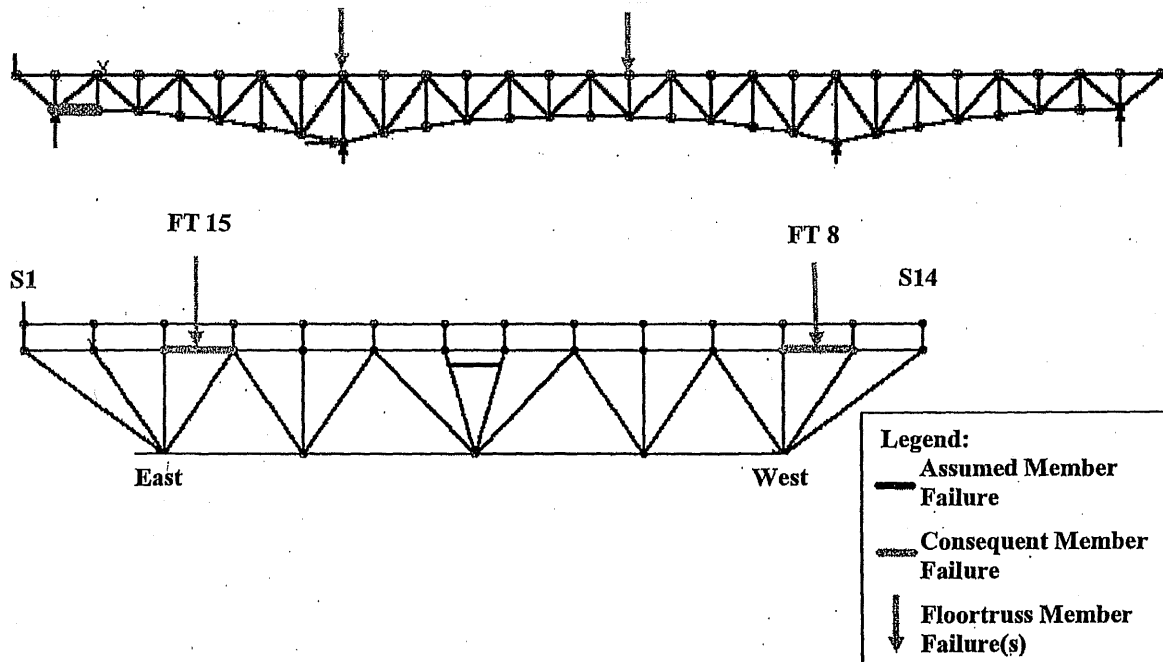


Figure 6-57: Load Case 4 – Failure of East Truss Lower Chord L1-L2
Consequent Member Failures with a Dynamic Impact Factor of 1.854

3. Failure of East Truss Upper Chord U0-U1 (South End Floorbeam)

Under the combined dead and live load on the intact structure prior to the removal of east truss upper chord U0-U1, five additional floor truss members were found to have interaction ratios greater than 1.0 compared to the dead load only condition, as shown in **Figure 6-58**. All of these members are located adjacent to floor trusses that support the stringers with the asymmetric expansion joint (Sections 6.7.1 and 6.7.2 and **Figure 3-21**), and the failures were attributed primarily to the out-of-plane bending.

Calculated force interaction ratios indicated that two consequent main truss member failures and fourteen consequent floor truss member failures would result from the failure of east truss upper chord U0-U1, when dynamic impact was not included (**Figure 6-59**). No consequent portal and sway frame member failures would occur but two upper lateral and lower lateral bracing consequent member failures would occur. When a dynamic

impact factor of 1.854 was included, four consequent main truss member failures and twenty-three consequent floor truss member failures would occur (Figure 6-60). No consequent portal and sway frame member failures would occur but three consequent upper lateral and lower lateral bracing member failures would occur. When the connection capacities are considered, two (U0-L1 and U1-L1) and five (U0-L1, U1-L1, L1-L2, SFB-U1, and U1-U2) consequent main truss member failures would occur without and with the 1.854 dynamic impact factor respectively. The results of calculated force interaction ratios are summarized in Table AIV-146A (member capacities) and Table AIV-146B (connection capacities) for main truss members and Table AIV-147 thru Table AIV-149 for floor truss members. For those floor truss members that have interaction ratios greater than 1.0 under the combined dead and live load in the intact condition, the sudden member failure does not cause significant changes to the force interaction ratio.

Table AIV-150 and Table AIV-151 list support reactions and maximum joint displacements and corresponding locations, respectively. The induced longitudinal reactions at the "locked" expansion bearings are relatively high (a maximum longitudinal to vertical force ratio of 0.24 at the east bearing of Pier 5 with a dynamic impact factor of 1.854), and are not expected to change the existing "locked" condition of the steel roller bearing. The displacements of the east truss upper joint U0 resulting from the member failure were extremely high, which indicated the instability of diagonal U0-L1 for supporting the weight of the approach span without the upper chord U0-U1.

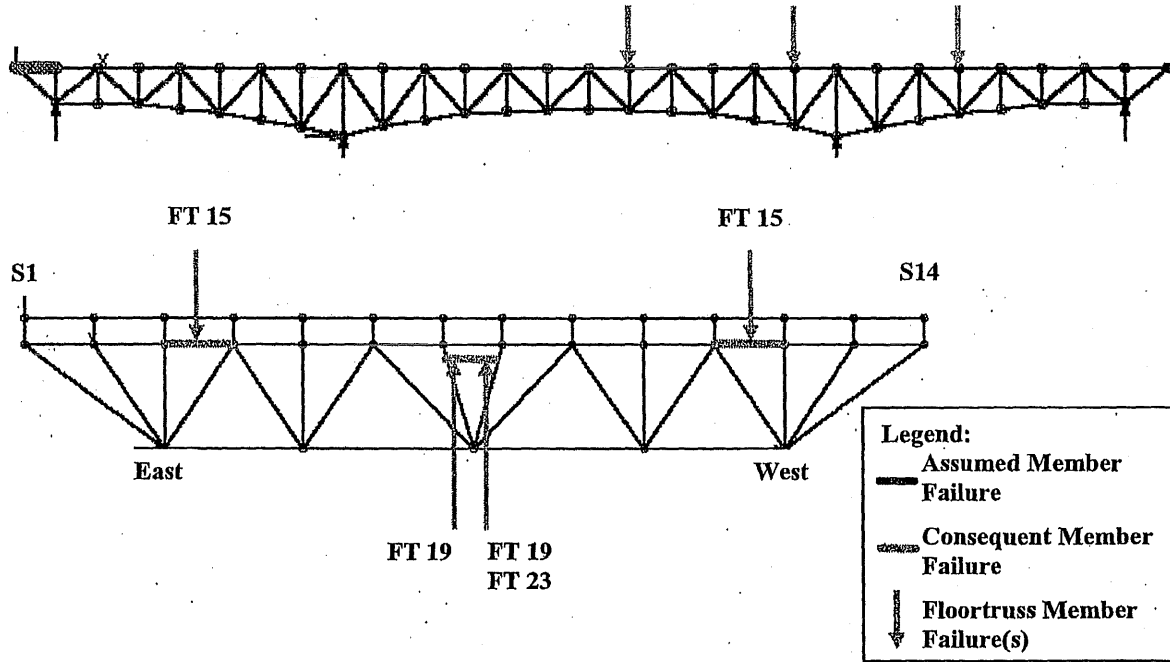


Figure 6-58: Load Case 4 – Failure of East Truss Upper Chord U0-U1
Additional Member Failures Due to DL+LL on Intact Structure

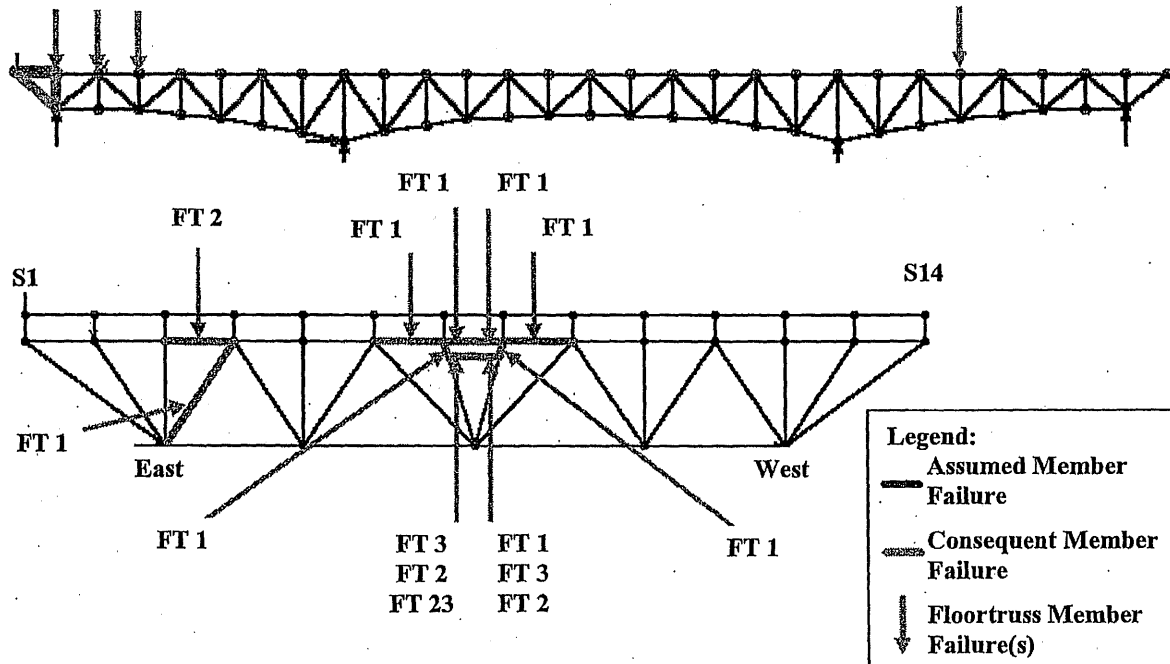


Figure 6-59: Load Case 4 – Failure of East Truss Upper Chord U0-U1
Consequent Member Failures without Dynamic Impact

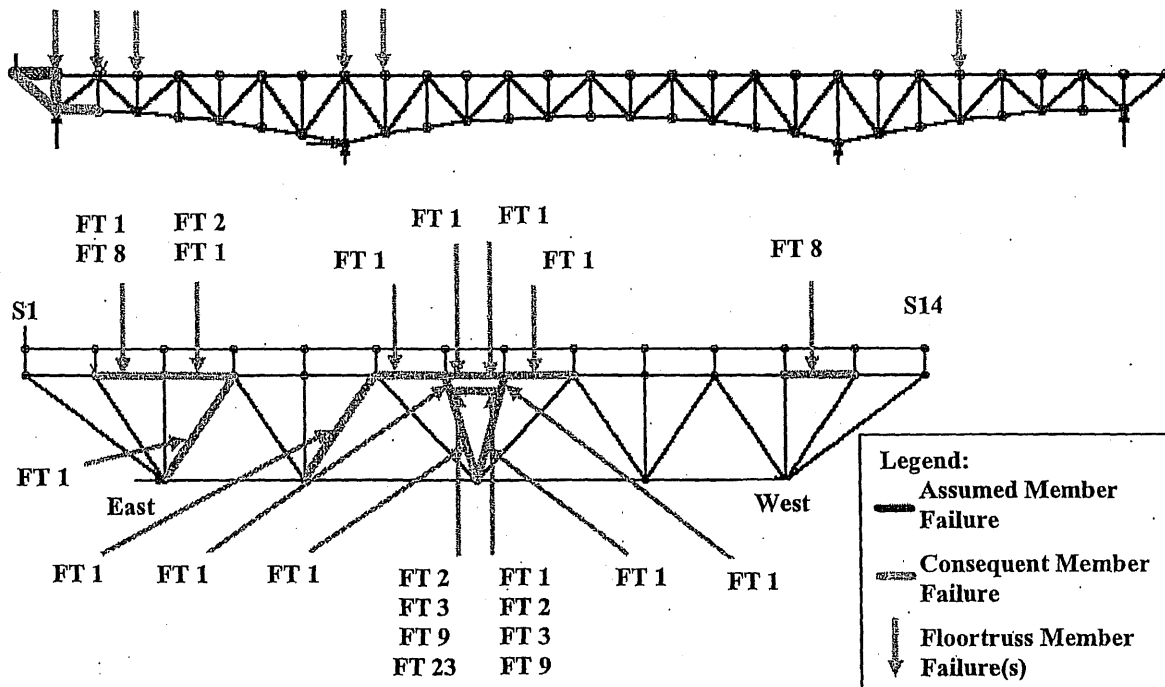


Figure 6-60: Load Case 4 – Failure of East Truss Upper Chord U0-U1
Consequent Member Failures with a Dynamic Impact Factor of 1.854

4. Failure of East Truss Upper Chord U4-U5

Under the combined dead and live load on the intact structure prior to the removal of east truss upper chord U4-U5, thirteen additional floor truss members were found to have interaction ratios greater than 1.0 compared to the dead load only condition, as shown in **Figure 6-61**. All of these members are located adjacent to the floor trusses that support the stringers with the asymmetric expansion joint (Sections 6.7.1 and 6.7.2 and **Figure 3-21**), and the high interaction ratios were attributed primarily to the out-of-plane bending.

As a result of the failure of east truss upper chord U4-U5, calculated force interaction ratios indicated no consequent failures of any main truss members, without or with the dynamic impact factor of 1.854. This is true for the investigation of the member capacities as well as the investigation of the connection capacities. Without the dynamic impact, four consequent floor truss member failures were found to occur (**Figure 6-61**),

No consequent portal/sway frame member or upper/lower lateral bracing member failures would occur. When a dynamic impact factor of 1.854 was included, ten consequent floor truss member failures were found to occur (**Figure 6-62**). No consequent portal/sway frame member failures would occur but two consequent upper/lower lateral bracing member failure would occur. The results of calculated force interaction ratios are summarized in **Table AIV-152A** (member capacities) and **Table AIV-152B** (connection capacities) for main truss members and **Tables AIV-153** through **AIV-155** for floor truss members. For some floor truss members that have interaction ratios greater than 1.0 under the dead load or the combined dead and live load in the intact condition, the sudden member failure did cause significant changes to the force interaction ratio.

Table AIV-156 and **Table AIV-157** list the support reactions and maximum joint displacements and corresponding locations, respectively. The induced longitudinal reactions at the “locked” expansion bearings are very low (a maximum longitudinal to vertical force ratio of 0.08 at the west bearing of Pier 6 with a dynamic impact factor of 1.854), and are not expected to change the existing “locked” condition of the steel roller bearing. The maximum joint displacements resulting from the member failure were low, a maximum of 1.4 inches of vertical deflection at panel point L5 with a dynamic impact factor of 1.854.

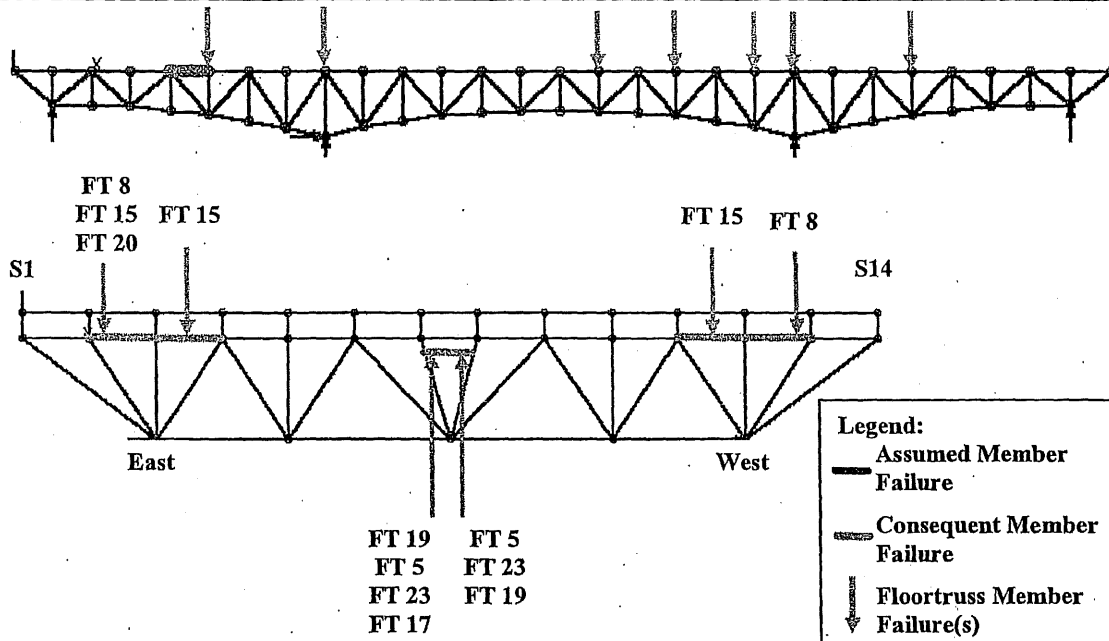


Figure 6-61: Load Case 4 – Failure of East Truss Upper Chord U4-U5
 Additional Member Failures Due to DL+LL on Intact Structure

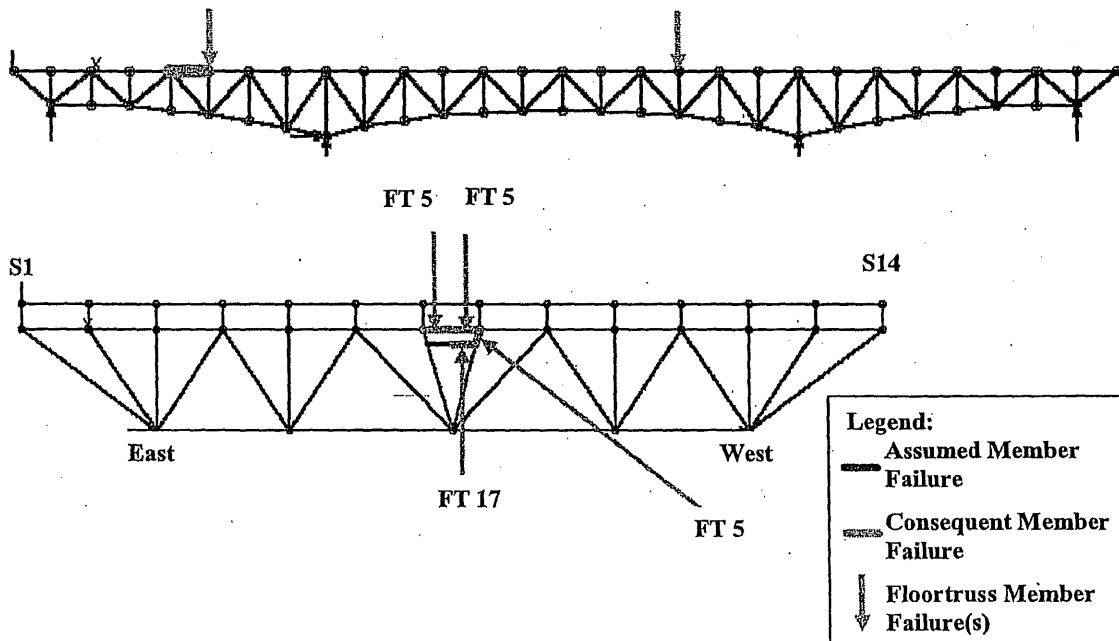


Figure 6-62: Load Case 4 – Failure of East Truss Upper Chord U4-U5
 Consequent Member Failures without Dynamic Impact

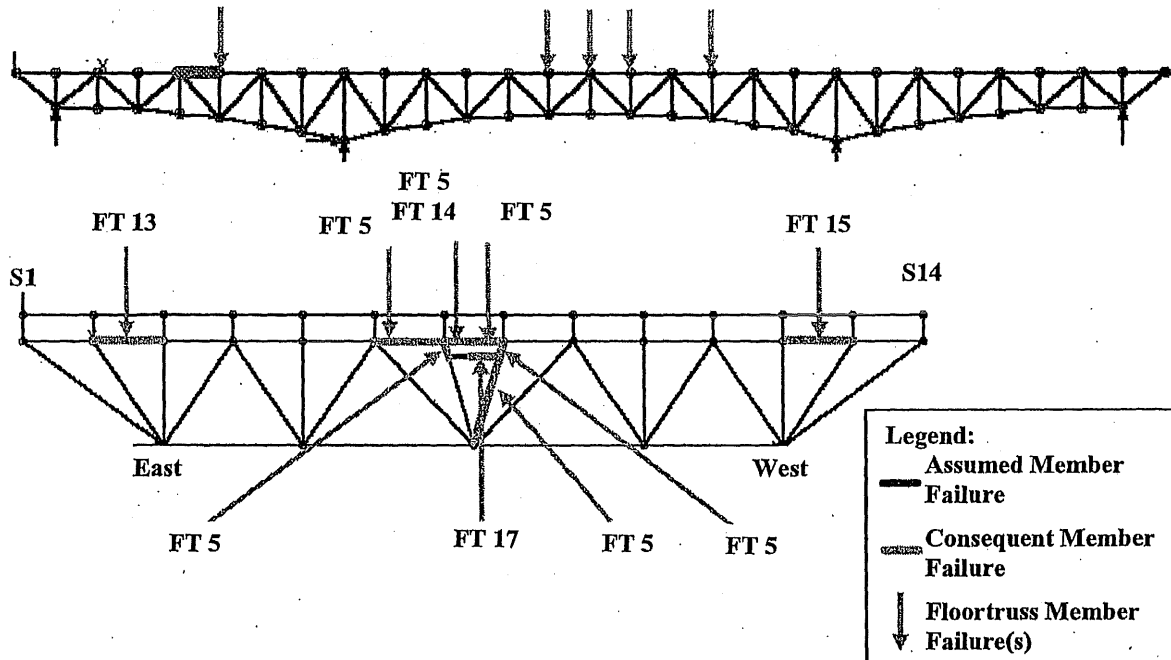


Figure 6-63: Load Case 4 – Failure of East Truss Upper Chord U4-U5
Consequent Member Failures with a Dynamic Impact Factor of 1.854

5. Failure of East Truss Upper Chord U4'-U3'

Member U4'-U3' was found to be subject to slightly higher forces than its counterpart U3-U4 due to different section properties and therefore used for the redundancy analysis. Under the combined dead and live load on the intact structure prior to the removal of east truss upper chord U4'-U3', eight additional floor truss members were found to have interaction ratios greater than 1.0 compared to the dead load only condition, as shown in Figure 6-64. All of these members are located adjacent to a floor truss that support the stringers with the asymmetric expansion joint (Sections 6.7.1 and 6.7.2 and Figure 3-21), and the failures were attributed primarily to the out-of-plane bending.

As a result of the failure of east truss upper chord U4'-U3', calculated force interaction ratios indicated no consequent failures of any structural members, without or with the dynamic impact factor of 1.854. This is true for the investigation of the member

capacities as well as the investigation of the connection capacities. The results of calculated force interaction ratios are summarized in **Table AIV-158A** (member capacities) and **Table AIV-158B** (connection capacities) for main truss members and **Tables AIV-159** through **AIV-161** for floor truss members. For those floor truss members that have interaction ratios greater than 1.0 under the dead load only in the intact condition, the sudden member failure did not cause significant changes to the force interaction ratio.

Table AIV-162 and **Table AIV-163** list the support reactions and maximum joint displacements and corresponding locations, respectively. The induced longitudinal reactions at the “locked” expansion bearings are very low (a maximum longitudinal to vertical force ratio of 0.03 at the east bearing of Pier 6 with a dynamic impact factor of 1.854), and are not expected to change the existing “locked” condition of the steel roller bearing. The maximum joint displacements resulting from the member failure were very low.

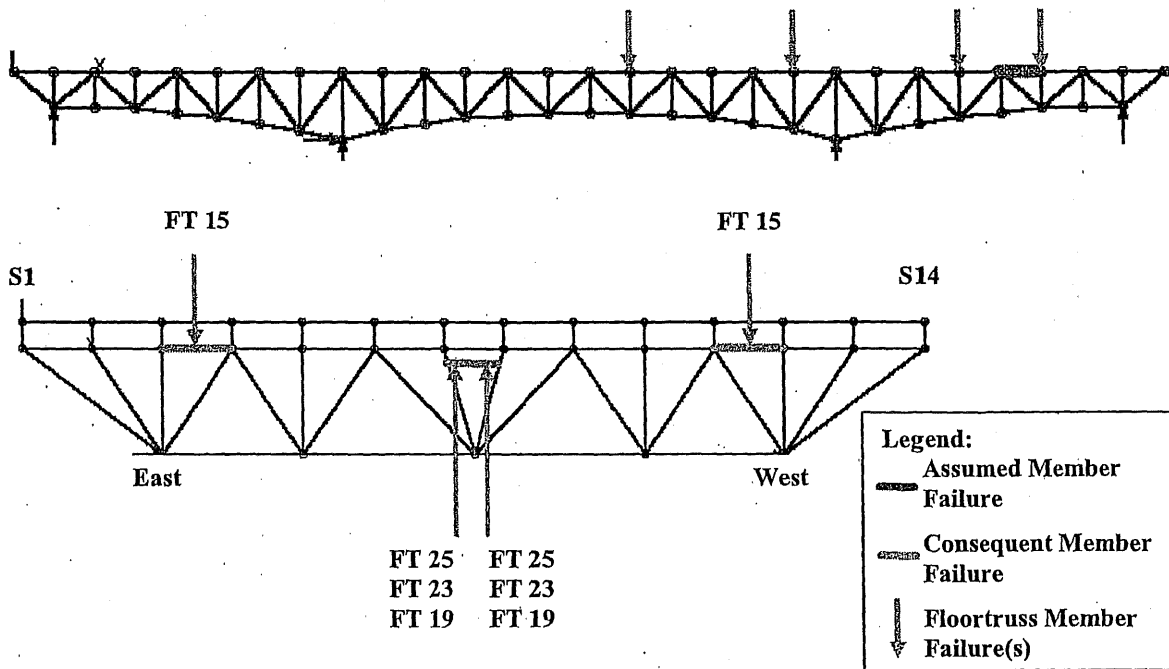


**Figure 6-64: Load Case 4 – Failure of East Truss Upper Chord U4'-U3'
Additional Member Failures Due to DL+LL on Intact Structure**

6. Failure of Critical Member L4-L5

Under the combined dead and live load on the intact structure prior to the removal of east truss lower chord L4-L5, seven additional floor truss members were found to have interaction ratios greater than 1.0 compared to the dead load only condition, as shown in **Figure 6-65**. All of these members are located adjacent to a floor truss that support the stringers with the asymmetric expansion joint (Sections 6.7.1 and 6.7.2 and **Figure 3-21**), and the failures were attributed primarily to the out-of-plane bending.

The calculated force interaction ratios indicated no consequent failures of any main truss members as a result of the failure of east truss lower chord L4-L5, without or with the dynamic impact factor of 1.854. This is true for the investigation of the member capacities as well as the investigation of the connection capacities. Without the dynamic impact, one consequent floor truss member failures were found to occur (**Figure 6-66**) but no consequent failures of any portal/sway frame or upper/lower lateral bracing members would occur. When a dynamic impact factor of 1.854 was included, one consequent floor truss member failure were found to occur (**Figure 6-67**). No portal/sway frame or upper/lower lateral bracing members would fail. The results of calculated force interaction ratios are summarized in **Table AIV-164A** (member capacities) and **Table AIV-164B** (connection capacities) for main truss members and **Tables AIV-165** through **AIV-167** for floor truss members. For those floor truss members that have interaction ratios greater than 1.0 under the combined dead and live load in the intact condition, the sudden member failure did not cause significant changes to the force interaction ratio.

Table AIV-168 and **Table AIV-169** list the support reactions and maximum joint deflections and locations respectively. The induced longitudinal reactions at the “locked” expansion bearings are low (a maximum longitudinal to vertical force ratio of 0.14 at the east bearing of Pier 5 with a dynamic impact factor of 1.854), and are not expected to

change the existing "locked" condition of the steel roller bearing. The maximum joint displacements resulting from the member failure were very low.

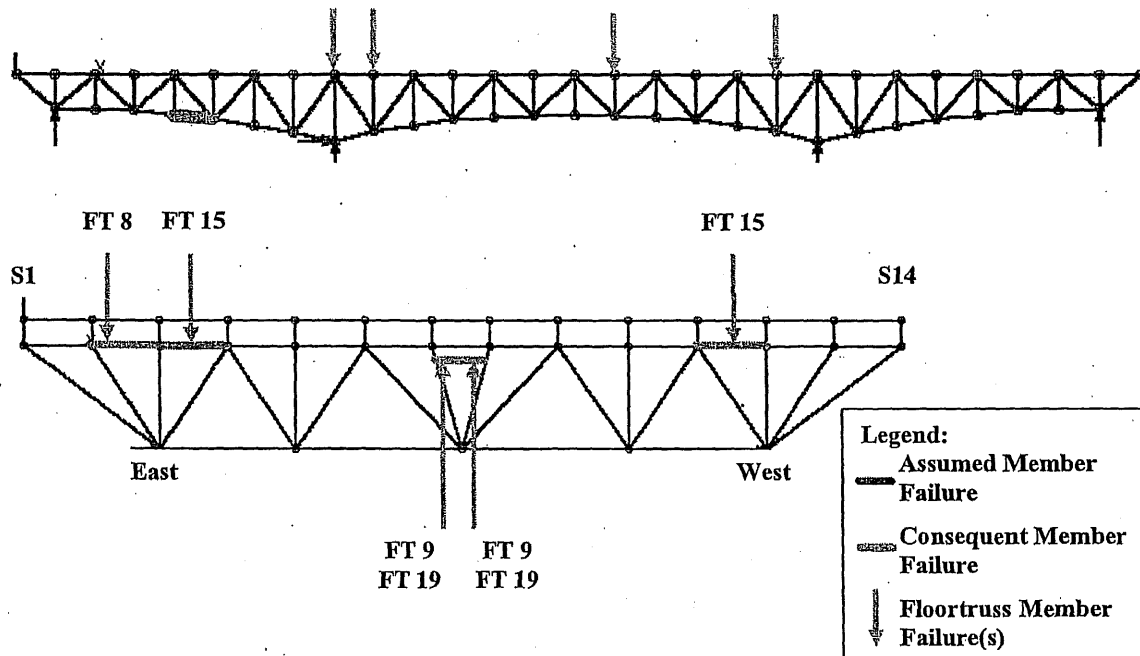


**Figure 6-65: Load Case 4 – Failure of East Truss Lower Chord L4-L5
Additional Member Failures Due to DL+LL on Intact Structure**

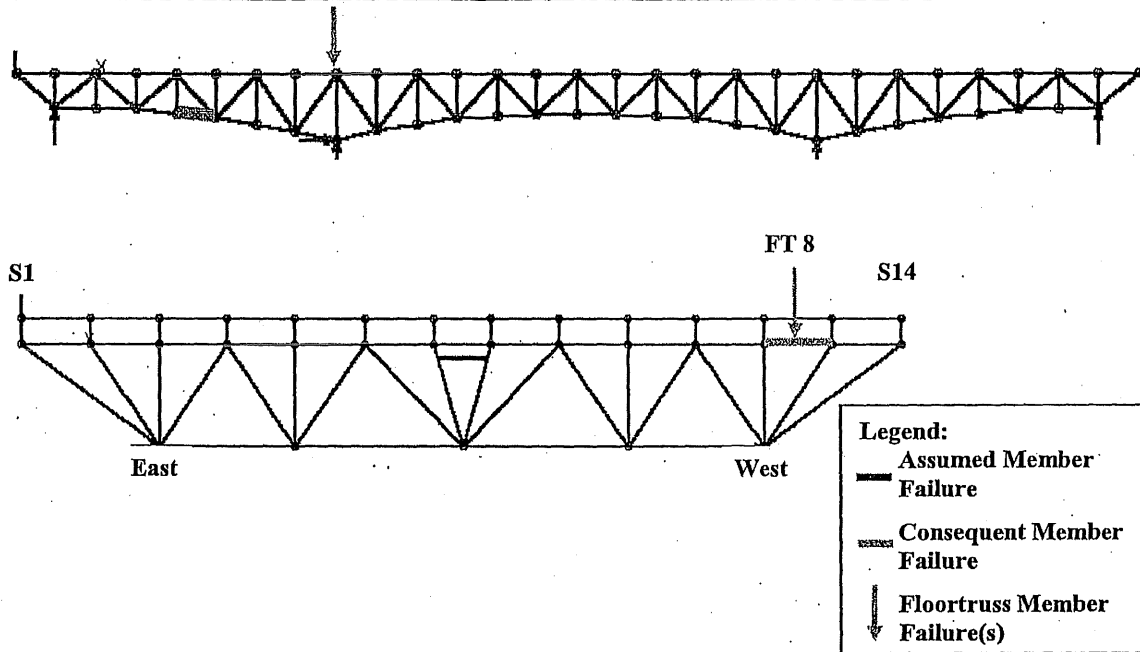


Figure 6-66: Load Case 4 – Failure of East Truss Lower Chord L4-L5
Consequent Member Failures without Dynamic Impact

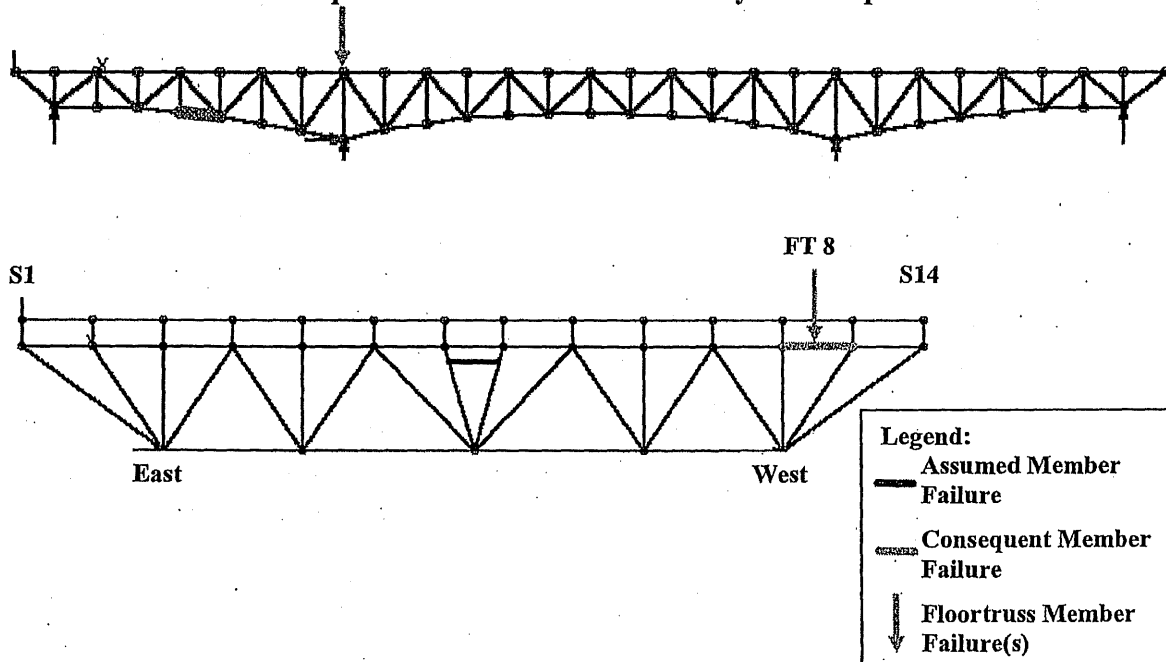


Figure 6-67: Load Case 4 – Failure of East Truss Lower Chord L4-L5
Consequent Member Failures with a Dynamic Impact Factor of 1.854

7. Failure of East Truss Lower Chord L12-L13

Under the combined dead and live load on the intact structure prior to the removal of east truss lower chord L12-L13, thirteen additional floor truss members were found to have interaction ratios greater than 1.0 compared to the dead load only condition, as shown in **Figure 6-68**. All of these members are located adjacent to a floor truss that support the stringers with the asymmetric expansion joint (**Sections 6.7.1 and 6.7.2 and Figure 3-21**), and the failures were attributed primarily to the out-of-plane bending.

Calculated force interaction ratios indicated that three consequent main truss member failures and three consequent floor truss member failures would occur resulting from the failure of east truss upper chord L12-L13, when dynamic impact was not included (**Figure 6-69**). No portal/sway frame members or upper/lower lateral bracing members would fail. When a dynamic impact factor of 1.854 was included, five consequent main truss member failures and five consequent floor truss member failures would occur (**Figure 6-70**). One portal/sway frame members would fail but no upper/lower lateral bracing member would fail. When the connection capacities are considered, three (L10-L11, L9-L10, and L8-L9) and six (L10-L11, L9-L10, L8-L9, L10'-L9', L11'-L10', and L9'-L8') consequent main truss member failures would occur without and with the 1.854 dynamic impact factor respectively. The results of calculated force interaction ratios are summarized in **Table AIV-170A** (member capacities) and **Table AIV-170B** (connection capacities) for main truss members and **Tables AIV-171 through AIV-173** for floor truss members. For some of the floor truss members that have interaction ratios greater than 1.0 under the combined dead and live load in the intact condition, the sudden member failure did cause significant changes to the force interaction ratio.

Table AIV-174 and **Table AIV-175** list the support reactions and maximum joint deflections and locations respectively. The induced longitudinal reactions at the "locked" expansion bearings were relatively low (a maximum longitudinal to vertical force ratio of 0.25 at the east bearing of Pier 6 with a dynamic impact factor of 1.854), and are not

expected to change the existing "locked" condition of the steel roller bearing. The maximum joint displacements resulting from the member failure were not very high (a maximum vertical deflection of 3.4 inches at panel point U12 with a dynamic impact factor of 1.854).

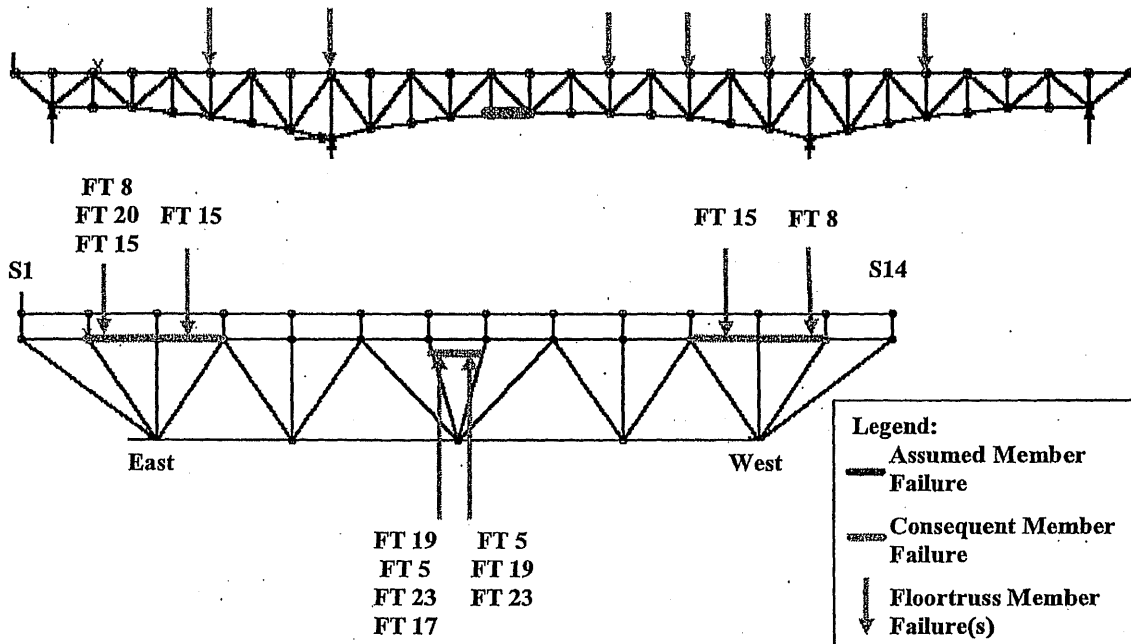


**Figure 6-68: Load Case 4 – Failure of East Truss Lower Chord L12-L13
Additional Member Failures Due to DL+LL on Intact Structure**

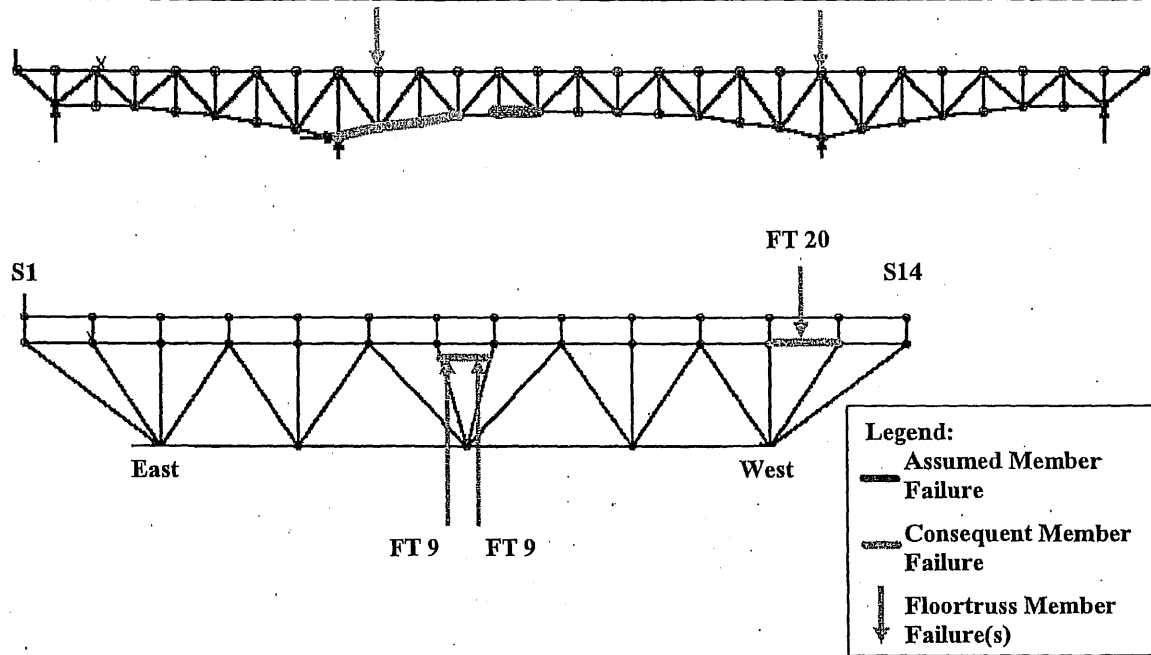


Figure 6-69: Load Case 4 – Failure of East Truss Lower Chord L12-L13
Consequent Member Failures without Dynamic Impact

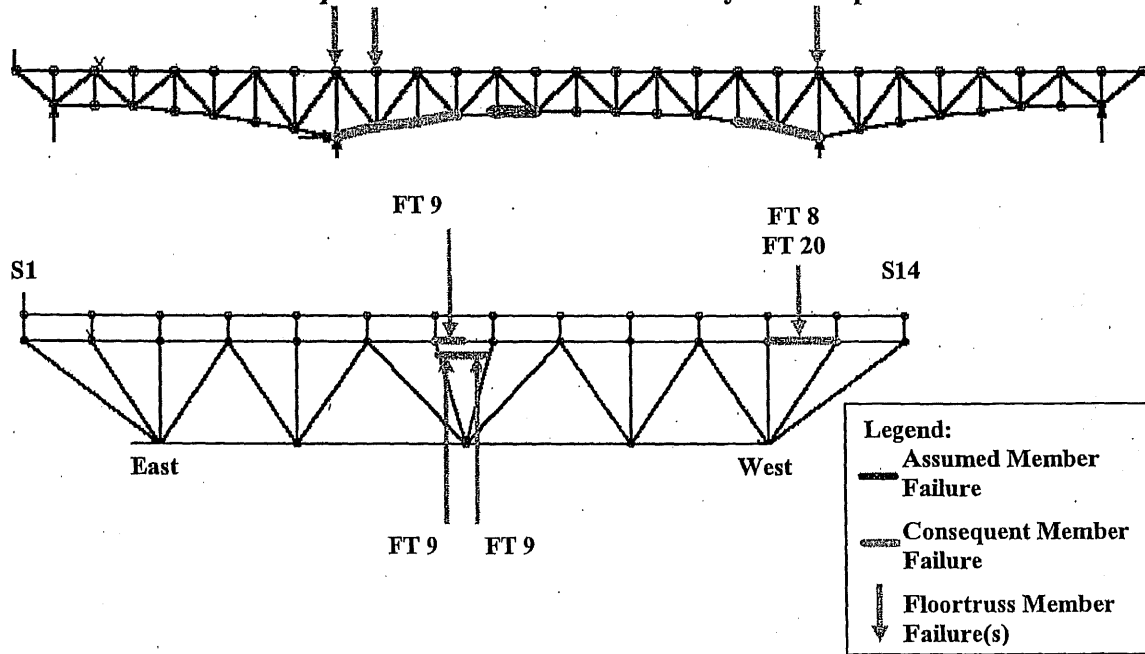


Figure 6-70: Load Case 4 – Failure of East Truss Lower Chord L12-L13
Consequent Member Failures with a Dynamic Impact Factor of 1.854

8. Failure of East Truss Lower Chord L13-L14

Under the combined dead and live load on the intact structure prior to the removal of east truss lower chord L13-L14, fifteen additional floor truss members were found to have interaction ratios greater than 1.0 compared to the dead load only condition, as shown in **Figure 6-71**. All of these members are located adjacent to floor trusses that support the stringers with the asymmetric expansion joint (Sections 6.7.1 and 6.7.2 and **Figure 3-21**), and the failures were attributed primarily to the out-of-plane bending.

Calculated force interaction ratios indicated that six consequent main truss member failures and five consequent floor truss member failures would occur resulting from the failure of east truss upper chord L13-L14, when dynamic impact was not included (**Figure 6-72**). One portal/sway frame member and three upper/lower lateral bracing members would fail. When a dynamic impact factor of 1.854 was included, seven consequent main truss member failures and fifteen consequent floor truss member failures would occur (**Figure 6-73**). Four portal/sway frame members and six upper/lower lateral bracing members would fail. When the connection capacities are considered, six (L10-L11, L11'-L10', L9-L10, L10'-L9', L8-L9, and L9'-L8') and seven (L10-L11, L11'-L10', L9-L10, L10'-L9', L8-L9, L9'-L8', and U14-L14 West) consequent main truss member failures would occur without and with the 1.854 dynamic impact factor respectively. The results of calculated force interaction ratios are summarized in **Table AIV-176A** (member capacities) and **Table AIV-176B** (connection capacities) for main truss members and **Tables AIV-177 through AIV-179** for floor truss members. For those floor truss members that have interaction ratios greater than 1.0 under dead load or combined dead and live load in the intact condition, the sudden member failure caused significant changes to the force interaction ratio in some of them.

Table AIV-180 and **Table AIV-181** list the support reactions and maximum joint deflections and locations respectively. The induced longitudinal reactions at the "locked" expansion bearings were relatively high, a maximum longitudinal to vertical force ratio

of 0.33 at the east bearing of Pier 6 with a dynamic impact factor of 1.854. This level of longitudinal force may not change the existing "locked" condition of the steel roller bearing, depending on the surface condition, since a frictional coefficient of 0.40 is generally accepted for steel. The maximum joint displacements resulting from the member failure were also relatively high, a maximum vertical deflection of 6.7 inches at panel point U14 with a dynamic impact factor of 1.854.

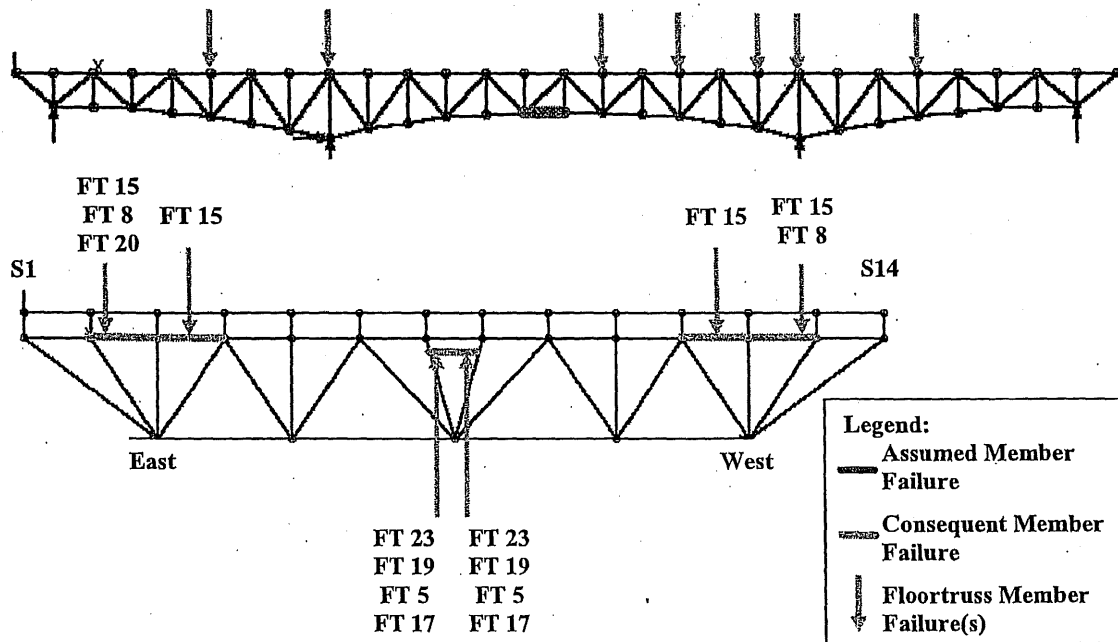


Figure 6-71: Load Case 4 – Failure of East Truss Lower Chord L13-L14
Additional Member Failures Due to DL+LL on Intact Structure

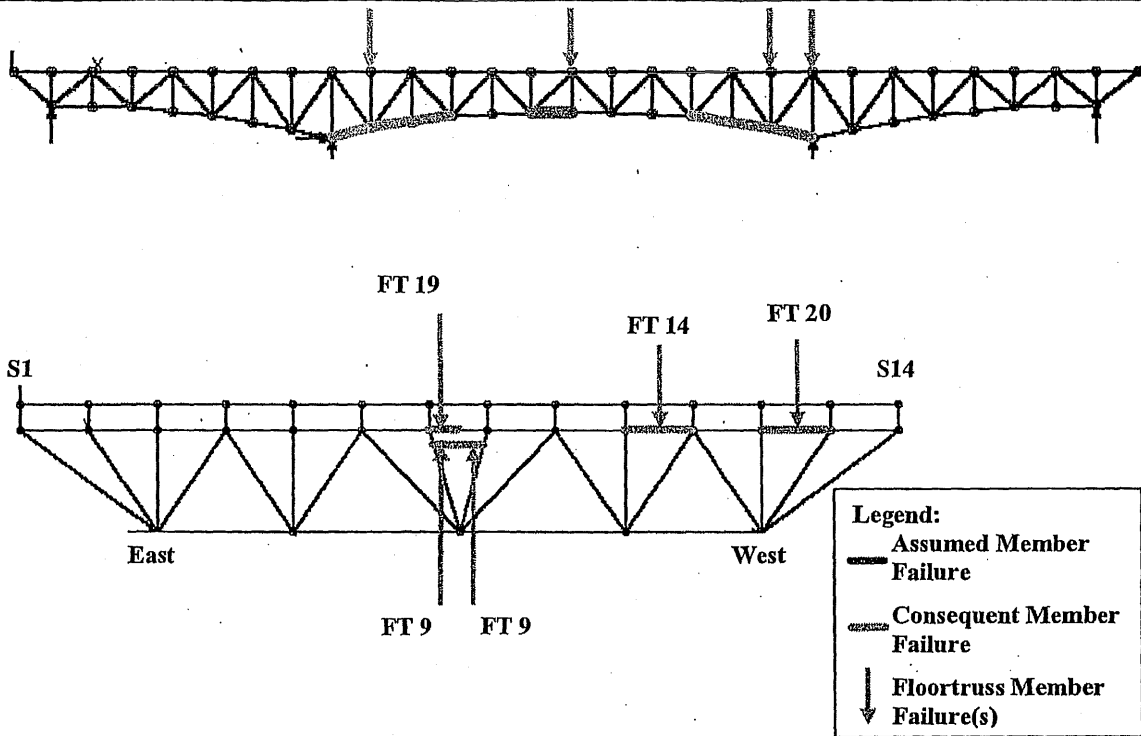


Figure 6-72: Load Case 4 – Failure of East Truss Lower Chord L13-L14
Consequent Member Failures without Dynamic Impact

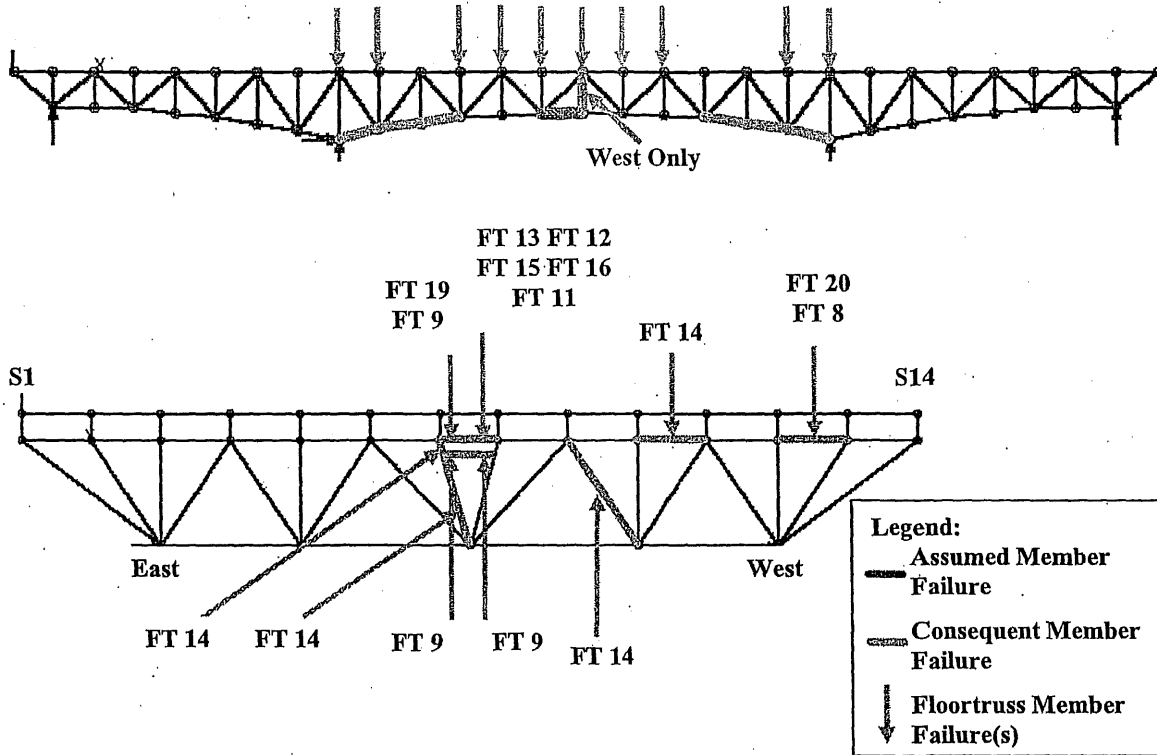


Figure 6-73: Load Case 4 – Failure of East Truss Lower Chord L13-L14
Consequent Member Failures with a Dynamic Impact Factor of 1.854

6.7.9 Stringers

For each of the four load cases, force effects in stringers were investigated for failure of critical truss members L3-U4 and L13-L14. Diagonal L3-U4 was selected since it is subject to the highest live load stress range. Bottom chord L13-L14 was selected since it causes the most severe consequent main-truss member failures.

The maximum force interaction ratio for stringers resulting from the failure of east truss diagonal L3-U4 was calculated to be 0.761 which occurs under Load Case 4 with a dynamic impact factor of 1.854. This ratio is only slightly greater than its counterpart of 0.738 for the same loading in the intact structural condition. This indicates insignificant consequent force effects on the stringers resulting from the main truss member failure. The stringer force results for the failure of

east truss diagonal L3-U4 are summarized in **Appendix IV** in **Table AIV-182** through **Table AIV-185**.

The maximum force interaction ratio resulting from the failure of east truss lower chord L13-L14 was calculated as 1.058 and 1.094, which occurred under Load Case 3, for including a dynamic impact factor of 1.854 and without dynamic impact, respectively. These values are only slightly greater than their counterpart of 1.015 under the same loading in the intact structural condition. This overstress is attributed to the asymmetrical stringer bearing layout about the deck expansion joint and likely also overestimated by assuming the end of the stringers to be rigidly connected to the floor beam in the computer model. The stringer force results for the failure of east truss lower chord L13-L14 are summarized in **Appendix IV** in **Table AIV-186** through **Table AIV-189**.

Since only one stringer member had a force interaction ratio greater than 1.0, it can be concluded that consequent failure of the stringers is not a concern. For this reason, no additional critical truss member failures were investigated for consequent stringer failures. In summary, the stringers are not expected to suffer significant force increase due to the failure of the critical truss members under investigation.

6.7.10 Deck

The force effects in the deck were evaluated for the failure of truss members L3-U4 and L13-L14 for Load Case 2, for the same reasons as those for the evaluation of stringers. Load Case 2 was selected because it is the most likely occurring situation and that truck loads are usually the governing load for deck strength.

For deck evaluation, a combined force ratio was calculated considering the bending moment and axial force at the mid-thickness of the deck for the longitudinal and transverse directions, respectively. The force effects in the deck, calculated from the finite element model, include the combined effect of dead and live load after the cure of deck concrete, and those resulting from the failure of the main truss members under investigation. The capacities of the deck in each

direction consisted of bending and tensile capacities of the reinforced concrete section at the ultimate state.

The deck evaluation indicated a few locations where the force interaction ratio exceeds 1.0 as shown in Table 6-5 and Table 6-6, resulting from the failure of east truss diagonal L3-L4 and lower chord L13-L14, respectively. An examination of the deck moment and force contours indicated that the overstressed areas are localized, as shown in Figure 6-74 to Figure 6-85, and therefore are not expected to impair the capacity of the deck to support the traffic load.

**Table 6-5: Deck Sections with Force Interaction Ratio Greater Than 1.0
Load Case 2 – Failure of East Truss Diagonal L3-U4**

Summary of Locations With Combined Stress Interactions Greater Than 1.0									
Location	Sign	Stress	Total Dead	Live	Dead + Live	W/O Dyn. Im.		W/ Dyn. Im.	
						Failed	Total	Failed	Total
Between FT2 and FT3 under rear wheels	Negative	MXX+NXX	0.13	0.84	0.97	0.22	1.20	0.41	1.39

**Table 6-6: Deck Sections with Force Interaction Ratio Greater Than 1.0
Load Case 2 – Failure of East Truss Lower Chord L13-L14**

Summary of Locations With Combined Stress Interactions Greater Than 1.0									
Location	Sign	Stress	Total Dead	Live	Dead + Live	W/O Dyn. Im.		W/ Dyn. Im.	
						Failed	Total	Failed	Total
FT11 - S14	Positive	MXX+NXX	0.73	0.06	0.79	0.35	1.14	0.66	1.45
FT14 - S12	Positive	MXX+NXX	0.22	0.59	0.81	0.15	0.96	0.27	1.08
FT11 - East Inner Deck Edge	Positive	MXX+NXX	0.40	-0.06	0.34	0.52	0.86	0.97	1.31
Between FT13 and FT14 - Between S1&S2 and	Negative	MXX+NXX	0.33	0.74	1.07	0.11	1.18	0.21	1.28
FT14 - S12	Positive	MYY+NYY	0.23	0.74	0.97	0.25	1.22	0.47	1.44

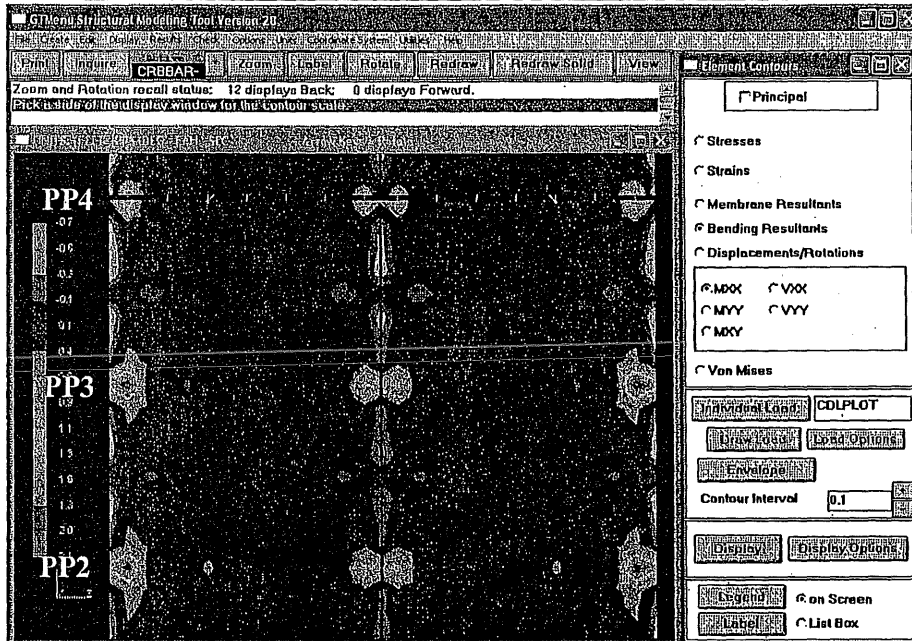


Figure 6-74: Deck Contours - Load Case 2 Failure of East Truss Diagonal L3-U4 Intact Structure - Bending about Transverse Axis Due to Composite Dead Load

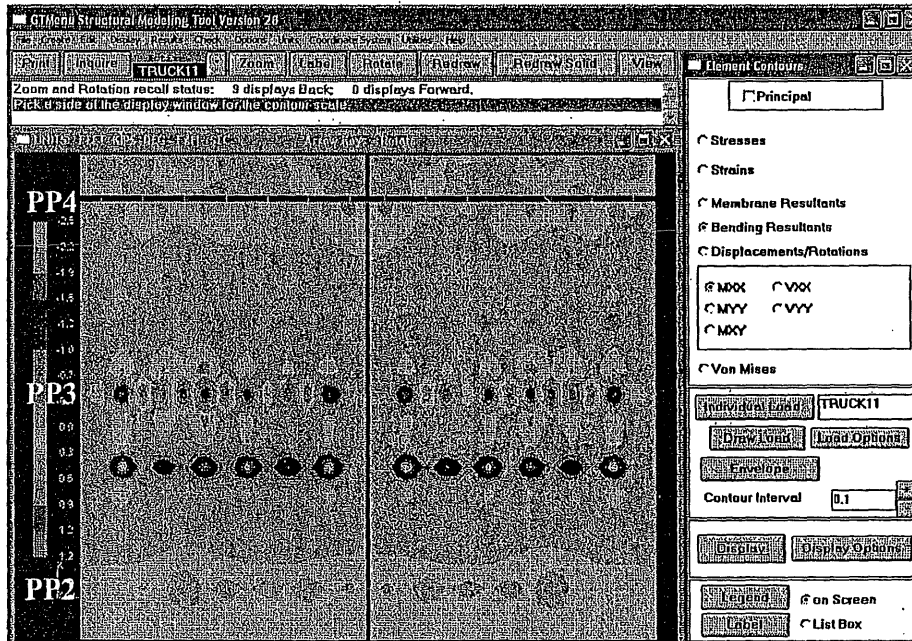


Figure 6-75: Deck Contours - Load Case 2 Failure of East Truss Diagonal L3-U4 Intact Structure - Bending about Transverse Axis Due to Live Load

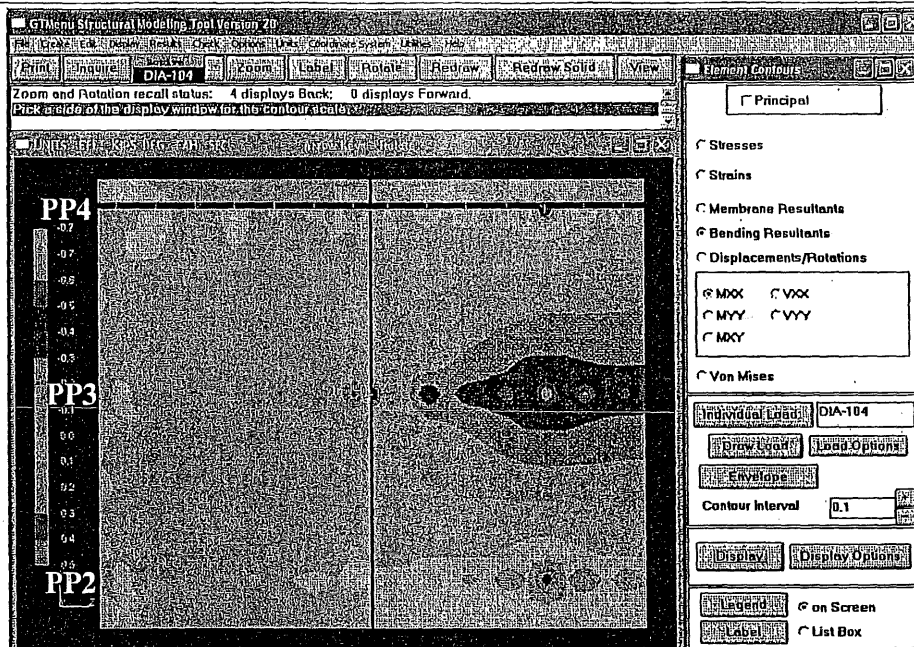


Figure 6-76: Deck Contours - Load Case 2 Failure of East Truss Diagonal L3-U4
Failed Structure - Bending about Transverse Axis Due to Failure Load

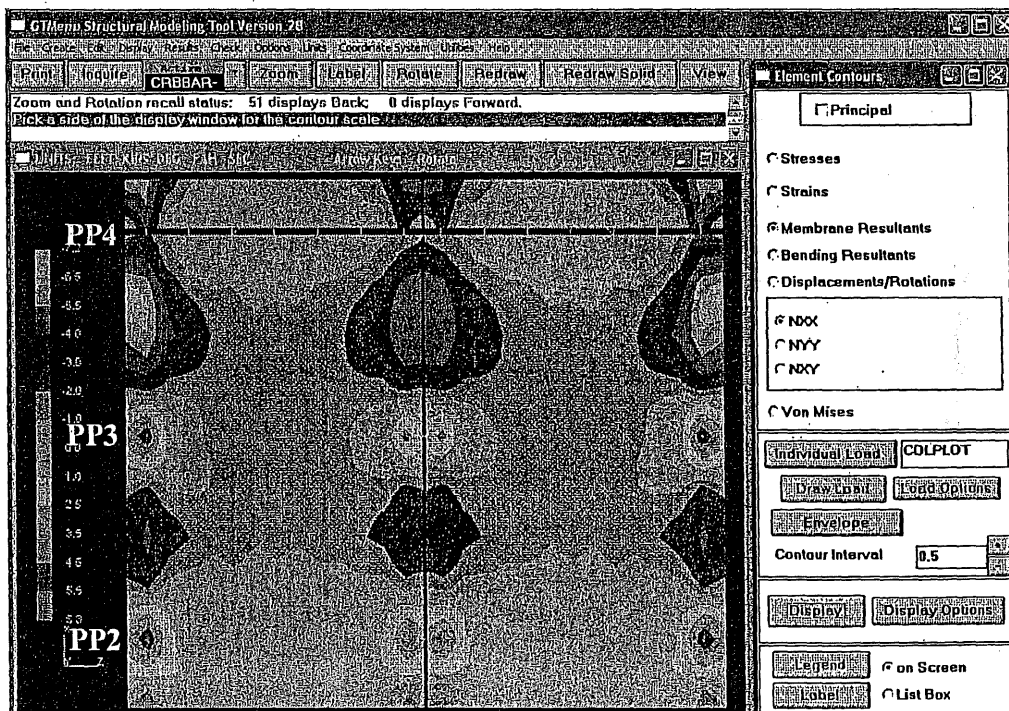


Figure 6-77: Deck Contours - Load Case 2 Failure of East Truss Diagonal L3-U4
Intact Structure - Force along Longitudinal Axis Due to Composite Dead Load

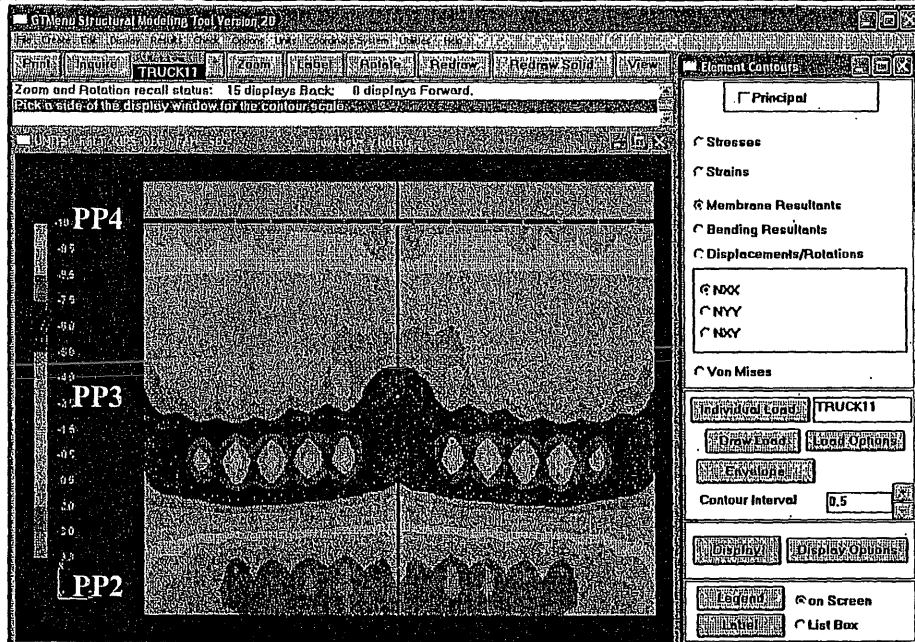


Figure 6-78: Deck Contours - Load Case 2 Failure of East Truss Diagonal L3-U4
Intact Structure - Force along Longitudinal Axis Due to Live Load

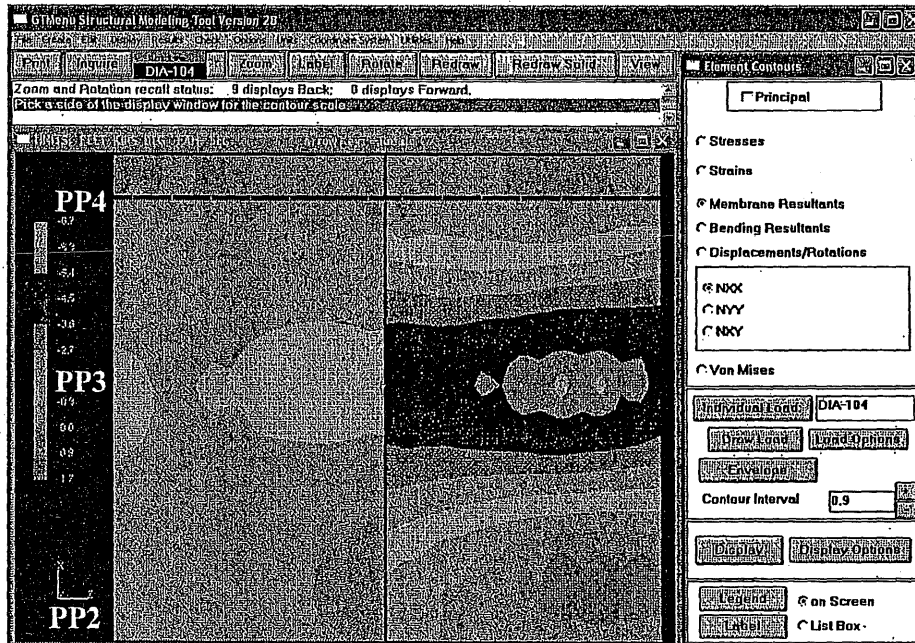


Figure 6-79: Deck Contours - Load Case 2 Failure of East Truss Diagonal L3-U4
Failed Structure - Force along Longitudinal Axis Due to Failure Load

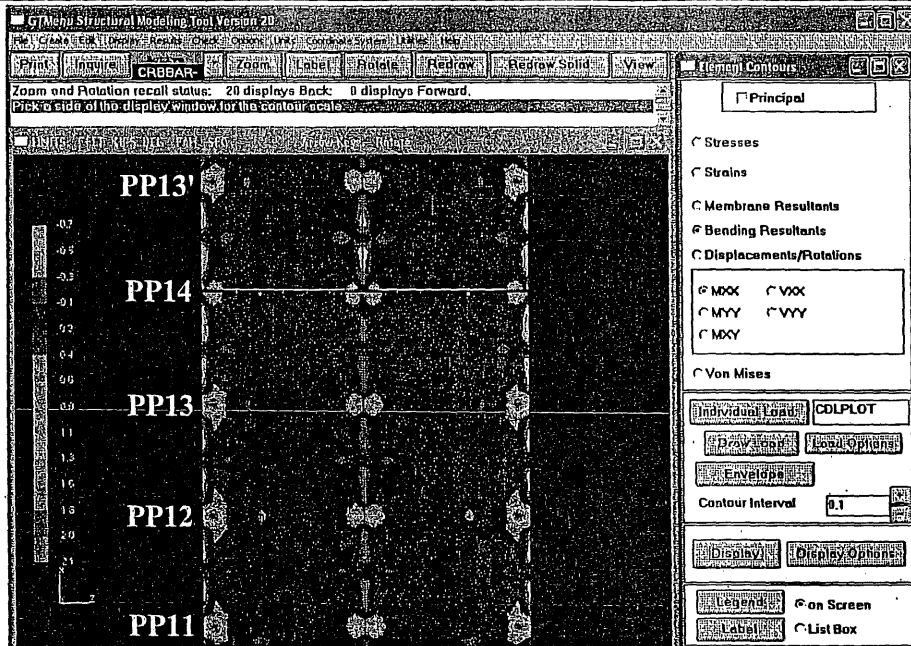


Figure 6-80: Deck Contours - Load Case 2 Failure of East Truss Lower Chord L13-L14 Intact Structure - Bending about Transverse Axis Due to Composite Dead Load

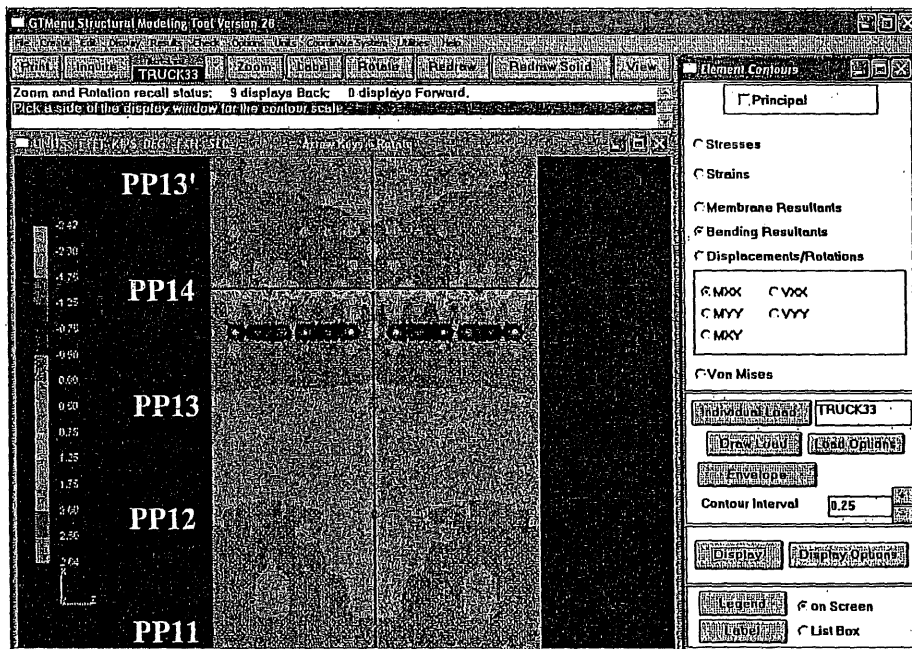


Figure 6-81: Deck Contours - Load Case 2 Failure of East Truss Lower Chord L13-L14 Intact Structure - Bending about Transverse Axis Due to Live Load

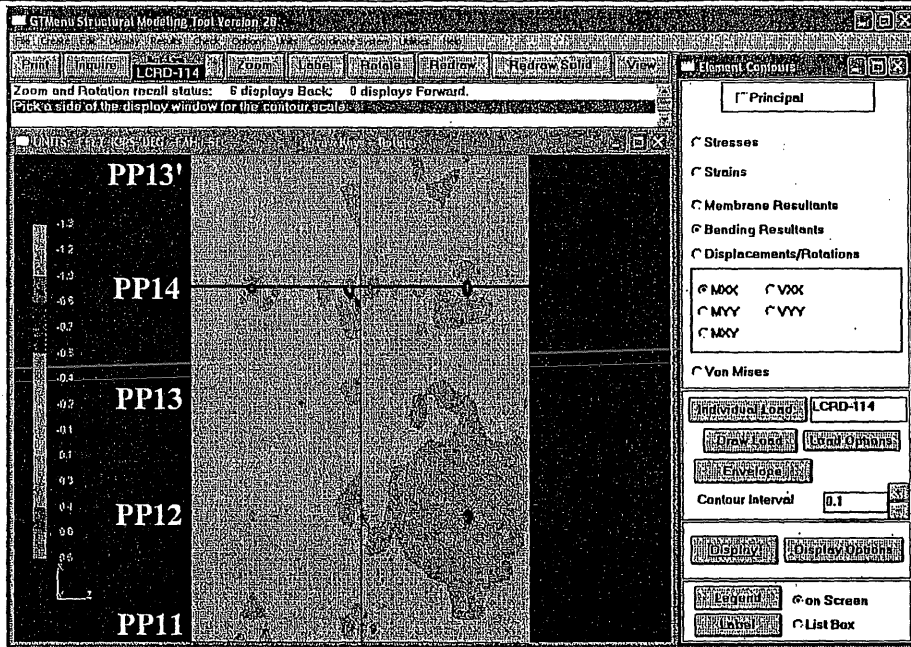


Figure 6-82: Deck Contours - Load Case 2 Failure of East Truss Lower Chord L13-L14
Failed Structure - Bending about Transverse Axis Due to Failure Load

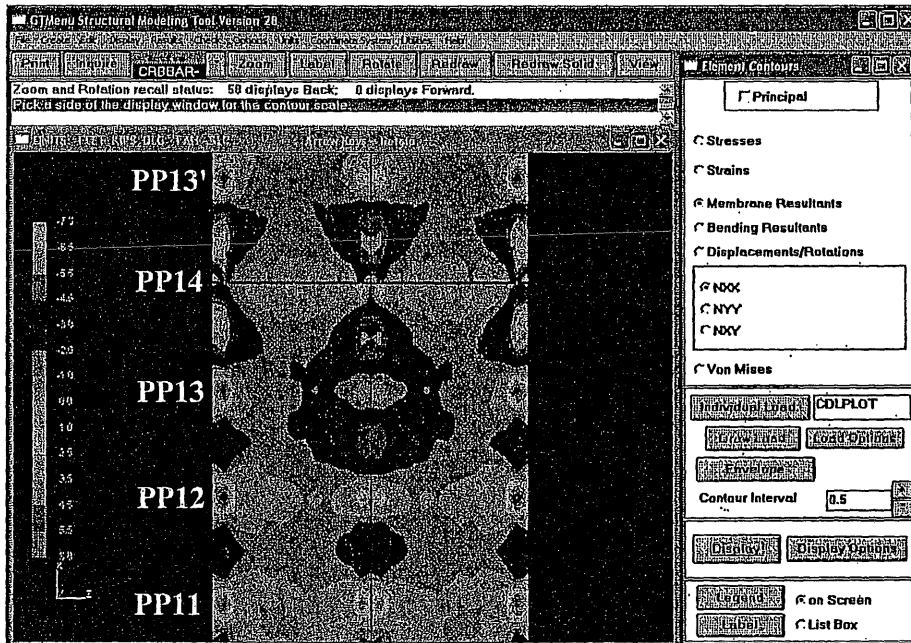


Figure 6-83: Deck Contours - Load Case 2 Failure of East Truss Lower Chord L13-L14
Intact Structure - Force along Longitudinal Axis Due to Composite Dead Load

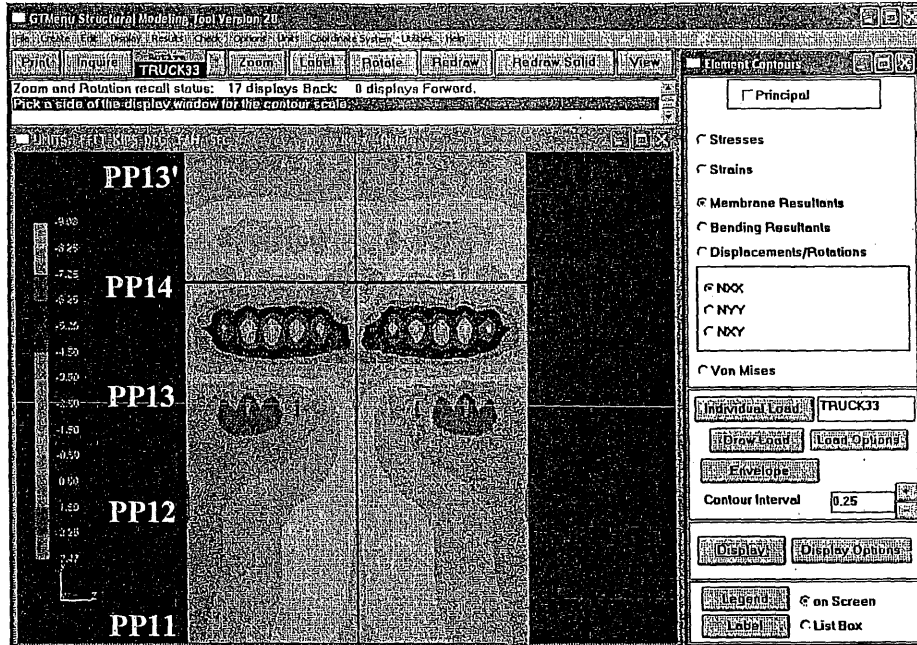


Figure 6-84: Deck Contours - Load Case 2 Failure of East Truss Lower Chord L13-L14
Intact Structure - Force along Longitudinal Axis Due to Live Load

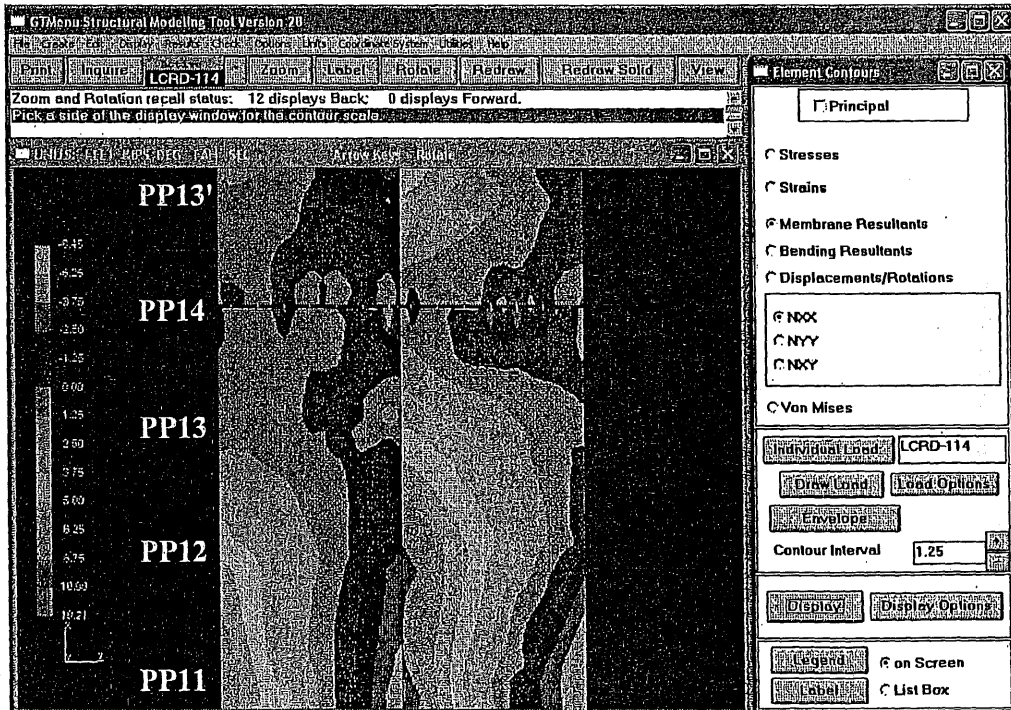


Figure 6-85: Deck Contours - Load Case 2 Failure of East Truss Lower Chord L13-L14
Failed Structure - Force along Longitudinal Axis Due to Failure Load

6.7.11 Summary of Fracture Critical Members

Table 6-7 and Table 6-8 present results of the redundancy analysis for all eight members under each of the four live load cases, based on member capacities and connection capacities, respectively. The tables summarize the number of additional main truss members that would fail as a result of the failure of the critical member both without and with the application of the dynamic impact factor. As shown in the tables, five of the eight critical members are fracture critical, i.e., their failure would result in the failure of at least one other main truss member and thus cause instability of the structural system. The five fracture critical main truss members are: Lower Chord L1-L2, Upper Chord U0-U1, Upper Chord U4-U5, Lower Chord L12-L13, and Lower Chord L13-L14. These five members actually represent twenty main truss members due to the nearly double symmetry of the trusses. Accounting for the connection capacities yields more total consequent main truss member failures, but Upper Chord U4-U5 is the only additional fracture critical member that would not be considered as such if the connection capacities were neglected.

Table 6-7. Consequent Main Truss Member Failures due to a Critical Member Failure (Based on Member Capacities)

Number of Consequent Member Failures - Member Capacities					
Critical Member	Dynamic Impact	Load Case	Load Case	Load Case	Load Case
		1	2	3	4
L3-U4 (Diagonal)	w/o Dynamic Impact	0	0	0	0
	w/ Dynamic Impact	0	0	0	0
L1-L2 (Lower Chord)	w/o Dynamic Impact	0	0	0	0
	w/ Dynamic Impact	0	0	1	0
U0-U1 (Upper Chord)	w/o Dynamic Impact	2	2	2	2
	w/ Dynamic Impact	3	4	6	4
U4-U5 (Upper Chord)	w/o Dynamic Impact	0	0	0	0
	w/ Dynamic Impact	0	0	0	0
U4'-U3' (Upper Chord)	w/o Dynamic Impact	0	0	0	0
	w/ Dynamic Impact	0	0	0	0
L4-L5 (Lower Chord)	w/o Dynamic Impact	0	0	0	0
	w/ Dynamic Impact	0	0	0	0
L12-L13 (Lower Chord)	w/o Dynamic Impact	0	2	4	3
	w/ Dynamic Impact	2	3	7	5
L13-L14 (Lower Chord)	w/o Dynamic Impact	0	4	7	6
	w/ Dynamic Impact	6	7	10	7

**Table 6-8. Consequent Main Truss Member Failures due to a Critical Member Failure
(Based on Connection Capacities)**

Number of Consequent Member Failures - Connection Capacities					
Critical Member	Dynamic Impact	Load Case	Load Case	Load Case	Load Case
		1	2	3	4
L3-U4 (Diagonal)	w/o Dynamic Impact	0	0	0	0
	w/ Dynamic Impact	0	0	0	0
L1-L2 (Lower Chord)	w/o Dynamic Impact	0	0	0	0
	w/ Dynamic Impact	0	0	2	1
U0-U1 (Upper Chord)	w/o Dynamic Impact	2	2	3	2
	w/ Dynamic Impact	4	5	6	5
U4-U5 (Upper Chord)	w/o Dynamic Impact	0	0	0	0
	w/ Dynamic Impact	0	0	1	0
U4'-U3' (Upper Chord)	w/o Dynamic Impact	0	0	0	0
	w/ Dynamic Impact	0	0	0	0
L4-L5 (Lower Chord)	w/o Dynamic Impact	0	0	0	0
	w/ Dynamic Impact	0	0	0	0
L12-L13 (Lower Chord)	w/o Dynamic Impact	1	2	5	3
	w/ Dynamic Impact	3	5	9	6
L13-L14 (Lower Chord)	w/o Dynamic Impact	0	4	9	6
	w/ Dynamic Impact	6	7	11	7

6.8 Effects of Truss Bearing Properties

In the redundancy analysis as discussed previously, the main truss bearings were assumed to behave "as-designed" under dead load and "locked" under live load, based on field observations and a calibration of the computer model with field testing data described in Section 3. The failure of each of the eight critical truss members under investigation would induce longitudinal forces at the "locked" truss expansion bearings; and these forces would tend to "unlock" the frozen expansion bearings for longitudinal movement. The possibility of this situation was evaluated to determine if it was likely to occur, and if it did, what the consequence would be. The longitudinal to vertical force ratio was used as the key parameter for comparison with the static frictional coefficient of the bearing.

6.8.1 Possibility of Movement of Locked Expansion Roller Bearings

As summarized in Section 6.7.4, the maximum longitudinal to vertical force ratio was found to be 0.34 from the redundancy analysis, resulting from the sudden failure of east truss lower chord L13-L14 with a dynamic impact of 1.854.

For a steel-to-steel contact, the frictional coefficient may vary in a wide range, heavily depending on the surface condition. For clean mill scale surface, according to "*Guide to Design Criteria for Bolted and Riveted joints*", by G.L. Kulak, J.W. Fisher and J.H.A. Struik, slip coefficient is listed as approximately 0.33 for A36 steel and 0.23 for A588 steel. For the roller bearings of Bridge 9340, as shown in **Figure 6-86**, the rollers were made of alloy steel forging ASTM A237-63T, Class D; the lower bearing plates were of Q-T high strength alloy steel MHD 3318; the upper bearing castings were of alloy steel casting MHD 3323; the pinion was of alloy steel forging MHD 3315, Type II; and the upper and lower racks were of structural steel MHD 3306 (ASTM A36). The expansion bearings at Piers 5 and 8 are similar except that there are three rollers rather than four. AASHTO *Standard Specifications for Highway Bridges* does not have specific values of coefficient of friction for steel. For the design of bronze or copper alloy sliding surfaces, the design coefficient of friction was specified as 0.1 for self-lubricating bronze component and 0.4 for other types.

Field bearing movement measurements (**Table 2-2**) indicated that the roller bearings moved due to a temperature fall of approximately 20°F, although the amount of movements were much smaller than the corresponding free thermal movement. The 3-D computer model consisting of the superstructure and the piers, with all expansion bearings fully locked, was used to evaluate the longitudinal to vertical force ratio for a temperature fall of 20°F. The results of the thermal analysis, in bearing reactions, are summarized in **Table 6-9**. As shown in the table, the bearings tend to move when the longitudinal to vertical force ratio is around 0.10.

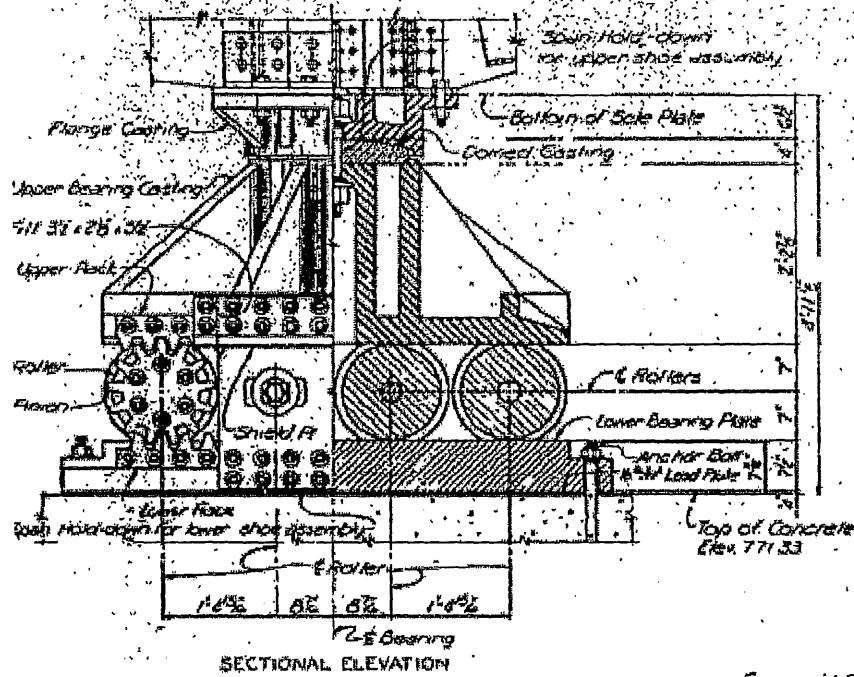


Figure 6-86: Pier 6 Expansion Bearing Assembly – Sectional Elevation

Table 6-9: Truss Bearing Reactions from 3-D Computer Model for $\Delta T = -20^{\circ}F$, All Expansion Bearings Fully Locked

Bearing Location	Type	Longitudinal Reaction R_l	Vertical Reaction R_v	Longitudinal to Vertical Force Ratio (R_l / R_v)
Pier 5 East	Expansion	155 kips	1,256 kips	0.12
Pier 6 East	Expansion	184 kips	4,230 kips	0.04
Pier 7 East	Fixed	272 kips	4,138 kips	0.07
Pier 8 East	Expansion	67 kips	1,666 kips	0.04

6.8.2 Consequence of Expansion Bearing Movement from Member Failure

If the roller bearings do move in the event of a truss member failure, one of the primary concerns is the deflections resulting from the event. The longitudinal bearing movement at each expansion pier needs to be checked since excessive movement may cause the rollers to move off the lower bearing plate.

A review of the original bearing plans indicates that the hold-down plate of the roller expansion bearings can accommodate a longitudinal movement of around 2 to 2½ inches from the neutral position through a slotted hole. Bearing movement in excess of that amount may cause damage to the hold-down plate and further movement may cause the rollers to move off their lower bearing plate.

Table 6-10 summarizes the predicted movements of truss expansion bearings resulting from the failure of east truss lower chord L12-L13, which is the worst case of all the eight critical truss members under investigation. As shown in the table, Pier 6 is subject to the highest longitudinal bearing movement, which is predicted to be 2.0 inches without dynamic impact and 3.7 inches with a dynamic impact factor of 1.854. As seen in **Table 6-10**, a sudden failure of east truss lower chord L12-L13 may likely cause damages to the bearing, depending on the position of the rollers prior to the occurrence of the member failure.

Table 6-10: Summary of Longitudinal Deflections at Bearings With L13-L14 Removed, Load Case 2, and Truss Bearings As-Designed

Longitudinal Bearing Deflections			
Failed Member	Location	w/o Dynamic Impact	w/ Dynamic Impact
		(inch)	(inch)
LC L13-L14	Pier 5 East	-1.3689	-2.5379
	Pier 6 East	-1.9869	-3.6837
	Pier 7 East	0.0000	0.0000
	Pier 8 East	-0.3499	-0.6487
	Pier 5 West	-1.3456	-2.4947
	Pier 6 West	-1.4701	-2.7256
	Pier 7 West	0.0000	0.0000
	Pier 8 West	-0.3629	-0.6728

More results of the redundancy analysis for this condition are summarized as follows:

1. Failure of East Truss Lower Chord L13-L14 for Load Case 2 with Truss Bearings and Stringer Bearings Assumed to Unlock After Critical Member Failure

Since the bearings are assumed to be locked until the critical member fails, the effects of dead and live load on the intact structure are the same as the Load Case 2 results, as shown in **Figure 6-34**.

Calculated force interaction ratios indicated that one consequent main truss member and twelve consequent floor truss member failures would occur resulting from the failure of east truss upper chord L13-L14, when dynamic impact was not included. Three portal/sway frame members and three upper/lower lateral bracing members would fail. When a dynamic impact factor of 1.854 was included, eight consequent main truss member failures and thirty-three consequent floor truss member failures would occur. Four portal/sway frame members and ten upper/lower lateral bracing members would

fail. When the connection capacities are considered, two (L11'-L10' and L10'-L9') and eight (L11'-L10', L10'-L9', L10-L11, L9-L10, U14-L14 West, L14-L13' West, L9'-L8', and L13-L14 West) consequent main truss member failures would occur without and with the 1.854 dynamic impact factor respectively. The results of calculated force interaction ratios are summarized in **Table AIV-190A** (member capacities) and **Table AIV-190B** (connection capacities) for main truss members and **Tables AIV-191** through **AIV-193** for floor truss members. For those floor truss members that have interaction ratios greater than 1.0 under dead load or combined dead and live load in the intact condition, the sudden member failure caused significant changes to the force interaction ratio in some of them.

Table AIV-194 and **Table AIV-195** list the support reactions and maximum joint deflections and locations respectively. The resulted longitudinal reactions at the formerly "locked" expansion bearings were very low, as expected assuming they would release after the failure of east truss lower chord L13-L14. This level of longitudinal force may not change the existing "locked" condition of the steel roller bearing, depending on the surface condition, since a frictional coefficient of 0.40 is generally accepted for steel. The maximum joint displacements resulting from the member failure were also found relatively high, a maximum vertical deflection of 9.6 inches at panel point U14 with a dynamic impact factor of 1.854.

The "locked" condition yields three more consequent main truss member failures than the "unlocked" condition with no dynamic impact and considering member capacities only. When connection capacities are considered, the "locked" condition yields two more consequent main truss member failures than the "unlocked" condition with no dynamic impact. The "unlocked" condition yields one more consequent main truss member failure than the "locked" condition with a dynamic impact factor of 1.854 and considering both member and connection capacities. For both without and with the 1.854 dynamic impact factor, significantly more floor truss members fail for the "unlocked" condition. Regardless of the bearing assumption that is made, east truss lower chord L13-L14 would

be considered fracture critical because its failure yields consequent main truss member failures.

The likelihood of the bearings “unlocking” after a critical member failure are discussed for each critical member and each load case in Section 6.7.5 through 6.7.8. For most of the critical members it was determined that it unlikely that the induced longitudinal forces would be sufficient to overcome the frictional resistance at the steel roller bearings. Although only east truss lower chord L13-L14 was analyzed since its failure produced the most consequent main truss member failures, similar results would be expected for the other critical members.

SECTION 7

7. RETROFIT SCHEMES FOR IMPROVING STRUCTURAL SAFETY AND PERFORMANCE

7.1 Contingency Repairs to Eight Critical Truss Members

URS investigated several alternatives for strengthening eight critical truss members for one half of each truss per the request of Mn/DOT. As discussed in Section 6.1, the eight members are identified as: L3-U4, L1-L2, U0-U1, U4-U5, U3-U4, L4-L5, L12-L13, and L13-L14. Due to the nearly double symmetry of the structure, these eight members actually represent thirty-two truss members on the bridge.

The initial approach of the contingency repair was to develop measures for adding some redundant or catch-up system, rather than making structural alterations. The general objective of the repair was to develop a concept to replace the strength of a member in an event that the member should completely fail due to a fracture initiated from a fatigue susceptible detail. The added benefit for this repair is that it would also reduce the live load stresses and thus retard or minimize the development of fatigue cracks in the repaired members.

7.1.1 Carbon Fiber Reinforced Polymer (CFRP) Plating

The use of Carbon Fiber Reinforced Polymer (CFRP) plating, or sheeting, involves bonding CFRP sheets, or strips, to the surfaces of the existing truss member to increase the strength of the member. In the case of a member failure, the CFRP plating, bonded beyond the predicted fracture section, would be expected to take over the member forces. This scheme was determined inappropriate for this application due to concerns about the CFRP-to-steel bond. The epoxy bonding may possibly be unsustainable under the loads and deformations caused by a sudden failure of the truss member. The truss member failure due to a section fracture would induce large shear forces and relative displacements on both sides of the failed section, in addition to axial force. These forces and displacements are extremely difficult for the CFRP plating to resist

since the CFRP is vulnerable in compression and shear (particularly in the out-of-plane direction) although high in unidirectional tensile strength.

7.1.2 Pre-Tensioned Bars

Another repair concept considered was to install some pre-tensioned steel or CFRP bars, or strands, around the truss members of concern. The pre-stressing bars would be anchored near both ends, or on the gusset joints, of the truss member and then pre-tensioned to a certain level. This concept was also determined to be an inappropriate solution for several reasons. First of all, the available space along the width of the truss members and the space required at the end to attach the pre-stressing head anchorage limit the number of steel or CFRP bars that can be used. Based on the required member loads and the dimensions of steel or CFRP bars, the number of bars required was determined to be impractical for actual placement. Additionally, this concept does not result in a satisfactory performance for members that are subjected to tension-compression reversal under the live load, nor does it provide proper strengthening for moment and shear capacity in case of a member failure. Finally, the application of pre-tensioning force into the truss members would also change the permanent load distribution in the 3-span continuous deck truss system, which may be detrimental to the structure.

7.1.3 High Performance Steel Plating

The steel plating concept involves installing steel plates on the exterior surfaces of both webs of the truss member. The retrofit plates would be bolted to the existing webs, or the gusset plates, with the anchor bolts properly located beyond the fatigue susceptible details of concern. The retrofit steel plates, and the bolted connections at both ends, are designed such that they provide equivalent capacity of the existing truss member. In the case of a member fracture initiated from a concerned fatigue detail, therefore, the retrofit plates would be able to take over all the member forces and replace the lost capacity. This repair concept does not affect the load distribution of the structural system except some minimal impact from the increased member stiffness. The steel plating repair concept was considered the most suitable solution and a preliminary design was performed along with conceptual plans for the eight selected critical truss members.

Based on Mn/DOT recommendations, high performance steel with a yield strength of 100 ksi was used for the retrofit plates. To minimize the plate weight for field erection and installation, two steel plates were used on each side of the truss member with each plate width equal to approximately one half of the member web depth. The one exception is diagonal L3-U4, which was designed with just one plate on each side with a width equal to approximately the entire member web depth, due to its relatively small size.

For the bolted connections to the existing truss member web, 1" diameter high strength ASTM A490 bolts were used in the design with AASHTO Class B contact surface for slip-critical connections. In addition to the primary connection bolts, stitch bolts would also be used along the length of the member with a minimum number of bolts to satisfy sealing and stitch bolt requirements. Based on discussions with Mn/DOT, the bolts were spaced at a maximum distance of 3'-0". The layout of bolt lines for each connection was set to correspond to the existing truss member connections in order to maintain the same net section in the existing web plates. There were eight lines of bolts on all members, except at diagonal L3-U4 which had only five lines of bolts.

The retrofit design loads were determined from the 3-D computer model of the existing structure using the highest member forces resulting from the load cases for redundancy analysis, as described in Section 6.5. Generally, Case 3 governed the design, which included eight lanes of standstill HS-20 truck and lane load without multiple presence factor or vehicle impact. The design of retrofit plates and connections was based on the interaction equations considering axial load and bending moments in two principal directions, following the provisions of the AASHTO *Guide Specifications for Strength Design of Truss Bridges (Load Factor Design)* (1985 with 1986 interims). The design loads of connection bolts were based on an elastic analysis of the bolt groups considering the combined effects of truss member axial force plus bending moments and shear forces in two principal directions. Fatigue of the bolted connections was also checked per current AASHTO fatigue provisions.

Conceptual plans have been prepared for the thirty-two members represented by the eight critical members and are included in Appendix V. Although the 3-span deck truss is generally a double symmetric structure, the difference in horizontal curvature, bridge width flaring, as well as the super-elevation, caused different member lengths and sizes between corresponding truss members in the original design. Additionally, the dead load effects at the two ends of the bridge are significantly different, which caused different plate sizes for corresponding members. This is primarily due to the different dead loads from the approach spans of different span lengths; the adjacent north and south approach span lengths are approximately 168 feet and 109 feet, respectively. Therefore, there exist geometric and/or loading variations for corresponding members between the east and west trusses, and/or between the north and south ends of the bridge.

Most of the eight critical truss members and their corresponding members have similar lengths, except for U0-U1 and U1'-U0'. Member U0-U1 at the south end is 40'-4" and 35'-8" long for the east and west truss, respectively. Member U1'-U0' at the north end, however, is 38'-0" long for both the east and west truss. For the development of final contract plans, it is important to field verify key dimensions for all members prior to manufacturing the retrofit plates.

The placement of retrofit plates and connection bolts has been made in accordance with the shop drawings. For members U3'-U4' and L13-L14, however, no shop drawings were available and the sizes and details for these members were estimated from adjacent members and from the contract plan documents. This information should also be verified prior to developing any final construction plans. All members except for the diagonal L3-U4 had adequate space between the diaphragm and the gusset to accomplish the required connection bolting. The connection at the ends of diagonal L3-U4 is accomplished by widening the retrofit plate and connecting it directly to the existing gusset plate on both sides of the existing connection.

There are some important issues involved with the construction of the steel plating retrofit. First of all, the bolt holes on the existing web plates shall be drilled with caution and then reamed to produce a smooth edge surface for better fatigue strength. The placement of the bolt lines along the member length shall be in alignment with the existing rivet/bolt lines to maintain the same

net section for the existing webs. Secondly, the two retrofit plates on each web of the truss member shall be installed one at a time. The drilling of bolt holes for the second plate shall not start until the complete installation of the first plate. This will eliminate the intermediate stage of having all open bolt holes exposed on any existing web at any time. Thirdly, all faying surfaces, existing or new, at the end connection areas shall be blast-cleaned as necessary and coated with a Class B coating to achieve the 0.50 slip coefficient. All high-strength bolts shall be installed with the required torque to achieve a slip critical connection. Finally, organic zinc rich paint shall be applied to the intermediate areas between the end connections and all interfaces between plates shall be properly caulked to prevent pack rust.

7.2 Deck Replacement for Reducing Stresses and Improving Redundancy

Another retrofit strategy is to alter the structural system by replacing the existing deck with a new deck that is continuous throughout the main truss spans and composite with the truss system. This structural alteration aims to reduce live load stresses in most members and improve structural redundancy. Combined with the steel plating member retrofit for the selected critical members as discussed in the previous section, the structural performance and redundancy of the redecked bridge is further improved.

The structural effects of this retrofit concept has been quantified using the 3-D computer model and is discussed in this section. Based on discussions with Mn/DOT a 9" total structural thickness was used in the analysis for the new deck. The new deck would be longitudinally and transversely continuous for the entire three truss spans without any joints. The existing deck, which has several transverse joints and a longitudinal joint, has a total thickness of 8.25", with 6" being structural and 2.25" being comprised of integral wearing surface and overlay wearing surface.

7.2.1 Alterations to the Computer Models

The utilization of a new continuous deck required some changes to the computer model. First of all, new finite elements were added to fill in the gaps in the deck at the longitudinal and

transverse joint locations of the existing deck. The thickness of the deck elements was also adjusted for the new deck. Additionally, member forces and moments due to the dead loads on the non-composite structure were reevaluated. For the existing structure, the 6" structural deck was poured monolithically with a 0.5" integral wearing surface. This portion of the deck weight (6.5" total thickness) was carried by the non-composite steel structure. In the computer model, it was assumed that the total overlays (2.25" thick) and all the barriers were carried by the composite deck-truss system with a deck element structural thickness of 6". With a new 9" thick monolithic deck in study, the entire weight of the uncured deck concrete would be carried by the non-composite steel system, and all the barriers would be carried by the composite deck-truss system with a deck element structural thickness of 9". It was assumed that the total weight of all the barriers would remain the same as those on the existing structure. The loads from the approach spans at both ends of the deck truss spans were also assumed to be unchanged. These loads were applied to the trusses prior to the installation of the deck and thus their effects are not affected by the deck replacement.

It is important to note that the condition of the truss expansion bearings was assumed to be "locked" for live load based on findings from a calibration study between the computer model and the University of Minnesota field test data. For dead load, however, the initial computer model used "as-designed" bearing condition since the original dead load was applied during construction when the bearings should be expected to behave as intended. Since the actual bearing condition is uncertain and erratic in nature, as discussed previously in Section 2, the dead load analysis for redecking considered both the "as-designed" and "locked" conditions for comparison purposes. With locked expansion bearings, an arch effect is induced, which tends to cause a variation in truss member force distribution compared with the intended 3-span continuous system.

7.2.2 Effect of Deck Replacement on Truss Member Axial Forces under Dead Load

Under the total dead load, the truss member axial force is summarized in **Table AV-1** in **Appendix V** for all the east truss members. It should be noted that all the lower chord members

in the north span from L8' to L1' are in compression under total dead load, most likely due to the heavier approach span load at the north end of the bridge.

Since the replacement deck (9" monolithic and continuous) differs from the existing deck (6" plus 2.25" overlay with joints) in deck thickness, dead load application, and continuity, four different cases were analyzed to isolate their structural effects, as shown in **Table AV-1**. Both the as-designed and locked bearing conditions were also considered in the analyses to quantify the impact of bearing condition.

The four cases analyzed are:

- Case 1: 6" existing deck with 2.25" overlay, as-designed bearing condition (baseline condition)
- Case 2: 6" continuous deck with 2.25" overlay, as-designed bearing condition (a hypothetical condition for the effect of deck continuity)
- Case 3: 9" monolithic and continuous deck, as-designed bearing condition (a redecked condition)
- Case 4: 9" monolithic and continuous deck, locked bearing condition for the dead load of deck concrete and barriers (another redecked condition)

There is a characteristic difference among the above cases in terms of the application of total dead load, which consists of the non-composite dead load (NCDL) and the composite dead load (CDL). The NCDL is the weight of wet concrete carried by the steel truss system alone; and the CDL is the dead load applied after the deck concrete cures and the deck-truss system becomes a composite structure. The NCDL in Case 1 and Case 2, consisting of a 6" structural deck and 0.5" integral wearing surface, is less than the NCDL in Case 3 and Case 4, consisting of a 9" monolithic deck. Contrarily, the SDL in Case 1 and Case 2, consisting of the side/median barriers and a 1.75" overlay over the entire deck, is greater than the SDL in Case 3 and Case 4, consisting of only the side/median barriers.

BRIDGE 9340 STUDY



From the analysis results summarized in **Table AV-1**, a continuous deck has been found to generally reduce truss member axial forces under the total dead load, compared with the existing deck. This is because the continuous deck helps resist the composite dead load with a more efficient, composite structural system. Comparing between Case 1 and Case 2 under the total dead load, the 6" continuous deck causes a maximum of 28% reduction in the upper chord axial force (occurring at U3-U4), a maximum of 90% reduction in the lower chord axial force (occurring at L2-L3), a maximum of 32% reduction in the diagonal member axial force (occurring in U4'-L3'), and a maximum of 31% reduction in the vertical member axial force (occurring at U5'-L5'). However, some members experience an axial force increase as a result of the continuous deck, all of which are located in the contra-flexural areas of the truss spans and are subject to very low force magnitudes. These members include some upper and lower chords located in the vicinities of Panel Points U4', L4, and L4' to L1'. Several vertical members also experience a minor axial force increase (U2-L2, U12-L12, U14-L14, U12'-L12' and U2'-L2'). These force increases are not considered detrimental because of the low magnitudes of the total forces. They are likely caused by the shifting of contra-flexural locations in the truss spans due to the continuous deck.

A comparison between Case 1 and Case 3 under the total dead load indicates that the axial force experiences insignificant changes for most truss members except some moderate increase for a few members. This is the combined result of a greater non-composite dead load (NCDL), which tends to cause higher truss member forces, and a continuous deck, which tends to reduce truss member forces under the composite dead load (CDL). If the new 9" deck would be poured in two steps, for example with 7" reinforced concrete and a 2" overlay, the truss member forces would be significantly reduced. Alternatively, the use of light-weight concrete for the new deck can also reduce dead load effects and should be evaluated in the final design of the deck replacement.

A comparison between Case 3 and Case 4 illustrates the effect of bearing condition on truss member axial forces. The different bearing conditions only apply to the NCDL of a 9" deck and the CDL of barriers, excluding the steel members. Generally, a change from the "as-designed" to the "locked" bearing condition causes the axial forces to decrease in the upper and lower chords. In the upper chords, the reduction is typically 9% to 68% with more significant changes in

members that have very low axial load. In the lower chords, the maximum axial force reduction is 52% occurring at L2-L3. Exceptions occur in the span contra-flexural areas where some upper chord members see a slight axial force increase and some compression lower chords in the main span adjacent to Piers 6 and 7 see an axial force increase of as much as 63% (L10'-L9'). This is most likely due to the arching affect caused by the locked bearings which tend to increase the compressive load in the lower truss chord members. For some lower/upper chord members in the span contra-flexural areas, such as L3-L4, L4-L5, L5'-L4', L4'-L3', and U4'-U3', the axial force under total dead load changes from compression to tension comparing between the as-designed and locked bearing conditions. This is likely caused by the shifting of contra-flexural locations due to the arching effect. For truss diagonal members, the change from the as-designed to locked bearing condition typically causes the axial force to decrease (49% maximum reduction occurring at U4'-L3'). However, exceptions occur in the side span members adjacent to Piers 5 and 8 where the increase can be as much as 60% (U2-L3) and 8% for member U14-L13'. In summary, the effect of bearing condition is complicated and can be significant on truss member forces. This effect should be considered in the final design of the deck replacement because of the uncertain and erratic nature of actual expansion bearings.

7.2.3 Effect of Deck Replacement on Truss Member Force Interaction Ratio under Dead Load

The previous section has discussed various effects of deck replacement on the axial force component of truss members. For deck replacement using a 9" monolithic and continuous slab, the force interaction ratio of axial force and bending moments in two principal directions will be discussed in this section under the total dead load. The purpose is to examine the combined force effects in the truss members due to the deck replacement. The force interaction ratios for the main truss members have been adjusted to account for connection capacities.

A comparison of the truss member force interaction ratios between the existing structure and the redecked structure is listed for all the east truss members in **Table AV-2 in Appendix V**. The bearing condition is as-designed for the existing structure and includes both the as-designed and locked for the redecked structure. The axial load portion of the interaction ratio is listed separately in the tables to quantify the contributions from the axial force and bending moments.

An observation of the tables indicates that the total interaction ratio of main truss members has similar response to the deck replacement as the axial load. The axial load is typically the primary contributor to the force interaction ratio except for members that have very low axial forces where the bending effects become dominant in the interaction ratio. For these main truss members, however, the total magnitude of the force interaction ratio is generally low.

A review of Table AV-2 indicates that a 9" monolithic and continuous new deck causes an increase of the total force interaction ratio in some, and a decrease in other, main truss members under total dead load. The magnitude of the change of the load effect, and whether or not the load effect increases or decreases, varies with the truss bearing condition, for the as-designed and locked conditions, as summarized in the tables. The impact of the deck replacement on the secondary members is relatively low. For floor truss members where the force interaction ratio has been found to exceed 1.0 in some members due to out-of-plane bending under the dead load in the existing condition, the number of members having a force interaction ratio greater than 1.0 with a 9" monolithic and continuous new deck actually decreases from 14 to 10, and 6, and the maximum value of the ratio decreases from 1.603 to 1.416, and 1.569, for the as-designed and locked bearing conditions, respectively. The effect on the portal and sway frame members is negligible with an increase in maximum interaction ratio from 0.101 to 0.107 (as-designed) and 0.103 (locked). For the upper and lower lateral bracing members the maximum force interaction ratio decreases from 0.516 to 0.485 for the as-designed bearing condition and increases to 0.558 for the locked bearing condition. For the stringer members the maximum force interaction ratio decreases from 0.654 to 0.524 for the as-designed bearing condition and increases to 0.841 for the locked bearing condition.

In summary, a 9" monolithic and continuous new deck causes load increase in some main truss members under the total dead load. This is primarily due to the increase of the non-composite dead load of the new deck. As discussed in the previous section, a 7" monolithic and continuous new deck with a 2" overlay would generally reduce truss member forces under total dead load and is thus more advantageous than a 9" monolithic slab for deck replacement.

7.2.4 Effect of Deck Replacement on Truss Member Forces under Live Load

A comparison of live load axial stress ranges was made and results summarized in **Table AV-3** in **Appendix V** for all east truss members for four different deck replacement options:

- Case 1: 6" existing deck with 2.25" overlay (baseline condition)
- Case 2: 6" continuous deck with 2.25" overlay. (a hypothetical condition for the effect of deck continuity)
- Case 3: 9" monolithic and continuous deck (a redecked condition)
- Case 4: 9" monolithic and continuous deck with all floor truss-to-main truss connections stiffened (another redecked condition)

For all the cases, the main truss expansion bearings and all stringer bearings were assumed locked. The live load used in the analysis was a single fatigue truck located 2 ft from the east curb moving from south to north.

As shown in **Table AV-3**, a continuous deck reduces live load stresses in almost all main truss members and the reduction is greater with a 9" thick than a 6" thick continuous deck. The largest reductions typically occur in the members near the existing deck joint locations (Panel Points 4, 8, 14, 8', and 4').

Using a 6" continuous replacement deck, the live load stress range reduces by as much as almost 30% in the upper chord members (U14-U13'), about 10% in the lower chord members (L13-L14 – one of the eight critical members), almost 5% in the diagonal members (L3'-U2'), and about 11% in the vertical members (U14-L14). Exceptions to this are the members in the side spans adjacent to Piers 6 and 7 (U7-U8 and U8'-U7'), where the live load stress range increases by about 3%. However, a further examination indicates that the increase of the stress range is due to an increase of the compressive component of the stress range. The tensile component actually decreased slightly due to the continuous deck.

The use of a 9" continuous replacement deck, instead of 6" in thickness, further reduces live load stress ranges with a maximum of additional 14% (U3-U4). This effect is more pronounced in the upper chords and insignificant in the lower chords and diagonals.

Case 4 was intended to investigate the effect of further enhancing the deck-truss composite action by stiffening the connections between the floor truss and the main truss. The existing connection is subject to out-of-plane bending of the web of the floor truss top chord, which has a pair of stiffeners on both sides of the web but, is not very stiff in the longitudinal direction of the bridge. Compared to a 9" continuous new deck, this additional stiffening further lowers the live load stress range in the top chords that are subject to tension. In the top chords above Piers 6 and 7, the additional reduction to the stress range is up to 14% (U8-U9). In the compression top chords near the middle of the center span, the maximum reduction of stress range is up to 20% (U14-U13'). For the top chords in the end cantilevers and in the span contra-flexural areas, some live load stress range increase up to 5% occurs. For the lower chords, diagonals, and verticals, the change in the live load stress range is negligible with maximum changes of 0.80%, 0.98%, and 1.38% respectively.

7.2.5 Effect of Deck Replacement on Bridge Redundancy

To investigate the effect of a continuous deck on bridge redundancy, a redundancy analysis was performed for truss lower chord L13-L14 and upper chord U7-U8 using Load Case 3 – eight lanes of standstill HS-20 truck and lane load. These two members were selected based on their nature of being fracture critical and the expectations of most significant impact on their behavior from a continuous deck. The results of the redundancy analysis of these two members represent a cluster of lower chords near the middle of the center span and clusters of upper chords above Piers 6 and 7, respectively. Load Case 3 was selected because it is the most severe of the four load cases studied in Section 6.

Two bridge conditions were analyzed for structural redundancy:

Case 1: 6" existing deck with 2.25" overlay (existing condition)

Case 2: 6" continuous deck with 2.25" overlay (a redecked condition)

Structural consequences were analyzed for the failure of each of the two truss members and the results are summarized in the following.

1. Failure of East Truss Lower Chord L13-L14

Redundancy analyses were performed for both the existing (Case 1) and a redecked (Case 2) condition, in which all expansion bearings of the trusses and the stringers were assumed to be locked.

For the existing condition (Case 1) without connection capacity adjustments, the calculated force interaction ratios indicated that six main truss members and twenty-five floor truss members would fail resulting from the failure of east truss lower chord L13-L14, when dynamic impact was not included. For the redecked condition (Case 2) without connection capacity adjustments, the number of consequent main truss member failures would be two less than in the existing structure; and the number of consequent floor truss member failures would be four less than the number that fail in the existing structure. The number of consequent member failures would be the same for both the portal/sway frames and the upper/lower lateral bracings for the redecked structure. When the connection capacity adjustments are applied, the same number of main truss members would fail for both the existing and the redecked structures.

When a dynamic impact factor of 1.854 was included without connection capacity adjustments, seven main truss members and thirty floor truss members would fail resulting from the failure of east truss lower chord L13-L14 in the existing condition (Case 1). Additionally, four portal/sway frame members and four upper/lower lateral bracing members would fail. For the redecked condition (Case 2) without connection capacity adjustments, the number of consequent main truss member failures would be the same as the existing structure; and the number of consequent floor truss member failures would be eight less than the existing structure. The number of consequent member failures for the redecked structure would be the same for the portal/sway frames and two

more for the upper/lower lateral bracings than the existing structure. When the connection capacity adjustments are applied, nine main truss members would fail in the existing condition while eight would fail in the redecked condition.

An examination of the deck forces at the cross section above Pier 6 and Pier 7 indicates that the maximum force interaction ratio for the intact redecked structure is 4.705 at Pier 6 and 7. After the failure of L13-L14 the maximum interaction ratio increases to 5.093 without dynamic impact and 5.426 with dynamic impact. This indicates that the capacity of the deck may likely be exceeded with the amount of reinforcement in the existing condition. These large interactions are due to the relatively low bending capacity in the longitudinal direction. The bending due to the superimposed dead load on the new deck alone exceeds the bending capacity.

In summary, replacing the existing deck with a continuous deck of the same thickness improves the structural redundancy by reducing the number of consequent member failures after the failure of truss lower chord L13-L14. Similar results would be expected if the same redundancy analysis was performed for lower chord L12-L13. However, the amount of longitudinal deck reinforcement above Piers 6 and 7 needs to be carefully determined in the final design of deck replacement.

2. Failure of East Truss Upper Chord U7-U8

Redundancy analyses were performed for both the existing (Case 1) and a redecked (Case 2) condition, in which all expansion bearings of the trusses and the stringers were assumed to be locked.

For the existing condition (Case 1) without connection capacity adjustments, the calculated force interaction ratios indicated that one main truss member and twenty-two floor truss members would fail resulting from the failure of east truss upper chord U7-U8, when dynamic impact was not included. For the redecked condition (Case 2) without connection capacity adjustments, the number of consequent main truss member failures

would be one less than the existing structure indicating zero failures; and the number of consequent floor truss member failures would be one less than the number that fail on the existing structure. No consequent member failures occur for both the portal/sway frames and the upper/lower lateral bracings for the existing or the redecked structure. When the connection capacity adjustments are applied, the same number of main truss members would fail for the existing structure and one member would fail for the redecked structure.

When a dynamic impact factor of 1.854 was included without connection capacity adjustments, two main truss members and twenty-six floor truss members would fail resulting from the failure of east truss upper chord U7-U8 in the existing condition (Case 1). No portal/sway frame members or upper/lower lateral bracing members would fail. For the redecked condition (Case 2) without connection capacity adjustments, the number of consequent main truss member failures would be the same as the existing structure; and the number of consequent floor truss member failures would be one more than the existing structure. No portal/sway frame members or upper/lower lateral bracing members would fail for the redecked structure. When the connection capacity adjustments are applied, two main truss members would fail in the existing condition while three would fail in the redecked condition.

As noted in the previous paragraph, for the failure of U7-U8 with the 1.854 dynamic impact factor applied, one more consequent member failure occurs for the redecked structure than the existing structure when the connection capacity adjustment factors are applied. For the existing structure U7-L7 (2.103) and U8-L8 (1.201) are the consequent failures. For the redecked structure U7-L7 (1.321), U10-U11 (1.140), and U8-L8 (1.017) are the consequent failures. Upper Chord U10-U11, which fails for the redecked structure but not the existing structure, has an interaction ratio of 0.982 for the existing structure. An examination of the force interaction for member U10-U11 under dead plus live load on the intact structure indicates a significantly higher value for the redecked structure (0.853) than for the existing structure (0.668). This difference in intact interaction ratios was determined to be primarily due to the difference in the dead load

force in the member due to the superimposed dead load (SDL). The larger force from the SDL on the redecked structure is expected because the SDL is supported by a continuous deck and some redistribution of the loads on the composite section is expected. Although an additional consequent member occurs for the redecked structure it is still a more favorable condition because the maximum interaction ratio has been significantly reduced.

An examination of the deck forces at the cross section above Pier 6 and Pier 7 indicates that the maximum force interaction ratio for the intact redecked structure is 4.485 at Pier 6 and 7. After the failure of L13-L14 the maximum interaction ratio increases to 7.611 without dynamic impact and 10.280 with dynamic impact. This indicates that the capacity of the deck may likely be exceeded with the amount of reinforcement in the existing condition. These large interactions are due to the relatively low bending capacity in the longitudinal direction. The bending due to the superimposed dead load on the new deck and the bending due to the member failure each exceed the bending capacity themselves.

In summary, replacing the existing deck with a continuous deck of the same thickness improves the structural redundancy by reducing the number of consequent member failures after the failure of truss upper chord U7-U8. Similar results would be expected if the same redundancy analysis was performed for upper chord U8-U9. However, the amount of longitudinal deck reinforcement above Piers 6 and 7 needs to be carefully determined in the final design of deck replacement.

7.2.6 Results Summary on Deck Replacement with a Continuous Slab

Results of analyses discussed above indicate that replacing the existing deck with a continuous deck of the same thickness throughout the truss spans significantly reduces stresses in most truss members under both dead and live loads. The largest stress reductions typically occur in the members near the existing deck joint locations. Some truss members near the span contra-flexural areas experience minor stress increases due to a continuous deck under both the dead and live loads, but the consequence is not detrimental since those member forces are of low

magnitudes. Under live load, further stress reduction can be achieved by using a thicker continuous deck and by stiffening the connections between the floor truss and the main truss. The further stress reduction due to each of these two measures, however, is insignificant to the upper chords and nearly negligible to the lower chords and diagonals. Therefore, further enhancement of the deck-truss composite action by stiffening the connections between the main truss and floor truss top chord does not seem to be worthwhile.

The casting of the new deck is critical to achieving the maximum benefit of stress reduction in truss members. Since the weight of wet concrete is carried by the steel system alone and any dead load applied after the deck concrete cures is carried more efficiently by the composite deck-truss system, the design and construction of the new deck should aim to minimize the thickness of the initial pour. For example, casting a continuous new deck with a 7" structural thickness plus a subsequently applied overlay is more advantageous than a monolithically poured 9" thickness. In addition, the use of light-weight concrete for the new deck should also be evaluated in the final design of deck replacement.

While the condition of the expansion bearings was assumed locked under live load, both "as-designed" and "locked" conditions were considered in the redecking dead load analysis for their uncertain and erratic nature. The analysis results indicated that the effect of bearing condition is complicated and can be significant on truss member forces. In the final design of deck replacement, both bearing conditions should be taken into consideration and the governing situation to be used in the design.

Redundancy analyses indicated that replacing the existing deck with a continuous deck of the same thickness typically improves the structural redundancy by reducing the number of consequent member failures after the failure of truss lower chord L13-L14, and the failure of truss upper chord U7-U8, respectively. However, the continuous deck would not eliminate consequent failures of main truss members and thus would not change the fracture-critical nature of either member. The amount of longitudinal deck reinforcement above Piers 6 and 7 shall be carefully determined in the final design of deck replacement.

SECTION 8

8. CONCEPTUAL PLAN FOR DECK REPLACEMENT

8.1 General Considerations

For the development of a conceptual plan for the deck replacement of Bridge 9340, the following considerations need to be taken into account:

- Maintain a minimum of four lanes open to traffic at any time during deck replacement construction
- Minimize traffic interruptions during necessary transportation and placement of construction materials and equipment
- Determine optimum plans for maintenance of traffic considering the ease of construction and the impact of unsymmetrical loading to the trusses

Since truss bridges have generally been designed with symmetrical dead load between the two trusses, it would be desirable to keep this loading condition during deck replacement. To achieve this, it would require a division of the deck replacement into two stages: one for the four center lanes and one for the four outer lanes (two along each side of the bridge). However, the layout of the traffic lanes and particularly the ramps at the bridge site makes it difficult for such lane division for deck replacement. It would be much easier to replace the half deck width on the east side and then the other half on the west side, or vice versa. As a result, the suitability of the structure, particularly the floor trusses, to the unsymmetrical half-deck loading condition was investigated and will be discussed in the following section.

Figure 8-1 is an aerial photo of the Bridge 9340 site.



Figure 8-1. Aerial Photo of Bridge 9340 Site

8.2 Deck Replacement Analysis

8.2.1 Structural Impact of Unsymmetrical Loading on Main Trusses

For proper development of a deck replacement sequence, it is important to understand whether the deck truss system is able to take transversely unbalanced loading since truss bridges are typically designed to carry symmetrical dead load about the longitudinal centerline. This information helps the deck replacement designer to consider more options for staging the construction work.

In order to evaluate whether the steel structure, consisting of the main trusses, the floor trusses and the lateral bracing system, is able to take an extreme laterally unbalanced loading condition, four different cases were analyzed:

- Case 1. Existing structure with half the deck and stringers removed – using unfactored load and ultimate capacity
- Case 2. Existing structure with half the deck and stringers removed – using LRFD factored load and capacity
- Case 3. Existing structure – using LRFD factored load and capacity
- Case 4. A redecked structure with a monolithic 9" deck – using LRFD factored load and capacity

For each case, member capacities were examined by checking the force interaction ratio of each member consisting of the force effects of axial force and in-plane and out-of-plane bending moments. The force interaction ratios were determined both without and with the connection capacity adjustments applied. The results are summarized in the subsequent sections 8.2.1.1 thru 8.2.1.4. It should be noted that the calculated force interaction ratios are somewhat conservative in terms of loading effect because each interaction ratio is calculated using the maximum axial force and maximum in-plane and out-of-plane bending moments caused by a truck crossing. These three maximum force effects, however, may not necessarily occur at the same time. A cursory check of some force interaction ratios revealed two important points: 1) A single truck

position may cause maximum axial load and one maximum bending moment simultaneously, but not the maximum value for all three components at the same time; and 2) the truck positions that cause the maximum axial load and bending moments are located no more than a floor truss spacing apart. Based on these findings it is believed that although the force interaction ratios are most likely overestimated, the amount of overestimation should be insignificant.

8.2.1.1 Case 1: Analysis of Existing Structure with Half the Deck and Stringers Removed – Using Unfactored Load and Ultimate Capacity

For this analysis, unfactored load was applied to the half-deck structure and checked against the ultimate capacity of the members. The purpose of this analysis is to provide a measurement of actual safety margin.

This condition includes complete removal of the west half of the deck and stringers from the longitudinal centerline, while the east half is in the existing condition and subjected to four lanes of unfactored LRFD design load with impact. The truss and stringer expansion bearings are assumed to be “as-designed” for the dead load and “locked” for the live load. The live load consists of four lanes of HS-20 truck load plus full-length lane load along the centerline of each lane, with a live load impact factor of 1.33 applied to the trucks only. No multiple-presence reduction was applied in order to represent the worst traffic situation. No load or resistance factors were used for a realistic assessment of the actual situation. Member capacities were examined by checking the force interaction ratio of each member consisting of axial force and in-plane and out-of-plane bending moments. The main truss member capacities were adjusted to account for their connection capacities.

The calculated force interaction ratios for all east truss members are presented in **Table AVI-1** and **AVI-2** in **Appendix VI** for the main truss members without and with the connection capacity adjustments applied, respectively. **Tables AVI-1** and **AVI-2** include the force interaction ratios under the Dead + Live Load, as well as breakdowns into the Dead Load and Live Load, respectively.

From this analysis for Case 1 for the member capacities only (without the connection capacity adjustments applied), zero main truss members have force interaction ratios exceeding 1.0 at one or both ends of the member with a maximum value of 0.940 (U1'-L1' Joint L1'). For these members the axial component is typically the primary contributor to the total force interaction ratio, with a maximum value of 0.668 versus the corresponding 0.940 total (U1'-L1' Joint L1'). For some of the members the contribution of the in-plane bending component is relatively significant with a maximum value of 0.449 versus the corresponding 0.864 total (SFB-U1 Joint SFB). The out-of-plane bending component typically has insignificant effect on the total force interaction ratio with a maximum value of 0.129 versus the corresponding 0.940 total (U1'-L1' Joint L1').

From this analysis for Case 1 with the connection capacity adjustment factors applied, two main truss members have force interaction ratios exceeding 1.0 at one or both ends of the member with a maximum value of 1.017 (U1'-L1' Joint L1'). For these two members the axial component is the primary contributor to the total force interaction ratio, with a maximum value of 0.723 versus the corresponding 1.017 total (U1'-L1' Joint L1'). For some of the members the contribution of the in-plane bending component is relatively significant with a maximum value of 0.492 versus the corresponding 0.945 total (SFB-U1 Joint SFB). The out-of-plane bending component typically has insignificant effect on the total force interaction ratio with a maximum value of 0.139 versus the corresponding 1.017 total (U1'-L1' Joint L1').

The calculated force interaction ratios for floor truss members are presented in **Table AVI-3** in **Appendix VI**. **Table AVI-3** includes the force interaction ratios under the Dead + Live Load, as well as breakdowns into the Dead Load and Live Load, respectively. Only floor truss members that have a force interaction ratio greater than 1.0 for at least one of the four cases evaluated are included in the table. From the analysis for Case 1, seven floor truss members at nine sections have a force interaction ratio greater than 1.0 with a maximum value of 1.230 (an upper chord at Panel Point 14). Typically the force interaction ratios greater than 1.0 occur on the upper chord members of the floor trusses, which are under tension. For these members, the primary contributor to the force interaction ratio is the out-of-plane bending, mostly due to the dead load. As discussed previously in Section 6.7.1, the asymmetry of stringer bearing releases at deck

expansion joints causes high out-of-plane bending in the floor truss top chords in the existing, full-deck condition. The half-deck configuration would further increase floor truss member forces due to the unbalanced dead load between the two trusses.

No other types of members have force interaction ratios greater than 1.0. The maximum total force interaction ratio is 0.335 for the portal and sway frame members, and 0.690 for the upper/lower lateral bracing members.

In summary for Case 1 of the half-deck condition, a force interaction ratio exceeding 1.0 occurs in zero main truss members without the connection capacity adjustment factors applied with a maximum value of 0.940, occurs in two main truss members with the connection capacity adjustment factors applied with a maximum value of 1.017, and in seven floor truss members with a maximum value of 1.230. The calculation of the force interaction ratios is based on unfactored load (four lanes of HS-20 truck and lane load) and unfactored ultimate member/connection capacities. It should be noted that the live load used in the analysis is significantly higher than the original design load. It should also be noted that many floor truss members have experienced a force interaction ratio greater than 1.0 under dead load in the existing full-deck condition, mainly due to the out-of-plane bending caused by the stringer bearing release asymmetry at deck expansion joint locations.

8.2.1.2 Case 2: Analysis of Existing Structure with Half the Deck and Stringers Removed – Using LRFD Factored Load and LRFD Factored Capacity

For this analysis, the LRFD factored load was applied to the half-deck structure and checked against the LRFD factored capacity, or resistance, of the members. This analysis is consistent with the current bridge design method in the state of Minnesota.

Similar to Case 1, this condition includes complete removal of the west half of the deck and stringers from the longitudinal centerline, while the east half is in the existing condition and subjected to four lanes of LRFD design load with impact. The truss and stringer expansion bearings are assumed to be “as-designed” for the dead load and “locked” for the live load. The

live load consists of four lanes of HS-20 truck load plus full-length lane load along the centerline of each lane, with a live load impact factor of 1.33 applied to the trucks only. A 0.65 multi-presence factor was applied to the live load. Load and resistance factors were applied to the loads and member capacities, respectively, in accordance with the LRFD specifications. Member capacities were examined by checking the force interaction ratio of each member consisting of the force effects of axial force and in-plane and out-of-plane bending moments. The main truss member capacities were adjusted to account for the connection capacities.

The calculated force interaction ratios for all east truss members are presented in **Table AVI-4** and **AVI-5** in **Appendix VI** for the main truss members without and with the connection capacity adjustments applied, respectively. **Tables AVI-4** and **AVI-5** include the force interaction ratios under the Dead + Live Load, as well as breakdowns into the Dead Load and Live Load, respectively.

Based on this analysis for Case 2 for the member capacities only (without the connection capacity adjustments applied), fourteen main truss members have a force interaction ratio exceeding 1.0 at one or both ends of the member with a maximum value of 1.358 (U0-L1 Joint U0). For thirteen of the fourteen members the axial component is the greatest contributor to the total force interaction ratio with a maximum value of 0.934 versus the corresponding 1.300 total (U1'-L1' Joint L1'). For some of the members the contribution of the in-plane bending component is relatively significant with a maximum value of 0.564 versus the corresponding 1.112 total (SFB-U1 Joint SFB). The out-of-plane bending component typically has insignificant effect on the total force interaction ratio with a maximum value of 0.171 versus the corresponding 1.300 total (U1'-L1' Joint L1').

Based on this analysis for Case 2 with the connection capacity adjustment factors applied, eighteen main truss members have a force interaction ratio exceeding 1.0 at one or both ends of the member with a maximum value of 1.453 (U0-L1 Joint U0). For seventeen of the eighteen members the axial component is the greatest contributor to the total force interaction ratio with a maximum value of 1.011 versus the corresponding 1.407 total (U1'-L1' Joint L1'). For some of the members the contribution of the in-plane bending component is relatively significant with a

maximum value of 0.617 versus the corresponding 1.218 total (SFB-U1 Joint SFB). The out-of-plane bending component typically has insignificant effect on the total force interaction ratio with a maximum value of 0.185 versus the corresponding 1.407 total (U1'-L1' Joint L1').

The calculated force interaction ratios for floor truss members are presented in **Table AVI-6** in **Appendix VI**. **Table AVI-6** includes the force interaction ratios under the Dead + Live Load, as well as breakdowns into the Dead Load and Live Load, respectively. Only floor truss members that have a force interaction ratio greater than 1.0 for at least one of the four cases evaluated are included in the table. Based on the analysis for Case 2, twenty floor truss members at thirty sections have a force interaction ratio greater than 1.0 with a maximum value of 1.533 (an upper chord at Panel Point 14). The majority of the force interaction ratios greater than 1.0 occur on the upper chord members of the floor trusses, which are under tension. For the majority of these members, the primary contributor to the interaction is the out-of-plane bending, mostly due to the dead load. As discussed previously in Section 6.7.1, the asymmetry of stringer bearing releases at deck expansion joints causes high out-of-plane bending in the floor truss top chords in the existing, full-deck condition. The half-deck configuration would further increase floor truss member forces due to the unbalanced dead load between the two trusses.

No other types of members have force interaction ratios greater than 1.0. The maximum total force interaction ratio is 0.443 for the portal and sway frame members, and 0.980 for the upper/lower lateral bracing members.

In summary for Case 2 of the half-deck condition, a force interaction ratio exceeding 1.0 occurs in fourteen main truss members without the connection capacity adjustment factors applied with a maximum value of 1.358, occurs in eighteen main truss members with the connection capacity adjustment factors applied with a maximum value of 1.453, and in twenty floor truss members with a maximum value of 1.533. The calculation of the force interaction ratios is based on the LRFD factored load and member/connection capacities. It should be noted that the LRFD live load is significantly higher than the original design load. It should also be noted that many floor truss members have experienced a force interaction ratio greater than 1.0 under dead load in the

existing full-deck condition, mainly due to the out-of-plane bending caused by the stringer bearing release asymmetry at deck expansion joint locations.

In order to better evaluate whether or not the removal of half the deck is detrimental, the existing full-deck structure was also analyzed for the force interaction ratios using the LRFD loads and member/connection capacities and compared with the half-deck results. This comparison was intended to better understand the significance of the calculated force interaction ratios that exceed 1.0.

8.2.1.3 Case 3: Analysis of Existing Structure – Using LRFD Factored Load and LRFD Factored Capacity

For this analysis, the LRFD factored load was applied to the existing full-deck structure and checked against the LRFD factored capacity, or resistance, of the members. This analysis is consistent with the current bridge design method in the state of Minnesota, and the results from the force interaction ratios are to be compared with those of the half-deck structure discussed above.

This condition includes the existing structure subjected to eight lanes of LRFD design load with impact. The truss and stringer expansion bearings are assumed to be “as-designed” for the dead load and “locked” for the live load. The live load consists of eight lanes of HS-20 truck load plus full-length lane load along the centerline of each lane, with a live load impact factor of 1.33 applied to the trucks only. A 0.65 multi-presence factor was applied to the live load. Load and resistance factors were applied to the loads and member capacities, respectively, in accordance with the LRFD specifications. Member capacities were examined by checking the force interaction ratio of each member consisting of the force effects of axial force and in-plane and out-of-plane bending moments. The main truss member capacities were adjusted to account for the connection capacities.

The calculated force interaction ratios for the east truss members are presented in **Table AVI-7** and **AVI-8** in **Appendix VI** for the main truss members without and with the connection

capacity adjustments applied, respectively. Tables AVI-7 and AVI-8 include the force interaction ratios under the Dead + Live Load, as well as breakdowns into the Dead Load and Live Load, respectively.

Based on this analysis for Case 3 for the member capacities only (without the connection capacity adjustments applied), twenty-four main truss members have a force interaction ratio greater than 1.0 at one or both ends of the member with a maximum value of 1.503 (U0-L1 Joint U0). For twenty-two of the twenty-four members the axial component is the greatest contributor to the total force interaction ratio with a maximum value of 0.952 versus the corresponding 1.339 total (U1'-L1' Joint L1'). For some of the members the contribution of the in-plane bending component is relatively significant with a maximum value of 0.610 versus the corresponding 1.274 total (U1'-NFB Joint NFB). The out-of-plane bending component typically has insignificant effect on the total force interaction ratio with a maximum value of 0.193 versus the corresponding 1.212 total (U1'-L1' at connection to the floor truss lower chord).

Based on this analysis for Case 3 with the connection capacity adjustment factors applied, thirty-five main truss members have a force interaction ratio greater than 1.0 at one or both ends of the member with a maximum value of 1.608 (U0-L1 Joint U0). For thirty-two of the thirty-five members the axial component is the greatest contributor to the total force interaction ratio with a maximum value of 1.030 versus the corresponding 1.449 total (U1'-L1' Joint L1'). For some of the members the contribution of the in-plane bending component is relatively significant with a maximum value of 0.666 versus the corresponding 1.307 total (SFB-U1 Joint SFB). The out-of-plane bending component typically has insignificant effect on the total force interaction ratio with a maximum value of 0.209 versus the corresponding 1.299 total (U1-L1 at connection to the floor truss lower chord).

The calculated force interaction ratios for floor truss members are presented in Table AVI-9 in Appendix VI. Table AVI-9 includes the force interaction ratios under the Dead + Live Load, as well as breakdowns into the Dead Load and Live Load, respectively. Only floor truss members that have a force interaction ratio greater than 1.0 for at least one of the four cases evaluated are included in the table. Based on the analysis for Case 3, one hundred and eight floor truss

members at one hundred forty-three sections have a force interaction ratio greater than 1.0 with a maximum interaction ratio of 2.441 (upper lateral bracing support at Panel Point 14). The majority of the force interaction ratios greater than 1.0 occur on the upper chords, diagonals, or upper lateral bracing support members. For the majority of the upper chord and upper lateral bracing support members, the primary contributor to the force interaction ratio is the out-of-plane bending, usually due to the dead load. As discussed previously in Section 6.7.1, the asymmetry of stringer bearing releases at deck expansion joints causes high out-of-plane bending in the floor truss top chords in the existing condition under dead load. For the majority of the floor truss diagonal members the primary contributor to the force interaction ratio is the axial load almost equally due to the dead load and the live load.

No portal or sway frame members have a total force interaction ratio greater than 1.0 with a maximum value of 0.266. Two upper lateral bracing members have a force interaction ratio greater than 1.0. These members span between Panel Point 14 and 13' and connect the center of the floor truss to the east and west main trusses with the force interaction ratio equal to 1.185 and 1.180, respectively.

In summary for Case 3 of the existing full-deck condition subjected to the LRFD factored load and member capacities, an excessive amount of members have force interaction ratios greater than 1.0. Twenty-four main truss members without the connection capacity adjustment factors applied have force interaction ratios greater than 1.0 with a maximum value of 1.503. Thirty-five main truss members with the connection capacity adjustment factors applied have force interaction ratios greater than 1.0 with a maximum value of 1.608. One hundred and eight floor truss members have force interaction ratios greater than 1.0 with a maximum value of 2.441. As discussed before, it should be noted that the LRFD live load is significantly higher than the original design load. It should also be noted that many floor truss members have experienced a force interaction ratio greater than 1.0 under dead load in the existing full-deck condition, mainly due to the out-of-plane bending caused by the stringer bearing release asymmetry at deck expansion joint locations.

Comparing between the full-deck (Case 3) and the half-deck (Case 2) conditions, it is seen that the calculated force interaction ratios of the half-deck condition (subject to four lanes of live load) are no worse than those of the full-deck condition (subject to eight lanes of live load) using the same multi-presence factor of 0.65.

8.2.1.4 Case 4: Analysis of a Redecked Structure— Using LRFD Factored Load and LRFD Factored Capacity

For this analysis, the LRFD factored load was applied to a redecked full-deck structure and checked against the LRFD factored capacity, or resistance, of the members. The redecked condition is for a monolithic 9" continuous composite deck. This analysis is consistent with the current bridge design method in the state of Minnesota, and the results from the force interaction ratios are to be compared with those of the existing full-deck structure discussed above.

This condition includes the structure with a new 9" monolithic continuous deck subjected to eight lanes of LRFD design load with impact. The truss and stringer expansion bearings are assumed to be "as-designed" for the dead load of the steel structure, "locked" for the dead loads of the new deck and barriers, and "locked" for the live load. The live load consists of eight lanes of HS-20 truck load plus full-length lane load along the centerline of each lane, with a live load impact factor of 1.33 applied to the trucks only. A 0.65 multi-presence factor was applied to the live load. Load and resistance factors were applied to the loads and member capacities, respectively, in accordance with the LRFD specifications. Member capacities were examined by checking the force interaction ratio of each member consisting of the force effects of axial force and in-plane and out-of-plane bending moments. The main truss member capacities were adjusted to account for the connection capacities.

The calculated force interaction ratios for the east truss members are presented in Table AVI-10 and AVI-11 in Appendix VI for the main truss members without and with the connection capacity adjustments applied, respectively. Tables AVI-10 and AVI-11 include the force interaction ratios under the Dead + Live Load, as well as breakdowns into the Dead Load and Live Load, respectively.

Based on this analysis for Case 4 for the member capacities only (without the capacity adjustments applied), twenty-eight main truss members have a force interaction ratio greater than 1.0 at one or both ends of the member with a maximum force interaction ratio of 1.611 (U1'-L1' Joint L1'). For twenty-five of the twenty-eight members the axial component is the greatest contributor to the total force interaction ratio with a maximum value of 1.091 versus the corresponding 1.210 total (L9-L10 Joint L9). For some of the members the contribution of the in-plane bending component is also significant with a maximum value of 0.769 versus the corresponding 1.070 total (L2'-L1' Joint L1'). The out-of-plane bending component typically has insignificant effect on the total force interaction ratio with a maximum value of 0.174 versus the corresponding 1.215 total (U1-L1 at connection to the floor truss lower chord).

Based on this analysis for Case 4 with the connection capacity adjustment factors applied, thirty-seven main truss members have a force interaction ratio greater than 1.0 at one or both ends of the member with a maximum force interaction ratio of 1.744 (U1'-L1' Joint L1'). For thirty-three of the thirty-seven members the axial component is the greatest contributor to the total force interaction ratio with a maximum value of 1.140 versus the corresponding 2.236 total (L10-L11 Joint L10). For some of the members the contribution of the in-plane bending component is also significant with a maximum value of 1.026 versus the corresponding 1.426 total (L2'-L1' Joint L1'). The out-of-plane bending component typically has insignificant effect on the total force interaction ratio with a maximum value of 0.189 versus the corresponding 1.315 total (U1-L1 at connection to the floor truss lower chord).

The calculated force interaction ratios for floor truss members are presented in **Table AVI-12** in **Appendix VI**. **Table AVI-12** includes the force interaction ratios under the Dead + Live Load, as well as breakdowns into the Dead Load and Live Load, respectively. Only floor truss members that have a force interaction ratio greater than 1.0 for at least one of the four cases evaluated are included in the table. Based on the analysis for Case 4, ninety-three floor truss members at one hundred twenty-three sections have a force interaction ratio greater than 1.0 with a maximum value of 2.600 (upper lateral bracing support at Panel Point 11). The majority of the force interaction ratios greater than 1.0 occur on the upper chords, diagonals, or upper lateral bracing support members. For the majority of the upper chord and upper lateral bracing support

members, the primary contributor to the interaction is the out-of-plane bending, usually due primarily to the dead load. As discussed previously in Section 6.7.1, the asymmetry of stringer bearing releases at deck expansion joints causes high out-of-plane bending in the floor truss top chords in the existing condition under dead load. For the majority of the diagonal members the primary contributor to the force interaction ratio is the axial load almost equally due to the dead load and the live load.

No portal or sway frame members have a total force interaction greater than 1.0 with a maximum value of 0.205. Four upper lateral bracing members have force interaction ratios greater than 1.0. Two of these members span between Panel Point 10 and 11 and connect the center of the floor truss to the east and west main trusses with force interaction ratios equal to 1.168 and 1.187 respectively. The other two members span between Panel Point 11' and 10' and connect the center of the floor truss to the east and west main trusses with force interaction ratios equal to 1.145 and 1.137 respectively.

In summary for Case 4 of the redecked condition with a monolithic 9" continuous composite deck subjected to the LRFD factored load and member capacities, an excessive amount of members have force interaction ratios greater than 1.0. Twenty-eight main truss members without the connection capacity adjustment factors applied have force interaction ratios greater than 1.0 with a maximum value of 1.611. Thirty-seven main truss members with the connection capacity adjustments applied have force interaction ratios greater than 1.0 with a maximum value of 1.744. Ninety-three floor truss members have force interaction ratios greater than 1.0 with a maximum value of 2.600. Compared with Case 3 of the existing condition, the force interaction ratios of the redecked condition are slightly higher in more than half of the members although also lower in some members. As discussed in Section 7, the member forces depend heavily on the casting sequence of the replacement deck and the condition of the truss bearings. It has been discovered in Section 7.2.2 that the construction of a replacement deck of 9" total thickness through an initial pour, for example of 7" thickness, plus an overlay can significantly reduce dead load force effects when compared to a monolithic 9" deck.

8.2.1.5 Comparison of Four Cases Evaluated

Comparison of calculated force interaction ratios among the four cases evaluated are summarized in **Table AVI-13** and **AVI-14** for main truss members without and with the connection capacity adjustment factors applied respectively, and **Table AVI-15** for floor truss members in **Appendix VI**. For Case 1 the maximum force interaction is less than 1.0 when the connections are not considered, and 1.017 when the connections are considered. This indicates that the actual design load should not cause overstress in any truss members for the half deck condition. For the remaining three cases, the maximum force interaction ratios are well above 1.0, considering the combined effects of axial force and in-plane and out-of-plane bending moments. As discussed in detail in **Section 4.4.5**, it should be noted that the live loads used in the analyses are significantly higher than the original design load. It should also be noted that many floor truss members have experienced a force interaction ratio greater than 1.0 under dead load in the existing condition, mainly due to the out-of-plane bending caused by the stringer bearing release asymmetry at deck expansion joint locations.

Comparing between the two half-deck structures, it is seen that the LRFD case (Case 2) typically has greater force interaction ratios (20% to 57% higher for main truss members and up to 56% higher for floor truss members) than the unfactored case (Case 1). The main truss results are the same both without and with the connection capacity adjustment factors applied. Case 1 and Case 2 are based on the same four-lane loading except Case 2 includes the LRFD load and resistance factors as well as the multi-presence reduction factor.

A comparison between the half-deck structure (Case 2) and the existing full-deck structure (Case 3) using the LRFD factors indicates that Case 3 has higher force effects than Case 2 both without and with the connection capacity adjustment factors applied. Both conditions yielded a significant amount of interaction ratios greater than 1.0 for both main truss and floor truss members. This indicates that the half-deck condition is no worse than the existing full-deck condition in terms of the LRFD loading and member resistance. For the main truss members, the interaction ratios are almost always higher in Case 3 than Case 2. The few truss members that have higher force interaction ratios in Case 2 fall into two categories: 1) the force interaction

ratio is greater than 1.0 but the difference is insignificant, e.g., U8-L8 has interaction ratios of 1.009 (Case 3 without connection capacity adjustment factors) and 1.032 (Case 2 without connection capacity adjustment factors), both greater than 1.0 but only about 2.26% different; and 2) the difference in force interaction ratio is relatively significant but the value of the ratio is significantly less than 1.0, e.g., U11'-L11' has interaction ratios of 0.242 (Case 3 without connection capacity adjustment factors) and 0.308 (Case 2 without connection capacity adjustment factors) with about a 27.65% difference but well below 1.0. For the floor truss members, the force interaction ratios are almost always higher in Case 3 than Case 2. The few members that have higher interaction ratios in Case 2 fall into the same two categories as for the main truss members. Based on these comparisons, the removal of half of the deck does not create a worse condition than what the existing structure is currently experiencing.

A comparison between the existing condition (Case 3) and a redecked condition with a monolithic 9" continuous composite deck (Case 4) using the LRFD factors indicates that Case 4 generally has higher force interaction ratios than Case 3 in main truss (both without and with the connection capacity adjustment factors applied) and floor truss members. As noted in **Section 7**, splitting the construction of a replacement deck of 9" total thickness into a 7" initial pour plus a 2" overlay can significantly reduce dead load force effects compared with a monolithic 9" deck. A continuous deck also significantly reduces live load effects compared with the existing deck that has several expansion joints. The member force effects also vary with truss bearing conditions used in the analysis, whether "as-designed" or "locked". From the analysis results in **Section 7**, it has been observed that the "locked" bearing condition tends to induce lower forces in the upper and lower truss chords compared with the "as-designed" condition due to the arching effects. Case 4 is just one potential structural condition among a number of possible situations. In the final design of deck replacement, various combinations of deck pouring and truss bearing support conditions should be investigated to determine the most appropriate solution.

8.2.2 Reinforced Concrete Pouring Sequence for Deck Replacement

For the three-span deck truss of a total length of 1,064 feet, the total volume of deck concrete is estimated to be 2,605 cubic yards for a 7-inch new deck, and 3,350 cubic yards for a 9-inch new deck. Assuming the deck replacement will be performed for approximately half of the bridge width at a time, the half-deck concrete volume is estimated to be 1.22 cubic yard per linear foot for a 7-inch new deck, and 1.57 cubic yards per linear foot for a 9-inch new deck. **Figure 8-2** depicts the bridge cross section with key deck dimensions marked.

From **Figure 8-2**, it is seen that the total width of the bridge deck is 108-ft between the existing side curbs, including the 4-ft median. This could potentially allow the maintenance of four traffic lanes in each of two half-deck construction stages while having the median area serving as a path for transporting concrete.

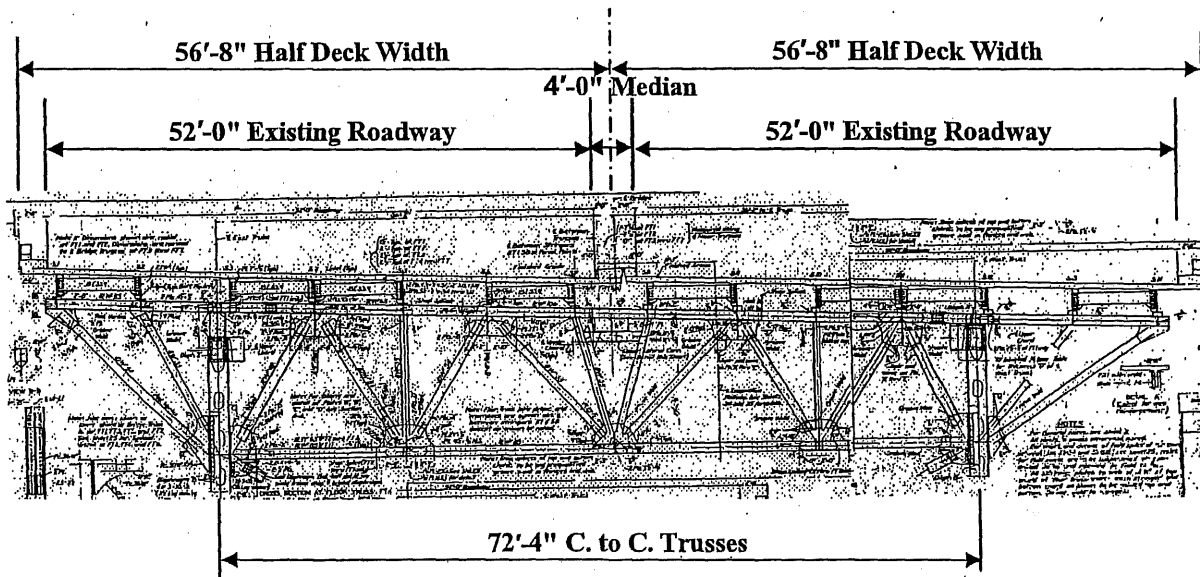


Figure 8-2. Bridge Cross Section with Key Deck Dimensions
 (For general dimensions only, not representing current median barriers)

Figure 8-3 shows longitudinal axial stress contours in a longitudinally continuous composite deck throughout the three-span deck truss. The contours were calculated using the 3-D computer

8.3 Summary and Conclusions

A preliminary analysis using the LRFD design load indicated that member forces in the main trusses and the floor trusses are no higher in a transversely unbalanced half-deck condition than the full-deck condition. However, since truss bridges have generally been designed with symmetrical dead load between the two trusses, it is more desirable to keep this symmetrical loading condition during deck replacement as much as possible. If the unbalanced half-deck procedure is to be considered, a more complete detailed analysis should be performed in the final design to evaluate the impact on all transverse members and their connections between the two main trusses.